NATURAL YELLOW DYES IN PERSIAN CARPETS: A HOLISTIC APPROACH

SAMANEH SHARIF

Mestre em conservação de objetos e artefatos culturais e históricos

NATURAL YELLOW DYES IN PERSIAN CARPETS: A HOLISTIC APPROACH

SAMANEH SHARIF

Mestre em conservação de objetos e artefatos culturais e históricos

Orientadora: Doutora Maria João Seixas de Melo,
Full Professor, Universidade NOVA de Lisboa

Júri:

Presidente: Doutor Carlos Manuel Agra Coelho,
Professor Catedrático, NOVA School of Science and Technology | FCT NOVA

Arguentes: Doutor Richard A. Laursen,
Professor Emeritus, Boston University, United States of America
Doutora Catia Clementi,
Researcher in Physical Chemistry, University of Perugia, Italy

Orientador: Doutora Maria João Seixas de Melo,
Full Professor, NOVA School of Science and Technology | FCT NOVA

Membros: Doutora Maria da Conceição Oliveira,
Researcher, Instituto Superior Técnico | University of Lisbon
Doutora Natércia do Carmo Valente Teixeira,
Researcher, Faculty of Science | University of Porto
Doutora Paula Sofia Fonseca Nabais,
Researcher, NOVA School of Science and Technology | FCT NOVA

DOUTORAMENTO EM CONSERVAÇÃO E RESTAURO DO PATRIMÓNIO

Universidade NOVA de Lisboa
setembro, 2021

Natural Yellow Dyes in Persian Carpets: A Holistic Approach

Acknowledgments

Resumo

A cor é um elemento importante que articula os padrões únicos dos tapetes persas e determina a sua identidade. No entanto, a ciência da conservação, e a investigação atual associada, têm um papel ativo na identificação de corantes amarelos naturais em têxteis históricos. Há mais de um milénio que são utilizadas diversas fontes vegetais locais para a obtenção de uma cor amarela em têxteis no Irão; no entanto, poucos estudos abordaram cientificamente este assunto. Como resultado, ainda existe uma grande lacuna no conhecimento e nos procedimentos das técnicas históricas de tingimento no Irão.

Efetivamente, a caracterização destas fontes de corantes amarelos em têxteis históricos é um desafio. Os corantes amarelos absorvem luz na região mais energética do espectro eletromagnético visível, resultando no desvanecimento e alteração da cor original em artefactos históricos. Ao analisar um tecido tingido histórico, não só a aquisição da amostra é limitada, como a quantidade de colorante é baixa. Além disso, é difícil criar uma base de dados universal de corantes amarelos naturais devido ao grande número de fontes locais, e a variedade de produtos de degradação presentes aquando da análise de amostras. Consequentemente, o perfil químico dos amarelos identificados pode não corresponder às referências existentes.

Os dados para este projecto doutoral foram coletados por meio de revisões de estudos persas e não persas e por meio da realização de entrevistas com mestres persas em alguns workshops ainda ativos, para investigar as fontes de corantes amarelos

disponíveis localmente.

A técnica multi-analítica HPLC-DAD-MS foi aplicada para analisar a composição da cor de amostras de lã tingida e as influências do processo de tingimento na composição química dos materiais corantes. Este estudo demonstra a sensibilidade e seletividade desta técnica analítica e a eficácia do método de extração suave para caracterizar flavonóides.

Finalmente, a estabilidade de sete flavonóides amarelos e o efeito dos solventes foram discutidos através da medição dos rendimentos quânticos de fotodegradação. Os dados indicam que a dupla ligação entre C3-C4 foi reconhecida como um ponto crítico das moléculas que formam o composto mais estável, o eriodictiol. Além disso, os amarelos mais estáveis beneficiam de um mecanismo foto-protetor mais forte devido à presença de OH em C5. Por outro lado, o OH em C3 aumenta a transferência de eletrões levando a uma maior reatividade. As estruturas mais instáveis- quercetina e kaempferol - foram submetidas à combinação de maior proteção e maior reatividade devido ao OH em C5 e C3, respectivamente.

A abordagem desta tese doutoral oferece informações essenciais sobre a proveniência e as características cronológicas dos têxteis persas, levando a uma melhor compreensão da abordagem de conservação preventiva para têxteis históricos.

Palavras-chave: corante natural; amarelo; tapete persa; HPLC-DAD-MS; fotodegradação; rendimento quântico

Abstract

Color is an important element that articulates the unique patterns of Persian carpets and ascertains their identity. However, conservation science and its state-of-the-art publications have an active role in identifying natural yellow dyes in historical textiles. The application of diverse local plant sources for yellow dyes in textiles has a history of a millennium in Iran; nevertheless, few studies have scientifically addressed this matter. As a result, the knowledge and procedures of historical dyeing techniques in Iran are not fully developed.

Characterization of the yellow dye sources in historical textiles is challenging. Yellow dyes absorb light in the most energetic region of the visible electromagnetic spectrum; this results in a tendency to fade and might change the original color in historical artifacts. While analyzing a historical dyed textile, not only the sample acquisition is limited, but also the amount of the coloring materials is low. Additionally, the database of natural yellow dyes is still incomplete due to the high number of local sources, and the degradation products are present in the analytical results. Consequently, the chemical profile of the identified yellows might not match the existing references.

The data for this study has been gathered through reviews of Persian and non-Persian studies and by conducting interviews with Persian dye masters in some remaining active workshops to investigate locally available Persian natural yellow dye sources.

A multi-analytical HPLC-DAD-MS technique has been applied to analyze the dye

composition of wool samples dyed and the influences of the dyeing process in the chemical composition of the dye materials. This study demonstrates the sensitivity and selectivity of this analytical technique and the effectiveness of the mild extraction method to characterize flavonoid yellow dyes.

Finally, the stability of seven yellow flavonoids and the effect of solvents on their stability were discussed by measuring their photodegradation quantum yield. The data indicates the double bond between C3-C4 was recognized as a critical point of the molecules that form the most stable compound, eriodictyol. In addition, the most stable yellows benefit from the more efficient photoprotective mechanism due to the presence of OH in C5. On the other hand, OH in C3 enhances the electron transfer and leads to higher reactivity. The most unstable structures- quercetin and kaempferol- were subjected to the combination of the higher protection and higher reactivity due to OH in C5, and C3, respectively.

The insight created by the approach of this thesis provides essential information about the provenance and chronological characteristics of Persian textiles, leading to a better understanding of the preventive conservation approach for historical textiles.

Keywords: natural dye; yellow; Persian carpet; HPLC-DAD-MS; photodegradation; quantum yield

Symbols and Notations

$Abs_{\lambda_{irr}}$	Absorption at irradiation wavelength
APCI	Atmospheric Pressure Chemical Ionization
API	Atmospheric Pressure Ionization
C	The concentration of the absorbing species per unit volume
Calc.	Calculated
Da	Dalton or unified atomic mass unit
DFT	Density Functional Theory
CID	Collision-Induced Dissociation
DART-MS	Direct Analysis in Real Time-Mass Spectrometry
DP	Degradation Product
E_a	Arrhenius activation energy
ESI	Electrospray Ionization
ESIPT	Excited State Intramolecular Proton Transfer
ESPT	Excited State Proton Transfer
FORS	Fiber Optics Reflectance Spectroscopy
hvP	Polychromatic irradiation
HPLC	High-Performance Liquid Chromatography
HPLC-DAD	High-Performance Liquid Chromatography coupled with a Diode Array Detector
HRMS	High Resolution Mass Spectrometry
I_{abs}	Total light absorbed
I_0	The intensity of the incident light
IR	Infrared
l	The absorption path-length
LC	Liquid Chromatography
MS	Mass Spectrometry
m/z	Mass-to-charge ratio
Obs.	Observed
oxA	Oxidation by electrochemical method
oxB	Oxidation by chemical compound
Pl.	Plant
QIT	Quadrupole Ion-Trap
QTOF	Quadrupole Time-of-Flight
RP	Reversed-Phase

RT, t_R	Retention Time
S_0	Singlet ground state
S_1	First singlet excited state
SERS	Surface-Enhanced Raman Spectroscopy
TLC	Thin Layer Chromatography
TOF	Time Of Flight
Tx	Textile
UHPLC	Ultra-High Performance Liquid Chromatography
UV-VIS	Ultraviolet-visible
VIS-FORS	Visible Fiber Optics Reflectance Spectroscopy
V_{sol}	Solution volume
ε	Molar absorptivity coefficient
λ_{max}	Maximum wavelength absorption in the ultraviolet-visible spectra
ϕ_R	Quantum yield

Contents

xvi

Index of figures

Index of tables

Synopsis

Systematic studies about yellow dye sources and dyeing procedures of Persian carpets are rare [1-5]. Traditional dyers were usually poorly educated, and their knowledge has passed on by oral transmission, which in some cases has led to even confusing information.

In this thesis, a three-stage methodology contributes to the study of natural yellow dye sources of Persian carpets (scheme 1).
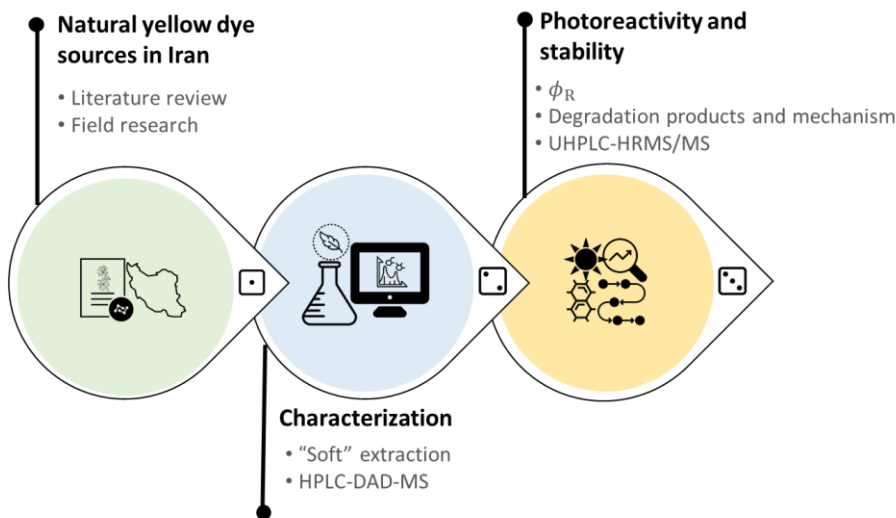
Scheme 1. The methodology developed in this research project for the investigation of yellow dyes.

In the first phase of this study, we made a list of yellow dye sources used in Persian carpets by reviewing the Persian [6-8] and non-Persian references [9-12]. Since the plants in our list were distributed in diverse locations of Iran as a vast country, we shortlisted our sources by focusing on the locally available natural yellow dyes in the center of Iran, where still few dye masters practice natural dyeing recipes in their workshops.

Aiming to have access to the production methods of Persian carpets, we documented the dyeing recipes. Knowing these recipes and the plant sources facilitates assessing the original appearance and chemical changes of the historical textiles over time. This, in turn, promotes our knowledge towards their conservation [12].

In undertaking this research, samples were supplied from the workshops, and some were personally collected from nature (Scheme 2). A highly esteemed botanist validated all the samples [13-15] because, in some cases, we witnessed conflicts between what dyers

3

call a plant and its botanical name [16].
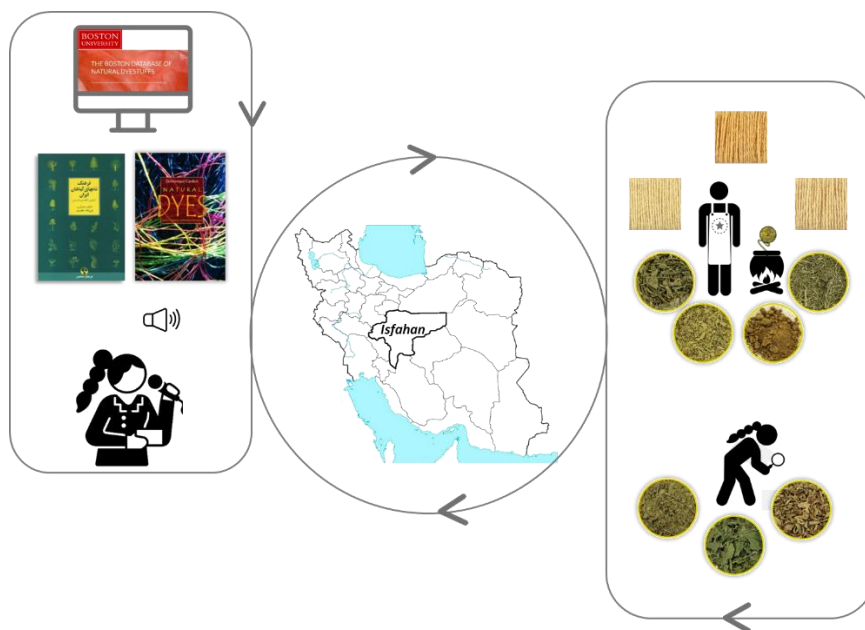
Scheme 2. The approach followed in this research project for collecting samples.

There are many factors to be considered while identifying yellow dyes; the characterization of the nature of the aglycone and its glycosylation state, the types of the substituents present and where they are attached to the aglycone, and the sequence of the glycan part [17].

Having reference chromatographic profiles is necessary to identify and differentiate yellow sources used to dye textiles. This detailed characterization was achievable by the development of micro-sampling separation techniques [18], which allowed comprehensive characterization of the yellow flavonoid dyes.

In the second phase, we intended to comprehensively characterize the composition of the selected Persian yellow dyes.

Three types of samples were analyzed to create a library of chromatographic profiles from yellow dye sources used in Persian carpets.

- The first group was the selected plant sources mentioned in the previous phase.
- In order to study the changes induced by the dyeing procedures in the original chemical composition of the plant extract, the second group was the wool samples dyed according to a medieval recipe with the extracts of the

4

dye sources in the first group.

- Aiming to understand the role of the dyeing procedure on the chemical profile of the yellow dyes, wool thread samples dyed by the skilled masters were acquired as the third group.

The mild extraction procedures [19,20] were performed for both the plants and the textiles to preserve the integrity of the yellow chromophore. The multi-analytical HPLC-DAD-MS technique analyzed the obtained extracts.

The combination of HPLC-DAD with mass spectrometry offers high sensitivity and selectivity, providing a database for identifying and characterizing flavonoid yellow dyes [21-23] (Scheme 3).
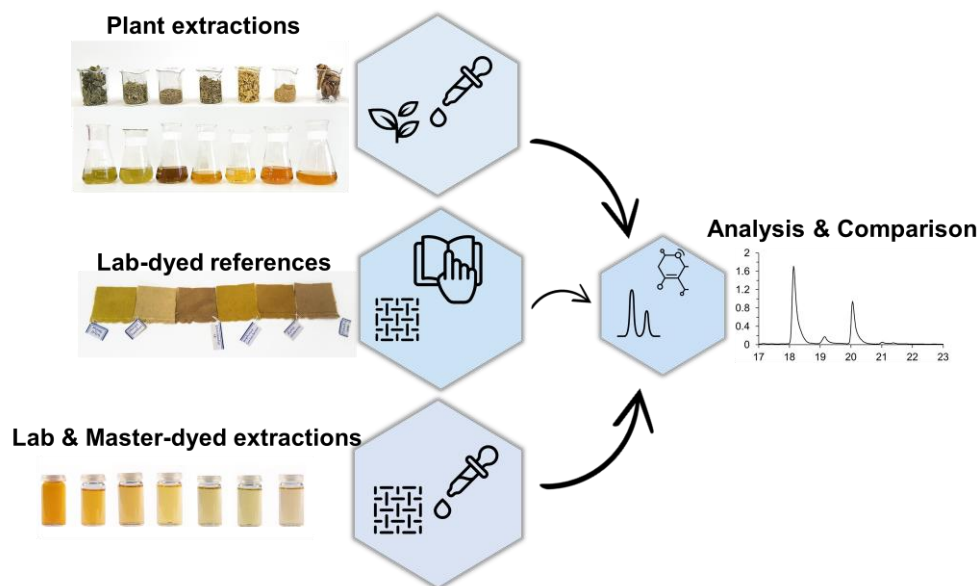
Scheme 3. The sample groups chosen in this research project for the HPLC-DAD-MS analysis.

Ultimately, to prove the credibility of our database, our chromatographic profiles were compared with the literature.

These results offer new markers for identifying yellow dye sources in Persian textiles and support the choice of stable chromophores by dye masters in the past [24] and present.

The spectral and chromatographic behavior of the dye molecules can change in the process of photoaging and mismatch with that of the standards. However, few studies

address all the necessary techniques required for the characterization of unknown degradation products.

In the third phase of this research, we highlighted the characterization of the photodegradation products, which act as markers for further analysis of the light faded natural yellow flavonoid dyes in historical textiles. For the first time in this work, we accurately quantified the relative stability of flavonoid yellows by calculating the quantum yield (ϕ_R) value [25]. The comparison of their relative stability delivers advanced knowledge toward the safety of dyed artworks. Flavonoid compounds in solution were irradiated by monochromatic light, and UV-VIS spectrophotometry provided the necessary data to calculate the ϕ_R values [26]. The photochemistry and overall reactivity of the flavonoids molecules were also addressed through a brief overview of their photophysics [27]. To investigate the effects of the environment on the stability of dyes, the monochromatic irradiation was also carried out in the proteinaceous gel to mimic the environment of the dyes in wool.

Photodegradation studies in less aggressive conditions produce an efficient total degradation of the molecules. However, to investigate the degradation mechanisms in faded artworks, polychromatic irradiation is suggested, which simulates natural aging mechanisms in shorter times [28]. Although the results may not be exactly the same as the degradation products, many intermediate and photodegradation products are in common.

In order to realize the degradation mechanism of the selected compounds, the identification of the degradation products is necessary [29]. In this regard, in addition to the HPLC-DAD-MS technique, HRMS/MS was also used to differentiate the same precursor ions that follow different fragmentation pathways, and different structure rearrangements (scheme 4).

6
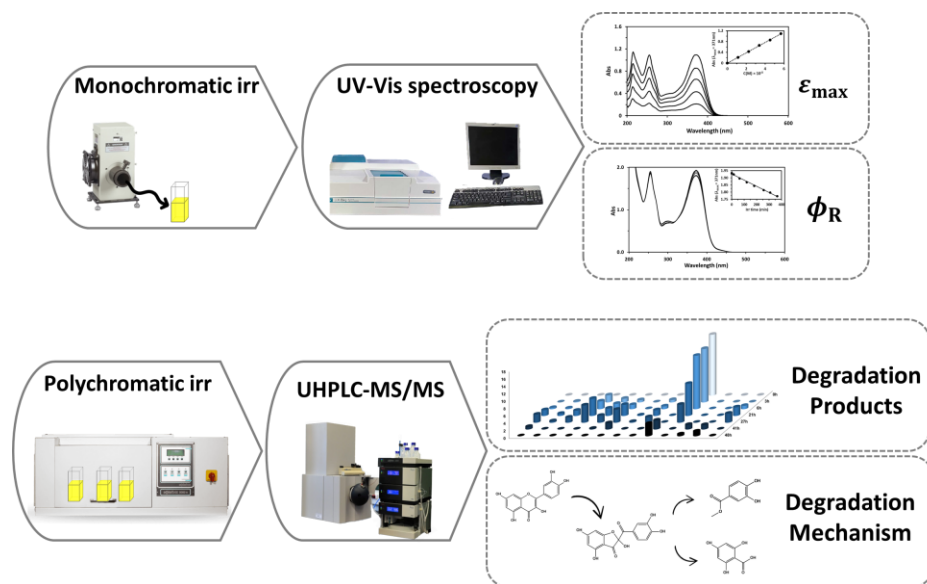
Scheme 4. The experiments carried out in this research project to study the stability of flavonoid yellows.

To prove the validity of the photochemical aging experiment, the results should follow the same degradation mechanism with the data acquired from the historical textile samples.

The accelerated aging study helps to understand the long-term behavior of historical textiles and evaluate their storage conditions. Hence, it provides significant data to develop preventive conservation strategies [30].

This doctoral work comprehensively studies the identification of biological yellow sources used to dye Persian carpets. This new insight may reveal important information about the chronology and the location, even the trade, and transport history of the ancient textiles.

The constructed database of HPLC-DAD retention times, UV-VIS spectra, along with the *m/z* values and fragment ions, offers detailed guidelines through a systematic analytical method.

The information gained from the photodegradation study can be applied within the conservation science to make the preventive plan improve the light stability of the dyed artworks, specially, historical Persian textiles.

References

1- Hallett, J. (2007). The knotted-pile carpet. In T. Pacheco Pereira & J. Hallett (Eds), *Carpets and paintings, 15th–18th centuries: the oriental carpet in Portugal* (pp. 23–30). Museu Nacional de Arte Antiga. ISBN 978-972-776-339-9

2-Heitor, M., Sousa, M., Melo, M. J., Hallett, J., Oliveira, M. C. (2007). The colors of the carpets. In T. Pacheco Pereira & J. Hallett (Eds), *Carpets and paintings, 15th–18th centuries: the oriental carpet in Portugal* (pp. 161-167). Museu Nacional de Arte Antiga. ISBN: 978-972-776-339-9

3- Armindo, E., Sousa, M., Melo, M. J., Hallett, J. A. (2008). A Persian carpet's paradise garden: discovering historical and technical aspects through carpet conservation and restoration. In J. Bridgland (Ed.), *The 15th triennial ICOM committee for conservation conference* (pp. 960-66). Allied Publishers Pvt. ISBN: 9788184243444

4- Santos, A. R. M. D. (2010). *The discovery of three lost 'Salting' carpets: science as a tool for revealing their history* [Master Thesis, New University of Lisbon]. NOVA University Repository. http://hdl.handle.net/10362/5146

5- Sharif, S., Nabais, P., Melo, M.J. (2021). Natural yellow dye sources in Persian carpets: a review. In J. Kirby (Ed.), *Dyes in History and Archaeology 35/36*. Archetype Publications. ISBN 9781909492813

6- Varzi, M. (1976). *The art and industry of carpet in Iran: an overview into history of dyeing, sketch and texture* (in Persian). Raz Publications.

7- Jahanshahi, V. (1996). *Process and methods of dyeing fibers with natural dyes* (in Persian). Scientific and Cultural Publications Co. ISBN 9646218008

8- Javidtash, I. (1996). *Dyeing method with plants and stability determination of 724 natural dyes* (in Persian). Research Institute of Forests and Rangelands.

9- Böhmer, H., Enez, N., Karadağ, R., Kwon, C., Fogelberg, L.E. (2002). *Koekboya: natural dyes and textiles, a color journey from Turkey to India and beyond* (L.E. Fogel-berg Trans.). REMHÖB-Verlag.

10- Cardon, D. (2007*). Natural dyes: sources, tradition, technology and science* (1st ed.) Archetype Publications. ISBN190498200X

11- Melo, M. J. (2009). History of natural dyes in the ancient Mediterranean world. In T. Bechtold, & R. Mussak (Eds.), *Handbook of Natural Colorants* (pp. 3–17), Wiley. Doi: 10.1002/9780470744970.ch1

12- Mouri, C., Mozaffarian, V., Zhang, X., & Laursen, R. (2014). Characterization of flavonols in plants used for textile dyeing and the significance of flavonol conjugates.

8

Dyes and Pigments, 100, 135-141. Doi: 10.1016/j.dyepig.2013.08.025

13- Ghahreman, A. (1978). *Flora of Iran* (vol. 7, 16, 20, 23), Research Institute of Forests and Rangelands.

14- Mozaffarian, V. (1996). *A dictionary of Iranian plant names: Latin, English, Persian*. Farhang e moaser. ISBN 9645545404

15- Mozaffarian, V. (2004). *Trees and shrubs of Iran* (in Persian). Farhang e moaser. ISBN 96486370302.

16- Sharif, S., Nabais, P., Melo, M. J., & Oliveira, M. C. (2020). Traditional yellow dyes used in the 21st century in central Iran: the knowledge of master dyers revealed by HPLC-DAD and UHPLC-HRMS/MS. *Molecules*, 25(4), 908. Doi: 10.3390/molecules25040908

17- Cuyckens, F., & Claeys, M. (2004). Mass spectrometry in the structural analysis of flavonoids. *Journal of Mass Spectrometry*, 39(4), 461-461. Doi: 10.1002/jms.622

18- Wouters, J. (1985). High-performance liquid chromatography of anthraquinones: analysis of plant and insect extracts and dyed textiles. *Studies in Conservation*, 30(3), 119. Doi: 10.2307/1505927

19- Zhang, X., & Laursen, R. A. (2005). Development of mild extraction methods for the Analysis of natural dyes in textiles of historical interest using LC-diode array detector-MS. *Analytical Chemistry*, 77(7), 2022-2025. Doi: 10.1021/ac048380k

20- Guinot, P., Andary, C. (2006, December 21-22). *Molecules involved in the dyeing process with flavonoids* [Conference presentation]. Dyes in History and Archaeology 25, Suceava, Romania.

21-Ferreira, E. S. B. (2001). New approaches towards the identification of yellow dyes in ancient textiles [Doctoral dissertation, University of Edinburgh]. University of Edin-burgh Repository. http://hdl.handle.net/1842/12020

22- Zhang, X., Boytner, R., Cabrera, J.S., Laursen, R. (2007). Identification of yellow dye types in pre-Columbian Andean textiles. *Analytical Chemistry*, 79, 1575-1582. Doi: 10.1021/ac061618f

23-Zhang, X., & Laursen, R. (2009). Application of LC–MS to the analysis of dyes in objects of historical interest. *International Journal of Mass Spectrometry*, 284(1-3), 108-114. Doi: 10.1016/j.ijms.2008.07.014

24- Zhang, X., Cardon, D., Cabrera, J. L., & Laursen, R. (2010). The role of glycosides in the light-stabilization of 3-hydroxyflavone (flavonol) dyes as revealed by HPLC. *Microchimica Acta*, 169(3-4), 327-334. Doi: 10.1007/s00604-010-0361-x

25- Melo, M. J., Ferreira, J. L., Parola, A. J., & Melo, J. S. (2016). Photochemistry for cultural heritage. G. Bergamini, S. Silvi (Eds.), *Applied photochemistry* (Vol. 92) (pp. 499-530). Springer, Cham. Doi: 10.1007/978-3-319-31671-0_13

26-Sousa, M. M., Miguel, C., Rodrigues, I., Parola, A. J., Pina, F., Melo, J. S., & Melo, M. J. (2008). A photochemical study on the blue dye indigo: from solution to ancient Andean textiles. *Photochemical & Photobiological Sciences*, 7(11), 1353. Doi: 10.1039/b809578g

27- Jørgensen, L. V., Cornett, C., Justesen, U., Skibsted, L. H., & Dragsted, L. O. (1998). Two-electron electrochemical oxidation of quercetin and kaempferol changes only the flavonoid C-ring. *Free Radical Research*, 29(4), 339-350. Doi: 10.1080/10715769800300381

28- Feller, R. L. (1995). *Accelerated aging: photochemical and thermal aspects*. Getty Publica-tions. ISBN 0892361255

29- Degano, I., Biesaga, M., Colombini, M. P., & Trojanowicz, M. (2011). Historical and archaeological textiles: An insight on degradation products of wool and silk yarns. *Journal of Chro-matography A*, 1218(34), 5837-5847. Doi: 10.1016/j.chroma.2011.06.095

30- Sharif, S., Nabais, P., Melo, M.J., Pina, F. and Oliveira, M.C. (2021). Photoreactivity and stability of flavonoid yellows used in cultural heritage. *Dyes and Pigments*, 110051. Doi: 10.1016/j.dyepig.2021.110051

Chapter 1. General introduction

Persian carpets have always been praised throughout history [1–3]. Given the fact that the organic nature of textiles is prone to deterioration, the oldest knotted textile regarded as the first carpet is the *Pazyryk* carpet, which dates to the 5th-4th century BC. A polychrome carpet with green, bright yellow, orange, and other shades of color [4]. After all the years, the rich and varied colors of this carpet prove the undeniable history of this art in Iran.

Color and design are two factors that have made Persian carpets unique. However, the long history of dyes and dyeing techniques in Iran lacks proper documentation, and the evidence of their recipes in the literature is hardly found. Two main reasons for the scarce information and documents about Persian dyes are the lack of formal knowledge in this context and the tradition of secrecy in the ancient eastern masters [5].

The earliest written evidence for textile dyeing in Iran can be found in the *Bundahishn* from the 9th century AD; one of the few references mentioned the application of saffron and turmeric as yellow dye sources for clothes dyeing [6].

The impressive natural dyes of Persia have been pointed out for many centuries; as an example, Richard Hakluyt, who traveled to Iran to learn the secrets of dyeing textiles, describes the colors of Persian carpet as "*so dyed as neither raine, wine nor yet vinegar can staine*" [7].

In his travel book [8], John Chardin describes Persian colors as rich, bright, and clear, not fading quickly. He also mentioned the pomegranate peel as a yellow dye source in Iran.

Nevertheless, by importing synthetic dyes to Iran, beginning in the middle of the Qajar dynasty (1789-1925), the exclusive presence of natural dyes in the Persian carpet was transformed [9]. It did not take long that the government defined some regulations to prevent the further application of these dyes in Persian carpets. This regulations booklet published in 1914 is considered the first historical Persian document about Persian carpets [10].

Even though the application of synthetic dyes never stopped, natural dyes as evidence of the authenticity of Persian carpets have been gaining increasing attention.

1- Yellow dye sources

Colors result from the absorption of specific wavelengths and the reflectance of the non-absorbed wavelengths in a dye molecule [11]. In general, colorants separate into two groups: pigments and dyes. Pigments are inorganic compounds that are insoluble in water and oil as their medium. In contrast, dyes are organic compounds that dissolve in a solvent. Additionally, dyes have the ability to penetrate the substrate they are applied to.

The chromophore and the auxochrome establish the structure of a dye where the former creates the color and the latter enriches it [12].
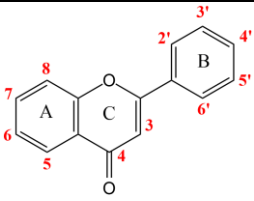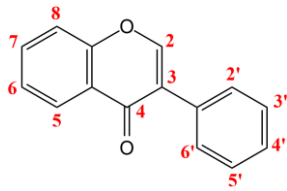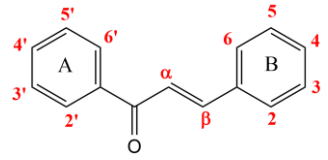
Yellow dyes are water-soluble, organic chemical structures, consisting of two larger categories, *flavonoids* and *carotenoids,* based on their chemical constitution [13].
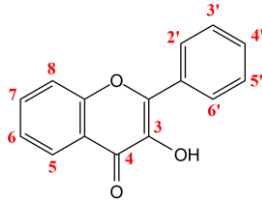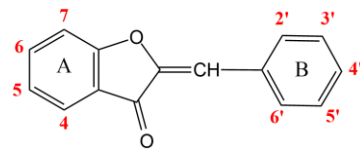
1.1 Flavonoid yellow dye sources

The most common flavonoids appear yellow in the natural environment of flowers [14]. Flavonoids are notable groups of polyphenolic compounds with a C_{15} (C_6-C_3-C_6) structural core. Their framework contains a chroman ring connected to the second aromatic ring at C-2 (flavone), C-3 (iso-flavone) or C-4 (neoflavone) positions [15]. These universal colorants have more than 8000 different structures [16].

Flavones, flavonols, flavanones, flavanols, chalcones, and aurones are typical examples of 12 classes that have been distinguished based on the oxidation level in the flavonoids' C-ring (Table 1) [15, 16]. The most common flavonoid chromophores in natural yellow dyes are flavones and flavonols [13, 17].

Table 1- The skeletons and numbering schemes for the main classes of flavonoids [24]

Flavone(a) Flavonol (b)	Isoflavone	Chalcone (a) Aurone (b)

Flavone(a) Flavonol (b)	Isoflavone	Chalcone (a) Aurone (b)
(b)		(b)
Luteolin, Apigenin (a) Kaempferol, Quercetin (b)	Genistein, Osajin, Auriculasin	Butein, Okanin (a) Sulfuretin, Leptosidin (b)

The presence or absence of the hydroxyl substituent in position 3 of the flavonoid molecule (or the protection of this position in the form of glycosides) defines their light sensitivity or resistance. This is why flavones and 3-*O*-substituted flavonols are less prone to degradation by oxidation and are used as dye sources [18]. The stability of flavonoids exposed to light will be discussed further in Chapter 4.

Flavonoid dye sources in plants are non-dominant compared to each other, and yellow dyes have been used from different local plant sources. Therefore, identifying these dye sources is important to achieve information about the origin of the textiles [18].

Flavonoids usually appear as *O*- or *C*-glycosides and as free aglycones in flowers, leaves, stems, or roots [16, 19–21]. However, in some cases when "low-temperature dried specimens" of *D. semibarbatum* and *Prangos* spp. have been analyzed, no aglycones were reported [22]. These compounds have been investigated widely during the last couple of decades (including [16, 19, 23–26]), and advances in molecular biology and also in analytical techniques have provided further information about their properties [24].

Flavonoids have been one of the main natural yellow, orange, and green (mixed with blue dyes) colorants in historical textiles. Still, they might have been degraded through time, complicating their identification process [14].

1.2 Non-flavonoid yellow dye sources

Several plants also produce non-flavonoid yellow dyes. They are fast and can be used directly to dye textiles, and the color obtained from them is considerably brighter

[18].

Carotenoid dyes with yellow and orange colors have been used in dyeing recipes for a long time. Saffron (*Crocus sativus* L.) is one of the most valued flowers globally, which makes its application on textile very uncommon [13, 14, 27]. However, the application of saffron was widespread in Persia in the Classical era [28]. Crocin, the gentiobiose diester of crocetin, is the main chromogen of saffron (Figure 1) [18].
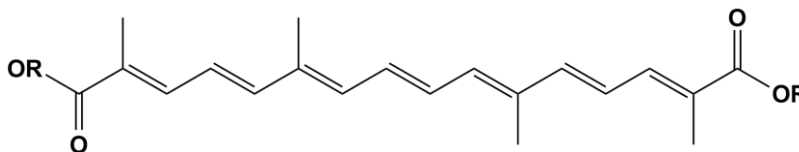
Figure 1- Structure of crocetin

2- Principles of dyeing technique

Persian carpets are usually made of silk and wool, the protein fibers which contain negatively -COO⁻ and positively -NH$_3^+$ groups. In the dyeing process, water should always be present as the diffusing agent of the dye molecules to the fibers [29].

According to the method they are applied to the textiles, natural dyes can be classified into mordant dyes and direct dyes.

Yellow dyes with plant sources are neutral and soluble in the water. They form metal complexes to bind them to the charged groups of molecules in the fibers. Metallic ions called mordants are incorporated to form bridges and convert the neutral molecules into positive complexes and bind them to the negative molecules of the fibers. This process is called mordant dyeing, which intensifies the color of the flavonoid chromophores and attaches them to the fibers [14, 27, 29].

The final color of the fiber depends on the type of mordant and is finalized only

16

after the mordanted fiber is treated with the dye molecules. Alum [1] is the most used mordant, but iron[2], copper[3], and tin[4] have also been applied [13]. Incorporating mordants with dye molecules increases the molecular weight, influences the extraction process and the absorption spectra [11].

The yellow carotenoid dyes like those from saffron are direct dyes that can easily bind to the protein fibers of the textiles without the use of mordants. The process is called non-ionic direct dyeing. There is usually a weaker affinity between the dyes and the fiber molecules in direct dyes [14, 29]. They yield brighter yellows and poor fastness [13].

2.1 Dyeing techniques

The dyeing method is important for outlining the amount of dye components retained in the textiles. These methods have been mostly passed on by word-of-mouth between generations and might reveal the social and cultural understanding [11].

Knowing and recreating the materials and techniques of the original recipes is a complex part of studying a historical artifact. The better this is done; the more detailed chemical information and standard data can be produced. Analytical investigations and manuscripts can provide enough data to relate a historical artifact to its period [29]. The HART methodology[5] applies the same logic to study the technical information about the sources in the documents, reconstruct historical materials, characterize and compare historical samples with the reconstructed simulations to analyze historical artworks [12]. Such approaches toward analyzing historical dyes have inspired studying undocumented recipes from workshops of Iran and other previously documented ones in the Persian reference collections (Table 2).

---

[1] A group of salts usually consisting of aluminum and another sulphate with hydration water. The most important alums are aluminium potassium sulphate [$Al_2(SO_4)_3.K_2SO_4.24H_2O$], aluminium ammonium sulphate, and aluminium sodium sulphate [13] .
[2] Ferrous sulfate [$FeSO_4$]
[3] Copper sulfate [$CuSO_4$]
[4] Stannous chloride [$SnCl_2$]
[5] The HART (Historically Accurate Reconstruction Techniques) methodology is a three-part model. It produces the reference materials with the maximum possible historical accuracy. This method also evaluates the condition and the original appearance of the artworks [12]

A list of the most common yellow dye plants that have been reported in Persian literature is described briefly in Appendix 1- section A1.1.

Many yellow dye sources are familiar in the neighboring countries of Iran. According to [17], the best-known yellow dye plants still being used in countries such as Turkey are weld, yellow larkspur, pomegranate, saffron, wild pistachio, and wine grape.

Table 2- Carpet dyeing recipes according to Persian literature

Dye source (colorant part)	Final color	Mordant	Additive	Thread	Mordanting	liquor ratio[6]	Reference
Pomegranate (rind)	Yellow	None	Sodium carbonate (2 gr)	Wool (1000 gr)	It doesn't need mordant, although alum or tin can be used.	40% L:R= 40:1	[31, 32, 33]
	Recipe: 1- Add dye at 40°C; 2- Increase the heat to 90°C for 30 min; 3- Remain at 90°C for 60 min. Considerations: it can create yellow to orange combined with *Reseda luteola*; it makes dark yellow without mordant.						
Turmeric (root)	Yellow to orange	Alum	Oxalic acid (10 gr)	Wool (1000 gr)	• Heat the solution of water and alum (45°C); • Add the wool fibers and heat the mixture for 30 min (90°C).	2-10% (light to dark yellow L:R= 40:1	[5, 31, 34]
	Recipe: 1- Add dye at 30°C; 2- Increase the heat to 60°C for 15 min; 3- Remain at 60°C for 90 min. Considerations: it can create yellow to orange combined with *Reseda luteola*; it makes dark yellow without mordant.						
Weld (flower, leave, and stem)	Bright yellow to orange	Alum (20gr)		Wool (1000 gr)	• Heat the solution of water and alum (70°C); • Add the wool fibers and heat the mixture again (90°C).	40% L/R = 30:1	[32, 34]
	Recipe: 1- Soak dyes in cold water for 6h; 2- Add to the dyebath in 60-70°C and continue (2h)						
		Potassium dichromate (50 gr)	Baking soda (10 gr)	Wool (1000 gr)	• Pour the chrome into 30°C water; • Add baking soda gradually; • Heat for 30 min (60°C); • Add the wool fibers and seal the lid (20 min).	40% L:R= 30:1	
	Recipe: 1- Soak dyes in cold water for 6h; 2- Add to the dye bath at 70°C and continue (1h); 3- Reduce the temperature slowly. A solution of water, soap, and bran for 20 min brighten the color.						
Grape tree (vine) (leave)	Yellow	Alum (20gr)		Wool (1000 gr)	• Heat the solution of water and alum; • Add the wool fibers and heat for 30 min at 80°C; • Reduce the temperature slowly.	75% L:R= 20:1	[32, 33]
	Recipe: 1- Add the solution (water + leaves powder) to the dyebath; 2- Heat the dyebath and add the mordanted wool at 70°C; 3- Continue at 80°C (30 min); 4- Reduce the temperature slowly. The dyed wools should be dried in the shadow.						
Onion	Red onion:	Alum	At step 2:	Wool	• Add alum to semi-warm water;	50% in step 1	[32, 34]

---

[6] Liquor ratio (L:R) compares the weight of the dry material being dyed to the water weight of the dyebath and is described as a ratio.

Dye source (colorant part)	Final color	Mordant	Additive	Thread	Mordanting	liquor ratio[6]	Reference
(skin)	yellow and orange	(10 gr)	salt (20 gr) sumac (10 gr)	(1000 gr)	• Add the wool and heat (70°C) for 30 min; • Reduce the temperature slowly; • Wash the mordanted wools.	and 70% in Step 2	
	Yellow onion: yellow and dark green	chrome				L:R= 15:1 to 20:1	

Recipe: Step 1: 1- Blend the peels in semi-warm water (30 min); 2- Mild heat (20 min); 3- Add the mordanted wools; 4- Heat to reach the boiling point (2h); 5- Stir the mixture every 10 min; 6- Keep it at the boiling point (2h); 7- Bring out the wools and put them in the air to dry.
Step 2: 1- Stir the peels in semi-warm water (30 min); 2- Mild heat (20 min); 3- Add the salt and sumac; 4- Heat to reach the boiling point (1h); 5- Add the wools (from step 1) gradually; 6- Heat to reach the boiling point (2h); 7- Stir the mixture continuously; 8- Bring out the wools and put them in the air to dry.

Dye source (colorant part)	Final color	Mordant	Additive	Thread	Mordanting	liquor ratio[6]	Reference
Chamomile (flower and stem)	Yellow	Alum/ chrome/ iron sulfate (2 gr)		Wool (1000 gr)	• Add iron sulfate to bath at 70°C; • Heat to reach 90°C; • Add the wool and keep the temperature for 15 min; • Reduce the temperature slowly; • Wash the mordanted wools and dry in the shadow.	75% L:R= 20:1 to 30:1	[32]

Recipe: 1- Boil the powder (1h); 2- Add it to the dyebath and increase the temperature to 70°C; 3- Add the mordanted wool and continue heating at 80 °C (1h); 4- Stir the wools continuously. A solution of water, soap, and bran for 20 min brighten the color.

Dye source (colorant part)	Final color	Mordant	Additive	Thread	Mordanting	liquor ratio[6]	Reference
White mulberry (leave)	Yellow to orange	Alum (10 gr)	Sodium hydroxide	Wool (1000 gr)	• Add the wool fibers at 70°C; • Heat to reach 80°C; • Keep the temperature for 30 min; • Reduce the temperature slowly; • Wash the mordanted wools with cold to semi-warm water.	75% L:R= 15:1 to 20:1	[32, 34]

Recipe: Step 1: 1- Add the powdered leaves and the mordanted fibers to the dyebath and heat to 80°C (30 min); 2- Continue for more 10 min; 3- Pull out the fibers.
Step 2: 1- Continue the dyeing at 80°C (70 min); 2- Reduce the temperature slowly and dry at the shadow

Dye source (colorant part)	Final color	Mordant	Additive	Thread	Mordanting	liquor ratio[6]	Reference
Safflower (flower)	Yellow	Alum (10 gr)		Silk (1000 gr)	• Heat the bath and add alum; • Add the silk fibers at 70°C; • Heat at 70°C for 1h; • Reduce the temperature slowly wash	75% L:R= 20:1 to 30:1	[32]

Dye source (colorant part)	Final color	Mordant	Additive	Thread	Mordanting	liquor ratio[6]	Reference
					the mordanted silk.		
	Recipe: 1- Boil the blossoms (1h) and add to the dyebath; 2- Add the mordanted silks at 70°C and continue (1h); 3- Reduce the temperature slowly and dry at the shadow. A solution of water, soap, and bran for 20 min brightens the color						
Fig tree (leave)	Crystal lemon	Alum (20 gr)		Wool (1000 gr)	• Heat the bath and add alum; • Add the wool fibers at 50°C; • Heat at 90°C for 40 min; • Reduce the temperature slowly and keep the fibers wet.	75% L:R= 15:1 to 20:1	[32]
	Recipe: 1- Heat the dyebath (70°C); 2- Add the mordanted wool after 30 min and heat to 90°C and continue (1h); 3- Stop heating and expose the fibers to air and dry them.						
Desert rod (flower)	Yellow, orange	Calcium hydroxide (10 gr)		Wool (1000 gr)	• Heat the bath and add mordant at 60°C, and heat more (70°C); • Add the wool fibers at 70°C (30 min); • Reduce the temperature slowly and keep the fibers wet.	75% L:R= 15:1 to 20:1	[32]
	Recipe: 1- Heat the dyebath (70°C) and add the dye and stir (30 min); 2- Heat to reach 80°C (30 min); 3- Add the mordanted wool and continue at 80 °C (70 min); 4- Stop heating and let the fibers cool down and dry them in the shadow, then rewash them. A solution of water, soap, and bran for 20 min brighten the color.						
Oak tree (middle skin between the fruit wall and the seed [testa])	Yellow, dark yellow, golden	None		Wool (1000 gr)	It does not need mordant, although chrome or aluminum sulfate can be used.	40% L:R= 20:1 to 30:1	[5, 32, 34]
	Recipe: 1- Add the dye and heat the dyebath (70°C); 2- Add the wool and increase the temperature to 90°C (1h); 3- Stop heating and let the dyebath in this state (30 min); 4- Let the fibers cool down and dry them in the shadow.						
Yellow larkspur (flower)	Yellow	Alum (100 gr)		Wool (1000 gr)	After mordanting, it is appropriately washed with water and dried.	3% L:R= 75:1	Banitaba, H. (Personal communication, August 12, 2019).
	Recipe: 1- Boil the dye in the water for 30 min; 2- Add more water to cool it down to 70°C; 3- add the mordanted wool fibers with another extra 5% of alum to the mixture; 4- Heat again to the boiling point and stir it for 1h; 5- Turn off the heat and let it rest for 10h to 12h. Add a small piece of walnut's green shell to the dyebath for more color stability. To change the hue color, madder and pomegranate can be added to the dye bath along with larkspur.						
Saffron (flower)	Yellow to orange	Alum	Oxalic acid (10 gr)	Silk (1000 gr)	• Heat the solution of water and alum; (45°C); • Add the wool fibers and heat the mixture for 30 min (90°C).	2-10% (light to dark yellow L:R= 40:1	[5]

Dye source (colorant part)	Final color	Mordant	Additive	Thread	Mordanting	liquor ratio[6]	Reference

Recipe: 1- Add dye at 30°C; 2- Increase the heat to 90°C during 15 min; 3- Remain at 90°C for 100 min.

3- Analytical techniques for characterization of flavonoid dyes

Several factors influence the precision of identification of historical textiles; the amount of sample, the deterioration process, and the previous effects of the storage environment are among these factors [35]. Historical evidence about dyeing recipes, along with complementary information of their trade and transport history, can help clarify the dyeing process. At the same time, chemical analysis can reveal the identity of the dye sources, the probable origin of historical textiles, and the past restoration practices. Hence, analytical chemistry and identification of natural dyes provide helpful information for historical, conservation, and archaeological studies.

There are different physical-chemistry techniques to characterize yellow dyes. However, simple chemical examinations or even infrared spectroscopy cannot usually characterize the compound and structure of the dyes in fabric [36]. It has been a big challenge for researchers to identify the exact dye sources; various techniques have been developed during the last decades that are briefly discussed in the following.

3.1 In-situ spectrophotometric techniques

Techniques such as reflectance and fluorescence spectroscopy have a major advantage in identifying dyes in historical textiles. They do not require the removal of samples and therefore do not damage the object. These methods are often used for the initial analysis of the dyes. They may even provide enough information to detect them or bring diagnostic data without destroying the fibers [37, 38, 39].

3.1.1 UV-VIS fluorescence spectroscopy

A good emission quantum yield of the molecules in organic dyes indicates that the application of the fluorescence spectroscopy method can be beneficial [40]. The excitation and the emission spectra help the further investigation of the organic dyes in historical samples [39, 41].

In a microspectrofluorimeter, a xenon lamp is used to create a spectrum from UV to near IR. It directs the excitation beams to the sample dyes, and its fluorescence

is directed back into the microscope [30, 39].

Microspectrofluorometry has proper reproducibility, high *S/N*, and fast data acquisition. Its spatial resolution helps in-depth profiling of the complex aged samples [30, 42].

Although the quality and efficiency of the emission quantum yield play an important role in adequately detecting the dyes. In this regard, the surrounding medium of the dyes affects the fluorescence emission of the molecules, creating a major challenge for identifying the historical dyed textiles [30]. This has led to very few complete fluorescence spectroscopy studies of dyed textiles (see, for example, [30, 39]). However, it has been widely used to identify anthraquinone colorants and their origins in lake pigments [30, 42].

3.1.2 UV-VIS reflectance spectroscopy

The illumination of materials and the capture of the reflected light is the primary detection element in the reflectance spectroscopy method [43]. Whether it is applied in a multi-analytical technique or independently, reflectance spectroscopy offers simple and useful results. It compares the variations and reflection extremes of an unknown sample with those of recognized ones [44]. Nevertheless, reflectance spectroscopy has had limited application for dyed textiles with low concentrations [44, 45], and most studies have focused on the analysis of spectra from paints and pigments [43, 46, 47].

However, there have already been many references to show the effectiveness of the fiber optics reflectance spectroscopy (FORS) as an inexpensive method for the screening or routine analysis of dyes in historical textiles [37, 39, 48–50].

FORS can support most of the visible and parts of the infrared regions in the range between 400 to 1655 nm [43]. It is a proper in-situ tool that is not affected by environmental light without a shield, and its probe does not need to touch the object [37]. However, this technique is not very selective for the different yellow dyes, many of which have the same chromophore [29, 37, 43, 50].

24

VIS-FORS does not provide satisfactory results to differentiate curcumin and flavonoid yellows in some cases. This happens when the spectra of yellow dyes and the wool fibers partially overlap, or the colors are of extreme paleness or intensity [51].

Even if in-situ spectrophotometric techniques cannot completely characterize the yellow dyestuff, their diagnostic purposes offer a useful preliminary tool to examine a large set of points on the textile. They provide their first interpretation and results in a short time and enable greater precision and significance when choosing areas for micro-sample acquisitions. In other words, they have exploratory applications for the multi-analytical techniques. They can also provide complementary knowledge about the changes in the chromatic and spectral behavior of materials during cleaning or treatment procedures and monitor the conditions of the objects against time [52, 53].

3.1.3 Surface enhanced Raman spectroscopy (SERS) and vibrational spectroscopy

Vibrational spectroscopy techniques determine the energy level from the vibration of chemical bonds [46].

Researchers have benefitted from SERS to identify natural organic dyes for many years. This non-separative technique requires only microscopic samples [54, 55]. However, some limitations restrict the analytical applications of this technique for the identification of historical dyes. The SERS spectrum is sensitive to chemical and instrumental variables; also, apart from target analytes, other compounds can have an affinity for SERS substrates and enhance the Raman signals [52, 56].

A general problem with all these spectroscopic techniques is that they do not allow for the separation of the dye components in the sample and provide little information about components with similar structures [11].

3.2 Micro-sampling separation techniques

In general, certain minor components can reveal the identity of the plant yellow dye sources [11]. These compounds are provided within complex mixtures in samples with very low amounts. The sensitivity and selectivity of the identification methods and efficiency of the separation technique are important for yellow flavonoid dyes because of

their limited quantity of samples in the textiles [52].

3.2.1 High-Performance Liquid Chromatography with Diode Array Detector (HPLC-DAD)

In the 1980s, High-performance liquid chromatography was applied for the first time to analyze dye extracts [57]. Since then, HPLC has been applied consistently to identify natural dyes in historical textiles.

In combination with appropriate detection devices, HPLC has the potential to separate, identify, and characterize components of the dye sources. This technique is now the most widely used method based on its successful analytical record, especially when distinguishing between different sources of yellow dyes with close chemical structure is difficult [58].

The separation of flavonoids in the chromatographic system depends on the mobile and stationary phases [11]. The analytes are soluble in the mobile phase, which is more polar than the stationary phase. Octyl (C8) or octadecyl (C18) reversed-phase (RP) are the most common columns for the separation of flavones, flavonols, and their glycosides. The stationary phase in these cases is a silica gel bead to which is bonded n-octyl or n-octadecyl groups [29, 59].

Proper elution time and resolution are the results of the selected gradient elution method (isocratic or gradient). A better separation is generally achieved with a gradient elution method than isocratic elution. Mixtures of methanol or acetonitrile with water are generally the best mobile phases for separating flavonoid dyes by RP-HPLC [29].

Adding limited amounts of a volatile acid—usually formic acid—to the mobile phases promotes the ionization of molecules in HPLC-MS [59].

As an advanced liquid chromatography technique, ultrahigh performance liquid chromatography (UHPLC) has improved HPLC detection limits for components in complex mixtures.

The smaller column particle size in most UHPLC has enhanced the resolution and improved limits of detection that lead to detecting minor dye components [52]. Additionally, the lower flow rate in UPLC, which means less solvent is used, provides economic and environment-friendly advantages for this method [60, 61].

26

Studying the flavonoids and dyes by HPLC demands a proper selection of the detectors [62].

HPLC-DAD identifies compounds based on the retention time of major peaks in chromatograms and comparison with the UV-VIS spectra. This leads to the detection of flavonoid dye sources in association with the known reference dye sources.

Retention time (RT or t_R) is the period between the injection of the sample and the detection of its components. It illustrates when the compounds have eluted from the column and can be compared with known reference samples [13]. However, the co-elution of the components makes their identification difficult by RT alone [11].

The chromatographic retention times on the hydrophobic C18-RP columns show that more polar compounds are eluted first [48]. It also highlights the increase of RT that goes along with a decrease of glycosylation in flavonols. Although the role of glycosylation's position on the retention time cannot be ignored [29], as for the saccharide residues, disaccharide rutinosides elute first. The order of elution for the monosaccharides is galactosides or glucosides, then arabinosides, and rhamnosides, respectively [59].

Diode array detectors (DAD) measure energy absorption in the 200-700 nm UV-VIS range. Since yellow dyes show strong absorption in the UV region, DAD can give information about their type of aglycone [13, 59].

The absorption spectra of most flavonoids are made of two characteristic bands, band I (300–440 nm) and band II (240–295 nm) that are attributed to the B-ring (cinnamoyl system) and A–ring (benzoyl system), respectively [63] (Figure 2 and Table 3).

The absorption maximum is influenced by adding functional groups to the aromatic chromophores, such as flavones and flavonols. The absorption bands shift to the longer wavelengths with an increase in oxygenation level. On the other hand, the methylation or glycosylation of 3-, 5- or 4' -hydroxyl group on the flavone or flavonol nucleus shifts it to shorter wavelengths [64] (See Appendix 1- section A1.2.).

Maximal absorption of most yellow compounds is about 350 nm, and monitoring yellow dyes at this wavelength offers the best selectivity and sensitivity [13, 29, 66, 67]. However, monitoring HPLC profiles at 350 nm sometimes shows peaks corresponding to non-colored compounds. Non-flavonoid peaks typically have masses of 354 Da, 516

Da or 336 Da and can be monitored in the range of 215-240 nm. As an example, chlorogenic acids (λ_{max}= 324 nm; mass= 354 Da) may be found in plant extracts and even in dyed wool or silk specimens.
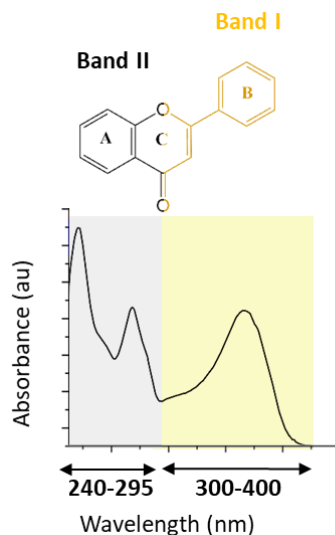
Figure 2- Classification of UV absorption bands in flavonoids [65]

Table 3- Band I & II in the UV spectra of some main classes of flavonoids [63]

Flavonoid	Band II	Band I
Flavones	240-285	304-350
Flavonols	240-285	352-385
Flavanones	270-295	303-304
Chalcones	220-270	340-390
Aurones		370-430

Analyzing the peaks in a chromatogram helps distinguish eluted compounds from the non-dye molecules or the degradation products. The injection peak is the first peak in a typical chromatogram, involving the compounds which are not usually dyestuffs [13]. In these cases, there might be a mixture of unknown compounds, treatment effects on the artifact, or deterioration products that affect the selectivity of the HPLC technique in the identification process of the dyed textiles [52].

Although DAD is a useful tool for the characterization and quantitative analysis of yellow components [35], as most flavonoids have a similar UV-VIS spectrum, it is not possible to identify flavonoid compounds with high certainty. Especially minor ones might fail to be identified- unless one has reference compounds for every possibility.

28

3.2.2 Mass spectrometry

Mass spectrometry began to be used to study the structure of natural dyes in historic textiles in the early 2000s [68]. This technique allows one to analyze organic compounds based on molecular mass, fragmentation patterns [52, 69, 70].

The MS detector is easily adapted to the HPLC technique and helps analyze the complex mixtures. This technique needs lower concentrations of chromophores with microgram-size samples due to its high selectivity and sensitivity [53]. In aging studies, HPLC-MS can reveal information to identify degradation products as a subset of unknown compounds without the existence of reference samples [52, 53]. Consequently, it is advantageous for the characterization of yellow dye sources and is quite helpful for studying aged historical textiles.

Two main functional elements are important for MS detection— the source that generates the ions and the analyzer that separates them will be discussed in the following.

3.2.2.1 Ion source

The analytes are ionized in the ion sources before analysis in the mass spectrometer. The internal energy transferred during the ionization process and the physical-chemical properties of the analyte that can be ionized are typical considerations when choosing the ionization technique [71].

Atmospheric Pressure Ionization (API) techniques are generally used with the HPLC method [72]. API nebulizes the column eluent from the HPLC, either by a heated nebulizer or an electrical field under atmospheric pressure. The former is done by the atmospheric pressure chemical ionization (APCI) and the latter by the Electrospray Ionization (ESI) [24, 73].

ESI has the highest sensitivity among different types of ion sources for flavonoids that are polar and have low molecular weight [62, 71, 75] (Table 4).

Table 4- Advantages and disadvantages of ESI ion source [71]

Ion Source	Electrospray (ESI)
Advantage	Effectively ionizes polar (non-volatile) compounds, < 100 Da to > 10^6 Da; Soft ionization often gives only adduct species; Compatible with HPLC; Applicable to noncovalent interactions;
Disadvantage	The efficiency of ionization depends on the polarity

In the ESI ion source, the solution passes through a capillary needle. An electrical charge (positive or negative) at the end of the needle nebulizes the solution and sprays it as droplets with the help of a high-velocity flow of N_2 gas. The droplets get smaller due to evaporative processes and capture positive or negative electrical charge on their surface and form $[M+H]^+$ or $[M-H]^-$ ions which then enter the mass analyzer [24, 72–74].

3.2.2.2 Mass analyzer

A mass analyzer is the mass spectrometer component that takes ionized molecules and separates them according to their *m/z* (mass to charge ratio) values. The mass analyzer measures the *m/z* value and isolates precursor ions created in the ion source to give the product ions. There are two main characteristics for measuring the performance of a mass analyzer; the resolution (the ability of a mass analyzer to yield distinct signals for two ions with a small *m/z* difference) and the mass accuracy (the difference between the exact and the measured *m/z* values) often expressed in parts per million (ppm).

In a Quadrupole Ion-Trap (QIT) mass analyzer, the ions are trapped and separated by an electric field one at a time according to their mass [74, 76]. This analyzer is a low-resolution device that separates ions in a three-dimensional radio frequency quadrupole field [76, 77]. It measures the *m/z* ratio but cannot express the constitution of the particular ions [76]. Specifically, isobaric ions will not be separated in low-resolution analyzers. These ions have the same nominal mass but different empirical formulas and thus different monoisotopic masses [71].

In a Time-of-Flight (TOF) mass analyzer, the ions of all *m/z* ratios are dispersed into the analyzer at a certain time while traversing in their field-free path. The accurate determination of their *m/z* ratios depends on the resolving power of the mass analyzer [72, 76,

30

77]. This analyzer is fast, simple, and possesses high resolution [76] (Table 5).

Table 5- Instrument performance according to mass analyzer type [71]

Mass Analyzer	Resolution	Accu-racy	Measurable m/z	Benefits	Limitations	Cost
Quadrupole ion trap (QIT)	Low	Low	Limited	Selected ion monitoring	Nominal mass only; time-con-suming	Cost-effi-cient
Time of Flight (TOF)	High	Precise	Unlimited mass range	Rapid acquisi-tion of spectra at high resolu-tion	No selected ion monitoring	More expensive

The soft ionization techniques (ESI, API) provide molecular weight information but cannot solely reveal the structure of natural dyes; therefore, the fragmentation pathways should also be obtained through the use of multi-analyzer mass spectrometers [24, 79]. Tandem mass spectrometry can provide helpful structural information by combining two or more analyzers within a single instrument to improve and extend analytical capabilities. Basically, a tandem mass spectrometer can be conceived in two ways: a *tandem in space* by coupling two physically distinct analyzers, or *tandem in time* by performing an appropriate sequence of events in an ion storage analyzer. The space combinations may involve mixed analyzer types (hybrid) as in a QTOF instrument, allowing MS/MS experiments [71]. The experiments in time can be achieved through time separation with ion trap devices, programming different steps that are successively carried out in the same mass analyzer, given MS$^{(n)}$ spectra.

Collision-induced dissociation (CID) can be applied since the soft-ionization methods do not produce several fragments. CID is the most commonly—used activation method to create fragment ions either at the in-source CID or in combination with tandem MS experiments. The MS/MS data can be achieved when an isolated precursor ion with a particular m/z is trapped and excited using a neutral gas [24, 78].

In tandem mass spectrometers, the precursor ions pass through a collision gas to gain sufficient energy to induce fragmentation [74]. This technique conducts two mass separations (MS-MS); the first operation isolates the precursor ion and is mainly applied to select specific ions arriving from the ion source; it also accelerates those ions to gain enough kinetic energy to enter the CID cell. These ions undergo the CID processes. The

second operation is to analyze the product ions and determine the *m/z* of the fragment ions formed [71].

QIT and TOF have been applied as mass analyzers in tandem mass spectrometry for the separation of dye molecules. The generation of the CID process in these two systems is different, so the MS/MS database cannot be exchanged between them. TOF provides better observation for the C-ring cleavage and accurate mass measurements of all MS/MS fragments. QIT, on the other hand, favors the losses of small molecules and helps to show fragmentation pathways [24].

Quadrupole Time of Flight (QTOF) transmitting devices follow the space concept of tandem mass spectrometry for MS/MS. Two separated analyzers may be mounted consecutively in QTOF. The first analyzer (quadrupole) is mainly used to select the precursor ions which are passed into the collision cell. The fragments formed in the CID cell, then, are transferred to the second analyzer (TOF). In TOF, they are separated according to their accurate *m/z* values yielding the high-resolution MS/MS spectrum. Different scan modes and MS experiments can be performed depending on the mass analyzer [71].

The type of mass analyzer cannot influence the fragmentation paths of dye molecules. However, it significantly changes the relative abundances of fragment ions. Hence, the most critical factor to consider while choosing the methods is their ability to detect the presence or absence of distinctive fragment ions for the isomeric compounds [70].

The analyte and the type of favored data determine the preferred level of kinetic energy needed for the ions. Too low energy may prevent the generation of the beneficial spectra, and too high energy may yield consecutive reactions and loss of information [78]. The original accelerating voltage and the collision gas type, and its pressure determine the nature and degree of fragmentation [71].

The inherent sensitivity, resolution, and rapid data acquisition of QTOF analyzers are major HPLC-MS/MS analysis assets.

4- Characterization of yellow dyes by HPLC-MS/MS: The interpretation of MS data

In HPLC-MS/MS method, ESI ionizes polar compounds effectively; therefore, both the molecular mass and fragmentation provide information for the identification of dyes.

The data of the MS[2] (and MS[3]) spectra of yellow dyes and the detection of the fragmentation ions provide important structural information to identify unknown compounds of dye sources [21, 24, 52, 65].

The creation of positive or negative ions helps identify polar flavonoid compounds extracted from textiles [65]. As most of the flavonoids are phenols, their mass spectral data in negative ion mode leads to a limited fragmentation [59], providing the largest parent ion [M-1]$^-$ and simplest overall spectrum [29]. It yields the molecular mass of the individual flavonoids, provides additional information after separation, and has high sensitivity, even when the concentration is low [59]. The negative mode can reveal anions in the fragmentation pathways and supplement structural information about flavonoid aglycones [20, 79]. Additionally, the interferences of the sample matrix are less effective on the negative ion mode [35].

Nevertheless, positive ion MS/MS spectra can reveal more fragments providing complementary information to confirm the identity of the flavonoid aglycones and clear the ambiguities [78].

In general, the diagnostic of the positive ion mode cannot provide all the information seen in the negative ion mode. Therefore, the structural information of the negative and positive modes is complimentary; some researchers use both fragmentations to characterize flavonoid aglycones [20].

Yellow dyes can be identified based on many important factors, including the characterization of the nature of the aglycone and its glycosylation state, the sequence of substituents attached to the aglycone, and their type [59]. Mass spectrometry provides detailed guidelines to identify and differentiate yellow dyes (Figure 3). For the detailed description, see Appendix 1- section A1.3.
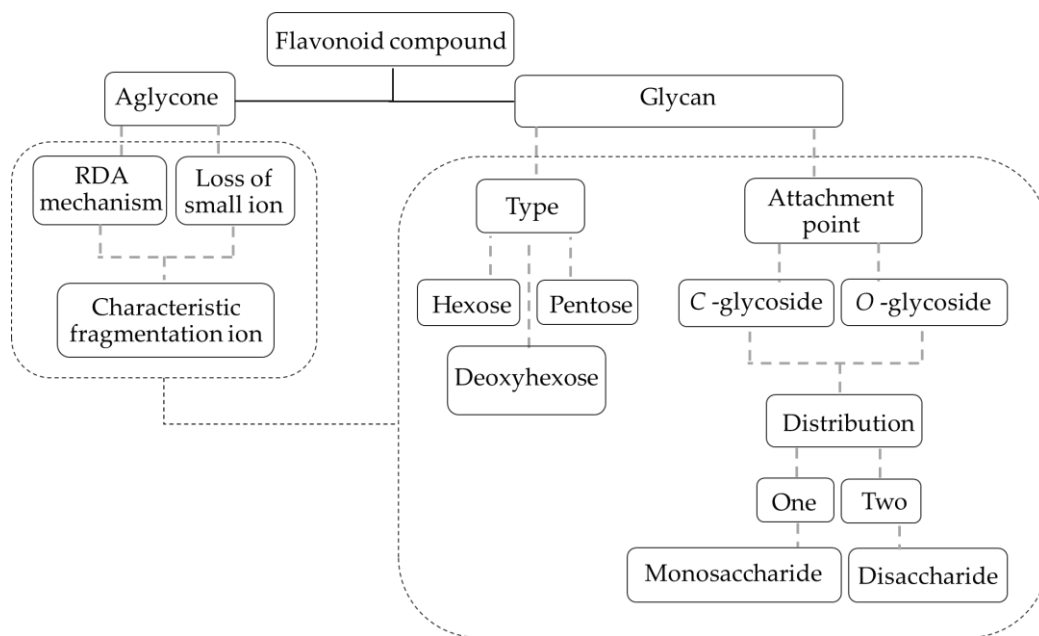
Figure 3- Methodology for mass spectrometric interpretation of dye components [21, 59]

Natural dyestuffs have complicated structures, and different compounds with various proportions participate in particular types of plants in diverse locations. Therefore, having reference samples and libraries is necessary to identify specific yellow dye sources. Following the same dyeing recipes for textiles helps create reliable reference libraries to characterize dye sources in historical textiles [13].

QIT-MS$^{(n)}$ and Q-TOF high-resolution MS/MS work as complementary techniques that provide sufficiently comprehensive data with a high degree of confidence to characterize dyes based on their detailed interpretation of the CID MS/MS spectra. IT-MS$^{(n)}$ reveals the fragmentation pathways, and Q-TOF determines the molecular formula of specific compounds [78].

For the known compounds, the standards and libraries are used to compare and confirm the identified dye sources. Structural information and molecular mass are used to determine the possible natural yellow dye source [29] (Figure 4).

34
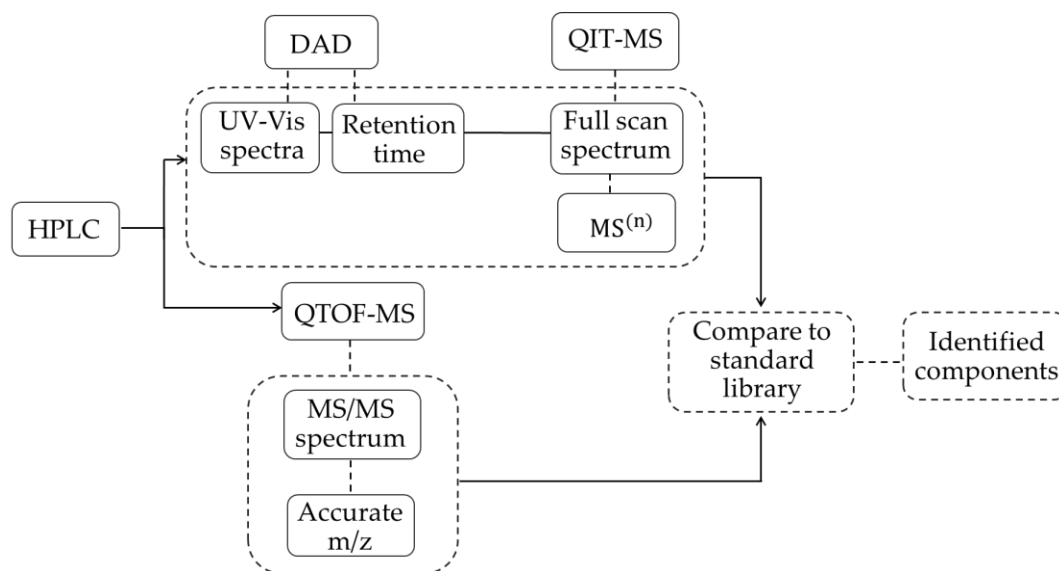
Figure 4- Strategy followed in this study to identify dye compounds

5- Extraction techniques

The high sensitivity of recent separation methods allows the extraction of thread samples in the ranges of µm in particle size, µg in mass, and/or mm in length (for examples, see [18, 36, 61, 83–89]). The solvent, extraction temperature, and pH are important factors that influence the extracted dyes [90].

To destroy the complexation of natural dyes with their mordants in the fibers, a chelation agent is needed. It neutralizes the dye molecules in the complex so that the extraction of the dye molecules by using water or some organic solvents could be possible. Water, as a polar solvent, penetrates the polar fibers. This process can benefit from the heat [29]. One of the reasons why little research was done on yellow dyestuffs is that by using strongly acidic conditions (as chelation agent), the extraction of dye molecules leads to hydrolysis of glycosides and thus the loss of valuable information [29, 91]. Conversely, by introducing weak acids, such as formic acid, or chelators, such as oxalic acid, mild (soft) extraction methods were introduced that prevented the problems presented by harsh extraction methods [92] (Figure 5).
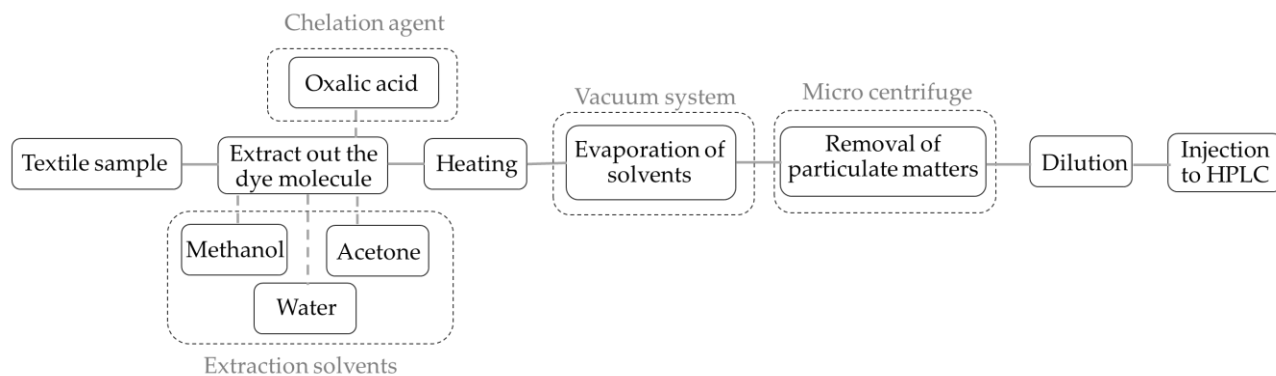
Figure 5- Textile extraction procedure

A combination of water and methanol, plus heating below the boiling temperature of the mixture, is required to extract dyes from the flavonoid plants [29]. The extract is then filtered or centrifuged to remove particulates (Figure 6).
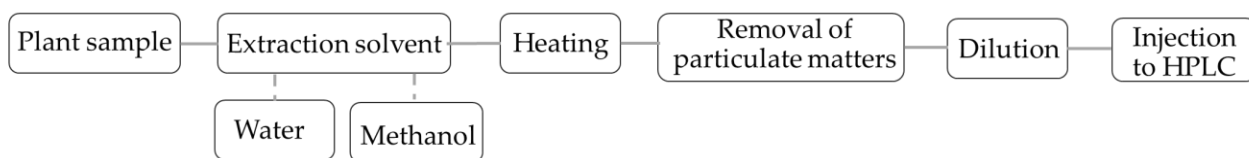
Figure 6- Plant extraction procedure

The amount of aglycones in the extracts of ancient textile fibers is far less than in plant extracts or even textiles dyed in the laboratories. Moreover, the dyeing process or the aging of the textiles may have deteriorating effects on the flavonoid aglycones. Therefore, mild extraction methods that prevent further loss of valuable information combined with the multi-analytical HPLC-DAD-MS technique can provide valuable information to identify the dye source(s) and the origin of the textiles under study [92].

6- Light degradation of natural yellow dyes

Yellow dyes in textiles are prone to fading—if exposed to light—because they absorb light in the higher energy range of the visible spectrum. The yellow in orange and green colors also fade, often causing objects to appear red or blue in historical textiles [11].

The photo-aging process not only has significant consequences on the artistic concept of artifacts, but it may also alter the dye molecules chemically. Hence, the spectral and chromatographic behavior of the dyes may not match that of the standards [93]. This change caused by photodegradation makes the identification of natural yellow dyes in historical textiles more complicated and time-consuming [68].

The photophysical and photochemical studies are important to determine the conditions that affect the naturally dyed objects, the changes in their colors [80], the environment of the dyes [42], and the technology applied to make the artifact [93]. The information gained from these studies can be applied to plan the strategies to prevent the fading and to improve the stability of the dyed artworks.

6.1 Photochemistry of yellow dyes

Photochemical processes are more relevant to natural dyes, particularly yellow dyes with poor lightfastness, as they are more likely to undergo photodegradation [80].

When a dye absorbs radiation, a molecule in the excited state is created [42, 94]. The resulting extra energy produces a molecule with entirely different properties such as its polarity, different acid-base, and redox properties from the ground state molecule [95].

The absorption coefficient is important to understand the type of transition associated with each band in the UV-VIS spectra and follows the Beer-Lambert law. This law, as illustrated in equation (1), describes that the absorbance of light in a medium is proportional to the absorption path length, (l), and to the concentration of absorbing species, (c), [96].

$$A = \varepsilon cl \tag{1}$$

When $l = 1$, the molar absorption coefficient, (ε), can be described by equation (2)

[96]:

$$\varepsilon = \frac{A}{c} \quad (l\ mol^{-1}\ cm^{-1}) \tag{2}$$

The characteristic bands of the UV-VIS absorption spectra of flavonoids were presented in Figure 2.

6.2 Quantum yield

Quantum yield (Φ_R) is a time-independent observable rate constant that can elucidate the characterization of photochemical reaction [95, 97]. As a matter of fact, the relative photostability of colorants is quantified by the quantum yield value [12].

The quantum yield determines " the number of moles of the species produced upon absorption of a mole of photons" with the following equation [97]:

$$\Phi = \frac{\text{Amount of reactant consumed or product formed}}{\text{Amount of photon absorbed}} \quad \text{per unit of time} \tag{3}$$

According to equation (3), The quantum yield equals one if every photon of absorbed light leads to the change or decomposition of one molecule [98].

Based on the concept of equation (3), the quantum yield of reaction (ϕ_R) in heterogeneous and in homogeneous media can be calculated by equation (4) [99].

$$\Phi_R = \frac{V_{sol} \cdot \Delta A}{1000 \cdot I_{Abs} \cdot \Delta t \cdot \Delta \varepsilon} \tag{4}$$

In equation (4), the volume of irradiated solution (mL) is illustrated by V_{sol}; the change in absorbance at the monitoring wavelength is ΔA; which is considered over the irradiation time period, Δt; and finally, the difference between the molar absorption coefficients of reagent and product at the monitoring wavelength is $\Delta \varepsilon$ [100]. The information about I_{Abs} will be discussed in the following section.

Beer's law can be applied whether in homogeneous (solution) or heterogeneous (transparent gels) media [100]. In this regard, using the collagen gel, which can simulate the wool environment, reveals the effect of the media on the light stability of dyes and also clarifies the probable photochemical behavior of dyes on historical textiles.

38

It is worth mentioning that the estimation of the quantum yield usually contains a 5 to 10 percent margin of error. Two main reasons for the errors are the quantum yield of the actinometer and the correction factors of the detection system [96].

6.3 Chemical actinometry

Actinometer is a chemical system that determines "the number of photons absorbed integrally or per time interval into the defined space of a chemical reactor" [101], preferably with a monochromatic incident light [97].

A photoactive compound with known quantum yield can be considered an actinometer. A good actinometer is independent of many factors, namely, the excitation wavelength, temperature, concentration, trace impurities, and oxygen. In addition, the number of reacted molecules for the actinometer should be determined by a convenient analytical method [97].

The actinometer is applied to calculate the intensity of the incident light (I_0). The I_0 can be obtained with the equation (5):

$$I_{Abs} = \frac{V_{sol} \cdot m}{1000 \cdot \Phi_R \cdot \Delta\varepsilon \cdot l} \tag{5}$$

I_{Abs} is defined as the total light absorption of the solution at the irradiation wavelength (λ_{irr}) and can be defined by $I_{Abs} = I_0 \left(1 - 10^{-Abs_{\lambda_{irr}}}\right)$ when $Abs < 2$, and is equal to I_0, when $Abs > 2$ [99].

6.4 Accelerated light aging of yellow dyes

Accelerated aging studies the degradation mechanisms in materials and considers their long-term behaviors. It is a predictive conservation model to understand better and evaluate the storage conditions of the historical textile.

The vague information about the previous conditions that were imposed on the artifacts highlights the necessity of applying low-energy UV as the source of accelerated aging. Meanwhile, it is important to notice that other environmental factors such as temperature and humidity are controlled during the accelerated light aging experiment, which may not happen in real conditions [80].

To set up the accelerating light aging experiment, dye solutions/ dyed samples are

deposited in glass and irradiated with two different light sources: the mercury monochromatic source (with a spectral distribution close to the maximum absorption of the molecule) to identify the intermediates; and the xenon polychromatic source (with a spectral distribution close to the solar spectrum) to identify the main photodegradation products in a much shorter time [95].

The photochemical damage is linearly correlated with the net exposure (i.e., intensity of irradiance (or illuminance) × exposure time) [80].

6.5 Photodegradation behavior of yellow dyes

The dye-aging processes noticeably depend on different conditions, which have been extensively investigated [98, 102, 103]. The observable lightfastness of naturally dyed textiles is influenced by internal factors, such as the concentration of the dye, the type of the fiber and mordant, and irradiation wavelength as external conditions (Figure 7) [104].
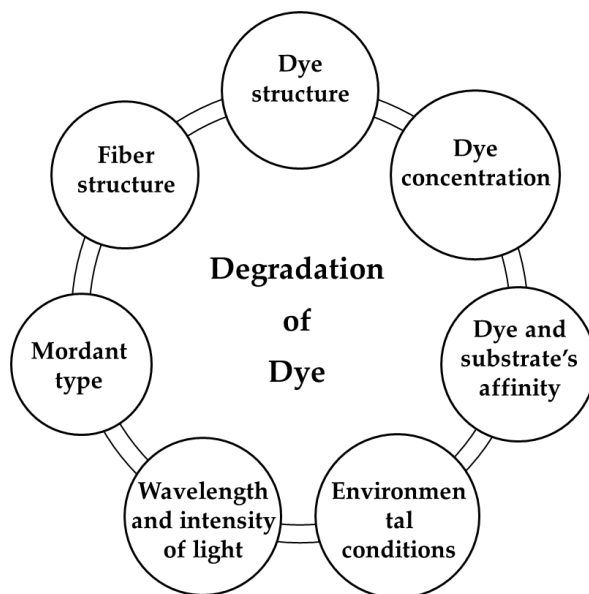
Figure 7- The lightfastness factors for natural dyes

The kinetics of degradation of a compound is influenced by its structures. So, for photophysical and photodegradation characterization of dye molecules, their structures should be well characterized first [95, 104].

The most sensitive yellow flavonoid dyes are the ones with a hydroxyl group in position

40

3 [105]. Nevertheless, when a sugar or other moiety replaces the proton of the 3-hydroxyl group in a flavonoid, light stability increases [22]. In addition, flavonoids without an OH group in position 3 are more stable, especially if they lack the C2-C3 double-bond [22, 104]. It is also reported that the higher electron density of the C2-C3 in flavonols results in their relatively low photostability [105].

This information explains why weld is more stable than larkspur and larkspur more than onionskin as yellow dye sources containing H, OR, and OH on position 3, respectively.

Understanding the photochemistry of the dye molecules is also achievable by overviewing the photophysics of these molecules:

It was previously discovered that the photostability of dyes is significantly influenced by proton transfer in the excited state [106].

Sisa and colleagues, from the same point of view, contributed that a "3-methoxy substituent increases the n, π^* character and the triplet state energy"; while a "7-methoxy substituent increases the π, π^* character of the excited state" [94].

The role of oxygen in obtaining the quantum yield should also be considered since photo-oxidation affects the general fading mechanism [95].

The C ring in the structure of flavonoids plays an important role in their reactivity to oxygen. Flavones and flavonols are chemically more reactive to atmospheric oxygen than flavanones and flavanes. In addition, in the presence of oxygen, the hydroxyl group in position 3 increases the rate of oxygen degradation by activating the C2-C3 double bond [107].

The oxidation pathways for the aglycones and glycosylated flavonoids are different. The former degrades when some of their bonds break, while the latter's degradation is caused by polymerization [104].

Besides the role of atmospheric oxygen in the light stability of flavonoid yellow dyes, the proper processing of plant materials plays an important role in this regard. The rapid heating of fresh buds or adding the fresh plant materials to the dye bath can inactivate the glycosidase enzyme in Pagoda trees and produce a light-stable dye [22].

6.6 Identification of photodegradation mechanism and products

The photodegradation products can reveal the plant used as a yellow dye source for historical textiles. But also understanding the molecular degradation mechanism is essential for setting up a preventive conservation protocol [95] [108].

Studying the chemical changes of degraded dyes under the light-aging process requires a technique that provides structural information [80]. It has been shown that ESI-QIT-MS/MS is a successful technique for identifying the nature of the photodegradation products in historical textiles, especially where the sample size is limited, and the concentration level of the dye extracts is very low [75].

Photo-oxidation is a common degradation path for flavonoids [80]. The oxidation of the C2-C3 bond along with the breaking of the C2–C3 and C3-C4 linkages decreases the concentration of the chromophores [109].

The photodegradation process of natural yellow dyes has rarely been studied in the literature, although new aspects of these dye sources can be identified by applying the knowledge of photochemistry. This topic has been fully addressed in chapter 4. The environmental conditions in the museum, especially light, can influence the dye structure in the textiles. Comprehending the degradation process and its mechanisms for affecting the molecular structure of the dyes is a significant step in this regard. Identifying and quantifying the effects of light on the dyes' degradation can control or reduce the risk of fading and improve the permanence of the dyed textiles. This can result in preventive conservation rules and sustainable strategies that enhance the storage condition of historical textiles.

7- The proposed study of natural yellow dyes in Persian carpets

Conservators, curators, archeologists, and chemists are the audiences of this study. Scientific and economical, even social and cultural progress, can be witnessed in a broader outlook by investigating production technologies and processes. In particular, dyeing techniques and materials may reveal the possible trade routes and connections during different eras, unmask national-historical secrecies, and authenticate a novel glimpse of the artworks.

Regarding what specifically addresses the conservators and chemists, this study aims to provide a database of HPLC-DAD retention times and UV-VIS spectra along with the mass values and fragment Ions through a systematic analytical method. The photochemical study of the dyes clarifies the degradation products and mechanisms and contributes to identifying faded yellow dyes. A scale of photostability based on reaction quantum yields is built on understanding and predicting the changes of color over time, resulting in better preservation of the dyed textiles. The new insight brought into natural yellow dyes and an assessment of the deterioration plays an important role in devising preventive conservation strategies and suggesting exhibition conditions.

The strategy that has been followed in this study to identify dye compounds is described in three successive chapters:

Chapter 2 presents a complete review of plants that have been reported as sources of natural yellow dyes in Persian carpets. The information is gathered from the literature and interviews, and the results are compared along with the reported identified yellow dye sources.

Chapter 3 analyzes seven natural yellow dye plants obtained from dye workshops of Iran; *Delphinium semibarbatum*, *Eremostachys laevigata*, *Prangos ferulacea*, *Morus alba*, *Pistacia vera*, *Punica granatum*, and *Vitis vinifera*. The dye composition of wool samples dyed with these sources and the changes induced by the dyeing procedures in the original chemical composition of the plant extract, raw materials, and dyed wools are characterized by HPLC–DAD and UHPLC–HRMS/MS.

The photostability of flavonoid dye compounds is discussed in Chapter 4. The photodegradation quantum yield for luteolin, quercetin, kaempferol, and their glucosides,

are calculated for the first time. Additionally, through artificial light aging of these compounds, the main degradation products are characterized by HPLC-DAD-MS and UHPLC–MS/MS.

References

[1] Jacoby, H. (1964). Materials used in the making of carpets. In A. U. Pope, & P. Ackerman (Eds.), *A survey of Persian art: from prehistoric times to the present* (Vol. 5) (2nd ed.). Meiji-Shobo.

[2] Edwards, A. C. (1975). *The Persian carpet: a survey of the carpet-weaving industry of Persia*. Gerald Duckworth.

[3] Wulff, H. E. (1966). *The traditional crafts of Persia, their development, technology, and influence on Eastern and Western civilizations*. MIT Press.

[4] Rudenko, S. I. (1970). *Frozen tombs of Siberia: the Pazyryk burials of iron-age horsemen* (M. W. Thompson, Trans.). University of California Press. ISBN 0520013956

[5] Varzi, M. (1971). *Art and industry of carpet in Iran: the history of painting, design and Carpet weaving* (in Persian). Raz Publications.

[6] Dādagī, F. (1991). *Bundahišn* (M. Bahar, Trans into new Persian. and Annot.). Tus publications. (Original book is based on three manuscripts were written in 1531, 1606, 1577).

[7] Hakluyt, R. (2014). *The principal navigations, voyages and discoveries of the English nation*. Cambridge University Press.

[8] Chardin, S. J. (1978). *The travels of Sir John Chardin into Persia and the East Indies*. Moses Pitt.

[9] Keddie, N. R. (1972). The economic history of Iran, 1800–1914, and its political impact an overview. *Iranian Studies*. 5(2-3), 58-78. Doi: 10.1080/00210867208701424

[10] Suresrafil, Sh. (1993). *Golden fall of Sarough carpet* (in Persian), Mirdashti publications.

[11] Zhang, X. (2008). *Analysis of natural yellow dyes using HPLC with diode array and mass spectrometric detection* [Doctoral dissertation, Boston University].

[12] Melo, M. J., Ferreira, J. L., Parola, A. J., & Melo, J. S. (2016). Photochemistry for cultural heritage. G. Bergamini, S. Silvi (Eds.), *Applied photochemistry* (Vol. 92) (pp. 499-530). Springer, Cham. Doi: 10.1007/978-3-319-31671-0_13

[13] Hofenk de Graaff, J. H., van Bömmel, M. R., Roelofs, W. G. Th. (2004). *The colorful past: origins, chemistry and identification of natural dyestuffs.* Archetype publications. ISBN 1873132131

[14] Cardon, D. (2007). *Natural dyes: sources, tradition, technology and science* (1st ed.) Archetype Publications. ISBN 190498200X

[15] Haslam, E. (1989). *Plant polyphenols: vegetable tannins revisited*. CUP Press. ISBN 0521321891

[16] Harborne, J. B. (Ed.). (1994). *The flavonoids: advances in research since 1986* (1s ed.).

CRC Press. ISBN 0412480700

[17] Böhmer, H., Enez, N., Karadağ, R., Kwon, C., Fogelberg, L.E. (2002). *Koekboya: natural dyes and textiles, a color journey from Turkey to India and beyond* (L.E. Fogel-berg Trans.). REMHÖB-Verlag.

[18] Ferreira, E. S., Hulme, A. N., Mcnab, H., & Quye, A. (2004). The natural constituents of historical textile dyes. *Chemical Society Reviews*, 33(6), 329-336 Doi: 10.1002/chin.200444268

[19] Gates, P. J., & Lopes, N. P. (2012). Characterization of flavonoid aglycones by negative ion chip-based nanospray tandem mass spectrometry. *International Journal of Analytical Chemistry*, 2012, 1-7. Doi: 10.1155/2012/259217

[20] Fabre, N., Rustan, I., Hoffmann, E. D., & Quetin-Leclercq, J. (2001). Determination of flavone, flavonol, and flavanone aglycones by negative ion liquid chromatography electrospray ion trap mass spectrometry. *Journal of the American Society for Mass Spectrometry*, 12(6), 707-715. Doi: 10.1016/s1044-0305(01)00226-4

[21] McNab, H., Ferreira, E.S., Hulme, A.N., Quye, A. (2009). Negative ion ESI–MS analysis of natural yellow dye flavonoids—An isotopic labeling study. *International Journal of Mass Spectrometry*, 284(1-3), 57-65. Doi: 10.1016/j.ijms.2008.05.039

[22] Zhang, X., Cardon, D., Cabrera, J. L., & Laursen, R. (2010). The role of glycosides in the light-stabilization of 3-hydroxyflavone (flavonol) dyes as revealed by HPLC. *Microchimica Acta*, 169(3-4), 327-334. Doi: 10.1007/s00604-010-0361-x

[23] Grotewold, E. (Ed.). (2005). *The science of flavonoids*. Springer. ISBN 038728821X

[24] Andersen, O. M., Markham, K. R. (2005). *Flavonoids: chemistry, biochemistry and applications*. CRC Press. ISBN 0849320216

[25] Williams, C. A., & Grayer, R. J. (2004). Anthocyanins and other flavonoids. *Natural product reports*, 21(4), 539-573.

[26] Chicaro, P., Pinto, E., Colepicolo, P., Lopes, J. L., & Lopes, N. P. (2004). Flavonoids from Lychnophora passerina (Asteraceae): Potential antioxidants and UV-protectants. *Biochemical Systematics and Ecology*, 32(3), 239-243. Doi: 10.1016/j.bse.2003.08.003

[27] Melo, M. J. (2009). History of natural dyes in the ancient Mediterranean world. In T. Bechtold, & R. Mussak (Eds.), *Handbook of Natural Colorants* (pp. 3–17), Wiley. Doi: 10.1002/9780470744970.ch1

[28] Brunello, F. (1973). *The art of dyeing in the history of mankind* (B. Hickey, Trans.). Neri Pozza.

[29] Laursen, R., Mouri, C., Zhang, X. (2019, March). *The Boston database of natural dyestuffs*. http://www.dyeanalysislcms.net

[30] Claro, A., Melo, M. J., Melo, J. S., Berg, K. J., Burnstock, A., Montague, M., & New-man, R. (2010). Identification of red colorants in van Gogh paintings and ancient Andean textiles by microspectrofluorimetry. *Journal of Cultural Heritage*, 11(1), 27-34. Doi: 10.1016/j.culher.2009.03.006

[31] Mirjalili, M. (2008). *Laboratory methods in natural fibers dyeing* (in Persian). Yazd IAU publications.

[32] Jahanshahi, V. (1996). *Process and methods of dyeing fibers with natural dyes* (in Persian). Scientific and Cultural Publications Co. ISBN 9646218008

[33] Afsharnia, S. (2008). *Natural dyeing* (in Persian). PNU publications. ISBN 9789643872922

[34] Veisian, M., Heidari M. E. (2009). *Natural dyeing of protein fibers (silk and wool)* (in Persian). National Carpet Center of Iran. ISBN 9789640427743

[35] Surowiec, I., Szostek, B., & Trojanowicz, M. (2007). HPLC-MS of anthraquinoids, flavonoids, and their degradation products in analysis of natural dyes in archeological objects. *Journal of Separation Science*, 30(13), 2070-2079. Doi: 10.1002/jssc.200700041

[36] Trojanowicz, M., Orska-Gawryś, J., Surowiec, I., Szostek, B., Urbaniak-Walczak, K., Kehl, J., & Wróbel, M. (2004). Chromatographic investigation of dyes extracted from Coptic textiles from the national museum in Warsaw. *Studies in Conservation*, 49(2), 115-130. Doi: 10.1179/sic.2004.49.2.115

[37] Gulmini, M., Idone, A., Diana, E., Gastaldi, D., Vaudan, D., & Aceto, M. (2013). Identification of dyestuffs in historical textiles: Strong and weak points of a non-invasive approach. *Dyes and Pigments*, 98(1), 136-145. Doi: 10.1016/j.dyepig.2013.02.010

[38] Laursen R. (2020). The analysis of dyes in textiles. *The Textile Museum Journal*. 47(1), 54-69.

[39] Nakamura, R., Tanaka, Y., Ogata, A., & Naruse, M. (2009). Dye analysis of Shosoin textiles using excitation–emission matrix fluorescence and ultraviolet–visible reflectance spectroscopic techniques. *Analytical Chemistry*, 81(14), 5691-5698. Doi: 10.1021/ac900428a

[40] Brunetti, B., Miliani, C., Rosi, F., Doherty, B., Monico, L., Romani, A., & Sgamellotti, A. (2016). Non-invasive investigations of paintings by portable instrumentation: the MOLAB experience. *Analytical Chemistry for Cultural Heritage*, 41-75. Doi: 10.1007/978-3-319-52804-5_2

[41] Romani, A., Clementi, C., Miliani, C., & Favaro, G. (2010). Fluorescence spectroscopy: a powerful technique for the noninvasive characterization of artwork. *Accounts of Chemical Research*, 43(6), 837-846. Doi: 10.1021/ar900291y

[42] Melo, M. J., & Claro, A. (2010). Bright light: microspectrofluorimetry for the characterization of lake pigments and dyes in works of art. *Accounts of Chemical Research*, 43(6), 857-866. Doi: 10.1021/ar9001894

[43] Leona, M., & Winter, J. (2001). Fiber optics reflectance spectroscopy: a unique tool for the investigation of Japanese paintings. *Studies in Conservation*, 46(3), 153. Doi: 10.2307/1506806

[44] Poldi, G. (2012, October 18-19). *Re-thinking to reflectance spectrometry as a tool to identify some classes of 9 dyes in old textiles and paintings in situ. Examples* [conference presentation]. Dyes in History and Archaeology 31, Antwerp, Belgium.

[45] Serrano, A., Sousa, M., Hallett, J., Lopes, J., Oliveira, C. (2011, October 12-15). *A New methodology for the analysis of Cochineal dyes in historical textiles* [conference presentation]. Dyes in History and Archaeology 30, Derby, England, UK.

[46] Smith, M., Thompson, K., & Lennard, F. (2017). A literature review of analytical techniques for materials characterization of painted textiles—Part 2: Spectroscopic and chromatographic analytical instrumentation. *Journal of the Institute of Conservation*, 40(3), 252-266. Doi: 10.1080/19455224.2017.1365739

[47] Aceto, M., Agostino, A., Fenoglio, G., Idone, A., Gulmini, M., Picollo, M., . . . Delaney, J. K. (2014). Characterization of colorants on illuminated manuscripts by portable fiber optic UV-visible-NIR reflectance spectrophotometry. *Analytical Methods*, 6(5), 1488. Doi: 10.1039/c3ay41904e

[48] Maynez-Rojas, M., Casanova-González, E., & Ruvalcaba-Sil, J. (2017). Identification of natural red and purple dyes on textiles by Fiber-optics Reflectance Spectroscopy. *Spectrochimica Acta Part A: Molecular and Biomolecular Spectroscopy*, 178, 239-250. Doi: 10.1016/j.saa.2017.02.019

[49] Gulmini, M., Idone, A., Davit, P., Moi, M., Carrillo, M., Ricci, C., . . . Aceto, M. (2016). The "Coptic" textiles of the "Museo Egizio" in Torino (Italy): A focus on dyes through a multi-technique approach. *Archaeological and Anthropological Sciences*, 9(4), 485-497. Doi: 10.1007/s12520-016-0376-2

[50] Angelini, L. G., Tozzi, S., Bracci, S., Quercioli, F., Radicati, B., & Picollo, M. (2010). Characterization of traditional dyes of the Mediterranean area by non-invasive UV-VIS-NIR reflectance spectroscopy. *Studies in Conservation*, 55(Sup2), 184-189. Doi: 10.1179/sic.2010.55.supplement-2.184

[51] Romani, A., Clementi, C., Miliani, C., Brunetti, B. G., Sgamellotti, A., & Favaro, G. (2008). Portable equipment for luminescence lifetime measurements on surfaces. *Applied Spectroscopy*, 62(12), 1395-1399. Doi: 10.1366/000370208786822250

[52] Shahid, M., Wertz, J., Degano, I., Aceto, M., Khan, M. I., & Quye, A. (2019). Analytical

methods for determination of anthraquinone dyes in historical textiles: A review. *Analytica Chimica Acta*, 1083, 58-87. Doi: 10.1016/j.aca.2019.07.009

[53] Degano, I., Ribechini, E., Modugno, F., & Colombini, M. P. (2009). Analytical methods for the characterization of organic dyes in artworks and in historical textiles. Applied Spectroscopy Reviews, 44(5), 363-410. Doi: 10.1080/05704920902937876

[54] Leona, M., Stenger, J., & Ferloni, E. (2006). Application of surface-enhanced Raman scattering techniques to the ultrasensitive identification of natural dyes in works of art. *Journal of Raman Spectroscopy*, 37(10), 981-992. Doi: 10.1002/jrs.1582

[55] Pozzi, F., Porcinai, S., Lombardi, J. R., & Leona, M. (2013). Statistical methods and library search approaches for fast and reliable identification of dyes using surface-enhanced Raman spectroscopy (SERS). *Analytical Methods*, 5(16), 4205. Doi: 10.1039/c3ay40673c

[56] Bhandari, D. (2011). *Surface-enhanced Raman scattering: substrate development and applications in analytical detection* [Doctoral dissertation, University of Tennessee]. University of Tennessee Repository. https://trace.tennessee.edu/utk_graddiss/949

[57] Wouters, J. (1985). High-performance liquid chromatography of anthraquinones: analysis of plant and insect extracts and dyed textiles. *Studies in Conservation*, 30(3), 119. Doi: 10.2307/1505927

[58] Brosseau, C. L., Gambardella, A., Casadio, F., Grzywacz, C. M., Wouters, J., & Duyne, R. P. (2009). Ad-hoc surface-enhanced Raman spectroscopy methodologies for the detection of artist dyestuffs: thin layer chromatography-surface enhanced Raman spectroscopy and in situ on the fiber analysis. *Analytical Chemistry*, 81(8), 3056-3062. Doi: 10.1021/ac802761v

[59] Cuyckens, F., & Claeys, M. (2004). Mass spectrometry in the structural analysis of flavonoids. *Journal of Mass Spectrometry*, 39(4), 461-461. Doi: 10.1002/jms.622

[60] Guillarme, D., Ruta, J., Rudaz, S., & Veuthey, J. (2009). New trends in fast and high-resolution liquid chromatography: A critical comparison of existing approaches. *Analytical and Bioanalytical Chemistry*, 397(3), 1069-1082. Doi: 10.1007/s00216-009-3305-8

[61] Serrano, A., van Bömmel, M., & Hallett, J. (2013). Evaluation between ultrahigh-pressure liquid chromatography and high-performance liquid chromatography analytical methods for characterizing natural dyestuffs. *Journal of Chromatography A*, 1318, 102-111. Doi: 10.1016/j.chroma.2013.09.062

[62] Ardrey, R. E. (2003). *Liquid chromatography-mass spectrometry: An introduction*. Wiley. ISBN 0471498017

[63] Harborne, J. B., Mabry, T. J., & Mabry, H. (1975). Ultraviolet-visible and proton magnetic resonance spectroscopy of flavonoids. In *The flavonoids* (pp. 45-77).

Springer. ISBN 9780123246028

[64] Mabry, T., Markham, K. R., & Thomas, M. B. (2012). The Ultraviolet Spectra of Fla-
vones and Flavonols. In *The systematic identification of flavonoids* (pp.41-57). Springer.
ISBN 978364288460

[65] Pinheiro, P. F., & Justino, G. C. (2012). Structural analysis of flavonoids and related
compounds-a review of spectroscopic applications. In V. Rao (Ed.), *Phytochemicals:
a global perspective of their role in nutrition and health* (pp. 33-56). IntechOpen. ISBN
9535102966

[66] Dong, M. W., & Wysocki, J. (2019). Ultraviolet detectors: perspectives, principles,
and practices. *LCGC North America*, 37(10), 750-759.

[67] Trojanowicz, M., Wójcik, L., & Urbaniak-Walczak, K. (2003). Identification of nat-
ural dyes in historical Coptic textiles by cappilary electrophoresis with diode array
detection. *Chemia analityczna*, 48(3), 607-620. Doi: 10.1016/s0021-9673(03)00083-9

[68] Ferreira, E. S., Quye, A., McNab, H., Wouters, J., Boon, J. J., & Hulme, A. N. (2002).
Development of analytical techniques for the study of natural yellow dyes in historic
textiles. In J. Kirby (Ed.), *Dyes in History & Archaeology 16/17* (pp. 179-186). Archetype
Publication. ISBN 1873132972

[69] Zhang, X., & Laursen, R. (2009). Application of LC–MS to the analysis of dyes in
objects of historical interest. *International Journal of Mass Spectrometry*, 284(1-3), 108-
114. Doi: 10.1016/j.ijms.2008.07.014

[70] Vukics, V., & Guttman, A. (2008). Structural characterization of flavonoid glyco-
sides by multi-stage mass spectrometry. *Mass Spectrometry Reviews*, 29(1), 1-16. Doi:
10.1002/mas.20212

[71] Greaves, J., & Roboz, J. (2014). *Mass spectrometry for the novice*. CRC Press. ISBN
1420094181

[72] Burinsky, D. J. (2006). Mass spectrometry. In S. Ahuja, N. Jespersen, (Eds.), *Com-
prehensive Analytical Chemistry 49* (pp. 319-396). Elsevier. Doi: 10.1016/S0166-
526X(06)47011-2.

[73] De Hoffmann, E., & Stroobant, V. (2007). *Mass spectrometry: principles and applica-
tions*. Wiley. p. 45. ISBN 0470033118

[74] Herbert, C. G., & Johnstone, R. A. (2002). *Mass spectrometry basics*. CRC Press. ISBN
0849313546

[75] Ferreira, E. S., Quye, A., Hulme, A. N., Wouters, J., & Boon, J. J. (1999). The analyt-
ical characterization of flavonoid photodegradation products: a novel approach to
identifying natural yellow dyes in ancient textiles. In *12th triennial ICOM committee
for conservation conference* (Vol. 1) (pp. 221-227). James & James. ISBN 1873936923

[76] Ardrey, R. E. (2003). *Liquid chromatography - mass spectrometry: An introduction*.

Wiley. ISBN 0471498017

[77] Gross, J. H. (2017). *Mass spectrometry: a textbook* (3rd ed.). Springer. ISBN 3319543970

[78] Wolfender, J., Waridel, P., Ndjoko, K., Hobby, K. R., Major, H. J., & Hostettmann, K. (2000). Evaluation of Q-TOF-MS/MS and multiple stage IT-MS[n] for the dereplication of flavonoids and related compounds in crude plant extracts. *Analusis*. 28(10), 895-906. Doi: 10.1051/analusis:2000280895

[79] Ma, Y. L., Li, Q. M., Heuvel, H. V., & Claeys, M. (1997). Characterization of flavone and flavonol aglycones by collision-induced dissociation tandem mass spectrometry. *Rapid Communications in Mass Spectrometry*, 11(12), 1357-1364. Doi: 10.1002/(sici)1097-0231(199708)11:12<1357::aid-rcm983>3.0.co;2-9

[80] Ferreira, E. S. B. (2001). *New approaches towards the identification of yellow dyes in ancient textiles* [Doctoral dissertation, University of Edinburgh]. University of Edinburgh Repository. http://hdl.handle.net/1842/12020

[81] Domon, B., & Costello, C. E. (1988). A systematic nomenclature for carbohydrate fragmentations in FAB-MS/MS spectra of glycoconjugates. *Glycoconjugate Journal*, 5(4), 397-409. Doi: 10.1007/bf01049915

[82] Cuyckens, F., Ma, Y. L., Pocsfalvi, G., & Claeysi, M. (2000). Tandem mass spectral strategies for the structural characterization of flavonoid glycosides. *Analusis*, 28(10), 888-895. Doi: 10.1051/analusis:2000280888

[83] Petroviciu, I., Albu, F., & Medvedovici, A. (2010). LC/MS and LC/MS/MS based protocol for identification of dyes in historic textiles. *Microchemical Journal*, 95(2), 247-254. Doi: 10.1016/j.microc.2009.12.009

[84] Petroviciu, I., Creanga, D., Melinte, I., Cretu, I., Medvedovici, A., & Albu, F. (2011). The Use of LC-MS in the Identification of Natural Dyes in the Epitaphios from Sucevita Monastery (15th century). *Revue Roumaine de Chimie*, 56(2), 161-168.

[85] Serrano, A., van Bömmel, M., & Hallett, J. (2013). Evaluation between ultrahigh-pressure liquid chromatography and high-performance liquid chromatography analytical methods for characterizing natural dyestuffs. *Journal of Chromatography A*, 1318, 102-111.

[86] Mouri, C., & Laursen, R. (2011). Identification and partial characterization of C-glycosylflavone markers in Asian plant dyes using liquid chromatography–tandem mass spectrometry. *Journal of Chromatography A*, 1218(41), 7325-7330. Doi: 10.1016/j.chroma.2011.08.048

[87] Mouri, C., & Laursen, R. (2012). Identification of anthraquinone markers for distinguishing Rubia species in madder-dyed textiles by HPLC. *Microchimica Acta*, 179(1-2), 105-113. Doi: 10.1007/s00604-012-0868-4

[88] Mouri, C., Aali, A., Zhang, X., & Laursen, R. (2014). Analysis of dyes in textiles from the Chehrabad salt mine in Iran. *Heritage Science*, 2(1). Doi: 10.1186/s40494-014-0020-3

[89] Shibayama, N., Wypyski, M., & Gagliardi-Mangilli, E. (2015). Analysis of natural dyes and metal threads used in 16th -18th century Persian/Safavid and Indian/Mughal vel-vets by HPLC-PDA and SEM-EDS to investigate the system to differentiate velvets of these two cultures. *Heritage Science*, 3(1). Doi: 10.1186/s40494-015-0037-2

[90] Robards, K., Li, X., Antolovich, M., & Boyd, S. (1997). Characterization of citrus by chromatographic analysis of flavonoids. *Journal of the Science of Food and Agriculture*, 75(1), 87-101. Doi: 10.1002/(sici)1097-0010(199709)75:1<87::aid-jsfa846>3.0.co;2-b

[91] Valianou, L., Karapanagiotis, I., & Chryssoulakis, Y. (2009). Comparison of extraction methods for the analysis of natural dyes in historical textiles by high-performance liquid chromatography. *Analytical and Bioanalytical Chemistry*, 395(7), 2175-2189. Doi: 10.1007/s00216-009-3137-6

[92] Zhang, X., & Laursen, R. A. (2005). Development of mild extraction methods for the Analysis of natural dyes in textiles of historical interest using LC-diode array detector-MS. *Analytical Chemistry*, 77(7), 2022-2025. Doi: 10.1021/ac048380k

[93] Clementi, C., Nowik, W., Romani, A., Cibin, F., & Favaro, G. (2007). A spectrometric and chromatographic approach to the study of aging of madder (*Rubia tinctorum* L.) dyestuff on wool. *Analytica Chimica Acta*, 596(1), 46-54. Doi: 10.1016/j.aca.2007.05.036

[94] Sisa, M., Bonnet, S. L., Ferreira, D., & Westhuizen, J. H. (2010). Photochemistry of Flavonoids. *Molecules*, 15(8), 5196-5245. Doi: 10.3390/molecules15085196

[95] Sousa, M. M. F. D. (2008). *A study on historical dyes used in textiles: dragon's blood, indigo, and mauve* [Doctoral dissertation, New University of Lisbon]. NOVA University Repository. http://hdl.handle.net/10362/50266

[96] Valeur, B., & Berberan-Santos, M. N. (2012). *Molecular fluorescence: principles and applications* (2nd ed.). Wiley-VCH Verlag & Co. KGaA. ISBN 3527328467

[97] Montalti, M., Credi, A., Prodi, L., & Gandolfi, M. T. (2006). *Handbook of photochemistry* (3rd ed.). CRC Press. ISBN 0367577909

[98] Feller, R. L. (1995). *Accelerated aging: photochemical and thermal aspects*. Getty Publications. ISBN 0892361255

[99] Sousa, M. M., Miguel, C., Rodrigues, I., Parola, A. J., Pina, F., Melo, J. S., & Melo, M. J. (2008). A photochemical study on the blue dye indigo: From solution to ancient Andean textiles. *Photochemical & Photobiological Sciences*, 7(11), 1353. Doi: 10.1039/b809578g

[100] Pina, F., & Hatton, T. A. (2008). Photochromic soft materials: flavylium compounds incorporated into pluronic F-127 hydrogel matrixes. *Langmuir*, 24(6), 2356-2364. Doi: 10.1021/la702733d

[101] Braslavsky, S. E. (2007). Glossary of terms used in photochemistry (3rd ed.) (IUPAC Recommendations 2006). *Pure and Applied Chemistry*, 79(3), 293-465. Doi: 10.1351/pac200779030293

[102] Giles, C. H., & Mckay, R. B. (1963). The lightfastness of dyes: a review. *Textile Research Journal*, 33(7), 528-577. Doi: 10.1177/004051756303300707

[103] Padfield, T., & Landi, S. (1966). The light-fastness of the natural dyes. *Studies in Conservation*, 11(4), 181. Doi: 10.2307/1505361

[104] Chaaban, H., Ioannou, I., Paris, C., Charbonnel, C., & Ghoul, M. (2017). The photostability of flavanones, flavonols and flavones and evolution of their antioxidant activity. Journal of Photochemistry and Photobiology A: Chemistry, 336, 131-139. Doi: 10.1016/j.jphotochem.2016.12.027

[105] Smith, G. J., Thomsen, S. J., Markham, K. R., Andary, C., & Cardon, D. (2000). The photostabilities of naturally occurring 5-hydroxyflavones, flavonols, their glycosides and their aluminum complexes. *Journal of Photochemistry and Photobiology A: Chemistry*, 136(1-2), 87-91. Doi: 10.1016/s1010-6030(00)00320-8

[106] Sharif, S., Nabais, P., Melo, M. J., Pina, F., & Oliveira, M. C. (2022). Photoreactivity and stability of flavonoid yellows used in cultural heritage. Manuscript submitted in Dyes and Pigments.

[107] Ramešová, Š., Sokolová, R., Degano, I., Bulíčková, J., Žabka, J., & Gál, M. (2012). On the stability of the bioactive flavonoids quercetin and luteolin under oxygen-free conditions. *Analytical and Bioanalytical Chemistry*, 402(2), 975-982. Doi: 10.1007/s00216-011-5504-3

[108] Quye, A., Wouters, J., & Boon, J. J. (1996). A preliminary study of light-aging effects on the analysis of natural flavonoid-dyed wools by photodiode array HPLC and by direct temperature mass spectrometry. In *11th triennial ICOM committee for conservation conference* (pp. 704-713). James and James. ISBN 1873936508

[109] Colombini, M. P., Andreotti, A., Baraldi, C., Degano, I., & Łucejko, J. J. (2007). Color fading in textiles: A model study on the decomposition of natural dyes. *Microchemical Journal*, 85(1), 174-182. Doi: 10.1016/j.microc.2006.04.002

[110] Mozaffarian, V. (2004). *Trees and shrubs of Iran* (in Persian). Farhang e moaser. ISBN 96486370302.

[111] Mozaffarian, V. (2012). *Recognition of medicinal and aromatic plants of Iran* (in Persian). Farhang e moaser. ISBN 9786001050231.

[112] Mozaffarian, V. (1996). *A dictionary of Iranian plant names (Latin, English, Persian),*

Farhang e moaser. ISBN 9645545404

[113] Javidtash, I. (1996). *Dyeing method with plants and stability determination of 724 natural dyes* (in Persian). Research Institute of Forests and Rangelands.

[114] Sadri, N. (2007). *Dyeing of fibers and yarns (wool, silk, cotton)* (in Persian). Amirkabir Publications.

[115] Justesen, U. (2000). Negative atmospheric pressure chemical ionization low-energy collision activation mass spectrometry for the characterization of flavonoids in extracts of fresh herbs. *Journal of Chromatography A*, 902(2), 369-379. Doi: 10.1016/s0021-9673(00)00861-x

Chapter 2. Natural Yellow Dye Sources in Persian Carpets: A Review

56

Abstract

Persian carpets are a precious product of art, culture, and traditions of craftsmen. Colors have a substantial role in different patterns of carpets, thus dyeing techniques have long been part of this unique industry in Persia.

In this paper, we present a complete review on plants that were used as a source of natural yellow dyes in Persian carpets; this review is based on local and international references, including interviews with the few remaining dye masters in workshops located at the central parts of Iran. These results are compared with studies in which the yellow colors of Persian textiles were characterized by high-performance liquid chromatography with diode array detection (HPLC–DAD) and/or the same with mass spectrometric examination in addition (HPLC–DAD–MS).

1. Introduction

Persian carpets are a precious product of art, culture, and traditions of craftsmen, and dyeing techniques have long been used to create their unique patterns. This paper reviews the plants that were used as a source of yellow dyes in these carpets and compares the results with studies that characterized the yellow colors of Persian textiles using high-performance liquid chromatography with diode array detection (HPLC–DAD) and with the addition of mass spectrometry (HPLC–DAD–MS). As well as local and international references, interviews with the few remaining dye masters in workshops in central Iran are included.

Local sources of yellow dyes retained their importance, and the identification of yellow dyes is useful for textile provenance studies [1]. Many plants in Iran could be regarded as natural sources of yellow dyes, but there are few references that describe them together with their historical dyeing methods. Moreover, as the yellow dyes are more prone to fading, the actual yellow colors might appear different from the original colors [2].

The most common flavonoids used to dye in yellow are flavonols and flavones [3]. The flavonol aglycones are characterized by a hydroxyl in position 3 of the pyran ring (C)

57

and flavones by its absence, Figure 8.
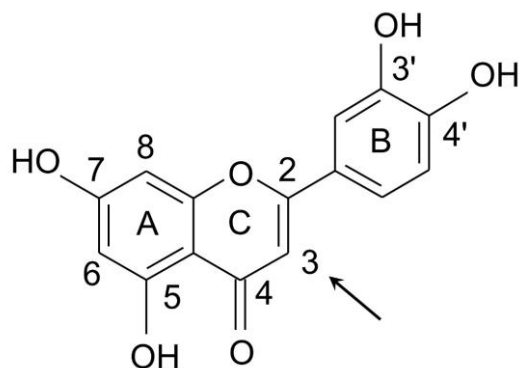
Figure 8- Aglycone structure present in flavonoid yellows; in position 3 an -OH group may also be present. In plants, flavonoids are present as glycosides.

In flavones such as luteolin, in which there is no 3-hydroxyl group, the colorants create a stable yellow chromophore [4]. This is the main reason for the wide application of plants with this kind of chromophore, like weld, *Reseda luteola*, in dyeing.

Flavonol aglycones, such as quercetin, kaempferol, and rhamnetin, display a much higher sensitivity to light which could account for their inferior application in dyeing [5].

2. Persian yellow natural dye sources

Our systematic research and interviews with dye masters indicate the use of the plants listed in Table 6 as natural sources of yellow dyes in Persian carpets. The English and Persian common names are given (in brackets) after the scientific name. Table 6 indicates the names, geographical provenance, parts of the plant and mordant used to dye as well as lightfastness data [6–8]. Lightfastness (in the right-hand column of Table 6) was assessed according to the comprehensive study by Javidtash [8], comparing the dyed textile samples to the eight ISO Blue Wool standard samples supplied by the Ciba-Geigy group: the higher the stated value (up to 8, the most stable to light) the more lightfast the dye-mordant combination described[7].

---

[7] The ISO blue wool standards are woolen fabrics dyed with eight different blue dyes of increasing fastness to light such that blue wool 1 is the least lightfast and blue wool 8 the most lightfast. For a given light exposure, blue wool 1 shows double the change seen in blue wool 2 and so on. Fading can be assessed by a color measurement method or against a greyscale chart.

Table 6- Names of the natural sources of yellow dyes in Iran, geographic distribution as well as data on the mordants used, lightfastness, and resulting colors [6–8]

Botanical name	English name	Persian name and phonetics	Family	Distribution	Part of the plant used	Mordant	Color on fiber	Lightfastness (5–8)
Delphinium semibarbatum	Lark-spur	Zaban dar ghafa /:zæban.dær.qæfa/	*Ranuncula-ceae*	North-east of Iran	Flower, stem	Al	Yellow	3 – 4
						Cu	Bright green pista-chio	5
						Cr	Dull yellow	6.5 – 7
						Fe	Brownish gray	7 – 7.5
Eremostachys spp.	Desert rod	Sonbol-e-biabani /:sɔːnbɔːl e biːɑːbɑːniː/	*Labiatae*	West of Iran	Leaf, stem		Not tested	
Pistacia vera	Pista-chio	Pesteh /:Pestɛ/	*Anacardi-aceae*	North-east and center of Iran	Leaf, stem, unripe fruit	Al	Bright yellow canary	4 – 5
						Cu	Mustard green	7
						Cr	Mustard green	7 – 8
						Fe	Brownish grey	7
Punica gran-atum	Pome-granate	Anar /:ænɔr/	*Punicaceae*	Iran (most parts)	Leaf, stem	Al	Yellowish khaki	7 – 8
						Cu	Olive green	7 – 8
						Cr	Brownish olive green	7 – 8
						Fe	Brownish dark grey	7 – 8
Morus alba	White mul-berry	Tūt-e- sefid /:tuĭt.e.sefid/	*Moraceae*	Iran (most parts)	Leaf	Al	Bright yellow canary	3 – 3.5
						Cu	Bright olive green	5.5 – 6
						Cr	Somber yellow lime	5.5 – 6
						Fe	Greyish brown	5.5 – 6
Prangos feru-lacea	Prangos	Jashir /:dʒæshir/	*Umbelliferae*	Some parts of East, center, South of Iran	Stem	Al	Bright yellow canary	3 – 4
						Cu	Bright olive green	5.5 – 6
						Cr	Dark lemon yellow	6.5 – 7
						Fe	Greyish brown	6.5 – 7
Quercus brantii	Oak tree	*dzaft* /:dʒæft/	*Fagaceae*	East, south-east of Iran	Peel of fruit	Al	Bright brown	3
						Cu	Brown	3 – 4

Botanical name	English name	Persian name and phonetics	Family	Distribution	Part of the plant used	Mordant	Color on fiber	Lightfastness (5–8)
						Cr	Brown	4 – 5
						Fe	Dark gray	4 – 5
Reseda luteola	Weld	Isparak /:ispæræk/	*Resedaceae*	North-west, west, north-east of Iran	Stem, leaf	Al	Lemon yellow	5
						Cu	Greenish khaki	6
						Cr	Dull yellow	6
						Fe	Brownish gray	7
Vitis vinifera	Grape	Angoor /:æŋgur/ or /:moʊ/	*Vitaceae*	Iran (most parts)	Stem, leaf	Al	Cream yellow	4
						Cu	Green pistachio	4.5
						Cr	Dark cream yellow	5.5 – 6
						Fe	Brownish gray	5 – 6

***Reseda luteola* L.** (weld; *isparak*)

The yellow flowers of this plant turn into small fruits with black seeds that can be planted. A biennial or perennial plant, its favorite location is the dark shaded areas near springs[9]. It has thick and strong branches, yellow or greenish-yellow flowers, leaves that are narrowly ovate or oblong-linear in shape, and is 30–120 cm in height. Weld grows in the Ardebil, Lorestan, and Khorasan regions of Iran [11] and is planted in early summer. The plants should be picked before the blossoms fall. All the aerial parts of this plant contain colorant materials, but the flowers are the main source [9].

Armindo *et al.* studied a 16th-century Persian carpet that was preserved in the monastery of Santa Clara-a-Vella (Coimbra) before integrating the collections of the National Museum Machado de Castro (Museu Nacional Machado de Castro) [12]. The results of their analysis of yellow dyes by HPLC–DAD demonstrates the existence of luteolin-7-*O*-glucoside as the main chromophore and lower amounts of luteolin, apigenin-7-*O*-glucoside, and apigenin.

Heitor *et al.* analyzed samples from eight Indo-Persian carpets by HPLC–DAD–MS [1]. The presence of luteolin and its glucoside, luteolin-7-*O*-glucoside, in the expected proportions suggests *Reseda luteola* as a possible source for all yellows; or a dyeing source with a similar profile for all yellows.

Hallet and Santos have also studied three Safavid Persian carpets that were identified in the palace of the Dukes of Bragança in Guimarães, Portugal [13]. A luteolin-based dye (possibly weld) was the source of yellow dyes in the carpets, and it was also mixed with indigo and madder to create green and orange, respectively.

The main chromophores responsible for the yellow color of weld extracts are luteolin and apigenin. The mordant dyeing process on wool and silk provides a saturated yellow with very good lightfastness [14], which is why it has been one of the primary colorants used for many centuries.

***Delphinium semibarbatum* Bien. ex Boiss.** (yellow larkspur; *zaban dar ghafa*)

Delphinium semibarbatum (*D. zalil*) grows in deserts on the eastern and central side of Iran; in Khorasan, Kashan, and Yazd on plains and foothill meadows, where it reaches

30–80 cm in height and has pale yellow flowers [11].

According to Cardon, one of the larkspur's species with yellow flowers is called *isparak* in central Asia [3]. However, in Iran, botanists and researchers in the field of dyeing use *isparak* when referring to weld. The plant mentioned by Cardon, *D. semibarbatum*, is called '*Zaban-dar-qafa*' or '*Zaban-pas-qafa*' [6]. *Zalil* is another common name.

In recent years in Iran, the use of *zalil* for dyeing has increased. The dye, which can be extracted from the flowers, leaves, and stems of the plant, when applied on silk or wool with a mordant, creates a bright and shiny shade of yellow with good stability [14]. When pomegranate peel or alum is used with a *zalil* dyeing, it also results in a bright and fast yellow [15].

The plant is rich in flavonols present as the 3-*O*-glycosides: quercetin, isorhamnetin and kaempferol. Only 5% of the glycosides are hydrolyzed to aglycones during extraction from dyed silk [3].

Kiumarsi *et al.* analyzed the extraction process of *D. semibarbatum* for dyeing silk yarns [16]: their results identified quercetin as the main yellow chromophore. Silk yarns dyed using the pre-mordanting technique possessed good lightfastness properties.

Mouri *et al.* characterized the major components of *D. semibarbatum* and found the 3-*O*-glucosides of kaempferol, quercetin, and isorhamnetin in similar amounts in the extracts [17]. Their work confirmed the existence of the glycosides in the dye rather than the aglycones. *Zalil* has good lightfastness- the reason it is widely used for yellow colors could be due to the low content of unsubstituted flavonols in the dye.

The use of larkspur in Persian textiles has been discussed by Shibayama *et al.* [18], who analyzed Persian Safavid velvets using HPLC–DAD. Most yellow samples were dyed with *D. semibarbatum*. The authors identified quercetin 3-*O*-hexoside, kaempferol 3-*O*-hexoside, and isorhamnetin 3-*O*-hexoside as the main colorants of larkspur, in agreement with the results of Mouri *et al.* [17].

Prangos ferulacea **Lindl.** (prangos; *jashir*)

Prangos ferulacea is a perennial and gramineous plant with bright green leaves, a tall stem 80–200 cm in height, and yellow blossoms. It is seen in the Markazi, Fars, Boyer-

Ahmad, Charmahal, Isfahan, Lorestan, Hamedan, and Kerman provinces and also in part of the Alborz mountains in Iran, which have cool and mild summers [11].

There are 15 different species of this plant in Iran, which are used as forage. Species such as *P. gaubae, P. calligonoides, P. cheilanthifolia, P. tuberculate*, and *P. crossoptera* are exclusive to Iran. Other species are also found in Anatolia, Caucasus, and central Asia [6].

The colorant materials, found in its leaves and stems, produce bright yellow to olive shades with different mordants. Dyers use a combination of yellow from *jashir* and blue from indigo to create a green color in carpets [10].

Mouri *et al.* studied different *Prangos* species and found flavonol 3-*O*-glycosides as the main yellow dyes [17]. 3-*O*-Glucuronides of quercetin, isorhamnetin, or rutin were the main components. Since the dried plant lacks free aglycones, it can be used directly for dyeing.

Vitis vinifera **L.** (grape; *angoor*)[8]

The leaves of the grape, which contain the colorant material, are reported to have been used in Persia [6, 9], and [15]. The dyeing process is similar to weld and produces yellow colors with alum on protein fibers [6]. However, the yellow color produced with grape leaves on an alum mordant is not recommended due to its poor lightfastness [14].

Mouri *et al.* identified quercetin 3-*O*-glucuronide as well as some other flavonol glycosides as the main components of *V. vinifera* [17]. This accords with the results by Böhmer that confirmed quercetin as the main chromophore [14], although Downey *et al.* identified both kaempferol and quercetin glucosides in Shiraz grape leaves [19].

Morus alba **L.** (white mulberry; *tut-e-sefid*)

Wild mulberry trees are scattered in the northern jungles, but the cultivated trees are found in Kordestan, Isfahan, north of Tehran, Kermanshah, and other areas of steppes or mountainous regions [11].

---

[8] It is also called '/:moʊ/'

The oval fruit, which can be found in different sizes, consists of small white drupe-lets; the leaves are heart-shaped with small jags and contain the colorant material (Figure 9). They also provide nourishment for silkworms.

Figure 9 - *Morus alba* **(Photo © M. Sharif)**

The leaves of this tree give a yellow dye that can be altered to orange, green, or even brown by using acids in the dyeing process. The dyes are characterized by a morin core and are applied to produce a yellow color for natural fibers [6].

Eremostachys **spp.** (desert rod; *Sonbol-e-biabani*)

Desert rod is one of the plants used as a yellow colorant in the west of Iran. It grows in Isfahan, Nahavand, Lorestan, Kordestan, and Charmahal. Different parts of the plant

contain colorant material, but most of the dyes are found in the flowers which are orange, yellow, or white [9].

There are 15 species of this perennial plant in Iran, five of which are exclusively found in Iran: *E. pulvinaris, E. codonocalyx, E. hyoscyamoides, E. azerbaijanica and E. adenantha*. Other species also grow in Anatolia, Afghanistan, Caucasus, Iraq, Pakistan, Turkmenistan, and Central Asia [6].

Light yellow, dark yellow, and yellow colors are obtained using aluminum, iron and chromium ions as mordants, respectively. All these colors are shown to have medium lightfastness[9]. We were unable to locate and collect this plant in Iran to confirm its scientific and common names.

Quercus brantii **Lindl.** (oak tree; *dzaft*)[10]

This oak species is a tall tree with lobed leaves; its blossoms have a greenish-yellow color, and the fruit is semi-oval, covered by fluff. A native tree that favors mild climates, it can be found in forests in Iran such as Lorestan, Kohgilouye, Kermanshah, Kordestan, Boushehr, and near Shiraz [11]. The dye is extracted from the seed coat[11] of the acorn.

It provides a yellow color with aluminum ions as mordant. Other mordants are not applicable due to the lack of stability against light [6]. The dye belongs to the quercetin family and also contains tannin, which strengthens the colorant properties [9].

Pistacia vera **L.** (pistachio; *pesteh*)

The pistachio tree grows in central and west Asia and the Mediterranean basin. Its height can reach up to 10 m in warm areas, but the trees that grow in mild climates sometimes resemble shrubs [20].

The hull (or husk) of the pistachio nut is used to dye yellow and pale brown; this is the outer fleshy layer of the pistachio that covers the hard shell containing the nut (see

---

[9] A research project by the Handicrafts Organization of Iran (1981), Tehran.
[10] The Persian oak's fruit is called '/:bælūt/' in Persian; but the part used for dyeing is the parenchyma, which is called '/:dʒæft/'.
[11] Testa

Appendix 2- section A2.1.) Using different mordants can diversify the final colors. The soft red or yellow hull is removed during the harvest season and dried. It can be used as a natural source of yellow dye.

According to a study by Kiumarsi and Parvinzadeh- Gashti, on wool yarns it produces light and dark shades of orange [21]. The authors found that the use of metal mordants with pistachio hull increases the dyeing ability properties and the colorfastness of the dyed yarns.

Punica granatum **L.** (pomegranate; *anar*)

The pomegranate grows in wide areas of Iran, including the north, north-east, north-west, west, and south. The tree blossoms in spring, and fruits ripen in late summer to early autumn [22].

This plant contains a large amount of tannins. In the past, pomegranate peel was used in combination with sodium carbonate for cotton dyeing, and when used with saffron, it gives various colors. The peel of the fruit, which is removed and dried during autumn, contains a brownish-yellow dyestuff. It is boiled in water, and the remaining color can be used after filtration. It can be applied without a mordant, but the yellowish fawn color is not durable [6].
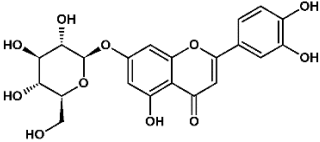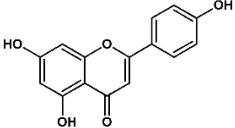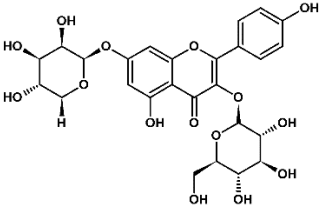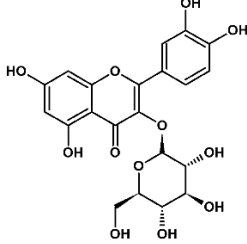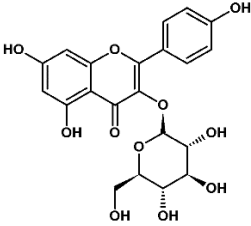
Ancient civilizations in the Mediterranean were familiar with the use of pomegranate as a dyestuff. Applying mordants such as alum or iron would result in golden yellow or grey colors, respectively.
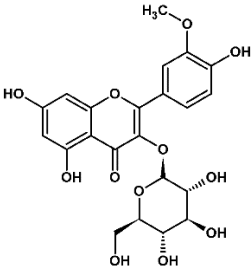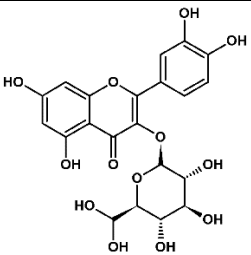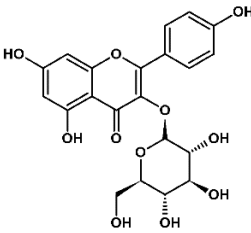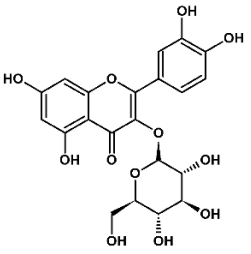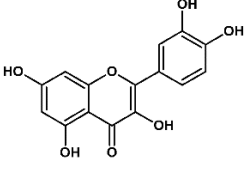
According to a study by Cardon, the colors from pomegranate were resistant to washing and light [3], but Böhmer *et al.* reported an unsatisfactory lightfastness result [14]. Tiwari *et al.* found the fastness to light, washing, and rubbing were very good in the case of wool but only just satisfactory when used on cotton fibers. The pomegranate peel dye provided them with a yellow color on cotton and brown on wool [23].

Middha *et al.* investigated the phenolic profile of *Punica granatum* fruit peel using high-performance liquid chromatography (HPLC) [24]. They identified five different flavonoids, phenolic acids, and their derivatives, including quercetin, rutin, gallic acid, el-

66

lagic acid, and punicalagin as major ellagitannin. Table 7 summarizes the main chromo-phores of the dyes in the study and their molecular structures, as well as the analytical and extraction methods used [6–8].

Table 7- Main natural sources of yellow dyes in Iran, together with the extraction and analytical methods used for their characterization

Botanical name	Components§	Structures	Authors & Analytical methods	Extraction methods
Reseda luteola	Luteolin-7-*O* glucoside; Luteolin Luteolin-3',7-*O*-diglucoside Luteolin-4'-*O*-glucoside		Wouters *et al.*, 1992 [25] HPLC-DAD	1 mg of yarn in 400 µL H_2O/MeOH/37% HCl (1/1/2) for 10 min at 100°C
			Pozzi, 2011 [26] SERS, with silver nanoparticles, λ_{exc} = 532nm	6 mL MeOH and 200 µL 37% HCl at 65°C for 60 min; the obtained solution was filtered and dried under a gentle stream of N_2
	Apigenin; Apigenin 7-*O* glucoside		Moiteiro *et al.*, 2008 [27] HPLC-DAD (Dionex system) and HPLC-MS	*R. luteola* was extracted with 15 mL of MeOH:H_2O (8:2) by sonication at 25°C for 10 min
	Kaempferol 3-*O*-glucoside-7-*O*-rhamnoside		Shibayama *et al.*, 2015 [18] HPLC-DAD	0.1-1 mg with 100 µL of 0.001 M Na_2EDTA in deionized MeOH:H_2O (2/3) at 60-70°C for 20 min. The sample was left for 1h in the solution; the extract was then evaporated. The residue was dissolved in 15 µL of 17.6% formic acid in deionized MeOH:H_2O (1/1)
Delphinium semibarbatum	Kaempferol 3-*O*-glucoside Quercetin 3-*O*-glucoside		Mouri *et al.*, 2014 [17] HPLC-DAD-MS	Extraction of raw material with MeOH:H_2O (1:1) at 65°C for 1 hour. Dyes extracted from textiles with a "soft method" (pyridine/water/1.0 M oxalic acid in water (95:95:10) at 100°C for 15 min)

68

Botanical name	Components§	Structures	Authors & Analytical methods	Extraction methods
	Isorhamnetin 3-O-glucoside		Shibayama et al., 2015 [18] HPLC-DAD	0.1-1 mg with 100 µL of 0.001 M Na₂EDTA in deionized MeOH:H₂O (2/3) at 60-70°C for 20 min. The sample was left for 1 hour in the solution; the extract was then evaporated. The residue was dissolved in 15 µL of 17.6% formic acid in deionized MeOH:H₂O (1/1)
Vitis vinifera	Quercetin 3-O-glucuronide		Mouri et al., 2014 [17] HPLC-DAD-MS	Extraction with MeOH:H₂O (1:1) at 65°C for 1 hour. Extraction of dyes with pyridine/water/1.0 M oxalic acid in water (95:95:10) at 100°C for 15 min
Morus alba	Astragalin Isoquercitrin Moracin M Moracin C		Yang et al., 2014 [28] HR-ESI-MS and NMR. Preparative HPLC .	The dried leaves were extracted twice (2 hours for each) with 95% EtOH under reflux and then the solvent was removed. The crude extract was suspended in water and extracted with ethyl acetate
Prangos Ferulacea	Flavonol 3-O-glycosides Quercetin 3-O-glucuronide Isorhamnetin/Rutin 3-O-glucuronide		Mouri et al., 2014 [29] HPLC-DAD-MS	Extraction with MeOH:H₂O (1:1) at 65°C for 1 hour. Extraction of dyes with pyridine/water/1.0 M oxalic acid in water (95:95:10) at 100º C for 15 min
Quercus brantii	Quercetin Rutin Flavonoid sulfate Flavon C and C-/O glycosides Apigenin, kaempferol, myricetin, naringenin,		Noori et al., 2015 [30] 2-Dimensional paper chromatography. UV spec. for ID	The material was boiled for 2 min in 5 ml of 70% EtOH. The mixture was cooled and left to extract for 24 h
			Çoruh et al. 2014 [31] HPLC-DAD	Extraction in methanol by using a rotating incubator at 30°C and

Botani- cal name	Components§	Structures	Authors & Ana- lytical methods	Extraction methods
			Other polyphe- nolic compounds are described	175 rpm overnight. The initial extract was then filtered

§ For each species, for the first name listed in this column, the molecular structure is represented in the third column. The main yellows, present in higher concentration, are in colored font.

3. Conclusions

The lack of historical sources on traditional dyeing techniques in Iran meant that this knowledge was preserved by oral transmission only and remained unknown to most researchers. Furthermore, traditional dyers were unaware of the scientific names of the plants, which can lead to confusing information regarding the natural dye sources. As part of future research, we intend to comprehensively characterize the natural sources of Persian yellow dyes [32]. Following their validation by botanists, analytical studies will complete the process of identification and characterization of dyes in historical textiles.

References

[1] Heitor, M., Sousa, M., Melo, M. J., Hallett, J., Oliveira, M. C. (2007). The colors of the carpets. In T. Pacheco Pereira & J. Hallett (Eds), *Carpets and paintings, 15th–18th centuries: the oriental carpet in Portugal* (pp. 161-167). Museu Nacional de Arte Antiga. ISBN: 978-972-776-339-9

[2] Ferreira, E. S., Hulme, A. N., McNab, H., & Quye, A. (2004). The natural constituents of historical textile dyes. *Chemical Society Reviews*, 33(6), 329-336.

[3] Cardon, D. (2007*). Natural dyes: sources, tradition, technology and science* (1st ed.) Archetype Publications. ISBN190498200X

[4] Zhang, X., Cardon, D., Cabrera, J. L., & Laursen, R. (2010). The role of glycosides in the light-stabilization of 3-hydroxyflavone (flavonol) dyes as revealed by HPLC. *Microchimica Acta*, 169(3-4), 327-334. Doi: 10.1007/s00604-010-0361-x

[5] Melo, M. J. (2009). History of natural dyes in the ancient Mediterranean world. In T. Bechtold, & R. Mussak (Eds.), *Handbook of Natural Colorants* (pp. 3–17), Wiley. Doi: 10.1002/9780470744970.ch1

[6] Mozaffarian, V. (1996). *A dictionary of Iranian plant names: Latin, English, Persian*. Farhang Mo'aser. ISBN 9645545404

[7] Varzi, M. (1976). *The art and industry of carpet in Iran: an overview into history of dyeing, sketch and texture* (in Persian). Raz Publications.

[8] Javidtash, I. (1996). *Dyeing method with plants and stability determination of 724 natural dyes* (in Persian). Research Institute of Forests and Rangelands.

[9] Jahanshahi-Afshar, V. (1996). *The Process and Methods of Dyeing Fibers with Natural Materials* (in Persian). University of Art.

[10] Qaranjing, K., Karimshahi, K., Pirkohan, R., Arami, M., Kharati, H. & Kiumarsi, A. (2007, November 20-21). *Optimization of dyeing conditions of wool fIbers with Jashir based on Taguchi's experiments* [Conference presentation] (in Persian). The 2nd National Seminar on the Hand-Knotted Carpet Research, Tehran, Iran.

[11] Ghahreman, A. (1978). *Flora of Iran* (vol. 7, 16, 20, 23), Research Institute of Forests and Rangelands.

[12] Armindo, E., Sousa, M., Melo, M. J., Hallett, J. A. (2008). A Persian carpet's paradise garden: discovering historical and technical aspects through carpet conservation and restoration. In J. Bridgland (Ed.), *The 15th triennial ICOM committee for conservation conference* (pp. 960-66). Allied Publishers Pvt. ISBN: 9788184243444

[13] Santos, R., Hallett, J. (2015). Interwoven knowledge: the understanding and conservation of three Islamic carpets. In A. Gerritsen, & G. Riello (Eds.), *Writing material*

culture history (pp. 257-64). Bloomsbury Publisher. ISBN-10: 147251856X

[14] Böhmer, H., Enez, N., Karadağ, R., Kwon, C., Fogelberg, L.E. (2002). *Koekboya: natural dyes and textiles, a color journey from Turkey to India and beyond* (L.E. Fogelberg Trans.). REMHÖB-Verlag.

[15] Wulff, H. E. (1966). *The traditional crafts of Persia* (1st ed.). MIT Press. ISBN 0262230259

[16] Kiumarsi, A., Gashti, M. P., Salehi, P., & Dayeni, M. (2016). Extraction of dyes fromDelphinium Zalilflowers and dyeing silk yarns. The Journal of The Textile Institute, 108(1), 66-70. Doi: 10.1080/00405000.2016.1153865

[17] Mouri, C., Mozaffarian, V., Zhang, X., & Laursen, R. (2014). Characterization of flavonols in plants used for textile dyeing and the significance of flavonol conjugates. *Dyes and Pigments*, 100, 135-141. Doi: 10.1016/j.dyepig.2013.08.025

[18] Shibayama, N., Wypyski, M., & Gagliardi-Mangilli, E. (2015). Analysis of natural dyes and metal threads used in 16th -18th century Persian/Safavid and Indian/Mughal velvets by HPLC-PDA and SEM-EDS to investigate the system to differentiate velvets of these two cultures. *Heritage Science*, 3(1). Doi: 10.1186/s40494-015-0037-2

[19] Downey, M. O., Harvey, J. S., & Robinson, S. P. (2003). Synthesis of flavonols and expression of flavonol synthase genes in the developing grape berries of Shiraz and Chardonnay (*Vitis vinifera* L.). *Australian Journal of Grape and Wine Research*, 9(2), 110-121. Doi: 10.1111/j.1755-0238.2003.tb00261.x.

[20] Sabeti, H. (2008). *Forests, Trees and Shrubs of Iran* (in Persian). Yazd University Press; p. 257

[21] Kiumarsi, A., & Gashti, M. P. (2015). Pistachio hulls, A new source of fruit waste for wool dyeing. *Journal of Textile Science & Engineering*, 05(01). Doi: 10.4172/2165-8064.1000185

[22] Mirjalili, A. (2016). *Flora of Iran; Punicaceae family* (Vol. 81) (in Persian). Research Institute of Forest and Rangelands.

[23] Tiwari, H. C., Singh, P., Mishra, P. K., & Srivastava, P. (2010). Evaluation of various techniques for extraction of natural colorants from pomegranate rind-ultrasound and enzyme assisted extraction. *Indian Journal of Fiber & Textile Research*, 35(3), 272-276.

[24] Middha, S. K., Usha, T., & Pande, V. (2013). HPLC Evaluation of Phenolic Profile, Nutritive Content, and Antioxidant Capacity of Extracts Obtained fromPunica granatumFruit Peel. *Advances in Pharmacological Sciences*, 2013, 1-6. Doi: 10.1155/2013/296236

[25] Wouters, J., & Rosario-Chirinos, N. (1992). Dye analysis of pre-Columbian Peruvian textiles with high-performance liquid chromatography and diode-array detection. *Journal of the American Institute for Conservation*, 31(2), 237-255. Doi: 10.1179/019713692806066637

[26] Pozzi, F. (2011). *Development of innovative analytical procedures for the identification of organic colorants of interest in art and archaeology* [Doctoral dissertation, University of Milan]. UniMi Repository. http://hdl.handle.net/2434/167821

[27] Moiteiro, C., Gaspar, H., Rodrigues, A. I., Lopes, J. F., & Carnide, V. (2008). HPLC quantification of dye flavonoids inReseda luteolaL. from Portugal. *Journal of Separation Science*, 31(21), 3683-3687. Doi: 10.1002/jssc.200800383

[28] Yang, Y., Yang, X., Xu, B., Zeng, G., Tan, J., He, X., . . . Zhou, Y. (2014). Chemical constituents of Morus alba L. and their inhibitory effect on 3T3-L1 preadipocyte proliferation and differentiation. *Fitoterapia*, 98, 222-227. Doi: 10.1016/j.fitote.2014.08.010

[29] Mouri, C., Aali, A., Zhang, X., & Laursen, R. (2014). Analysis of dyes in textiles from the Chehrabad salt mine in Iran. *Heritage Science*, 2(1). Doi: 10.1186/s40494-014-0020-3

[30] Noori, M., Talebi, M., & Ahmadi, T. (2015). Comparative Studies of Leaf, Gall and Bark Flavonoids in Collected *Quercus brantii* Lindl. (Fagaceae) from Lorestan Province, Iran. *International Journal of Plant Research*, 5(2), 42-49. Doi: 10.5923/j.plant.20150502.03

[31] Çoruh, N., Nebigil, C., & Özgökce, F. (2014). Rapid and comprehensive separation for the phenolic constituents of *Quercus brantii* acorns by Rp-Hplc-Dad. *Journal of Liquid Chromatography & Related Technologies*, 37(6), 907-915. Doi: 10.1080/10826076.2012.759126

[32] Sharif, S., Nabais, P., Melo, M. J., & Oliveira, M. C. (2020). Traditional yellow dyes used in the 21st century in central Iran: the knowledge of master dyers revealed by HPLC-DAD and UHPLC-HRMS/MS. *Molecules*, 25(4), 908. Doi: 10.3390/molecules25040908

Chapter 3. Traditional Yellow Dyes Used in the 21st Century in Central Iran: The Knowledge of Master Dyers Revealed by HPLC-DAD and UHPLC-HRMS/MS

76

Abstract

This work provides new knowledge on natural yellows used in Iran. Seven biological sources were selected based on interviews with dye masters in Isfahan workshops (Iran). *Delphinium semibarbatum*, *Eremostachys laevigata*, *Prangos ferulacea*, *Morus alba*, *Pistacia vera*, *Punica granatum*, and *Vitis vinifera* are currently used in these workshops. Aiming to study the dye composition of wool samples dyed with the extracts of the selected biological sources, and the changes induced by the dyeing procedures in the original chemical composition of the plant extract, raw materials and dyed wool (by us and in the workshops) were analyzed by HPLC–DAD and UHPLC–HRMS/MS. In solutions extracted from the textiles, the main yellows for *E. laevigata* are luteolin-*O*-glycosides. In the other plant sources, the main chromophores are based on 3-*O*-glycosides of kaempferol, quercetin, and isorhamnetin. In pistachio hulls, myricitin derivatives were detected, and we propose their use as markers. Generally, the solutions extracted from the wool displayed a higher amount of more polar compounds, but also a higher amount of aglycones. Importantly, the chromatographic profiles of the samples we prepared compared well with 17th c. yellows in Persian carpets, and therefore can be considered highly characterized references for the study of Persian yellows.

Keywords: dye analysis; soft extraction methods; Persian dyes; flavonoids; HPLC; mass spectrometry; yellow colors; conservation

1. Introduction

1.1 Medieval oriental carpets: an inherited knowledge for skilled practitioners

In medieval times, dyeing was a craft exclusive to a few skilled individuals who made brilliant, fast colors using inherited recipes [1, 2]. The knotted-pile oriental carpet, a surface composed of warp, weft, and knot, was an artistic object as well as a luxury good and, as such, also an object of status [2]. Medieval Persian carpets were made with brilliant, fast colors from a handful of natural dyestuffs. These natural dyes give very attractive non-uniform colors, which present differences in shade and intensity around a certain hue that create the illusion of movement—a vibrato effect [2]. Although we have evidence that the sources for red and blue were widely traded [1], recent research has shown

that yellow dye plants may have been regional [3–5]. This was corroborated in our case study on natural yellow dyes used in Isfahan, a province in the central part of Iran (covering an area of 107,029 km^2). Our research focused on the study of natural colorants used to dye yellow in Persia, in Isfahan, where, in the 21st century, dyeing with natural dyes is still practiced in workshops by skilled masters. Our main goal was to provide reference chromatographic profiles for dyes that were used to dye textiles in yellow, or combined with other dyes such as madder to create orange and brown hues. Thus, these profiles refer to solutions extracted from textiles. In this work, extracts from reference materials were compared with those obtained from wool threads dyed in Isfahan workshops, and with published data on the characterization of yellows in Persian carpets. In the next section, we describe how the plant sources were selected for this study and the main yellow dyes were found in their extracts. This description is followed by a summary of the chromophores and plant sources that have been identified in the literature as being used to dye yellow in historical artworks, in particular Persian carpets. Whenever possible, we selected data collected by HPLC-DAD-MS (high-performance liquid chromatography equipped with diode array and mass spectrometry detectors) using mild extraction procedures that preserved the integrity of the natural yellow chromophores, avoiding hydrolysis of the glycosidic linkages [3, 5].

1.2 Yellow flavonoids extracted from plants in Persia and 21st c. Iran

Recently we prepared a review on plants that were used as sources of natural yellow dyes in Persian carpets [6], Figure 10-12. The plants studied in the present work were selected based on that review (in particular, on data gathered regarding Persian and Iranian flora sources [7, 8]), on recent characterization of yellows on Persian textiles, and on interviews with the few remaining dye masters in workshops located in Isfahan (central Iran)[12]. Cross-referencing the data gathered, we arrived at the list of nine plants that are found in Table 8. The species selected were in agreement with what is described in the reference book by Dominique Cardon [1], and with recent research carried out by Richard Laursen's group at Boston University [3, 4, 9–11]. The fundamental yellow chromophores

---

[12] In Isfahan workshops, *Reseda luteola* and *Quercus brantii* are not being used by the dye masters that we interviewed, and for that reason, they were not included.

that were extracted from these plants are flavonoids based on the flavone and flavonol chromophore, Figure 10-12. In literature, flavone-based yellows are considered more stable than flavonols, but the latter might be stabilized by transforming the OH group in position 3 into an *O*-glycoside [5, 10].

Luteolin
$C_{15}H_{10}O_6$ MW 286.239

Luteolin-*O*-glucoside
$C_{21}H_{20}O_{11}$ MW 448.38

Luteolin-*O*-di-glucoside
$C_{27}H_{30}O_{16}$ MW 610.521

Luteolin-7-*O*-malonyl hexose
$C_{24}H_{22}O_{14}$ MW 534.426
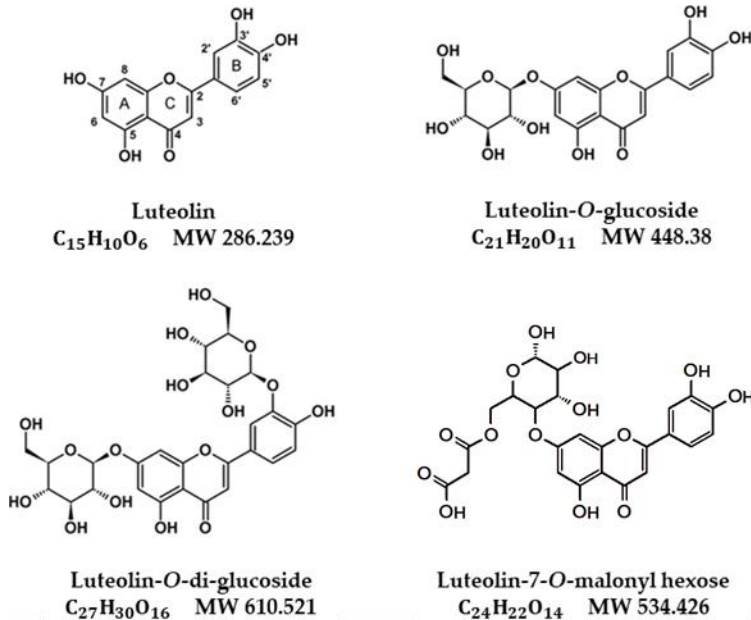
Figure 10- Luteolin-based chromophores (flavones).

Quercetin-3-*O*-glucoside
$C_{21}H_{20}O_{12}$ MW 464.38

Quercetin-3-*O*-glucuronide
$C_{21}H_{18}O_{13}$ MW 478.36

Quercetin-3-*O*-rutinoside (rutin)
$C_{27}H_{30}O_{16}$ MW 610.521

Isorhamnetin
$C_{16}H_{12}O_7$ MW 316.26
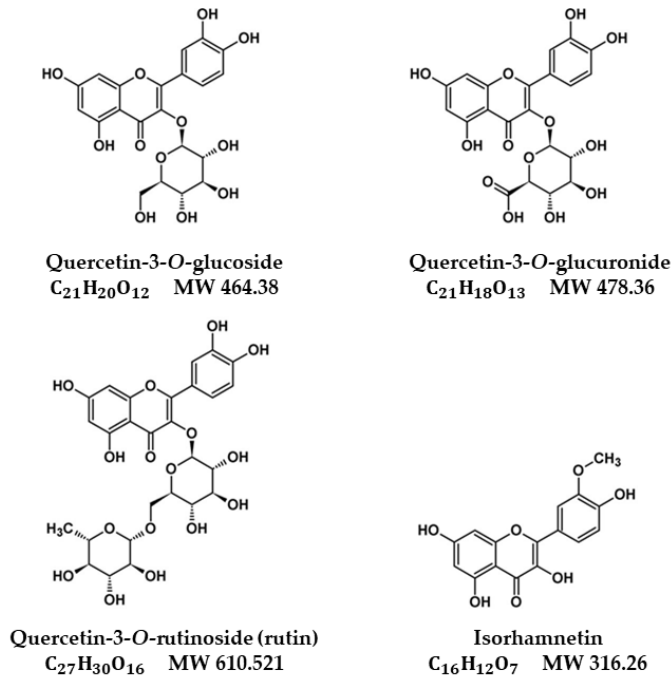
Figure 11- Quercetin-based chromophores (flavonols).

Kaempferol-3-*O*-glucoside
$C_{21}H_{20}O_{11}$ MW 448.101

Kaempferol-3-*O*-acetyl-glucose
$C_{23}H_{22}O_{12}$ MW 490.111
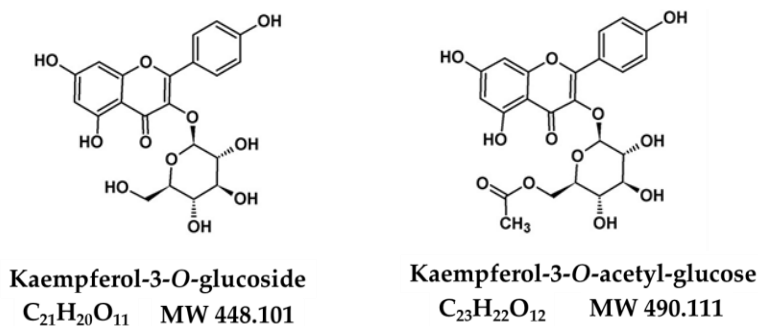
Figure 12- Kaempferol-based chromophores (flavonols).

Most of the plant extracts have been analyzed by HPLC-DAD or HPLC-DAD-MS [4–6, 12–15], and, for some, accurate quantifications of the yellow flavonoids have been published [16, 17]. On the other hand, chromatographic profiles of extracts from textiles dyed with these plants could only be found in cultural heritage studies for *D. semibarbatum*, Table 8. For this biological source, we had access to both the characterization of the plant extracts and of the solutions extracted from textiles [18]. For the other natural sources studied in this work, data on the yellow chromophores were only available for the plant extracts. Yellows present in the leaves of *Pistacia vera* were also analyzed by Laursen's group, but they are not described here, because it is the pistachio hull that is used in Isfahan workshops [6]. In this group, Mouri *et al.* studied by HPLC-MS, *D. semibarbatum*, *P. ferulacea*, and *V. vinifera* extracts, which were obtained using water: methanol (1:1, *v:v*) [4], Table 8. *Delphinium semibarbatum* is characterized by nearly equimolar amounts of the 3-*O*-glucosides of kaempferol, quercetin, and isorhamnetin [4] Figure 11 and 12). Flavonol 3-*O*-glycosides were also the yellows found in all the twelve species of *Prangos* analyzed, displaying as major compounds 3-*O*-glucuronides of quercetin and isorhamnetin, or rutin [4] (Table 8). The first was also found to be the main yellow chromophore in extracts of *Vitis vinifera* leaves [4] (Table 8). Hmamouchi *et al.* [13] also studied *Vitis* leaves that were extracted with water: methanol (80:20, *v:v*). The aglycones in this study were identified in HPLC chromatograms obtained at 340 nm by comparison with references, whereas sugars were analyzed by TLC. Together with 3-*O*-glycosides of quercetin, the presence of apigenin-7-glucoside and luteolin-7-glucoside was also reported, which agreed with the analysis carried out by TLC by Böhmer *et al.* after hydrolysis with strong acids such as sulfuric or hydrochloric acids [14].

Table 8- Main components described in literature for the plant sources. Plant origin, and analytical, and extraction methods are described.

Plant Source	Reference	Origin	Equipment	Extraction	Main Yellow Flavonoids [1]
Delphinium semibarbatum	Mouri *et al.* [4]	Uzbekistan, Turkey	HPLC-DAD-MS	MeOH:H_2O (1:1, *v:v*) @65°C	Kae-3-*O*-Glc, Que-3-*O*-Glc, Irh-3-*O*-Glc
Prangos spp. (12 species)	Mouri *et al.* [4]	Iran	HPLC-DAD-MS	MeOH:H_2O (1:1, *v:v*) @65°C	Que-3-*O*-Glr, Irh-3-*O* Glr
Vitis vinifera (leaves)	Mouri *et al.* [4]	Iran	HPLC-DAD-MS	MeOH:H_2O (1:1, *v:v*) @65°C	Que-3-*O*-Glr, other flavonol glycosides (minor amounts)
Punica granatum (peel)	El-Hadary and Fawzy Ramadan [15]	Egypt	HPLC-DAD	MeOH: H_2O (4:1, *v:v*) @ rt	Que, Kae-3-(2-*p*-coumaroyl) Glc, Api-6-Rha- 8-galactose, Lut-7-Glc
Eremostachys azerbaijanica (aerial parts)	Asnaashari *et al.* [19]	Iran	HPLC @220 nm; NMR	*n*-hexane, CH_2Cl_2 and MeOH	Lut-7-*O*-Rut
Morus alba (leaves)	Katsube *et al.* [20]	Japan	HPLC-MS, NMR	EtOH:H_2O	Que 3-(6-malonyl)-Glc, rutin, Que-3-*O*-Glc
Morus alba (var. *korin* and var.*morettiana*) (leaves)	Dugo *et al.* [21]	Italy	HPLC-DAD-MS	EtOH (95%) @ rt	Kae-3-*O*-Rha-Glc, Kae-3-*O*-Glc, rutin, isoquercetin
Pistacia vera (hull)	Ersan *et al.* [22]	Turkey	HPLC-DAD-MS, UHPLC-DAD-ELSD	MeOH:H_2O:HCOOH (80:19:1, *v:v:v*)	Que-3-*O*-galactoside, Que-3-*O*-Glr, Que-3-*O*-Glc, Que-galloyl hexoside Que-pentoside

[1] Abbreviations: Que, quercetin; Kae, kaempferol; Lut, luteolin; Api, apigenin; Irh, isorhamnetin; Glc, glucoside; Glr, glucuronide; Hex: hexoside; Pent: pentoside; rt, room temperature.

For pomegranate and *Eremostachys* species, the data available on yellow flavonoids is scarce. In the case of *Punica granatum*, this is because extractions were carried out in strong acidic media, and for this reason, the compounds identified were mainly flavonoid aglycones [14, 15]. More recently, dihydrokaempferol-hexose was identified by HPLC-MS [16]. The extracts of its peel are dominated by the presence of polygalloyl esters of glucose (being punicalagin a marker for *Punica)*, and gallic and ellagic acids [16, 17]. The main aglycones are listed in Table 8. For *Eremostachys* spp., luteolin-7-*O*-rutinoside was identified by Asnaashari *et al.* [19]; chromatograms were obtained by monitoring at 220 nm, and the identification was performed via proton nuclear magnetic resonance (H-NMR; Table 8).

For mulberry leaves and pistachio hulls, a complete identification of the main yellow flavonoids together with accurate quantifications was published by Dugo *et al.* and Ersan *et al.*, respectively [19, 20]. For *Morus alba*, the flavonoid profile is dependent on the cultivars, as shown by Dugo *et al.*; for the morettiana cultivar, the two main yellow flavonoids were identified as rutin and isoquercitrin (quercetin 3-glucoside), in agreement with previous studies by Katsube *et al.* [20]. This author identified quercetin 3-(6-malonyl)-glucoside as the major flavonol glycoside, together with rutin and isoquercitrin, by HPLC-MS and H-NMR. For the korin cultivar, Dugo *et al.* observed a distribution over a wider number of flavonol glycosides, including kaempferol 3-*O*-glycosides, which were present in lower relative concentrations when compared to the morettiana cultivar [21] (Table 8).

Ersan *et al.* showed that flavonol glycosides comprise 5.7–16.3% of total phenolic constituents in pistachio hulls, anacardic acids being the major compounds (64.6–80.4% of total phenolics), followed by gallotannins (13.4–21.2%), such as β-glucogallin, gallic acid, and penta-*O*-galloyl-β-D-glucose [22] (Table 8). Quercetin 3-*O*-galactoside and quercetin 3-*O*-glucuronide were found to be the major yellow flavonoids together with quercetin 3-*O*-glucoside [22] (Table 8). As minor compounds, Ersan et al. tentatively identified myricetin 3-*O*-galactoside, myricetin hexuronide, myricetin hexosides, quercetin pentoside, quercetin hexosides, and traces of kaempferol hexosides and pentoside [22].

In summary, with the exception of *Eremostachys* species, characterized by a flavone chromophore of the luteolin type (Figure 10), in all the other plants, the main chromophores are based on flavonol 3-*O*-glycosides, which display a higher stability to light

when compared to the parent aglycones shown in Figure 11 and 12. For this reason, Mouri *et al.* concluded that "the dried plant can be used directly for dyeing and no precautions need be taken in drying it" (as is not the case with *Sophora japonica*); this was possibly one of the reasons why these plants were selected in the past to dye textiles [4]. It is also interesting to note that in two of the six plants, in the parts chosen to be extracted (peel for pomegranate and hull for pistachio), the phenolic fraction is dominated by gallotannins (polygalloyl esters of glucose), and it is known that these compounds play an important auxiliary function in textile dyeing [1].

1.3 Yellow dyes analyzed in Persian textiles

HPLC-DAD-MS remains one of the best methods available for identifying the colorants used in historical works, and can provide information as to where, when, and how historical and archaeological textiles were made, allowing their quantification when a calibration curve is used [23]. The main published works using HPLC-DAD or HPLC-DAD-MS for characterizing yellows in Persian textiles were carried out at Boston University, at the University NOVA of Lisbon (Department of Conservation and Restoration), and at the Metropolitan Museum of Art, MET, (New York) [18,24–26]. The main results are listed in Table 9 and show that in the Portuguese collections, the main chromophores are based on luteolin-7-*O*-glucosides, and in the MET collection, on flavonol 3-*O*-glycosides. In two of the publications, the authors proposed as plant sources *Reseda luteola* [25], and *Delphinium semibarbatum* and *Carthamus tinctoria* [18]. For more details, please see below.

One "small silk Kashan", one "tree and animal", and seven "Indo-Persian design" wool carpets from the 17th century, in the collection of "Museu Nacional de Arte Antiga", were studied by Heitor *et al.* by HPLC-DAD and LC-MS [24]. Except for the small silk Kashan, luteolin-7-*O*-glucoside was identified as the major yellow chromophore, together with minor amounts of luteolin and apigenin. Orange colors were obtained by adding alizarin, in various amounts, to the previously described yellow. In the "small silk Kashan", the yellow extracts were characterized by the presence of rutin, quercetin, and (iso)-rhamnetin-3-*O*-glucoside, as well as small percentages of luteolin and isoquercetin, suggesting golden rod or Persian berries as possible dye sources. In all the samples, aluminum ion was identified as the mordant by ICP-AES.

A "vine scroll" carpet held in the "Museu Nacional Machado de Castro" from the Safavid period (late 16th to early 17th century) composed of wool pile and silk wrap was analyzed by HPLC-DAD by Armindo *et al.* [25]. As in previous studies, luteolin-7-*O*-glucoside was detected as the main chromophore in yellows, together with minor amounts of luteolin, apigenin-7-*O*-glucoside, and apigenin (Figure 10 and Table 9). As in the previous case, alizarin was detected in orange colors admixed with yellow dyes. ICP-AES analysis revealed aluminum ion as the mordant.

Santos *et al.* analyzed three Persian carpets which were knotted in wool on a silk foundation with metal (silver) thread decors [26]. These Safavid carpets, known as the "Salting carpets", were discovered in the palace of the Dukes of Bragança in Guimarães. The authors proposed *Reseda luteola* as the source for yellows and a combination of *Reseda luteola* and madder for orange (Table 9).

Persian velvets embellished with metal threads in the MET collection were studied by Shibayama *et al.* by HPLC-DAD [19]. These authors proposed the use of yellow larkspur *(Delphinium semibarbatum)* based on the identification of quercetin 3-*O*-hexoside, kaempferol 3-*O*-hexoside, and isorhamnetin 3-*O*-hexoside as the main flavonoids (Figure 10 and Table 9). In two samples, a combination of yellow larkspur with another plant source containing luteolin, luteolin-7-*O*-glucoside, and apigenin was found, a mixture similar to what was found in the "small silk Kashan" [24]. In another sample from a different velvet, kaempferol-3-*O*-glucoside was identified as the major chromophore together with minor amounts of carthamin and quinochalcone, which indicates that safflower plant (*Carthamus tinctoria*) may have been one of the dye sources.

In summary, in historical Persian textiles, flavone chromophores such as luteolin-7-*O*-glucoside have been found as the main sources for yellows. Oranges were obtained by adding alizarin (probably extracted from madder, *Rubia tinctorum*) to the yellows.

Table 9- Yellow flavonoids identified in Persian textiles, analytical methods used in their identification, and number of samples analyzed.

Dye source	Reference	Location [1]	Equipment	Artwork [2]	Main yellow flavonoids
Luteolin based	Heitor [24]	MNAA	HPLC-DAD, LC-MS	16th c. wool carpets, 9 samples	Lut-7-*O*-Glc low amounts of Lut, Api
R. cartharicus or *Solidago virgaurea*	Heitor [24]	MNAA	HPLC-DAD, LC-MS	16th c. silk carpet, 5 samples	Rutin, quercetrin, (iso)-rhamnetin-3-*O*-Glc, and low percentage of Lut, isoquercitin
Luteolin based	Armindo *et al.* [25]	MNMC	HPLC-DAD	Late 16th c. wool carpet, 2 samples	Lut-7-*O*-Glc, low amounts of Lut, Api-7-*O*-Glc, Api
Reseda luteola	Santos [26]	Palace of Bragança	HPLC-DAD HPLC-MS	15–17th c. wool carpet, 7 samples	Lut-di-*O*-Glc, Lut-7-*O*-Glc, Api-7-*O*-Glc, Lut
Delphinium semibarbatum	Shibayama *et al.* [18]	MET	HPLC-PDA	16–18th c. silk velvet, 13 samples	Que3-*O*-hexoside, Kae-3-*O*-hexoside, and Irh-3-*O*-hexoside
D. semibarbatum + *R. luteola*	Shibayama *et al.* [18]	MET	HPLC-PDA	16–18th c. silk velvet, 2 samples	Lut, Lut-7-*O*-Glc, Api
Unknown flavonoid-containing plant + *Carthamus tinctoria*	Shibayama *et al.* [18]	MET	HPLC-PDA	16–18th c. silk velvet, 1 sample	Kae-3-*O*-Glc, minor amounts of quinochalcone and carthamin

[1] Abbreviations: MNAA, Museu Nacional de Arte Antiga (Portugal); MNMC, Museu Nacional Machado de Castro (Portugal); Palace of Bragança, Palace of the Dukes of Bragança (Portugal); MET, Metropolitan Museum of Art (New York, USA). [2] Samples were extracted using "soft" extraction methods. For more details, please see references.

1.4 Design and main objectives

In this work, plant extracts were used to dye wool references with alum as mordant, based on the essential steps used in medieval times to dye textiles, and the extracts obtained from both the plant and from the dyed wool references were characterized by HPLC-DAD-HRMS/MS. The latter were compared with wool threads dyed in Isfahan workshops and with published data on the characterization of yellows in Persian carpets. Additionally, the chromatographic profiles obtained from the plant extracts were compared with extracts from the dyed textiles, and the changes observed are discussed. Chromatographic profiles for solutions extracted from wool textiles dyed with *E. laevigata*, *P. ferulacea*, *M. alba*, and *P. vera* (hull) were for the first time obtained and the changes induced by the dyeing procedure discussed. Extraction was performed using mild extraction procedures [4] to retain the glycoside moiety, avoiding decomposition that occurs in strong acidic media to their parent aglycons. This research will provide new knowledge on the past and current natural yellows used to dye in Iran, which is important information for their preservation for future generations.

2. Results and Discussion

2.1. Plants selected and collected in Iran

In the workshops in Isfahan, the sources for yellow were obtained from plants (Table 10). Based on the interviews in Isfahan dyeing workshops, three plants may have been used in Iran as sources for yellow as a main color: *Delphinium semibarbatum*, *Eremostachys laevigata*, and *Prangos ferulacea;* however, in Isfahan workshops, only *D. semibarbatum* is currently used as the main source for saturated yellows (Table 10). The other plants are used to produce orange and brown colors or as co-dyes to create shades and/or intensify the yellow color (Table 10). Shades of yellow, orange, or brown colors are produced by combining *D. semibarbatum* with other dyes extracted from *Eremostachys laevigata, Morus alba, Vitis vinifera, Punica granatum*, and *Pistacia vera*. The color palette for yellows is thus variegated, as certain sources are used to create the main yellow colors and others are combined to produce oranges, dark yellows, and brownish colors.

Table 10- Plant sources and parts used to dye yellow in Isfahan workshops, together with the place and date of their acquisition. Prangos may be used as main yellow in other regions of Iran.

Scientific name	Icon §	Common name	Color type	Parts of the plant used	Acquired/Collected
Delphinium semibarbatum		Yellow larkspur	Main	Flower	In the workshop of H. Banitaba/ Tudeshk, August 2016
Eremostachys laevigata		Desert rod	Main	Leaf, stem (crushed)	In the workshop of R. Zakeri/Murcheh khvort, August 2016
Prangos ferulacea		Prangos	Secondary	Leaf, stem (crushed)	In the workshop of R. Zakeri/Murcheh khvort, August 2016
Punica granatum		Pomegranate	Secondary	Peel (powder)	In the workshop of H. Banitaba/ Tudeshk, August 2016
Morus alba		White mulberry	Secondary	Leaf	Collected August 2016
Pistacia vera		Pistachio	Secondary	Hull	Collected August 2016
Vitis vinifera		Vine	Secondary	Leaf	Collected August 2016

§ Icons as used in Figure 14. The icons for *E. laevigata*, *P. ferulacea*, and *P. granatum* do not identify the plant, but that it was acquired as a crushed or powdered material.

Eremostachys laevigata is the only species that produces luteolin-based chromophores (Figure 10); the crushed leaves and stems were supplied by the workshop of R. Zakeri, and it was used as such to produce the plant extracts to dye our wool samples (Figure 13). *Prangos ferulacea* came from the same workshop, as did crushed leaves and stems, and the flowers of *Delphinium semibarbatum* were obtained from a workshop located in Tudeshk. Both species are a source of quercetin and kaempferol glycosides (Figure 11 and 12). The secondary colors, *Morus alba* leaves, and *Pistacia vera* hulls, were collected from nature by the author; *Punica granatum* was acquired in one of the workshops (Table 8 and 10).
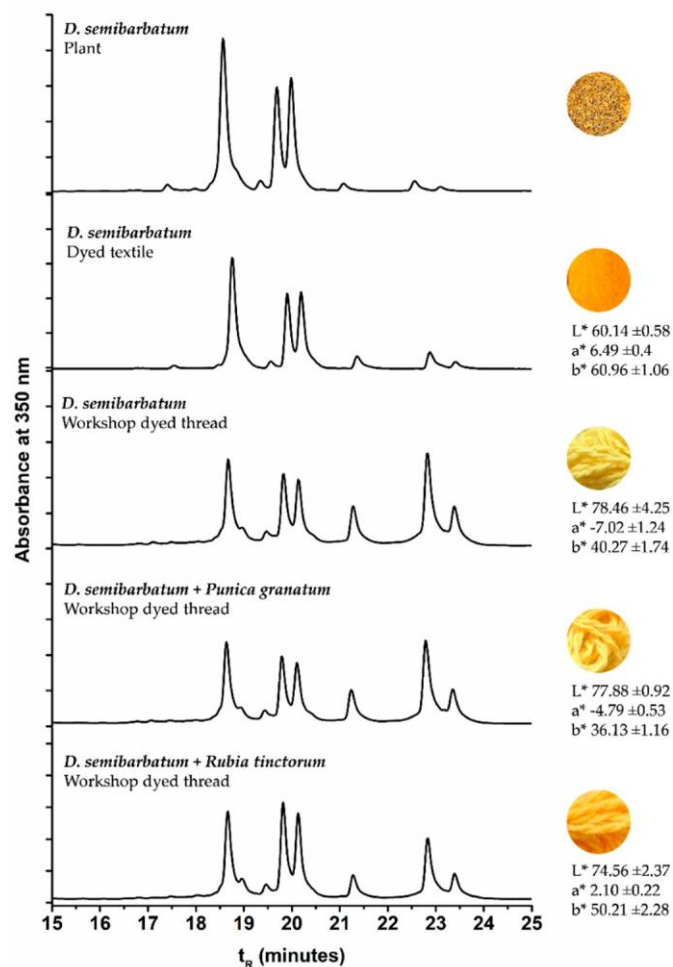
Figure 13 - HPLC-DAD profiles for *D. semibarbatum* extract compared with the extracts from our reference sample and samples acquired at the workshop, together with the L*, a*, b* coordinates[13].

2.2 Characterization by UHPLC- HRMS/MS and HPLC-DAD of the main chromophores in the plants collected in Isfahan and in dyed wool references

Extracts of plant material and dyed wool were analyzed by HPLC-DAD and UHPLC-HR tandem mass spectrometry to fully characterize the main yellow chromophores present in the biological sources. The information is summarized in Table A.3.1[14]. Compounds were identified based on their UV-VIS data and accurate *m/z* values released as deproto-

---

[13] The first three major peaks in the all chromatograms are the glucosides of quercetin, kaempferol, and isorhamnetin. Other peaks in the lower three chromatograms are the aglycones of quercetin, kaempferol, and isorhamnetin

[14] See Appendix 2 for all the tables and figures related to this chapter.

nated molecules [M–H]⁻, considering the accuracy and precision of the measurement parameters, such as error (ppm) and mSigma. Each molecular formula was validated by extracting the ion chromatograms from the raw data, and the accurate mass, isotopic, and fragmentation pattern were evaluated. The typical UV-VIS spectra obtained for major yellow components revealed a band I with a maximum of absorption between 350 and 370 nm, pointing to a flavonol structure (Table A3.2). The compounds were confirmed by comparison with analytical standards or published data.

Delphinium semibarbatum: The main yellow chromophores present in this plant are *O*-glucosides of quercetin, kaempferol, and isorhamnetin, according to the study of Mouri *et al.* [4]. Two minor compounds with *m/z* 609.1461 and 447.0929 were also identified and attributed based on the MS/MS fragmentation patterns to a quercetin-*O*-di-glycoside and to a kaempferol-*O*-hexoside, respectively.

The latter was assigned to a kaempferol structure based on the absence of the fragment *m/z* 133.0283 [^{1,3}B]⁻, which is a diagnostic fragment of luteolin derivatives, in the ESI(-) tandem mass spectrum[15]. The HRMS of plant extracts confirmed that *D. semibarbatum* contains a very low content of aglycones; however, in dyed wool extracts, the appearance of signals at *m/z* 301.0358, 285.0412, and 315.0519, indicates that during the preparation of the dyed wool references, deglycosylation of flavonol glycosides occurred.

Eremostachys laevigata: UV-VIS data of the flavonoid compounds present in this plant lay in the 340–350 nm region, suggesting the presence of flavone structures (Table A.3.2-B). The HRMS/MS data confirmed that the main yellow components were luteolin-*O*-glycosides derivatives. Peaks at t_R 18.37 (6.18) and 20.28 (6.49) min were assigned to luteolin-pentoside-hexoside (*m/z* 579.1362) and luteolin-7-*O*-acetyl-glucoside (*m/z* 489,1040); the smaller one at t_R 19.38 (6.49) min was attributed to a luteolin-7-*O*-glucoside by comparision with a standard. Based on the fragmentation patterns observed in the MS/MS spectrum, peaks at 18.58 (6.37) and 21.55 (8.08) min were identified as luteolin-7-*O*-rutinoside and a malonyl derivative of luteolin glucoside, respectively. In the dyed

---

[15] According to: (Fabre, N., Rustan, I., de Hoffmann, E., & Quetin-Leclercq, J. (2001). Determination of flavone, flavonol, and flavanone aglycones by negative ion liquid chromatography electrospray ion trap mass spectrometry. *Journal of the American Society for Mass Spectrometry*, 12(6), 707-715).

wool extracts, the luteolin-malonyl-glucoside was found together with the luteolin agly-cone.

Morus alba: The UV-VIS spectra showed a maximum at 350 nm for plant and dyed wool extracts, indicating that the main yellow compounds had a flavonol structure (Table A3.2-C). Based on the HRMS/MS spectra, the more intense signals at 18.63 (6.08) and 19.03 (6.41) min were identified as rutin and quercetin-3-*O*-glucoside, respectively, in accord-ance with previous results [20, 21]. Minor peaks eluting at 19.77 (6.66), 19.87 (7.03), and 20.33 (7.43) min were assigned to *O*-glycoside derivatives of kaempferol. Although the more abundant yellow components were flavonol 3-*O*-glucosides, signals related to their aglycones were not found in the dyed wool extracts.

Pistacia vera: In this study, the plant extract was obtained from the pistachio hulls and not from leaves, as reported by Mouri *et al.* [4]. However, both parts of these speci-mens seemed to have similar flavonoid profiles, and the hull flavonoid profile assessed in our study was also in accordance with Ersan *et al.* [22]. HPLC profiles are shown in Table A3.2-D, having characteristic UV-VIS absorption around 350 nm pointing to fla-vonol glycosides. Peak 1 at t_R 17.25 (5.71) min was observed with the co-elution of two compounds with *m/z* 493.0628 and 479.0834 assigned to myricetin-*O*-glucuronide and quercetin-*O*-glucoside, respectively. Peak 3 (R_t 6.45 min) results from co-elution of two compounds: quercetin-3-*O*-glucuronide (*m/z* 477.0675) and quercetin-3-*O*-glucoside (*m/z* 463.0883), the main constituents of the extract. The smaller peaks were attributable to quercetin and kaempferol glycoside derivatives. The MS/MS spectrum also exhibited a deprotonated molecule with *m/z* 447.0940 (t_R 6.98 min), which gave fragments with *m/z* 285.0406 and 284.0331, attributed to luteolin-7-*O*-glucoside by comparison with the stand-ard. The peak at t_R 22.00 (9.16) min was assigned to the aglycone, luteolin.

The identification of small amounts of luteolin and its glycoside derivative in pista-chio hulls has been previously reported in the literature [22]. Since myricetin derivatives are not usually found as yellow chromophores in plants, the two myricetin glycosides can be used as distinctive markers for plant identification.

Prangos ferulacea: As found in previous studies by the Laursen group [4], the primary yellow dyes present in the P. *ferulacea* extracts were glucuronic derivatives of quercetin and isorhamnetin, along with minor amounts of rutin. No signal of free aglycones was

found in the HPLC chromatograms of the textiles (Table A3.2-E).

Punica granatum: HPLC extracts of the peel of pomegranate were dominated by the main peak eluting at t_R 19.38 (6.24) min assigned to ellagic acid, by comparison with the analytical standard. The three peaks eluting at lower retention times were identified as ellagitannins characteristic of this species: peak 1 was assigned as punicalin (MW 782), and the other two as forms alpha and beta of punicalagin (MW 1.084,74) which, in the ESI(−) tandem mass spectrum, appeared as double-charged deprotonated molecules at *m/z* 541.0272. The smaller peaks at higher retention times were due to ellagic acid derivatives. The HPLC profile displayed in Table A3.2-F indicates that during the preparation of dyed wool references, degradation of the ellagitannins occurred.

Vitis vinifera: The HPLC profile of grape leaf extract also presented a dominant peak at t_R 18.60 (6.46) min, identified as quercetin-*O*-glucuronide in accordance with reported literature data [4] (Table A3.2-G). The smaller peaks 2 and 3 were attributed as two kaempferol-3-*O*-glycoside isomers, isomer 3 being assigned to kaempferol-3-*O*-glucoside by comparison with the analytical standard. Although studies by the Laursen group reported that "in any event, no free aglycones were seen" [4], in our dyed wool extract, a signal at t_R 21.23 (9.27) min was clearly identified as quercetin, indicating that some deglycosylation of the quercetin–glucuronide can occur.

2.3 Comparison of the chromatographic profiles of the main chromophores in the dyed wool by HPLC-DAD

In Table 11, we compare the variation of the chromatographic profiles of plant and wool extracts for *E. laevigata*, *P. vera*, and *M. alba*, and in Table 12, we calculated the differences in the main peak ratios for all the species. As a general trend, we observed that the compounds that were more polar (more OH groups or more sugar substituents) were found in higher amounts in the wool extracts (Table 12). On the other hand, in the wool extracts, we also found the parent aglycones, which were not usually detected in the plant extracts (Table A3.1). It is possible that they were formed through the hydrolysis of the glycosidic bonds, by heating during the dyeing procedure.

Table 11- HPLC-DAD profiles for the extracts of the plant (upper) and dyed wool (lower) for *Eremostachys laevigata*, *Morus alba*, and *Pistacia vera*. The retention times, t_R, for the main chromatographic peaks are given together with the wavelengths of the main absorption bands

Name	Chromatogram @350 nm	t_R (min)	λ_{max} (nm)	Main chromophores
Eremostachys laevigata		18.15	254, 348	Lut- Hex-Pent
		19.15	256, 345	Lut-7-*O*-Glc
		20.07	254, 350	Lut-acetyl-Hex
		18.37	254, 349	
		19.38	256, 344	
		20.28	254, 350	
Morus alba		18.35	256, 356	Que-3-*O*-rutinoside
		18.70	255, 355	Que-3-*O*-Glc
		19.43	264, 348	Kae-3-*O*-rutinoside
		18.63	256, 356	
		19.03	255, 355	
		19.77	264, 348	
Pistacia vera		16.94	262, 357	Myr-3-*O*-Glc
		18.26	258, 355	Que-3-*O*-Glr
		21.58	254, 350	Lut
		17.25	264, 358	
		18.62	258, 355	
		22.00	254, 350	

Table 12- Comparison of the main chromophores[1] extracted from the plants and the dyed wool: the ratios were obtained by normalizing the areas of the main chromophores, a b c, by the main peak in the chromatogram (HPLC-DAD). For more details, please see Table A.2.

Name	Plant extract	Wool extract	Peak a	Peak b	Peak c
D. semibarbatum	a:b = 1.85 a:c = 1.49	a:b = 1.94 a:c = 1.55	Que-3-*O*-Glc	Kae-3-*O*-Glc	Irh-*O*-Glc
E. laevigata	a:b = 5.92 a:c =2.04	a:b = 12.4 a:c = 6.24	Lut- Hex-Pent	Lut-7-*O*-Glc	Lut-acetyl-Hex
P. ferulacea	b:a = 1.84	b:a = 2.01	Que-3-*O*-Glr	Irh-3-*O*-Glr	-
M. alba	a:b = 1.08 a:c =1.83	a:b = 3.67 a:c = 4.18	Que-3-*O*-Rut	Que-3-*O*-Glc	Kae-3-*O*-Rut
P. vera	b:a = 6.26 b:c = 4.80	b:a = 3.83 b:c = 2.84	Myr-3-*O*-Glc	Que-3-*O*-Glr	Lut
P. granatum	c:a = 1.48 c:b = 0.89	c:a = 1.84 c:b = 2.04	Punicalin	Punicalagin B	Ellagic acid
V. vinifera	a:b = 6.62	a:b = 7.17	Que-*O*-Glr	Kae-3-*O*-Glc	-

[1] Glc — glucose and Glr — glucuronide.

2.4 Characterization of the main chromophores in wool threads of a workshop in the center of Iran

Samples were extracted and the solutions analyzed by HPLC-DAD-LRMS and HPLC-DAD (Figure 13). The colors of the threads were measured in the CIELAB color system (Figure 13). It was interesting to observe that in the workshop samples, the parent aglycones were present in relatively large amounts, reinforcing the trend already described in the extracts of our wool references. This means that, possibly, wool threads were dyed with higher temperatures and/or over longer periods than our reference samples. By HPLC-DAD-LRMS, it was possible to detect the presence of alizarin in the samples dyed with both *D. semibarbatum* and *R. tinctorum*, but in much lower amounts when compared with samples from 17th c. Persian carpets [23]. In these historical samples, alizarin was detected only in orange colors, where it may have been used in higher amounts than in the workshop samples. In the extracts of *D. semibarbatum + P. granatum*, it was possible to detect the presence of ellagic acid, but not the punicalagin isomers. It is worth noting that when comparing the chromatographic profiles for *D. semibarbatum + R. tinctorum* and *D. semibarbatum + P. granatum*, the latter presented higher amounts of the parent aglycones (closer to the profile of historical samples dyed only with *D. semibarbatum*). As a general trend, all the extracts obtained from the workshop presented significantly higher concentrations of the parent aglycones when compared with our dyed wool extracts. On

the other hand, our dyed samples, in terms of aglycone concentration, compared well with extracts obtained from 17th c. Persian carpets [24].

3. Materials and Methods

3.1 Materials

All solvents used were HPLC grade. Methanol was purchased from Merck, perchloric acid (HClO$_4$) ACS reagent, and acetone ≥99.5% from Honeywell Riedel-de Haen. For all the chromatographic studies as well as dye extraction, Millipore ultrapure water was used. For UHPLC-HRMS, LC-MS–grade Optima methanol, acetonitrile, water, and LC-MS-grade formic acid were acquired from Fisher Scientific.

Quercetin (C$_{15}$H$_{10}$O$_7$), luteolin (C$_{15}$H$_{10}$O$_6$), kaempferol (C$_{15}$H$_{10}$O$_6$), isorhamnetin (C$_{16}$H$_{12}$O$_7$), apigenin (C$_{15}$H$_{10}$O$_5$), ellagic acid (C$_{14}$H$_6$O$_8$), luteolin-7-O-glucoside (C$_{21}$H$_{20}$O$_{11}$), Luteolin-3′,7-di-O-glucoside (C$_{27}$H$_{30}$O$_{16}$), kaempferol-3-O-glucoside (C$_{21}$H$_{20}$O$_{11}$), quercetin-3-O-glucoside (C$_{21}$H$_{19}$O$_{12}$), quercetin-3-O-glucuronide (C$_{21}$H$_{18}$O$_{13}$), and rutin (C$_{27}$H$_{30}$O$_{16}$) analytical standards were purchased from Extrasynthese.

3.2 The plants: collection and preparation

Four plants were obtained from a workshop located in Isfahan province of Iran in August 2016: the flowers of *Delphinium semibarbatum*[16], crushed leaves and stems of *Prangos ferulacea* and *Eremostachys laevigata*, and powdered peel of *Punica granatum*. The first two species were obtained in the workshop of R. Zakeri, Murcheh Khvort[17] (coordinates 33°05′24.7″N 51°28′40.8″E), while the latter two were acquired from the workshop of Banitaba (coordinates 32°41′37.9″N 52°43′31.2″E) of Tudeshk[18] (Figure 13).

The other three species were collected from plants growing in nature in the province of Isfahan: the tree leaves of *Morus alba* and *Vitis vinifera* and the hull of the fresh *Pistacia vera* were collected at ites with geographical coordinates of 32°42′22.4″N 52°43′43.5″E,

---

[16] This plant was called "*Isparak*" by master dyers of that workshop and NOT "*Zaban dar gafa*" or "*Zalil*".
[17] Murcheh Khvort is a city in the central district of Shahin Shahr and Meymeh county, Isfahan province, Iran.
[18] Tudeshk is a city in Kuhpayeh district, Isfahan County, Isfahan province, Iran.

94

33°26'48.6"N 51°10'14.7"E, and 32°51'37.1"N 53°05'11.5"E, respectively, Figure 14. These samples were dried spread in a tray, in the dark, in a ventilated area, at 30–40°C.

Figure 14 - Geographical distribution of the collected plant sources used to dye yellow in Isfahan province, Iran [27].

3.3 Preparation of dyed wool references

In this work, wool references[19] were mordanted with Al^{3+} and dyed with the plant extracts once only following a model procedure based on the steps necessary to dye yellow in medieval times that were adapted by Dominique Cardon [1]. According to the protocol provided by D. Cardon, 5 × 5 cm² of unbleached woven wool fabric was pre-mordanted with 16% (of the mass of the wool) alum ($KAl(SO_4)_2 \cdot 12H_2O$) and 2% (mass of the wool) potassium hydrogen tartrate ($KC_4H_5O_6$). The textiles were boiled for two hours. After being taken out of the mordant bath, the mordanted textile was allowed to cool down for about one day, and it was then washed in water.

---

[19] The unbleached wool broadcloth was obtained from the *Île-de-France* breed of sheep, woven at *Eric Car-lier's* workshop in Payrin-Augmontel, France. These wool references were acquired from breeders from the region around Paris, washed and then woven in the workshop.

Dry plant material (1 g) was placed in 100 mL of water and heated until the bath was nearly at the boiling point (92–95°C); the bath was then allowed to cool down to 25°C with the plant material still in. The pre-mordanted textile was added at this point, and the bath was heated again to the boiling point (100°C); it was allowed to boil, containing both the plant material and the textile for 45 min.

3.4 Yellow dyed wools from a workshop in the center of Iran

Three yellow dyed wool yarn samples from the workshop of H. Banitaba (coordinates 32°41'37.9"N 52°43'31.2"E) near Isfahan were acquired. The samples ranged from light to darker shades of yellow and were dyed using: (a) *Delphinium semibarbatum*; (b) *Delphinium semibarbatum* and *Punica granatum*; (c) *Delphinium semibarbatum* and *Rubia tinctorum*.

3.5 Extraction of plants, dyed textiles or fibers

In this work, we extracted two samples from biological sources and two samples from dyed wool textiles and threads. The extractions were replicated twice for the HPLC-DAD analysis and once for the UHPLC-HRMS. Each replicate was analyzed at least twice by HPLC-DAD and UHPLC-HRMS/MS. The samples of plant specimens were extracted by placing 1 g of the dry plant material (as supplied by the workshop or as collected from nature) with 100 mL of methanol:water (70:30, *v:v*) and heating in a water bath at 60°C for one hour, as described in Reference [4]. The extracts were filtered through cotton (a piece of cotton in a glass Pasteur pipette) and centrifuged at 12,000 rpm for about 10 min. The supernatant liquid was gently removed and centrifuged for about 5 min. Before analysis, the solution was diluted with methanol:water (70:30, *v:v*) if necessary.

The dye from the textiles was extracted by placing it in a 5 mL balloon, 1 g of textile with 3 mL of a mixture of 0.2 M oxalic acid:methanol:acetone:water (0.1:3:3:4, *v:v*), as described in Reference [28]. The solution was left to evaporate in a vacuum line, the thread was removed, then the residues were dissolved in 400 µL of methanol/water, 7:3 (*v/v*); the tubes were centrifuged, and the upper 25 µL of the solution was removed for analysis.

3.6 HPLC-DAD and UHPLC-HRMS equipment

The analysis of both plant material and dyed wool extracts was carried out in a Thermo Finnigan Surveyor® HPLC-DAD system with a Thermo Finnigan Surveyor PDA (Thermo Finnigan, San Jose, CA, USA), an autosampler, and a gradient pump. The sample separations were performed in a reversed-phase column, RP-18 Nucleosil column (Macherey-Nagel) with 5-µm particle size column (250 mm × 4.6 mm), with a flow rate of 1.7 mL/min with the column at a constant temperature of 35 °C. The samples were injected via a Rheodyne injector with a 25 µL loop. The elution gradient consisted of two solvents: A, methanol, and B, 0.1% (*v/v*) perchloric acid aqueous solution. The gradient elution program used was 0–2 min isocratic 7% A, 2–8 min linear gradient to 15% A, 8–25 min linear gradient to 75% A, 25–27 min linear gradient to 80% A, 27–29 min linear gradient to 100% A, and 29–30 min isocratic 100% A (10 min re-equilibration time). The eluted peaks were monitored at 350 nm.

Aliquots of 3 µL of both plant material and dyed wool extracts were also analyzed on a UHPLC Elute system coupled on-line with a quadrupole time-of-flight Impact II mass spectrometer equipped with an ESI source (Bruker Daltoniks, Bremen, Germany). Chromatographic separation was carried out on an RF-C18 Halo column (150 mm × 2.1 mm, 2.7-µm particle size, Advanced Materials Technology). The mobile phase consisted of water (A) and acetonitrile (B), containing 0.1% formic acid, at a flow rate of 600 µL/min. The elution conditions were as follows: 0–18 min, linear gradient to 50% B; 18–20 min, linear gradient to 90% B; 20–23 min, isocratic 90% B; and 23–24 min, linear gradient to 0% B (followed by 11 min re-equilibration time). The column and the autosampler were maintained at 45°C and 8°C, respectively. High-resolution mass spectra were acquired in both ESI ionization modes. The mass spectrometric parameters were set as follows: end-plate offset: 500V; capillary voltage: 4.0 or −2.5 kV; nebulizer: 4 bars; dry gas: 8 L/min; heater temperature: 200 °C. Internal calibration was achieved with an ammonium formate solution introduced to the ion source via a 20 µL loop at the beginning of each analysis, using a six-port valve. Calibration was then performed using a high-precision calibration (HPC) mode. The acquisition was performed in full scan mode in the *m/z* 100–1000 range and in a

data-dependent MS/MS mode with an acquisition rate of 3 Hz using a dynamic method with a fixed cycle time of 3 s, and an isolation window of 0.03 Da. Data acquisition and processing were performed using Data Analysis 4.2 software.

3.7 Colorimetry

To measure color, a portable Data Color International colorimeter spectrophotometer was used. The optical system of the measuring head used diffuse illumination from a pulsed Xenon arc lamp over the 8mm diameter measuring area, with $0°$ viewing angle geometry. Color coordinates were calculated by defining the D65 illuminant and the $10°$ observer. The calibration was performed with a white bright standard plate and a total black standard. The color data were presented in the CIE-Lab system. The values represented are an average of three points.

4. Conclusions

Seven plants used for dyeing in yellow Persian textiles were studied by HPLC-DAD and UHPLC-HRMS/MS: *Delphinium semibarbatum*, *Eremostachys laevigata*, *Prangos ferulacea*, *Morus alba*, *Pistacia vera*, *Punica granatum*, and *Vitis vinifera*. The main yellows for *E. laevigata* were luteolin-*O*-glycosides derivatives (luteolin-pentoside-hexoside), this being the only plant in which this stable chromophore was identified. The other extracts were characterized by less stable 3-hydroxy flavone structures such as quercetin, kaempferol, and isorhamnetin, although always in the form of 3-*O*-glycosides, which will have a protective effect on the dye stability. For *Pistacia vera* (hulls), together with the main yellows (quercetin-3-*O*-glucoside and 3-*O*-glucuronide), myricetin derivatives were also detected as minor compounds, and we propose that they may be used as markers for plant identification.

Overall, we observed that the extracts from the wool samples displayed a higher amount of more polar chromophores, but, at the same time, in most of the extracts, a small amount of the parent aglycones was also detected (that were not seen in the plant ex-

98

tracts). Mild extraction methods were used to prevent hydrolysis of the glycosidic linkages, so hydrolysis was possibly a result of the temperature used during the dyeing [3, 29].

Besides our dyed wool references, we were also able to analyze samples from a workshop active in Isfahan: wool threads dyed with *Delphinium semibarbatum*, as a single dye or applied together with *Rubia tinctorum* or *Punica granatum*. Our analysis showed that the threads were, in fact, dyed with these plant sources. Interestingly, in the workshop samples, a high proportion of aglycones was detected. Moreover, when comparing our *Delphinium semibarbatum* extracts and the workshop extracts with previous studies on 17th c. Persian carpets, the profiles compared better with our dyeing procedure, i.e., parent aglycones were not present in high concentrations. This indicates that even when using similar natural sources for yellows, the methods used to dye in the workshops are different; possibly, the dye baths are heated at higher temperatures or for longer time periods. It is also possible to conclude that our dyed wool samples may be used as highly characterized references in future research work.

As to future work, it would be interesting to gather information on other workshops established in other regions of Iran, to verify whether the main biological sources for yellows are also flavonol-based or if other, flavone-based natural sources are preferred.

References

[1] Cardon, D. (2007). *Natural dyes: sources, tradition, technology and science* (1st ed.) Archetype Publications. ISBN 190498200X

[2] Hallett, J. (2007). The knotted-pile carpet. In T. Pacheco Pereira & J. Hallett (Eds), *Carpets and paintings, 15th–18th centuries: the oriental carpet in Portugal* (pp. 23–30). Museu Nacional de Arte Antiga. ISBN 978-972-776-339-9

[3] Zhang, X., & Laursen, R. A. (2005). Development of mild extraction methods for the analysis of natural dyes in textiles of historical interest using LC-diode array detector-MS. *Analytical Chemistry*, 77(7), 2022-2025. Doi: 10.1021/ac048380k

[4] Mouri, C., Mozaffarian, V., Zhang, X., & Laursen, R. (2014). Characterization of flavonols in plants used for textile dyeing and the significance of flavonol conjugates. *Dyes and Pigments*, 100, 135-141. Doi: 10.1016/j.dyepig.2013.08.025

[5] Melo, M. J. (2009). History of natural dyes in the ancient Mediterranean world. In T. Bechtold, & R. Mussak (Eds.), *Handbook of Natural Colorants* (pp. 3–17), Wiley. Doi: 10.1002/9780470744970.ch1

[6] Sharif, S., Nabais, P., Melo, M.J. (2021). Natural yellow dye sources in Persian carpets: a review. In J. Kirby (Ed.), *Dyes in History and Archaeology 35/36*. Archetype Publications. ISBN 9781909492813

[7] Ghahreman, A. (1978). *Flora of Iran*. Research Institute of Forests and Rangelands.

[8] Mozaffarian, V. (1996). *A dictionary of Iranian plant names: Latin, English, Persian*. Farhang e moaser. ISBN 9645545404

[9] Zhang, X., & Laursen, R. (2009). Application of LC–MS to the analysis of dyes in objects of historical interest. *International Journal of Mass Spectrometry*, 284(1-3), 108-114. Doi: 10.1016/j.ijms.2008.07.014

[10] Zhang, X., Cardon, D., Cabrera, J. L., & Laursen, R. (2010). The role of glycosides in the light-stabilization of 3-hydroxyflavone (flavonol) dyes as revealed by HPLC. *Microchimica Acta*, 169(3-4), 327-334. Doi: 10.1007/s00604-010-0361-x

[11] Mouri, C., & Laursen, R. (2011). Identification and partial characterization of C-glycosylflavone markers in Asian plant dyes using liquid chromatography–tandem mass spectrometry. *Journal of Chromatography A*, 1218(41), 7325-7330. Doi: 10.1016/j.chroma.2011.08.048

[12] Marques, R., Sousa, M. M., Oliveira, M. C., & Melo, M. J. (2009). Characterization of weld (*Reseda luteola* L.) and spurge flax (*Daphne gnidium* L.) by high-performance liquid chromatography–diode array detection–mass spectrometry in Arraiolos historical textiles. *Journal of Chromatography* A, 1216(9), 1395-1402. Doi:

10.1016/j.chroma.2008.12.083

[13] Hmamouchi, M., Es-Safi, N., Lahrichi, M., Fruchier, A., & Essassi, E. M. (1996). Flavones and flavonols in leaves of some Moroccan *Vitis vinifera* cultivars. American *Journal of Enology and Viticulture*, 47(2), 186-192.

[14] Böhmer, H., Enez, N., Karadağ, R., Kwon, C., Fogelberg, L.E. (2002). *Dye plants in Turkey and surrounding areas. In Koekboya natural dyes and textiles: A color journey from Turkey to India and beyond* (L.E. Fogelberg Trans.). REMHÖB-Verlag; p. 161. ISBN 3936713014

[15] El-Hadary, A. E., & Ramadan, M. F. (2019). Phenolic profiles, antihyperglycemic, antihyperlipidemic, and antioxidant properties of pomegranate (*Punica granatum*) peel extract. *Journal of Food Biochemistry*, 43(4). Doi: 10.1111/jfbc.12803

[16] Fischer, U. A., Carle, R., & Kammerer, D. R. (2011). Identification and quantification of phenolic compounds from pomegranate (*Punica granatum* L.) peel, mesocarp, aril and differently produced juices by HPLC-DAD–ESI/MS^n. *Food Chemistry*, 127(2), 807-821. Doi: 10.1016/j.foodchem.2010.12.156

[17] Mathon, C., Chater, J. M., Green, A., Merhaut, D. J., Mauk, P. A., Preece, J. E., & Larive, C. K. (2019). Quantification of punicalagins in commercial preparations and pomegranate cultivars, by liquid chromatography–mass spectrometry. *Journal of the Science of Food and Agriculture*, 99(8), 4036-4042. Doi: 10.1002/jsfa.9631

[18] Shibayama, N., Wypyski, M., & Gagliardi-Mangilli, E. (2015). Analysis of natural dyes and metal threads used in 16th -18th century Persian/Safavid and Indian/Mughal velvets by HPLC-PDA and SEM-EDS to investigate the system to differentiate velvets of these two cultures. *Heritage Science*, 3(1). Doi: 10.1186/s40494-015-0037-2

[19] Asnaashari, S., Afshar, F. H., Ebrahimi, A., Moghadam, S. B., & Delazar, A. (2016). Chemical composition and radical scavenging activity of essential oil and methanolic extract of *Eremostachys azerbaijanica* Rech. f. from Iran. *Research in pharmaceutical sciences*, 11(2), 113.

[20] Katsube, T., Imawaka, N., Kawano, Y., Yamazaki, Y., Shiwaku, K., & Yamane, Y. (2006). Antioxidant flavonol glycosides in mulberry (*Morus alba* L.) leaves isolated based on LDL antioxidant activity. *Food Chemistry*, 97(1), 25-31. Doi: 10.1016/j.foodchem.2005.03.019

[21] Dugo, P., Donato, P., Cacciola, F., Germanò, M. P., Rapisarda, A., & Mondello, L. (2009). Characterization of the polyphenolic fraction of *Morus alba* leaves extracts by HPLC coupled to a hybrid IT-TOF MS system. *Journal of Separation Science, 32(21)*, 3627-3634. Doi: 10.1002/jssc.200900348

[22] Erşan, S., Üstündağ, Ö G., Carle, R., & Schweiggert, R. M. (2017). Determination of

pistachio (Pistacia vera L.) hull (exo- and mesocarp) phenolics by HPLC-DAD-ESI/MS[n] and UHPLC-DAD-ELSD after ultrasound-assisted extraction. *Journal of Food Composition and Analysis*, 62, 103-114. Doi: 10.1016/j.jfca.2017.04.013

[23] Sousa, M. M., Miguel, C., Rodrigues, I., Parola, A. J., Pina, F., Melo, J. S., & Melo, M. J. (2008). A photochemical study on the blue dye indigo: From solution to ancient Andean textiles. *Photochemical & Photobiological Sciences*, 7(11), 1353. Doi: 10.1039/b809578g

[24] Heitor, M.V.V. (2007). *A cor dos tapetes: análise de materiais de tapetes persas dos séculos XVI e XVII.* [Master Thesis, New University of Lisbon]. NOVA University Repository. http://hdl.handle.net/10362/2162

[25] Armindo, E., Sousa, M., Melo, M.J., Hallett, J.A. (2008). A Persian carpet's paradise garden: discovering historical and technical aspects through carpet conservation and restoration. In J. Bridgland (Ed*.), The 15th triennial ICOM committee for conservation conference* (pp. 960-966). Allied Publishers Pvt. ISBN 978-81-8424-344-4

[26] Santos, A. R. M. D. (2010). *The discovery of three lost 'Salting' carpets: science as a tool for revealing their history* [Master Thesis, New University of Lisbon]. NOVA University Repository. http://hdl.handle.net/10362/5146

[27] Isfahan Municipality Maps Electronic System. (2019, September). http://mapservice.isfahan.ir

[28] Guinot, P., Andary, C. (2006, December 21-22). *Molecules involved in the dyeing process with flavonoids* [Conference presentation]. Dyes in History and Archaeology 25, Suceava, Romania.

[29] Lombardi, L., Serafini, I., Guiso, M., Sciubba, F., & Bianco, A. (2016). A new approach to the mild extraction of madder dyes from lake and textile. *Microchemical Journal*, 126, 373–380. https://doi.org/10.1016/j.microc.2015.12.021

Chapter 4. Photoreactivity and Stability of Flavonoid Yellows Used in Cultural Heritage

104

Abstract

Flavonoid yellows are historical dyes widely found in cultural heritage, in particular those based on the glycosides of luteolin, quercetin, and kaempferol. In this research, for the first time, the photodegradation quantum yields (Φ_R) were calculated for luteolin, quercetin, and kaempferol as well as their glucosides luteolin-7-*O*-glucoside, quercetin-3-*O*-glucuronide, kaempferol-3-*O*-glucoside and compared to the reactivity of eriodictyol. The results are discussed within the current state of art on the mechanisms of degradation for these antioxidant compounds, which are reviewed in the introduction. Φ_R values were obtained in solution irradiating at 313 nm and 366 nm, providing the quantification of the stability of flavonoid yellows. In particular, by irradiating at 366 nm, a very good stability scale is obtained, with Φ_R values for luteolin and the 3-*O*-glycosides of quercetin and kaempferol on the order of 10^{-6}. The more reactive quercetin and kaempferol are characterized by Φ_R values of *ca.* 3×10^{-5}. The relative stability of these yellows can be explained by a photoprotective mechanism based on excited state proton transfer, which is more efficient when there is an OH in C5 position. In addition, electron transfer, and consequently oxidation, is also enhanced through the OH in position C3 when compared to C5.

Solvents effects were also studied, and to mimic the environment of the dye in wool, irradiation was carried out at 366 nm in a proteinaceous gel. In this gel, the Φ_R values increased for all the molecules studied, reaching 1×10^{-4} and 2×10^{-4} for kaempferol and quercetin, respectively. This drastic enhancement shows that the environment has a major impact on stability. The main degradation products were also studied by irradiation with a xenon source ($\lambda_{irr} \geq 300$ nm) and characterized by HPLC-DAD-MS and LC-HRMS/MS. These data, on the reaction mechanism, show that the double bond between C2 and C3, in the C ring, is the most reactive point of the molecules, as in all the flavonoids degradation started by solvent attack, followed in some cases by ring opening and the formation of low molecular weight hydroxyl compounds such as benzoic acids, in agreement with the general reaction scheme proposed in literature.

Keywords: hydroxyflavones; historical yellow dyes; HPLC; mass spectrometry; conservation

1. Introduction

This paper focuses on the study of the stability of yellow dyes that have been used since historical times, based on luteolin (Lut), a flavone, and on the flavonols quercetin (Que) and kaempferol (Kae) and their substituted 3-*O*-glycosides, Figure 15. These flavonoid yellows have been used as paints to create works of art, or to dye fibers in beautiful objects such as Persian carpets in medieval times [1-3]. Flavonoids are ubiquitous in plants, but to be used to dye textiles, they need to be present in sufficient quantity and be resistant to fading [2]. As elegantly summarized by Zhang *et al.* in [2]: "It seems likely that early dyers learned by trial and error over centuries which plants produced the best dyes and which times were best for harvesting them."

The main difference between the two classes selected in this study (see Figure 15) lies in the hydroxyl group in position 3, which is absent in the flavone luteolin. We also included in this study eriodictyol, considering the importance of the double bond between C2 and C3 (present in the studied flavone and flavonols, but absent in eriodictyol), Figure 15. These molecules are important to preserve in cultural heritage [2, 4, 5], but most publications on their stability derive from their fundamental importance for life, acting as anti-oxidants [6, 7]. For example, the flavonol rutin, or vitamin P, was first separated from lemon peel and studied in 1936 by Bentsáth [8] and later by Bondarev [9]. 3-Hydroxyflavone and 5-hydroxyflavone, which are present in the basic structures of the flavonols and flavones, were also extensively studied due to their extremely interesting photophysical properties [10, 11, 12]. In particular, the observed photochemical stability is a consequence of an excited state proton transfer, which acts as a protective mechanism to dissipate the excess energy absorbed by the molecule. Such a protector mechanism is shared with other fundamental historical dyes: indigo blue and anthraquinone reds, as well as the DNA bases [13, 14]. Due to these extraordinary properties, they have been used in a variety of applications that range from additives in sunscreens to components in solar cells [6, 7].

Despite a large number of publications on the stability of these flavonoids, and important contributions that led to fundamental advances [6, 7], it is very rare to find published values for the quantum yields of reaction. To fill this lacuna, in this paper quantum yields of photodegradation (Φ_R) are measured, in homogeneous (methanol/water, 7:3

v/v) and heterogeneous (proteinaceous gel) media, for the neutral forms [15]. Our results show that these values are essential to understanding their stability and are an accurate way to quantify the relative stability of these colorants. In this work, we also compare the main degradation products, in homogeneous media, with what is described in the literature (sections 1.2 and 1.3). The Φ_R values were obtained by monochromatic irradiation at 313 nm and 366 nm, and the photoproducts were mainly characterized by polychromatic irradiation with a Xenon lamp (λ_{irr}> 300 nm), with the exception of quercetin for which data using monochromatic irradiation is also available. The data necessary for the calculation of the Φ_R was acquired by UV-VIS spectrophotometry, and the main degradation products were identified and characterized by HPLC-DAD-MS and LC-HRMS/MS.

To understand the photochemistry and overall reactivity of these molecules, we will provide a brief overview of their photophysics, i.e., of the fundamental processes of energy dissipation in the excited state, as well as their mechanisms of antioxidant action.
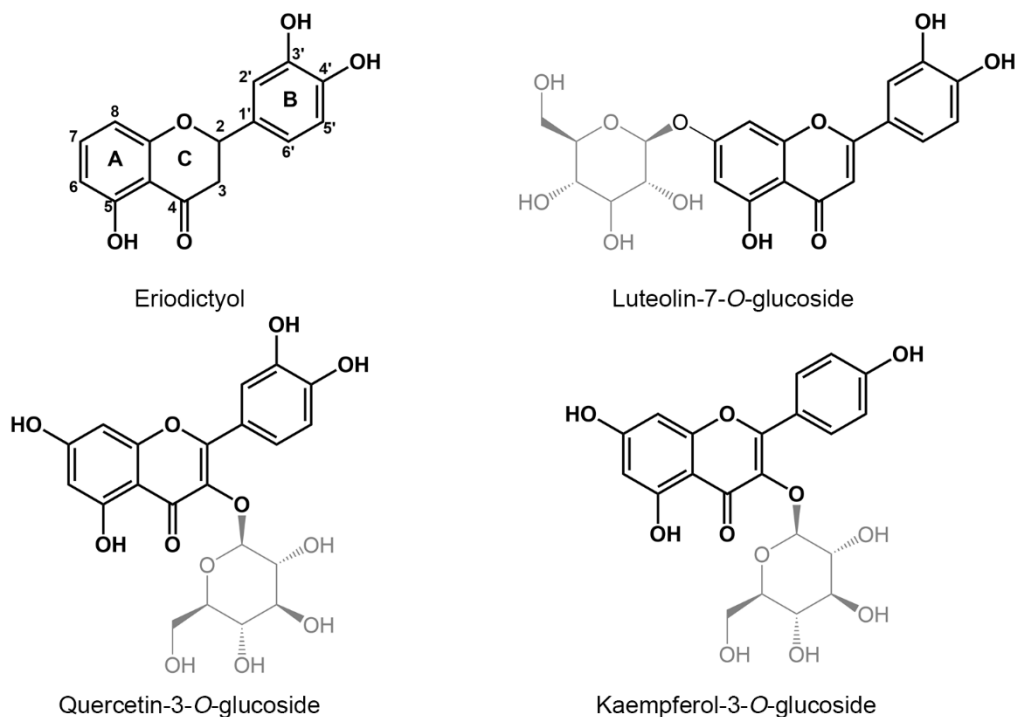

Figure 15- Luteolin, a flavone, and the flavonols, quercetin and kaempferol and their substituted 3-*O*-glycosides are the main natural yellow dyes used in the 21st c. in central Iran. For eriodictyol the numbering of the atoms and ring label is presented; luteolin, quercetin and kaempferol chromophores are highlighted in bold, while the glucosides, bound to the 7-OH or 3-OH of the aglycones, are in grey.

1.1 Photoprotective mechanisms in flavonoid yellows

"The observation of yellow to yellow-green luminescence spots is taken as the preliminary diagnosis for the flavonols, e.g., kaempferol, quercetin, myricetin. This yellow luminescence could not be the normal singlet-singlet fluorescence of the corresponding initial molecules (…)". This observation is made by Sengupta and Kasha in their groundbreaking publication in 1979 [10]. It was based on the fact that 3-hydroxyflavone (3-HF) and quercetin "have their first singlet-singlet absorption band at about 352 and 380 nm (onsets at 370 nm and 420 nm), respectively", for this reason it is not expected that the decay of the excited molecule would lead to a brilliant yellow to yellow-green fluorescence. To understand the reason behind this "anomalous" fluorescence that was used to identify, at the time, flavonols, they chose to study 3-hydroxyflavone, "as the skeletal precursor of the flavonols", proving that "the yellow region luminescence in these molecules is from a tautomer of the parent molecule, produced by excited state proton transfer" [10]. The authors showed that, in deuterated solvents, two bands are observed for 3-HF, at *ca.* 400 nm (the emission of the excited neutral form) and at *ca.* 540 nm (the tautomer formed in the excited state, which is responsible for the yellow-green luminescence), Figure 16. It was also proposed that the drastic change in the pK_a of the carbonyl and hydroxyl group, in the excited state, is based on the formation of a pyrylium structure, in which the phenyl ring (B) is coplanar with the pyrone ring (C), Figure 16. Considering that it will also be useful for discussing the degradation mechanisms, we have included as Scheme A4.1[20] the multi-equilibria in solution based on the benzopyrylium ring present in flavylium salts and anthocyanins.

---

[20] See Appendix 3 for all the schemes, tables and figures related to this chapter.
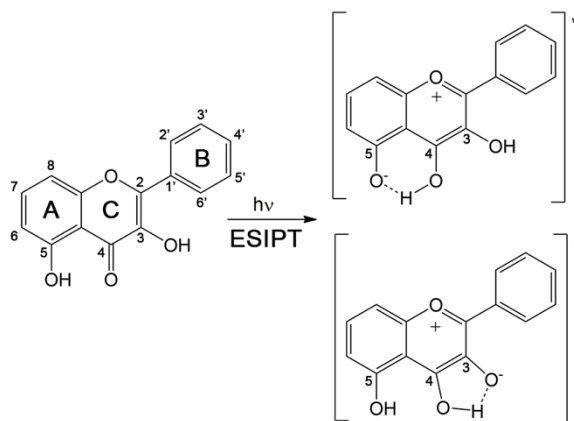
Figure 16- The drastic change in the pK_a of the carbonyl and hydroxyl group in C3 and C5, in the excited state, promotes an ultrafast excited proton transfer, which acts as a photoprotective mechanism for these yellow dyes. The 5-Hydroxyflavone proton transfer in the excited state involves an intramolecular hydrogen bond six-membered ring which is stronger than that in the 3-hydroxyflavone possessing a five-membered ring, allowing for a more efficient ESIPT. For more details, please see text.

In 1985, Strandjord *et al.*, confirmed the importance of co-planarity with the phenyl group to enhance this photoprotective mechanism. They proved that for 3-hydroxyflavone, substituents in the B ring influence the proton transfer mechanism, in particular in the ortho position (C4'): "compounds fall into two groups depending on whether the ortho position in the phenyl ring is substituted with a methyl group. The ortho compounds are less acidic, and less hydrogen-bond donating. They also exhibit weaker intramolecular hydrogen bond and a E_a" [11].

Chou *et al.* added another extremely relevant contribution by showing that 5-hydroxyflavone proton transfer in the excited state involves a six-membered ring intramolecular hydrogen bond which is stronger than that in 3-hydroxyflavone, which possesses a five-membered ring hydrogen bond, allowing for a more efficient excited state intramolecular proton transfer (ESIPT). This was demonstrated by IR and NMR data. In this case, emission from the tautomer formed in the excited state was observed at *ca.* 700 nm, being characterized by very low quantum yields of fluorescence (5×10^{-6}) and an ultrafast rate of ESIPT (>160 fs^{-1}). At this point, both 3-hydroxyflavone and 5-hydroxyflavone are considered as prototypes for studying the dynamics of excited state proton transfer

(ESPT) [12−16]. The importance of these six and five-membered rings in the excited state was also supported by density-functional theory (DFT) calculations, showing that the stronger the hydrogen bond in the 5-hydroxyflavone, the more likely the ESIPT process is to occur [17]. An identical work was published in the following year, 2017 [18]. More on the causes behind this efficient ESIPT continues to be investigated in recent publications [19-21].

Other flavonols such as quercetin and its glycoside rutin were also studied [9, 22]. For the latter it was shown that ESPT can take place between the carbonyl and the 2'-OH from the glucose unit close to the glycoside bond [22]. A similar phenomenon was observed for quercetin, studied by Liu *et al.* [23], in which it was observed a strong intramolecular hydrogen bond "between the -OH group of the glucose and carbonyl oxygen at the 4-position, or another -OH of the sugar and the -OH at the B ring". The fluorescence emission spectra of the several species in solution and pK_as of luteolin and apigenin were published by Favaro *et al.* [24].

1.2 Mechanisms of antioxidant action

The study of the mechanisms of degradation for these antioxidant compounds may be approached by studying the products formed by electrochemical methods or by promoting oxidation using chemicals such as DPPH (diphenylpicrylhydrazyl).

In 1998, Jørgensen *et al.* [6] identified the oxidation products of quercetin and kaempferol, in non-aqueous solutions (acetonitrile), formed in a two-electron process using bulk electrolysis. The main degradation products, which are colorless and more polar than the parent compounds, were isolated and characterized by HPLC-MS and NMR, their structures are shown in Figure 17. The mechanism for its formation was discussed in-depth by the authors as well as by Hajji *et al.*, Figure 17 and Table 13 [25]. Hajji *et al.* used chemical reagents such as DPPH (diphenylpicrylhydrazyl) to promote oxidation. In organic solvents, quercetin is oxidized in a 2-hydrogen process and, in water, in a two-electron-two-proton process [6, 26]. The quinone structure formed into this redox reaction, *p*-quinonemethide (**VI**), suffers solvent addition and ring opening being transformed in the main product **XI**, 2-(3,4-dihydroxybenzoyl)-2,4,6-trihydroxybenzofuran-

3(2H)-one. To explain this mechanism, Jørgensen *et al.* compared it to the multi-state equilibria found in anthocyanins, Scheme A4.1, in which the flavylium cation is attacked by the solvent forming a colorless hemiketal that will open forming *cis* and *trans* chalcones [6, 27, 28]; in the case of anthocyanins or flavylium salts, solvent attack on the hemiketal is not preceded by a redox reaction and the equilibrium may be fully reversible [27, 28]. The formation of radical species was also discussed by Jørgensen *et al.* [6] and Dangles *et al.* [29], by loss of H•, neutral or anion radicals can be formed in 4′-OH and 3-OH. It is possible that the pseudo six-membered ring discussed in 1.1 contributes to the overall planarity and stability of these radicals. Jørgensen *et al.* [6] also note that "the most frequently reported oxidation product of quercetin is a so-called depside or phenolic carboxylic acid ester (**XII**), Table 13. It is noteworthy, that none of the investigations provided ^{13}C NMR data, since the most striking difference between this molecular structure and **XI,** is the number of carbon atoms (14 vs. 15)." Final products in the oxidation of quercetin have also been reported to be 2,4,6-trihydroxybenzaldehyde and 3,4-dihydroxybenzoic acid [29].

Luteolin was also included in this study and although it was consumed during electrolysis, no oxidation products were detected by HPLC [6]. Based on the percentage of HPLC area found for the parent molecule (Lut 40%, Kae 10%, Que 0%), luteolin was considered more stable than the 3-OH flavonols studied (quercetin and kaempferol), and it was suggested that "the presence of the 3-OH group is crucial in determining the oxidation mechanism" [6]. These results were confirmed for the neutral form of quercetin in aqueous media by Sokolová *et al.* [26], which by cyclic voltammetry was oxidized by a 2e$^-$ / 2H$^+$ process [6], forming **XI** as oxidation product, Figure 17. The oxidation of luteolin was also studied by this group, and the oxidation products identified by HPLC-MS are depicted in Figure 18, being the main oxidation product 3,4-dihydroxybenzoic acid. Similarly to quercetin, the neutral form of luteolin in aqueous solution "is oxidized by a 2e$^-$ / 2H$^+$ process". It is possible that the first oxidation products formed are hydroxy-luteolin and 3,5-dihydroxy-2-(2-oxoacetyl) phenyl-3,4-dihydroxybenzoate, Figure 18. The latter, in the presence of oxygen decomposes to the low molecular weight compounds identified as 3,4-dihydroxybenzoic acid and 2,5,7-trihydroxy-4H-1-benzopyran-4-one, Figure 18.
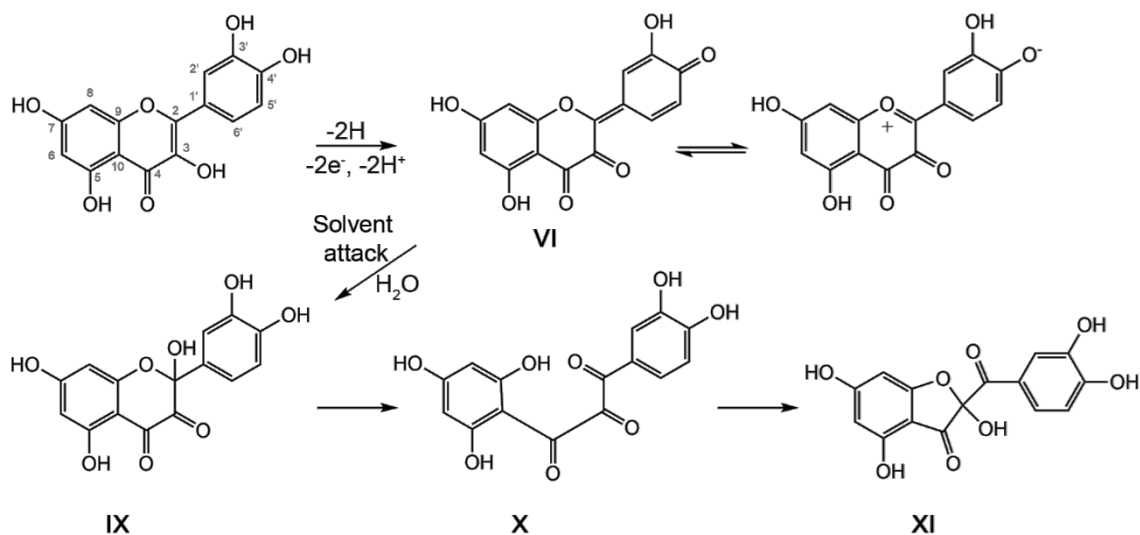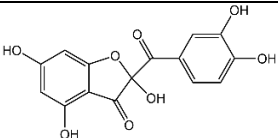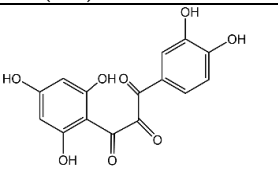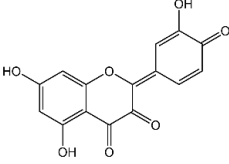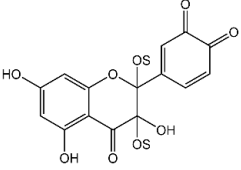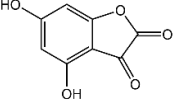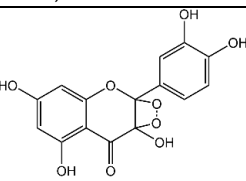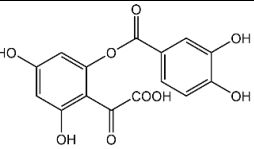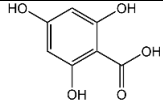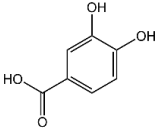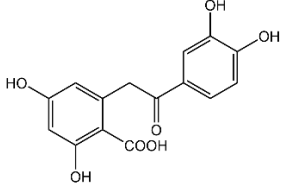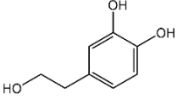
Figure 17- Mechanism proposed for the oxidation of quercetin adapted from several studies [6, 25, 26]. The main intermediates and the main product identified (XI) are numbered following the first mechanistical proposal by Jørgensen. The p-quinonemethide (VI) is formed by two-electron oxidation of quercetin. This structure, by analogy with anthocyanins, is transformed into a hemiketal (IX) by solvent addition, followed by ring opening (X). Finally, X is converted into the main oxidation product XI, 2-(3,4-dihydroxybenzoyl)-2,4,6-trihydroxybenzofuran-3(2H)-one. This colorless and more polar compound XI is also an antioxidant. Compounds were characterized by HPLC-MS. The main compound was isolated and identified by ^{13}C- and ^{1}H-NMR.

Table 13- Molecular structures of the main degradation products of quercetin, the methods used to identify them and to promote degradation; oxA, oxidation by electrochemical methods; oxB, oxidation by chemical compounds, e.g., DPPH; hνP, polychromatic irradiation, e.g., using Xenon lamps.

Structure	Identification methods	How (oxA; oxB; hνP)	Authors and Year
XI- 3(2H)-benzofuranone	Separation & NMR (^{13}C and ^{1}H); HPLC-MS ^{1}H-NMR; HPLC-MS	oxA	Jørgensen *et al.* **1998** Hajji *et al.* **2006**
X- chalcantrione	Separation & NMR (^{13}C and ^{1}H); HPLC-MS	oxA	Jørgensen *et al.* **1998**

112

Structure	Identification methods	How (oxA; oxB; h𝜈P)	Authors and Year
VI- ortho-quinone	Separation & NMR (^{13}C and ^{1}H); HPLC-MS ^{1}H-NMR; HPLC-MS	oxA	Jørgensen *et al.* **1998** Hajji *et al.* **2006**
4- hemiketal species[#]	^{1}H-NMR NMR (^{13}C and ^{1}H); HPLC-MS	oxB	Dangles *et al.* **1998** Innocenti *et al.* **2012**
5- 4,6-dihydroxy-1-benzo-furan-2,3-dione	^{1}H-NMR; HPLC-MS	oxB	Hajji *et al.* **2006**
6- depside with a four-membered hydroperoxide	Isolation; structures confirmed by synthesis	h𝜈P	Matsuura *et al.* **1967**
7- depside	Isolation; structures confirmed by synthesis HPLC-MS	h𝜈P h𝜈P	Matsuura *et al.* **1967** Ferreira *et al.* **2002**
8- 2,4,6-trihydroxybenzoic acid	HPLC-MS; structures confirmed by synthesis Separation & NMR (^{13}C and ^{1}H); HPLC-MS	h𝜈P h𝜈P	Ferreira *et al.* **2002** Fahlman and Krol **2009**
9- 3,4-duhydroxybenzoic acid	HPLC-MS; structures confirmed by synthesis	h𝜈P	Ferreira *et al.* **2002**

Structure	Identification methods	How (oxA; oxB; hνP)	Authors and Year
10- 2-(3',4'-dihydroxyben- zoyloxy)-4,6-dihy- droxybenzoic acid	Separation & NMR (^{13}C and ^{1}H); HPLC-MS	hνP	Fahlman and Krol **2009**
11- hydroxytyrosol	Separation & NMR (^{13}C and ^{1}H); HPLC-MS	hνP	Krol and Fahlman **2009**

[#] Other hemiketal species can be formed, by the attack of a single solvent molecule, for example IX.

3,5-dihydroxy-2-(2-oxoacetyl)phenyl-3,4-dihydroxybenzoate

6-hydroxy-luteolin

2,5,7-trihydroxy-4H-1-benzopyran-4-one
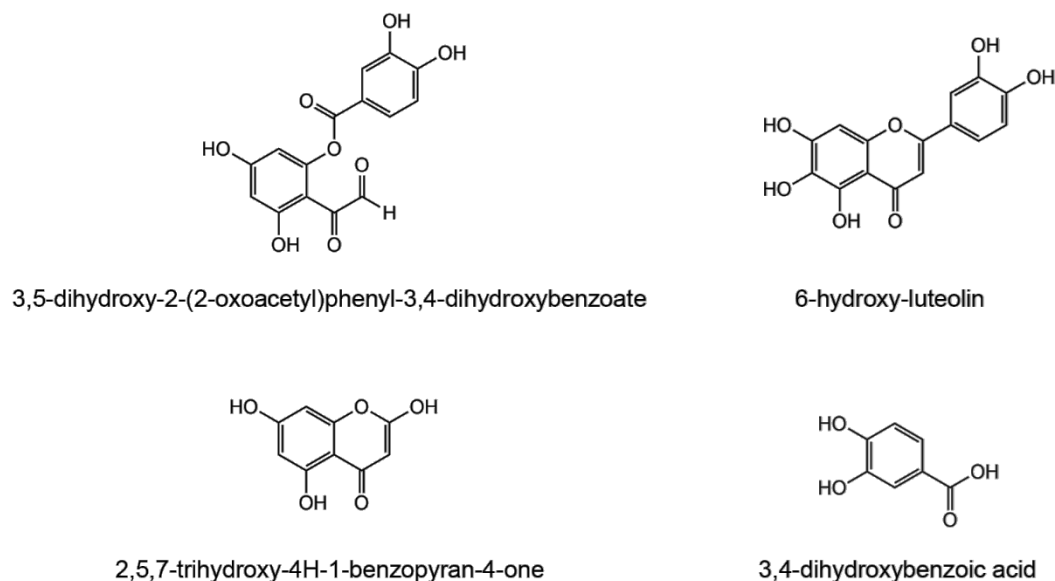
3,4-dihydroxybenzoic acid

Figure 18- Molecular structures for the main products identified in the oxidation of luteolin pro-posed by Sokolová *et al.* [50]. In the first row are depicted the minor products, the major product is 3,4-dihydroxybenzoic acid. Compounds were characterized by HPLC-MS.

1.3 Photostability and stability of flavonoid yellows used in cultural heritage: an integrated mechanism

In a seminal paper, Zhang, Cardon, Cabrera and Laursen demonstrated the importance of 3-*O*-glycoside substitution in the light stabilization of 3-hydroxyflavones [2].

114

This work provided "an explanation for why 3-*O*-substituted, rather than unsubstituted, 3-hydroxyflavones" were used as sources for yellows in historical textiles. The authors show that certain plants have enzymes that can hydrolyze the glycoside bonds in the 3-position; for example, if, after being collected, the plants are dried under conditions that do not denature enzymes. Ancient dyers had to know how to process plants to produce a stable yellow dye, including inactivating these enzymes by heat (roasting, steaming or boiling) as described for the buds of the Pagoda tree in Chinese written sources [2]. This technology of using heat to inactivate plant enzymes was available for many centuries, having been used in China since the eighth century to make green tea [2].

In previous studies of flavonoids used as historical dyes, it has been proposed to correlate relative photostabilities with redox potentials [30, 31]. In addition, several groups in the field of cultural heritage, identified degradation products both in artificially aged reference samples as well as in historical textiles, by using HPLC-MS [5, 32]. Key markers for the identification of the original molecule are also discussed in these works. Ferreira *et al.*, proposed a scheme for the photooxidation of quercetin, depicted in Scheme A4.2, in which the main degradation products are depside, 2,4,6-trihydroxy and 3,4-di-hydroxy benzoic acids, Table 13. These main products and the overall mechanism were confirmed by Colombini *et al.* [5], both for the aluminum ion-complexes as well as the parent molecule. However, in another publication by this group [33], in 2011, it is discussed that the benzoic acids could originally be present in the dyed yarns, concluding that "the presence of 4-hydroxybenzoic acid in yarn extracts is a strong indication of aging, whereas the detection of di- and tri-hydroxybenzoic acids does not imply that the textile was subjected to aging". This is somewhat in contradiction to an earlier publication by Zhang *et al.*, in which the authors consider that "the hydroxybenzoic acids must have been produced after dyeing; otherwise, they would have been washed away during the dyeing process" [34]. In this research, "a number of pre-Columbian textiles, most discovered in northern Peru and dating to the Late Intermediate Period (*ca.* 1050-1200 AD), were analyzed by high-performance liquid chromatography with diode array and mass spectrometric detection, after extraction of the dyes with formic acid and methanol" [34]. In some extracts, various hydroxybenzoic acids were identified [34].

Very few authors report the calculation of quantum yields of degradation when studying the photostability of flavonoids. In the few cases in which they are reported, it

is not clear how they were calculated. For quercetin, by irradiation at 254 nm of 3-hydroxfalvone, a quantum yield *ca.* 1 was obtained [35]; while using polychromatic irradiation, a value of *ca.* 10^{-4} was calculated [36]. A final note of caution, photodegradation induced using 254 nm is not aimed at reproducing the mechanisms at play in natural conditions, but to produce an efficient total degradation of the molecule (based on different dissociative pathways). For this reason, although common compounds can be identified, the data discussed cannot be used to extrapolate degradation mechanisms in under less aggressive conditions, like those selected in this work (λ_{irr}> 300 nm).

Overall, although it is generally agreed that the absence of an OH in position 3 leads to an increase in stability, the information on the stability of the 3-substituted compounds is contradictory for quercetin, kaempferol, morin or their glucosylated derivatives [36—40]. Even though, there is a faster visible color loss for compounds with an OH in the 3 position, it is possible that the first direct degradation products are photo and electrochemically stable [6].

Given the importance of quercetin as an anti-oxidant, the number of published studies on it is very high. Sometimes the results are contradictory, and there are also few studies that use all the necessary techniques for an accurate characterization of unknown products found during degradation. Thus, and following a methodology similar to that used in section 1.2, relevant publications were selected, from which we highlight the study by Fahlman & Krol 2009 [7]. These authors consider that "The UV energy absorbed by quercetin may be dissipated as heat, light or through decomposition of quercetin. (…) The effect of UV radiation has not been studied in as much detail as have other oxidative systems" [7]. Thus, the studies on quercetin photochemistry will serve as a model for other flavonols with an OH at C3 [4, 7, 32, 41]. When we compare the results obtained by "oxidative decomposition" with those obtained by light absorption, usually polychromatic irradiation at wavelengths ≥ 300 nm, we see that it shares the general mechanism already discussed for electrochemical oxidation, for the first time proposed by Jørgensen: solvent attack with formation of a hemiketal, followed by opening of the C ring and formation of a chalcone, **X,** Figure 17 and Scheme A4.1. These chalcones may be stable if not irradiated, Table 13. By irradiation they are converted into benzoic acids, whose substitution pattern depends on the parent molecule. In the case of quercetin irradiation, the final products are 2,4,6-trihydroxybenzoic acid and 3,4-dihydroxybenzoic acid, Table 13

116

[4, 5, 7, 32]. In many of the studies, the main product results from the solvent attack at position 2, with the formation of a "hemiketal" structure as for example, **IX** [35]. In addition to what was observed for electrochemical oxidation, as first proposed by Matsuura *et al.* in 1967, the loss of CO results in a phenolic carboxylic acid ester, usually called depside, **7** in Table 13 [4, 5, 7, 12, 28, 32, 42].

2. MATERIALS AND METHODS

2.1. Materials

2.1.1 Dyes, reference compounds and solvents

All reagents were of analytical grade. Spectroscopic or equivalent grade solvents and Millipore filtered water were used for all the spectroscopic studies. Water, acetonitrile and formic acid LC-MS grade Optima® were from Fisher Chemical (Hampton, NH, USA). Flavonoid dyes luteolin (C.I. Natural Yellow 2), luteolin-7-*O*-glucoside, quercetin (CI Natural Yellow 10), quercetin-3-*O*-glucuronide (Que-3OGlr), kaempferol, kaempferol-3-*O*-glucoside, and eriodictyol, were acquired from Extrasynthese and TCI Europe N.V.

2.2. Sample preparation and irradiation

Monochromatic irradiation was carried out in quartz cells, with continuous magnetic stirring, at room temperature (293 K). For homogeneous media, the 3 mL solutions were irradiated at 313 nm and 366 nm; for heterogeneous media, proteinaceous gels, at 366 nm. UV-VIS spectra were acquired at each irradiation time.

Gels were prepared with food-grade gelatine (Vahiné) sheets, which were kept in cold water, overnight, previous to gelification. Then a 20% solution was prepared with 0.8 g of gelatine dissolved in 4 mL of hot water (at *ca.* 80ºC) with constant stirring; these liquid gels were left to cool until *ca.* 30ºC and were added to a quartz cell. Mother solutions of the flavonoid yellows of *ca.* 1-2x10^{-3} M, in methanol:water (7:3, v:v), were used to prepare *ca.* 10^{-4} M solutions. The flavonoid solutions were added slowly to the cells, under stirring.

Polychromatic irradiation was carried out in quartz cells, using 3 mL of 1×10^{-3} M of flavonoid dyes in methanol. The PTFE (polytetrafluoroethylene) lids of the quartz cells

117

were sealed with UHU allplast acrylic ester / PVC copolymer glue, and kept for 30 min to completely dry and avoid evaporation or loss of material, after which they were placed in the aging chamber. UV-VIS spectra were acquired upon diluting 41-49 µL of the irradiated solution in 500 µL of methanol:water (7:3, v:v). These irradiated solutions were also characterized by HPLC-DAD-MS and LC-HRMS/MS.

2.3. Equipment

2.3.1 Monochromatic Irradiation.

Monochromatic irradiations were performed, at 293 K, using a photochemical reactor (Newport) equipped with a 200 W Xe/ Hg arc lamp and a 2-mm interference filter (Oriel) to isolate wavelengths, (bandpass 16 nm).

The intensity of the incident light (I_0) at 366 nm was calculated using a diarylethene derivative (1,2-bis[2-methyl-5-(4-methylpyridyl)-3-thienyl] cyclopentene) [43], whereas for 313 nm potassium hexacyanocobaltate (III) was used at concentrations of 10^{-2} M (in H_2O, pH = 2) [44]. The I_0 was calculated, with correction for the absorbed light according to equation (1):

$$I_0 = V_{sol} \, (\Delta A/\Delta\varepsilon)/1000 \, \Phi_R \, \Delta t \qquad (1)$$

where, V_{sol} is the volume of irradiated solution in mL (3 mL); ΔA is the change in absorbance at the monitoring wavelength over the irradiation time period, Δt; $\Delta\varepsilon$ is the difference between the molar absorption coefficients of reagent and product at the monitoring wavelength. The quantum yield of reaction (Φ_R) for DAE is 0.34, and 0.31 for potassium hexacyanocobaltate (III). The value for the incident light (I_0) at 366 nm and 313 nm was calculated 2.61×10^{-6} and 1.22×10^{-6} (mol min^{-1}), respectively.

The quantum yields of reaction in homogeneous media were calculated with equation (1) rearranged as:

$$\Phi_R = V_{sol} \, (\Delta A/\Delta\varepsilon)/1000 \, I_{abs} \, \Delta t \qquad (2)$$

Where, I_{abs} is the light absorbed by the solution at the irradiation wavelength; I_{abs} was made equal to $I_0 \times (1 - 10^{-A_{irr}})$ when $A < 2$ and to I_0 when $A > 2$.

The quantum yield in heterogeneous media was calculated as in the homogeneous media using eqation (2). The irradiated volume, calculated through the measurement of

118

the optical path (1 cm) exposed to light, was 3 mL. Estimated errors for the Φ_R are 10% and are the result of three independent measurements.

2.3.2 Polychromatic Irradiation and color loss calculation

The irradiation experiment was carried out in a CO.FO.ME.GRA accelerated aging apparatus (SolarBox 3000e) equipped with a Xenon-arc light source (λ_{irr}> 300 nm) with constant irradiation of 800 W/m^2 and black standard temperature of 50°C, cooled with air conditioning (inside the camera temperature was maintained at approximately 25°C).

The percentage of color loss was calculated considering the maximum of absorbance of each compound in the visible region. With exposure to light, this maximum of absorbance will decrease, allow the calculation of the difference as: (Abs_f x 100%)/ Abs_0= Abs_f %, where Abs_f is the absorbance maximum after several hours of irradiation, and Abs_0 is the absorbance maximum at t=0h. After this, the color loss is calculated as: 100% - Abs_f% = color loss%.

2.3.3 HPLC-DAD-MS and LC-HRMS/MS analysis

The irradiated solutions were analyzed by HPLC-DAD-MS on a Dionex Ultimate 3000SD system with a diode array detector coupled online to a LCQ Fleet ion trap mass spectrometer equipped with an ESI ion source (Thermo Scientific, Waltham, MA, USA). Separations were carried out with a Kinetex C18 column 100 Å (150 x 2.6 mm, 5 μm particle size, Phenomenex) at a controlled temperature of 35°C, using a flow rate of 0.3 mLmin^{-1}. The mobile phase was 0.1% of acid formic in water (v/v, eluent A) and acetonitrile (eluent B). The elution gradient was as follows: 0-2 min linear gradient to 7% B; 2-22 min linear gradient to 80 % B, 22-23 min linear gradient to 100 % B, 23-27 min linear isocratic to 100% B, 27-28 min linear gradient to 7% B, and then the column was re-equilibrated with 7 % B for 7-min. The mass spectrometer was operated in the ESI positive and negative ion modes, with the following optimized parameters: ion spray voltage, ±4. 5 kV; capillary voltage, 16/-18 V; tube lens offset, -70/58 V; sheath gas (N$_2$), 40 arbitrary units; auxiliary gas (N$_2$), 20 arbitrary units; capillary temperature, 270°C. Spectra typically corresponds to an average of 20–35 scans, and were recorded in a range between 100-

1000 Da.

To further characterize the degradation products, the irradiated solutions were also analyzed by liquid chromatography (UHPLC Elute system) interfaced with a QqTOF Impact II mass spectrometer equipped with an ESI source (Bruker Daltoniks, Bremen, Germany). Chromatographic separations were carried out on a Kinetex C18 column 100 Å (100 mm x 2.1 mm, 2.6 µm particle size; Phenomenex). The mobile phase consisted of water (A) and acetonitrile (B), containing 0.1% (v/v) formic acid. The elution conditions were as follows: 0-2 min, linear gradient to 5% B; 2-15 min, linear gradient to 80% B; 15-16 min, linear gradient to 100% B; and 16-20 min, isocratic 100 % B; 20-21 min linear gradient to 5% B (followed by 6 min re-equilibration time). The injected volume was 3 µL, the flow rate 350 µLmin^{-1}, the column and the autosampler were maintained at 45°C and 8°C, respectively. High resolution tandem mass spectra were acquired in the ESI negative mode. The mass spectrometer parameters were set as follows: end plate offset: 500V; capillary voltage: -2.5 kV; nebulizer: 4 bars; dry gas: 8 L/min; dry temperature: 200°C. Internal calibration performed on the high-precision calibration mode (HPC) was achieved with a solution of 10 mM ammonium formate introduced to the ion source via a loop of 20 µL at the beginning of each analysis, using a six-port valve. Tandem mass spectra were obtained in a data-dependent-acquisition (DDA) mode, in a range between 100-1000 *m/z*, an acquisition rate of 5 Hz, and using a dynamic method with a fixed cycle time of 3s, and an isolation window of 0.03 Da. Data acquisition and processing were performed using the Data Analysis 4.2 software (Bruker Daltonics).

2.3.4 UV-VIS absorption spectroscopy

The UV-VIS absorption spectra were recorded on a Cary 100 Bio UV-VIS Varian spectrophotometer, at room temperature. The spectra were acquired in the range 200-800 nm, with an average scan time of 0.1 seconds/nm and scan rate of 600 nm/min.

3. RESULTS AND DISCUSSION

3.1 UV-VIS spectra

The absorption maxima (λ_{max}) and respective molar absorption coefficients (ε_{max}) for the UV-VIS spectra of the flavonoids and eriodictyol are listed in Table 14. The UV-VIS spectra from which λ_{max} were calculated are available as Supporting Information, Tables A4.1-A4.2. For the compounds studied in homogeneous media (methanol/water, 7:3 v/v) and heterogeneous media (proteinaceous gel), the ε_{max} ranges between 18000 and 23000 Mol^{-1} cm^{-1}, with a majority around 20000 Mol^{-1} cm^{-1} in agreement with a π-π^* transition [12, 45] and with values published in literature [7, 46]

Table 14- Absorption maxima, in the visible range, and respective molar extinction coefficients, ε, in solution MeOH:H$_2$O (7:3; v/v) and in proteinaceous gel at T = 293 K; ε values for the irradiation wavelength 366 nm and 313 nm in MeOH:H$_2$O are also given.

Dyes	MeOH:H$_2$O (7:3)		Proteinaceous gel		MeOH:H$_2$O (7:3)	
	λ_{max} (nm)	ε_{max} (Mol^{-1} cm^{-1})	λ_{max} (nm)	ε_{max} (Mol^{-1} cm^{-1})	ε_{366} (Mol^{-1} cm^{-1})	ε_{313} (Mol^{-1} cm^{-1})
Luteolin	350	2.21×10^4	350	2.32×10^4	1.82×10^4	1.15×10^4
Luteolin-7*O*Glc	351	2.01×10^4	351	2.23×10^4	1.63×10^4	9.66×10^3
Quercetin	371	1.92×10^4	372	1.73×10^4	1.90×10^4	7.05×10^3
Quercetin 3*O*Glr	360	1.82×10^4	352	1.01×10^4	1.71×10^4	1.07×10^4
Kaempferol	366	2.26×10^4	365	1.79×10^4	2.26×10^4	1.19×10^4
Kaempferol-3*O*Glc	348	1.82×10^4	345	2.01×10^4	1.42×10^4	1.35×10^4
Eriodictyol	290	1.89×10^4	280	1.46×10^4	3.84×10^2	5.76×10^3

The absorption spectra of flavonoids exhibit two characteristic bands, band I (300–440 nm) and band II (240–295 nm), which are influenced by the substitution pattern of the B-ring and the A–ring, respectively [46]. More specifically, for flavones, band I is found between 304-350 nm, while for flavonols (3-OH) between 352-385 nm [46]. According to the literature, it is possible to identify band I from 350 nm (luteolin) to *ca.* 370 nm (quercetin) and band II *ca.* 255 nm for all compounds, Table 14. As described by Markham and Mabry [46], "the absence of hydroxyl groups in either ring is usually evidenced by the relatively weak intensity of the relevant band", explaining why eriodictyol, lacking an OH substituent in ring A, displays a single band at 295 nm with a small shoulder at *ca.* 335 nm.

3.2 Monochromatic irradiation of flavonoid yellows

   3.2.1 Quantum yields of reaction at 313 nm and 366 nm

For the first time, to the best of our knowledge, the quantum yields of photodegradation, Φ_R, are measured for the flavonoid yellows listed in Table 15. For an accurate determination of reaction quantum yields we should ensure measurement accuracy for a single phenomenon as well as for the light absorbed. For this reason, values of Φ_R have been calculated at initial times to guarantee that a single event is being measured per photon absorbed at a specific wavelength, in this case, the degradation of the colorant at 313 nm or 366 nm, Figure 19 and Tables A4.1-A4.2.

In homogeneous media with irradiation at 313 nm, Φ_R values range from 1.8×10^{-5} to 1.4×10^{-5}, with the exception of eriodictyol with 1.7×10^{-6}, for the colorants studied, Table 15. Quercetin with a Φ_R value of 7×10^{-5} is the least stable of the series. Φ_R values below or equal to 10^{-6} are assigned to the lightfast pigment indigo in stable environments (for λ_{irr} 610 nm), one of the most stable natural dyes used in the past [13]. Luteolin with a Φ_R of 1.4×10^{-6} can be compared with the value for indigo (Φ_R of 9×10^{-6}), obtained by irradiating indigo in water at 335 nm, is the more stable yellow in these conditions. The almost ten-fold higher values observed for quercetin show that some of these flavonoid yellows are not as stable as indigo blues. In figure 19, the spectral evolution under irradiation shows a decrease of absorbance at 371 nm and slight increase at about 260 nm; this is in agreement with the absorption maxima observed for the identified degradation products, which will be discussed in next section.

However, when irradiation is carried out at 366 nm in homogenous media, a different mechanism is possibly at play, and values ranging from 2.8×10^{-5} to 8.7×10^{-6} were calculated. Importantly, this irradiation wavelength allows an even better discrimination of its stability, allowing to be built a stability scale in which we found in the 10^{-6} scale luteolin, its 7-*O*-glucoside as well as all 3-*O*-glycosides of quercetin and kaempferol. Quercetin and kaempferol are characterized by a Φ_R value of *ca.* 3×10^{-5}. With this excitation wavelength it was not possible to calculate Φ_R for eriodictyol, because it does not absorb. The values calculated for luteolin and the 3-*O*-glycoside derivatives are now closer to the values obtained for indigo in stable environments, reflecting an increase in stability for these chromophores.

122

In the proteinaceous gel, which mimics the environment of wool fibers, by irradiating again at 366 nm, a different scenario is observed: the Φ_R values increase for all the molecules studied, reaching 1x10⁻⁴ and 2x10⁻⁴ for kaempferol and quercetin, respectively. A drastic increase in instability was observed by changing the media.

Table 15- Quantum yields of reaction, Φ_R, irradiating at 366 nm for the flavonoid dyes in solution MeOH:H₂O (7:3; v/v) and in proteinaceous gel at T = 293 K; in solution Φ_R values were also acquired irradiating at λ_{irr} 313 nm.

	Φ_R @313 nm MeOH:H₂O	Φ_R @366 nm MeOH:H₂O	Φ_R @366 nm proteinaceous gel
Luteolin	1.38×10^{-5}	5.99×10^{-6}	3.07×10^{-5}
Luteolin-7*O*Glc	1.84×10^{-5}	8.67×10^{-6}	2.43×10^{-5}
Quercetin	6.97×10^{-5}	3.10×10^{-5}	2.08×10^{-4}
Quercetin-3*O*Glr	4.95×10^{-5}	7.15×10^{-6}	3.04×10^{-5}
Kaempferol	4.63×10^{-5}	2.81×10^{-5}	1.09×10^{-4}
Kaempferol-3*O*Glc	2.79×10^{-5}	6.46×10^{-6}	2.55×10^{-5}
Eriodictyol	1.67×10^{-6}	-	-
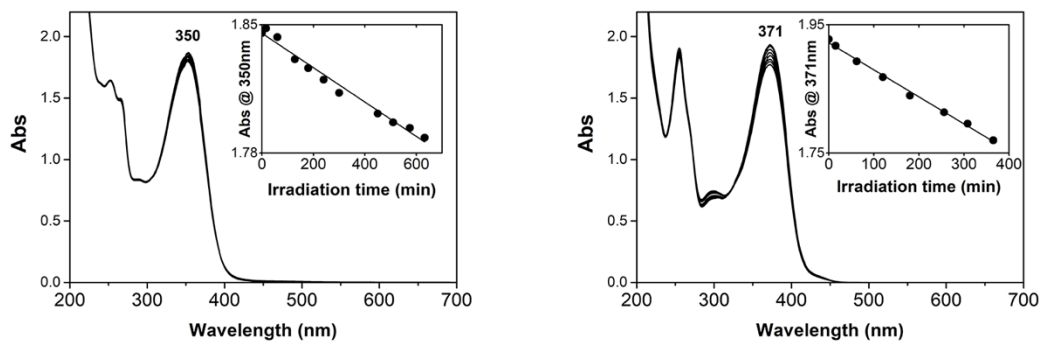
Figure 19- UV-VIS spectra evolution by irradiation at 313 nm, in a MeOH:H₂O solution, left luteolin and right quercetin. In the inset are plotted the values at absorbance maxima vs irradiation time, from which Φ_R is calculated (equations 1 and 2).

The Φ_R values allow us to propose that the more stable chromophores are luteolin and the 3-*O*-glycosides of quercetin and kaempferol, with safer excited state deactivation channels that compete with photoreactions, and that the impact of solvent on stability has wider implications for the role of the medium on the lightfastness of these colorants. All the flavonoids studied display the 5-OH substitution that allows the formation of a safe proton transfer in the excited state through a six-membered ring, Figure 16. Possibly because of this stronger OH bond established within the six-membered ring, the 3-OH

cannot compete with it forming the 5-membered ring depicted in Figure 16, thus being unable to protect this O-H bond through ESIPT. In addition, by determining 1.7x10^{-6} as the Φ_R value for eriodictyol, we showed that the double between C2 and C3 is critical for the stability of the molecule. Thus, the more this C2=C3 is stabilized when going to the excited state, the more stable the chromophore will be; stabilization can be promoted through, e.g., substituents on rings A or B [11, 12]. The C2=C3 double bond is thus one of the weak points of these systems, being the first to react by solvent attack, as first proven by Jørgensen *et al.* [6], Figure 17.

3.2.2 Identification of degradation products, irradiation at 366 nm, by HPLC-DAD and HRMS

In order to identify degradation products (DPs), the solutions of flavonoid dyes, in homogeneous media and submitted to monochromatic irradiation at 366 nm, were analyzed by HPLC-DAD-MS and LC-HRMS/MS. The results obtained indicate that kaempferol and quercetin solutions are prone to degradation via ring opening as a result of oxidation and solvent addition, Tables 16 and 17. For quercetin, a hydroxybenzoic acid and its methyl ester were identified that arise from oxidation of the C2-C3 bond, Table 16.

After 420 min of irradiation, the HPLC chromatograms showed only a peak assigned to the parent molecule, except for those of quercetin and kaempferol. The quercetin solution, at 150 min of irradiation, already displayed several degradation products, identified by LC-HRMS/MS, as listed in Table 16. The identified DPs are in accordance with those in Table 13. Ring-opening of quercetin is visible through the formation of chalcantrione (*m/z* 317, t_R 4.90 min), and other degradation products were identified such as 3,4-dihydroxybenzoic acid methyl ester (*m/z* 167, t_R 5.40 min) and 2,4,6-trihydroxybenzoic acid (*m/z* 169, t_R 5.92 min), as well as two depsides (*m/z* 349, t_R 5.42 min, *m/z* 363, t_R 6.50 min). The fragmentation paths supporting the proposed DPs structures are presented in Table A4.5.

At 180 min of irradiation, chromatograms of kaempferol indicate a decrease in kaempferol signal (*m/z* 285, t_R 8.0 min), and the appearance of two new peaks at *m/z* 333 (t_R 6.03 min) and *m/z* 347 (t_R 7.26 min). Based on high-resolution accurate measurements

the two degradation products were assigned to the ionic structures $[C_{16}H_{13}O_8]^-$ (m/z 333.0600) and $[C_{17}H_{16}O_8]^-$ (m/z 347.0763), which result from oxidation that follows from solvent addition to the C2=C3 double bond and are shown in Table 17. Both precursor ions dissociated via similar fragmentation paths. The more relevant fragment corresponds to the aglycone radical ion, m/z 284.0313, formed by the consecutive losses of one water molecule and one methoxy radical, or one methanol and one methoxy radical, from precursor ions m/z 333.0600 and 347.0763, respectively, as described in Table A4.5. At 300 min of irradiation, a new peak with m/z 317.0654 was observed and was attributed to a $[C_{15}H_{10}O_8]$ structure shown in Table 17, formed in a reaction where oxidized kaempferol incorporated one methanol molecule, as supported by the MS/MS data presented in Table A4.5.

Table 16- Quercetin in homogeneous media (MeOH:H₂O) at 150h of irradiation; the main degradation products were identified by HPLC-DAD-MS and characterized by LC-HRMS/MS (λ_{irr}= 366 nm).
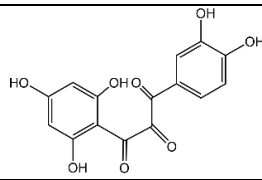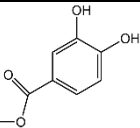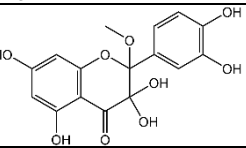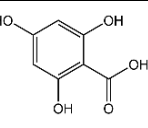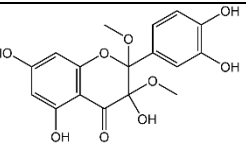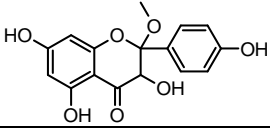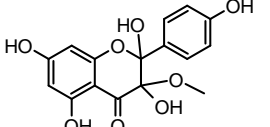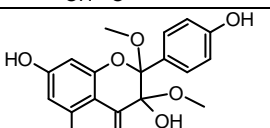
Proposed molecular structures	ESI(-)/MS (m/z) (Δppm; mSigma)	Ion formula	t_R (min)	λ_{max} (nm)
	317.0338 (+3.7; 17.1)	$[C_{15}H_9O_8]^-$	4.90	238; 294
	167.0322 (+4.8; 11.2)	$[C_8H_7O_4]^-$	5.40	260, 294
	349.0549 (+4.5; 6.0)	$[C_{16}H_{13}O_9]^-$	5.42	292
	169.0138 (+2.6;12.1)	$[C_7H_5O_5]^-$	5.92	260; 298
	363.0716 (+1.6; 8.7)	$[C_{17}H_{15}O_9]^-$	6.50	294

Table 17- Kaempferol in homogeneous media (MeOH:H₂O) at 180 min of irradiation. The main degradation products were identified by HPLC-DAD-MS and characterized by LC-HRMS/MS (λ_{irr}= 366 nm). For details, please see Table A4.5.

Proposed molecular structures	ESI(-)/MS (m/z) (Δppm; mSigma)	Ion formula	t_R (min)	λ_{max} (nm)
	317.0654 (+4.9; 17.3)	$[C_{16}H_{13}O_7]^-$	5.06	-
	333.0604 (+3.6; 10.6)	$[C_{16}H_{13}O_8]^-$	6.03	292
	347.0763 (+2.5; 15.6)	$[C_{17}H_{15}O_8]^-$	7.26	288

3.3 Polychromatic irradiation in homogeneous media: degradation products identified by HPLC-DAD and LC-HRMS/MS

To better understand the fundamental degradation mechanism at play for the three types of molecules, aging experiments using a more intense light source and polychromatic radiation were carried out (Xenon lamp, λ_{irr}> 300 nm), Table A4.3. These studies allow the simulation, in much shorter times, of degradation that occurs during natural aging and can be used to obtain information on the products present on faded artworks. The color loss, in percentage, was measured at the maximum of absorbance for each compound; for more details, please see section 2.3.2. The results show that quercetin is the chromophore with the fastest color loss rate (95% at 40h), opposed to luteolin (64% at 130h), Figure 20. At 40h luteolin presented a 14% color disappearance, luteolin-7-*O*-glucoside had 29% and quercetin-3-*O*-glucuronide 14.5%. Hence, in agreement with the Φ_R values, when a glycoside is present in the 3-hydroxyl group of quercetin, a significant decrease in the color loss rate is observed.

126
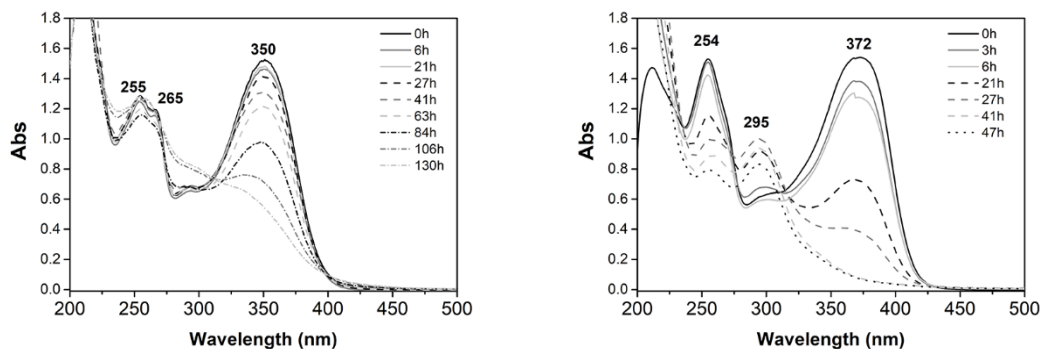
Figure 20- UV-VIS spectra in MeOH during irradiation with a Xenon source (λ_{irr} > 300 nm); *left* luteolin and *right* quercetin. At 40h luteolin showed a 14% color loss while quercetin had a 95% color loss; when measured at the maximum of absorbance (350 and 372 nm, respectively).

Overall, the typologies of the main products obtained are in agreement with that found in the literature for electrochemical degradation, Figure 17 and Table 13. No direct degradation products resulting from the loss of carbon monoxide were detected in our experimental conditions [5, 46- 50], Tables 18 and 19. In all the flavonoids studied solvent addition occurred, followed in some cases by ring opening and the formation of low molecular weight hydroxyl compounds such as benzoic acids. For quercetin-3-*O*-glucuronide, when 76% color loss was observed (measured at 358 nm), only products resulting from solvent attack were identified, Table 19. In addition, for the glycosylated flavonoids small peaks at higher *m/z* values suggest the formation of dimers or trimers. The experimental data that supported these findings are discussed below.
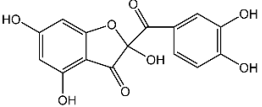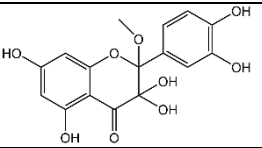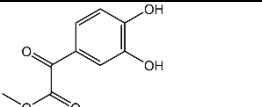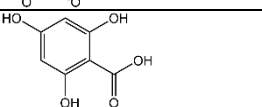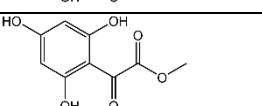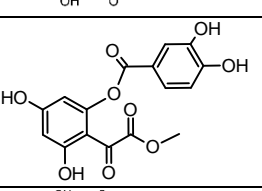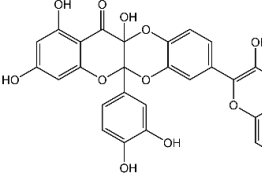
To characterize the oxidized products of the flavonoid dyes, aliquots of the oxidized solutions were collected and monitored with both HPLC with a DAD detector coupled on-line with a mass spectrometer, and HR tandem mass spectrometry. HPLC-DAD-MS and LC-HRMS/MS data are summarized in Table A4.4, Figures A4.2-A4.6, and Table A4.5, respectively. The chromatographic profiles indicate that the peak intensity of each yellow dye decreases, and new peaks appear and increase over time, revealing a wide variety of degradation products. The variation in the peak areas of each dye ion and their main DPs as a function of the irradiation time is also shown in 3D graph, Figures A4.7-A4.11. DPs were identified based on the accurate *m/z* values of the deprotonated molecules [M-H]⁻, the elemental composition of each peak was predicted using the algorithm Smart Formula 3D, and values with mass deviation (Δ) lower than 5 ppm and mSigma < 25 were considered acceptable. Molecular formulas were then validated by extracting

127

ionic chromatograms from the raw data, and accurate masses, isotopic patterns and fragmentation paths were evaluated, supporting the respective proposed chemical structures.

3.3.1 Identification of degradation products of quercetin and quercetin-3-O-glucuronide

Quercetin solutions in methanol, after polychromatic irradiation, present complex profiles. Both the DAD and MS chromatograms exhibit several peaks indicating that extensive degradation has occurred as the irradiation time increases, as shown in Figure A4.3

Table 18- Quercetin in MeOH (λ_{irr}> 300 nm); the main degradation products were identified by HPLC-DAD-MS and characterized by LC-HRMS/MS. For more details, please see Table A4.5.

Proposed molecular structures	ESI(-)/MS (*m/z*) (Δppm; mSigma)	Ion formula	t_R (min)	λ_{max} (nm)	Obs
	317.0297 (+0.2; 3.3)	$[C_{15}H_9O_8]^-$	5.45	274	Minor compound until 27h irr.
	349.0562 (+1.0; 4.3)	$[C_{16}H_{13}O_9]^-$	6.05	290	Major compound between 3h and 27h irr.
	195.0293 (-0.6; 3.2)	$[C_9H_7O_5]^-$	6.37	292	Observed until 27h irr.
	169.0140 (+0.3; 1.6)	$[C_7H_5O_5]^-$	6.54	260; 298	Major compound at 27h irr.
	211.0248 (-3.8; 9.9)	$[C_9H_7O_6]^-$	7.15	300	Major compound at 48h irr.
	347.0422 (-3.9; 19.8)	$[C_{16}H_{11}O_9]^-$	8.23	298	Observed at 41h and 48h irr.
	601.0628 (-0.7; 10.7)	$[C_{30}H_{17}O_{14}]^-$	9.72	304; 362	Observed until 27h irr.

128

The more relevant data summarized in Table 18 indicate that degradation of quercetin in methanol (t_R 7.95 min, m/z 301), occurs via oxidation with solvent addition followed by hydrolysis leading to low molecular weight hydroxyl compounds. HPLC-DAD-MS data recorded at 3h of irradiation displayed three peaks that in the UV-VIS spectra share a single band around 290 nm. The first two compounds, co-eluting at t_R 6.05 min, yield two ions with m/z 331 and 349 (the more abundant ion), the t_R 9.29 min produced an ion with m/z 363 Table A4.5. Based on accurate mass measurements the three ions are assigned to $[C_{16}H_{11}O_8]^-$, $[C_{16}H_{13}O_9]^-$ and $[C_{17}H_{15}O_9]^-$ structures, respectively. To characterize the proposed structures, collision induced dissociation (CID) experiments were performed. HR tandem mass spectrometric results presented in Table A4.5 indicate that the three precursor ions follow common fragmentation pathways. The most relevant fragmentation gave rise to a fragment ion with m/z 299.0197 assigned to a $[C_{15}H_7O_7]^-$, a quinone form of quercetin. Based on this data it is proposed that DP 331, 349 and 363 are deprotonated molecules formed from oxidized quinone-methide forms, by the addition of one methanol, one methanol plus one water, and two methanol molecules, respectively. The fact that no signal was found for the deprotonated molecule of the quinoid structure indicates that solvent addition is a fast process. Similar results are reported by Hvattum *et al.* [51].
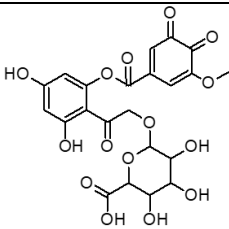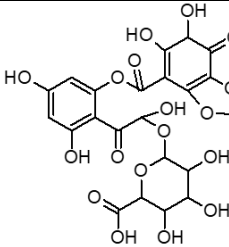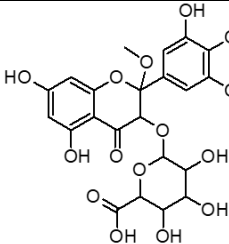
The mass spectrum also displayed an ion attributed to a deprotonated molecule with m/z 317.0297, assigned to a benzofuranone structure with a molecular formula $[C_{15}H_{10}O_8]$. A small peak with m/z 333.0255 (t_R 6.97 min) was attributed to a $[C_{15}H_9O_9]^-$ ion. It is proposed that this ion corresponds to a substituted depside form, an open–oxo-acetic acid structure, which subsequently hydrolyzed giving 2,4,6-trihydroxybenzoic acid (t_R 6.54 min, m/z 169) and methyl 3,4-dihydroxyphenylglyoxylate (t_R 6.37 min, m/z 195). At 6h of irradiation the formation of a new peak (DP601) was observed that had a longer retention time (t_R 9.72 min). It had m/z 601, and a UV-VIS spectrum with two bands ranging from 270-304 nm, and a band at 362 nm. The HR-tandem mass spectrum of the precursor ion m/z 601.0628 gave a fragment ion with m/z 299 due to the loss of 302 Da, indicating the presence of a doubly linked dimer formed through a concerted reaction between the B-ring of the o-quinone moiety and the C2-C3 double bond of C-ring of another quercetin unit, as proposed by Krishnamachari *et al.* [52]. At 27h of irradiation, a small peak at t_R 8.23 min, with m/z 347 was identified. From accurate mass measurements,

a molecular formula of [$C_{16}H_{12}O_9$] assigned as a methoxy depside form (DP347) has been proposed. At longer irradiation times, the DP347 depside hydrolyzed giving the methyl ester of 2,4,6-trihydroxyphenylglyoxylic acid (t_R 7.15 min, m/z 211), the main peak in the HPLC-DAD-MS at 48h of irradiation, Figure A4.3. The variation of the peak area of quercetin ion and its main DPs as a function of the irradiation time is shown in 3D graph, Figure A4.7.

When comparing data from Table 16 with monochromatic irradiation (λ_{irr}= 366 nm) of quercetin and form Table 18, (λ_{irr}> 300 nm), it is possible to see that three degradations products were found in both experiments, with DP317, DP349 and DP169, all sharing a similar degradation mechanism.

Table 19 summarizes the main degradation products of quercetin-3-O-glucuronide in methanol (t_R 6.10 min, m/z 477). Only at around 106h of irradiation was observed the appearance of degradation products resulting mainly from addition of solvent molecules. In addition to the species formed by solvent attack (m/z 523 and 587), very small peaks with higher m/z values were detected on the HRMS spectra (between 700-1200 Da, data not included). These values can correspond to dimers and trimers of quercetin-3-O-glucuronide, as reported in previous studies on photodegradation of rutin [38], in which these products were identified by LC-MS.

Table 19- Quercetin-3-*O*-glucuronide in MeOH (λ_{irr}> 300 nm); the main degradation products were identified by HPLC-DAD-MS and characterized by LC-HRMS/MS. For more details, please see Table A4.5.
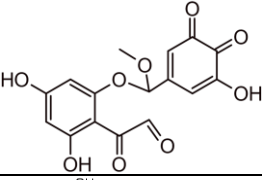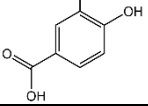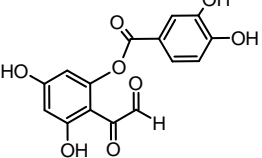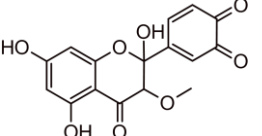
Proposed molecular structures	ESI(-)/MS (*m/z*) (Δ ppm; mSigma)	Ion formula	t_R (min)	λ_{max} (nm)	Obs
	523.0730 (-0.1; 23.1)	$[C_{22}H_{19}O_{15}]^-$	4.63	292; 294	Major compound at 190h irr.
	587.0859 (-2.3; 10.5)	$[C_{23}H_{23}O_{18}]^-$	5.43	260; 296	Minor compound at 190h irr.
	539.1054 (-2.1; 6.8)	$[C_{23}H_{23}O_{15}]^-$	6.46	258; 352	2 isomers, appeared at 147 h irr; major compounds at 190h irr,

3.3.3 Identification of degradation products of luteolin and luteolin-7-O-glucoside

HPLC-DAD-MS analysis of the methanolic solutions of luteolin (t_R 7.96 min; *m/z* 285) did not show any significant qualitative change until 63h of irradiation; only luteolin was present. At 84h irradiation, the chromatogram recorded at 290 nm showed three small signals that in the mass spectrum yielded ions with *m/z* 347, 153 and 317. The last one was attributed to a depside $[C_{15}H_9O_8]^-$ structure as shown in Table 20. According to Sokolová 2016 [50], due to the absence of the hydroxyl group at C3 in the structure of luteolin, the depside form may correspond to an "oxobenzaldehyde". This assumption is supported by the HRMS/MS data of the precursor ions *m/z* 317.0295 identified in both quercetin and luteolin solutions, which follow different fragmentation pathways indicating different structure rearrangements, Scheme A4.4-A4.5. Subsequent decomposition of
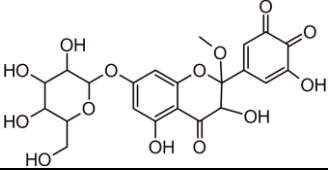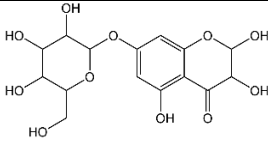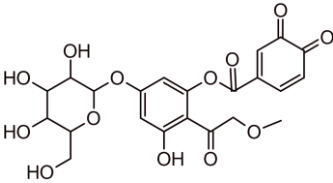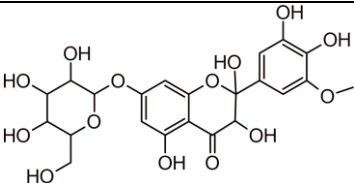
the open structure gives rise to the 3,4-dihydroxybenzoic acid (*m/z* 153). At 147h of irradiation, the signal corresponding to luteolin had a very low intensity; the more abundant deprotonated molecules are due to degradation products from solvent addition, Table A4.5, Figures A4.6 and A4.9.

Table 20- Luteolin in MeOH (λ_{irr}> 300 nm); the main degradation products were identified by HPLC-DAD-MS and characterized by LC-HRMS/MS. For more details, please see Table A4.5.

Proposed molecular structures	ESI(-)/MS (*m/z*) (Δppm; mSigma)	Ion formula	t_R (min)	λ_{max} (nm)	Obs
	347.0401 (+2.3; 10.01)	$[C_{16}H_{11}O_9]^-$	5.66	304	Minor compound until 147h irr.
	153.0192 (+0.6; 6.7)	$[C_7H_5O_4]^-$	5.87	292	Major compound at 147h irr.
	317.0295 (+2.5; 1.3)	$[C_{15}H_9O_8]^-$	6.25	302	Minor compound until 147h irr
	331.0448 (+3.2; 8.4)	$[C_{16}H_{11}O_8]^-$	8.18	318	Major isomers at 147h irr.

The decomposition of luteolin-7-*O*-glucoside (t_R 6.61min, *m/z* 447) with 80% color loss (measured at 350 nm), was also assessed by HPLC-DAD-MS and LC-HRMS/MS. At 67 h of irradiation, peaks with very low intensity assigned to degradation products were observed, Table 21 and Figure A4.6. As mentioned in the literature, degradation of luteolin-7-*O*-glucoside proceeds through addition of solvent molecules and C ring opening. DP373, the major peak at 130h of irradiation, was assigned to a decomposition product, Table A4.5. At longer irradiation times, the HRMS/MS spectra also displayed very small signals at higher *m/z* values that may have resulted from dimer degradation products present in the irradiated solutions (data not included).
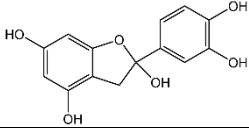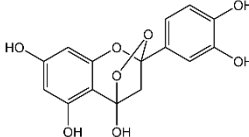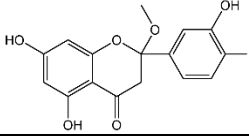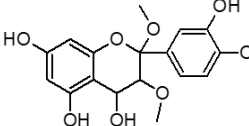
Table 21- Luteolin-7-*O*-glucoside in MeOH (λ_{max}> 300 nm); the main degradation products were identified by HPLC-DAD-MS and characterized by LC-HRMS/MS. For more details, please see Table A4.5

Proposed molecular structures	ESI(-)/MS(m/z) (Δppm; mSigma)	Ion formula	t_R (min)	λ_{max} (nm)	Obs
	509.0935 (-3.7; 6.4)	$[C_{22}H_{21}O_{14}]^-$	4.79	258; 290	Major compound at 67h irr.
	373.0796 (-5.2; 19.1)	$[C_{15}H_{17}O_{11}]^-$	6.18	294	Major compound from 67h irr.
	493.1000 (-2.6; 10.2)	$[C_{22}H_{21}O_{13}]^-$	6.92	262; 328	Observed from 106 h irr.
	511.1110 (-3.3; 3.2)	$[C_{22}H_{23}O_{14}]^-$	7.48	260; 320	2 isomers, appear at 106 h irr; major compounds at 130h irr,

3.3.4 Identification of degradation products of eriodictyol

In Table 22 the main degradation products are listed along with the proposed structures supported by HRMS/MS analysis. At 102 h of irradiation, the deprotonated molecule of the eriodictyol is a minor signal, while DP349, resulting from the addition of two methanol molecules dominates the mass spectrum. DP319, probably a product of the oxidation of eriodictyol, decomposes leading to DP275, Table A4.5. The variation in the peak areas of eriodictyol ion and its main DPs as a function of the irradiation time is also shown in 3D graph, Figure A4.11.

Table 22- Eriodictyol in MeOH (λ_{irr}> 300 nm); the main degradation products were identified by HPLC-DAD-MS and characterized by LC-HRMS/MS. For more details, please see Table A4.5.

Proposed molecular structures	ESI(-)/MS (*m/z*) (Δppm; mSigma)	Ion formula	t_R (min)	λ_{max} (nm)	Obs
	275.0563 (-0.8; 4.6)	$[C_{14}H_{11}O_6]^-$	6.51	288	Minor compound until 62h irr
	319.0459 (+0.3; 13.9)	$[C_{15}H_{11}O_8]^-$	6.96	286	Minor compound until 102h irr
	317.0666 (-0.6; 3.4)	$[C_{16}H_{13}O_7]^-$	8.57	288	Observed from 21h irr.
	349.0932 (-1.0; 5.9)	$[C_{17}H_{17}O_8]^-$	9.83	289	Main compound at 102h irr.

4- Conclusions

Photodegradation studies, using irradiation wavelengths > 300 nm, can be used to simulate natural aging mechanisms, in times much faster than other techniques such as thermal aging. To achieve this goal, it is necessary to prove that natural and photochemical aging share the same degradation mechanism. In our case study, we need to show that the main intermediates and main degradation products, in solution and in proteinaceous gel that mimic a wool environment, are similar to those found in ancient textiles. Our data show that this is the case. Although in ancient textiles flavonoid dyes are usually complexed to the fiber through aluminum ions, at the level of the main degradation products, our data compares with that found in ancient textiles by Zhang *et al.* [34] and Degano *et al.* [33]: benzoic acids, whose substitution pattern depends on the parent molecule, and depside type molecules, Table 13 and Figure 18. In doing so, we show that our data, performed in solution and proteinaceous media, relate to data acquired on textile fibers, namely on the main products characterized in ancient textiles. Based on these data, we can also add that it is very likely that the various hydroxybenzoic acids detected in pre-Columbian Andean textiles studied by Zhang *et al.* were the result of natural aging during the hundreds of years of burial [34].

134

Thus, this study is a fundamental starting point for understanding the degradation of flavonoid yellows in works of art. However, bearing in mind that the studied dyes are used in textiles in combination with a metal mordant, we expect that this will influence the absolute values of the quantum yields of reaction, Φ_R, but not the relative stability scale. As we observed when comparing the values in methanol/water solution with the proteinaceous media, in which the stability of the dyes decreased. It is important to highlight that the Φ_R values obtained in solution irradiating at 366 nm provide a scale to accurately measure the stability of flavonoid yellows: Lut-7-*O*-Glc > Que-3-*O*-Glr > Kae-3-*O*-Glc ≈ luteolin >> quercetin ≥ kaempferol. These Φ_R values fully agree with the levels of degradation observed using a more intense light source (Xenon lamp and polychromatic irradiation); a first phase characterized by intermediates resulting from solvent attack (with or without opening of the C ring) and, a second phase in which low molecular weight products such as benzoic acids are formed.

The higher stability of luteolin yellows is explained by the absence of an OH in position C3 and by the high protective effect offered by excited state proton transfer based on the 5-hydroxyflavone six-membered ring, which is more stable than that the 3-hydroxyflavone five-membered ring, Figure 16. Nagaoka *et al.* also showed that electron transfer to other compounds is enhanced through the OH in position C3 when compared to OH in C5 [53]. The combination of these two effects: higher protection due to OH in C5 and higher reactivity by electron injection caused by OH in C3 makes quercetin and kaempferol the most unstable structures. When the OH in C3 is protected by a monosaccharide, electron transfer & oxidation are avoided, and the molecules attain a stability comparable to luteolin. On the other hand, when the ESPT mechanism becomes less efficient due to solvent interference in the hydrogen bond needed to form the six-membered ring based on C5-OH, as seen in the proteinaceous gel, a drastic loss of stability was observed (*ca.* one order of magnitude).

For eriodictyol it was only possible to calculate Φ_R by irradiating at 313 nm (as it does not absorb at 366 nm); with a 1.7×10^{-6} value, it is the most stable compound of the series, showing that another critical point for stability is the double bond between C2-C3.

We hope that this new knowledge on these fascinating molecules used in the past, on textiles and paintings, will contribute to a better preservation of flavonoid yellows in

cultural heritage.

5. References

[1] Cardon, D. (2007). *Natural dyes: sources, tradition, technology and science* (1st ed.) Archetype Publications. ISBN 190498200X

[2] Zhang, X., Cardon, D., Cabrera, J. L., & Laursen, R. (2010). The role of glycosides in the light-stabilization of 3-hydroxyflavone (flavonol) dyes as revealed by HPLC. Microchimica Acta, 169(3-4), 327-334. Doi: 10.1007/s00604-010-0361-x

[3] Sharif, S., Nabais, P., Melo, M. J., & Oliveira, M. C. (2020). Traditional yellow dyes used in the 21st century in central Iran: the knowledge of master dyers revealed by HPLC-DAD and UHPLC-HRMS/MS. *Molecules*, 25(4), 908. Doi: 10.3390/molecules25040908

[4] Ferreira, E. S. B. (2001). *New approaches towards the identification of yellow dyes in ancient textiles* [Doctoral dissertation, University of Edinburgh]. University of Edinburgh Repository. http://hdl.handle.net/1842/12020

[5] Colombini, M. P., Andreotti, A., Baraldi, C., Degano, I., & Łucejko, J. J. (2007). Color fading in textiles: A model study on the decomposition of natural dyes. *Microchemical Journal*, 85(1), 174-182. Doi: 10.1016/j.microc.2006.04.002

[6] Jørgensen, L. V., Cornett, C., Justesen, U., Skibsted, L. H., & Dragsted, L. O. (1998). Two-electron electrochemical oxidation of quercetin and kaempferol changes only the flavonoid C-ring. *Free Radical Research*, 29(4), 339-350. Doi: 10.1080/10715769800300381

[7] Fahlman, B. M., & Krol, E. S. (2009). UVA and UVB radiation-induced oxidation products of quercetin. *Journal of Photochemistry and Photobiology B: Biology*, 97(3), 123-131. Doi: 10.1016/j.jphotobiol.2009.08.009

[8] Bentsáth, A., Rusznyák, S., & Szent-Györgyi, A. (1936). Vitamin nature of flavones. *Nature*, 138(3497), 798-798. Doi: 10.1038/138798a0

[9] Bondarev, S. L., Knyukshto, V. N., Tikhomirov, S. A., & Buganov, O. V. (2016). Mechanism for highly efficient non-radiative deactivation of electronic excitation in rutin. *Journal of Applied Spectroscopy*, 82(6), 929-935. Doi: 10.1007/s10812-016-0207-3

[10] Sengupta, P. K., & Kasha, M. (1979). Excited state proton-transfer spectroscopy of 3-hydroxyflavone and quercetin. *Chemical Physics Letters*, 68(2-3), 382-385. Doi: 10.1016/0009-2614(79)87221-8

[11] Strandjord, A. J., Smith, D. E., & Barbara, P. F. (1985). Structural effects on the proton-

transfer kinetics of 3-hydroxyflavones. *The Journal of Physical Chemistry*, 89(11), 2362-2366. Doi: 10.1021/j100257a042

[12] Chou, P., Chen, Y., Yu, W., & Cheng, Y. (2001). Spectroscopy and dynamics of excited-state intramolecular proton-transfer reaction in 5-hydroxyflavone. *Chemical Physics Letters*, 340(1-2), 89-97. Doi: 10.1016/s0009-2614(01)00399-2

[13] Miliani, C., Monico, L., Melo, M. J., Fantacci, S., Angelin, E. M., Romani, A., & Janssens, K. (2018). Photochemistry of artists' dyes and pigments: towards better understanding and prevention of color change in works of art. *Angewandte Chemie International Edition*, 57(25), 7324-7334. Doi: 10.1002/anie.201802801

[14] Kleinermanns, K., Nachtigallová, D., & Vries, M. S. (2013). Excited state dynamics of DNA bases. *International Reviews in Physical Chemistry*, 32(2), 308-342. Doi: 10.1080/0144235x.2012.760884

[15] Sousa, M. M., Miguel, C., Rodrigues, I., Parola, A. J., Pina, F., Melo, J. S., & Melo, M. J. (2008). A photochemical study on the blue dye indigo: from solution to ancient Andean textiles. *Photochemical & Photobiological Sciences*, 7(11), 1353. Doi: 10.1039/b809578g

[16] Wei, Y., Zhang, Z., Chen, Y., Wu, C., Liu, Z., Ho, S., . . . Chou, P. (2019). Mechanochromism induced through the interplay between excimer reaction and excited state intramolecular proton transfer. *Communications Chemistry*, 2(1). Doi: 10.1038/s42004-019-0113-8

[17] Yang, Y., Zhao, J., & Li, Y. (2016). Theoretical study of the ESIPT process for a new natural product quercetin. *Scientific Reports*, 6(1). Doi: 10.1038/srep32152

[18] Yang, D., Yang, G., Zhao, J., Zheng, R., Wang, Y., & Lv, J. (2017). A theoretical assignment on excited-state intramolecular proton transfer mechanism for quercetin. *Journal of Physical Organic Chemistry*, 30(11). Doi: 10.1002/poc.3684

[19] Protti, S., & Mezzetti, A. (2015). Solvent effects on the photophysics and photoreactivity of 3-hydroxyflavone: a combined spectroscopic and kinetic study. *Journal of Molecular Liquids*, 205, 110-114. Doi: 10.1016/j.molliq.2014.12.001

[20] Anand, N., Welke, K., Irle, S., & Vennapusa, S. R. (2019). Nonadiabatic excited-state intramolecular proton transfer in 3-hydroxyflavone: S2 state involvement via multi-mode effect. *The Journal of Chemical Physics*, 151(21), 214304. Doi: 10.1063/1.5127271

[21] Das, S., Mukherjee, S., Chakrabarty, S., & Chattopadhyay, N. (2020). Hydroxyl group-directed solvation of excited-state intramolecular proton transfer probes in water: a demonstration from the fluorescence anisotropy of hydroxyflavones. *The Journal of Physical Chemistry A*, 125(1), 57-64. Doi: 10.1021/acs.jpca.0c08023.s001

138

[22] Simkovitch, R., & Huppert, D. (2017). Intramolecular excited-state hydrogen transfer in rutin and quercetin. *Israel Journal of Chemistry*, 57(5), 393-402. Doi: 10.1002/ijch.201600112

[23] Liu, H. B., Yu, D., Shin, S. C., Park, H. R., Park, J. K., & Bark, K. M. (2009). Spectroscopic properties of quercetin derivatives, quercetin-3-*O*-rhamnoside and quercetin-3-*O*-rutinoside, in hydro-organic mixed solvents. *Photochemistry and photobiology*, 85(4), 934-942. Doi: 10.1111/j.1751-1097.2009.00550.x

[24] Favaro, G., Clementi, C., Romani, A., & Vickackaite, V. (2007). Acidichromism and ionochromism of luteolin and apigenin, the main components of the naturally occurring yellow weld: a spectrophotometric and fluorimetric study. *Journal of Fluorescence*, 17(6), 707-714. Doi: 10.1007/s10895-007-0222-0

[25] Hajji, H. E., Nkhili, E., Tomao, V., & Dangles, O. (2006). Interactions of quercetin with iron and copper ions: Complexation and autoxidation. *Free Radical Research*, 40(3), 303-320. Doi: 10.1080/10715760500484351

[26] Sokolová, R., Ramešová, Š, Degano, I., Hromadová, M., Gál, M., & Žabka, J. (2012). The oxidation of natural flavonoid quercetin. *Chemical Communications*, 48(28), 3433. Doi: 10.1039/c2cc18018a

[27] Pina, F., Melo, M. J., Laia, C. A., Parola, A. J., & Lima, J. C. (2012). Chemistry and applications of flavylium compounds: A handful of colors. *Chemical Society Reviews*., 41(2), 869-908. Doi: 10.1039/c1cs15126f

[28] Pina, F., Alejo-Armijo, A., Clemente, A., Mendoza, J., Seco, A., Basílio, N., & Parola, A. J. (2021). Evolution of Flavylium-Based Color Systems in Plants: What Physical Chemistry Can Tell Us. *International Journal of Molecular Sciences*, 22(8), 3833. Doi: 10.3390/ijms22083833

[29] Dangles, O., Dufour, C., & Bret, S. (1999). Flavonol–serum albumin complexation. Two-electron oxidation of flavonols and their complexes with serum albumin. *Journal of the Chemical Society, Perkin Transactions 2*, (4), 737-744. Doi: 10.1039/a810017i

[30] Smith, G. J., Thomsen, S. J., Markham, K. R., Andary, C., & Cardon, D. (2000). The photostabilities of naturally occurring 5-hydroxyflavones, flavonols, their glycosides and their aluminum complexes. *Journal of Photochemistry and Photobiology A: Chemistry*, 136(1-2), 87-91. Doi: 10.1016/s1010-6030(00)00320-8

[31] Dunford, C. L., Smith, G. J., Swinny, E. E., & Markham, K. R. (2003). The fluorescence and photostabilities of naturally occurring isoflavones. *Photochemical & Photobiological Sciences*, 2(5), 611-615. Doi: 10.1039/b300078h

[32] Ferreira, E. S., & Quye, A. (2002). Photo-oxidation products of quercetin and morin as

markers for the characterization of natural flavonoid yellow dyes in ancient textiles. In Kirby, J. (Ed.), *Dyes in history and archaeology 18* (pp. 63-72). Archetype. ISBN 1873132336

[33] Degano, I., Biesaga, M., Colombini, M. P., & Trojanowicz, M. (2011). Historical and archaeological textiles: An insight on degradation products of wool and silk yarns. *Journal of Chromatography A*, 1218(34), 5837-5847. Doi: 10.1016/j.chroma.2011.06.095

[34] Zhang, X., Boytner, R., Cabrera, J.S., Laursen, R. (2007). Identification of yellow dye types in pre-Columbian Andean textiles. *Analytical Chemistry*, 79, 1575-1582. Doi: 10.1021/ac061618f

[35] Tommasini, S., Calabrò, M., Donato, P., Raneri, D., Guglielmo, G., Ficarra, P., & Ficarra, R. (2004). Comparative photodegradation studies on 3-hydroxyflavone: influence of different media, pH and light sources. *Journal of Pharmaceutical and Biomedical Analysis*, 35(2), 389-397. Doi: 10.1016/s0731-7085(03)00586-7

[36] Dall'Acqua, S., Miolo, G., Innocenti, G., & Caffieri, S. (2012). The photodegradation of quercetin: relation to oxidation. *Molecules*, 17(8), 8898-8907. Doi: 10.3390/molecules17088898

[37] Mezzetti, A., Protti, S., Lapouge, C., & Cornard, J. (2011). Protic equilibria as the key factor of quercetin emission in solution. Relevance to biochemical and analytical studies. *Physical Chemistry Chemical Physics*, 13(15), 6858. Doi: 10.1039/c0cp00714e

[38] Chaaban, H., Ioannou, I., Paris, C., Charbonnel, C., & Ghoul, M. (2017). The photostability of flavanones, flavonols and flavones and evolution of their antioxidant activity. *Journal of Photochemistry and Photobiology A: Chemistry*, 336, 131-139. Doi: 10.1016/j.jphotochem.2016.12.027

[39] Dunford, C. L., Smith, G. J., Swinny, E. E., & Markham, K. R. (2003). The fluorescence and photostabilities of naturally occurring isoflavones. *Photochemical & Photobiological Sciences*, 2(5), 611. Doi: 10.1039/b300078h

[40] Smith, G. J., Thomsen, S. J., Markham, K. R., Andary, C., & Cardon, D. (2000). The photostabilities of naturally occurring 5-hydroxyflavones, flavonols, their glycosides and their aluminum complexes. *Journal of Photochemistry and Photobiology A: Chemistry*, 136(1-2), 87-91. Doi: 10.1016/s1010-6030(00)00320-8

[41] Momić, T., Savić, J., Černigoj, U., Trebše, P., & Vasić, V. (2007). Protolytic equilibria and photodegradation of quercetin in aqueous solution. *Collection of Czechoslovak Chemical Communications*, 72(11), 1447-1460. Doi: 10.1135/cccc20071447

[42] Matsuura, T., Matsushima, H., & Sakamoto, H. (1967). Photosensitized oxygenation of 3-hydroxyflavones. Possible model for biological oxygenation. *Journal of the American Chemical Society*, 89(24), 6370-6371. Doi: 10.1021/ja01000a078

[43] Ferreira, P., Ventura, B., Barbieri, A., Da Silva, J. P., Laia, C. A., Parola, A. J., & Basílio, N. (2019). A visible–near-infrared light-responsive host–guest pair with nanomolar affinity in water. *Chemistry–A European Journal*, 25(14), 3477-3482. Doi: 10.1002/chem.201806105

[44] Pina, F., Moggi, L., Manfrin, M. F., Balzani, V., Hosseini, M. W., & Lehn, J. M. (1989). Photochemistry of supramolecular systems-size and charge effects in the photoaquation of adducts of the hexacyanocobaltate (III) anion with polyammonium macrocyclic receptors. *Gazzetta Chimica Italiana*, 119(1), 65-67. Doi: 10.1021/ic00039a020

[45] Valeur, B., & Berberan-Santos, M. N. (2012). *Molecular fluorescence: principles and applications* (2nd ed.). Wiley-VCH Verlag & Co. KGaA. ISBN 9783527328376

[46] Markham, K. R., Mabry, T. J. (1975). Ultraviolet-visible and proton magnetic resonance spectroscopy of flavonoids. In J. B. Harborne, T. J. Mabry, H. Mabry (Eds.), *The flavonoids* (pp. 45-77). Springer. ISBN 9780123246028

[47] Studer, S. L., Brewer, W. E., Martinez, M. L., & Chou, P. T. (1989). Time-resolved study of the photooxygenation of 3-hydroxyflavone. *Journal of the American Chemical Society*, 111(19), 7643-7644. Doi: 10.1002/chin.199001076

[48] Abdolahzadeh, S., Boyle, N. M., Hage, R., Boer, J. W., & Browne, W. R. (2018). Metal-Catalyzed Photooxidation of Flavones in Aqueous Media. *European Journal of Inorganic Chemistry*, 2018(23), 2621-2630. Doi: 10.1002/ejic.201800288

[49] Russo, M., S☐tacko, P., Nachtigallová, D., & Klán, P. (2020). Mechanisms of orthogonal photodecarbonylation reactions of 3-hydroxyflavone-based acid–base forms. *The Journal of Organic Chemistry*, 85(5), 3527-3537. Doi: 10.1021/acs.joc.9b03248

[50] Sokolová, R., Ramešová, Š, Kocábová, J., Kolivoška, V., Degano, I., & Pitzalis, E. (2016). On the difference in decomposition of taxifolin and luteolin vs. fisetin and quercetin in aqueous media. *Monatshefte Für Chemie - Chemical Monthly*, 147(8), 1375-1383. Doi: 10.1007/s00706-016-1737-3

[51] Hvattum, E., Stenstrøm, Y., & Ekeberg, D. (2004). Study of the reaction products of flavonols with 2,2-diphenyl-1-picrylhydrazyl using liquid chromatography coupled with negative electrospray ionization tandem mass spectrometry. *Journal of Mass Spectrometry*, 39(12), 1570-1581. Doi: 10.1002/jms.756

[52] Krishnamachari, V., Levine, L. H., & Paré, P. W. (2002). Flavonoid oxidation by the radical generator AIBN: a unified mechanism for quercetin radical scavenging. *Journal of Agricultural and Food Chemistry*, 50(15), 4357-4363. Doi: 10.1021/jf020045e

[53] Nagaoka, S., Bandoh, Y., Matsuhiroya, S., Inoue, K., Nagashima, U., & Ohara, K. (2021).

Activity correlation among singlet-oxygen quenching, free-radical scavenging and excited-state proton-transfer in hydroxyflavones: Substituent and solvent effects. *Journal of Photochemistry and Photobiology A: Chemistry*, 409, 113122. Doi: 10.1016/j.jphotochem.2020.113122

Ongoing study

Flavonoid yellow dyes are complex systems, and their photophysical properties may be strongly influenced by metal ion complexation [1]. In addition, the involved process in their photochemical mechanisms is affected by the type of substrates [2].

Following the detailed study of photostability of flavonoids in homogenous and heterogeneous media and identification of their degradation products [3], we studied a wool sample-set in order to understand the photochemical behavior of studied natural yellow dye sources on a proteinous substrate and in the presence of aluminum ions (mordants).

The samples were selected in three categories:

1-Three wool samples lab-dyed with: the flowers of *Delphinium semibarbatum*, crushed leaves, and stems of *Prangos ferulacea* and *Eremostachys laevigata* (plants were obtained from the dyeing workshops [locations explained in Chapter 3, sections 3.2];

2- Two textiles dyed by *Reseda luteola* (100 and 200% plant:textile weight), accomplished by a dye expert (Dominique Cardon);

3- Three wool threads from a dyeing workshop [location explained in Chapter 3, sections 3.3]; dyed with: *Delphinium semibarbatum* (3% plant:thread weight), *Delphinium semibarbatum* together with (2% plant:thread weight) Rubia tinctorum (1% plant:thread weight), *Delphinium semibarbatum* (3% plant:thread weight) together with *Punica granatum* (1% plant:thread weight).
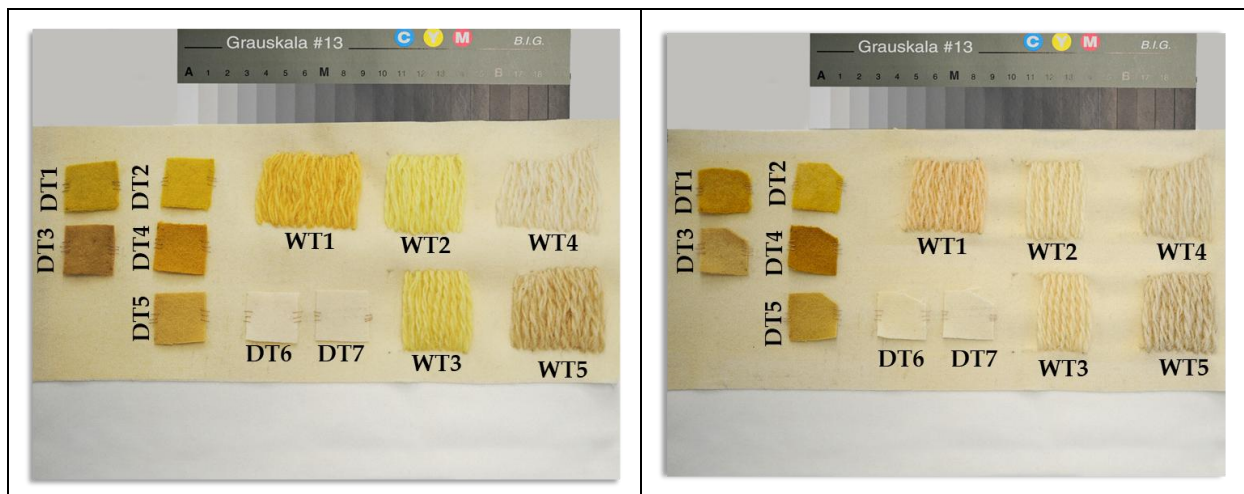
Figure 21- Irradiation of sample-set at 0h (left) and at 126h (right).

146

Table 23- Sample code name and sample identification. For the Dyed Textiles (DT) and the Workshop Threads (WT), a weighted amount is also shown

DT 1	Weld 100%	0,250g
DT 2	Weld 200%	0,240g
DT 3	*Eremostachys laevigata*	0,231g
DT 4	*Delphinium semibarbatum*	0,248g
DT 5	*Prangos ferrulacea*	0,237g
DT 6	Mordanted textile	0,228g
DT 7	Unmordanted textile	0,214g
WT 1	*Delphinium semibarbatum + Rubia tinctorum*	0,579g
WT 2	*Delphinium semibarbatum*	0,439g
WT 3	*Delphinium semibarbatum + Punica granatum*	0,390g
WT 4	Unmordanted thread	0,474g
WT 5	Mordanted thread	0,669g

The dyed textiles and the workshop threads were sewn into a broadcloth base. This base is the same unbleached wool used to prepare the DT samples. The dyed textiles were sewn on the sides with three points by 100% unbleached cotton thread. The workshop threads were sewn directly into the broadcloth base. The minimum amount possible of the thread was left in the back.

The sample-set was exposed to polychromatic irradiation (as explained in Chapter 4, section 2.3.2). Artificially induced changes to natural yellow dyed wools by accelerated light exposure were studied at 0h, 24h, and 126h and compared by two different experimental approaches:

1- Colorimetry

The in-situ colorimetry technique provides information about chromatic properties. For measuring color, a portable colorimetry spectrophotometer, Data Color International, was used. Its measuring head's optical system uses diffuse illumination from a pulsed Xenon arc lamp over the nine mm-diameter measuring area, with a 0° viewing angle geometry. Color coordinates were calculated, defining the D65 illuminant and the 10° observer. The calibration was performed with a bright white standard plate and a total black standard. Color, as perceived by the human eye, may be represented in a three-dimensional system. The color data are presented in the CIE-Lab system. In the Lab cartesian

system, L*, relative brightness, is represented by the z-axis. Variations in relative brightness range from white (L*=100) to black (L*=0). The (a*, b*) pair represents the hue of the object. The red/green y-axis plots a* ranging from negative values (green) to positive (red). The yellow/blue x-axis plots b* going from negative (blue) to positive numbers (yellow). The values represented are an average of three points. Total color variation (ΔE^*) was calculated according to the expression $\Delta E^* = [(\Delta L^*)^2 + (\Delta a^*)^2 + (\Delta b^*)^2]^{1/2}$.

For colorimetry measurement of the textile samples, it was important to ensure that the CIELAB coordinated measurements were excluded from the sample. Hence, a filter paper base fitted below the sewn dyed textile and workshop samples was prepared. This base was folded to achieve ten sheets of filter paper.

The result showed workshop threads were more prone to fading compared to the other samples. The amount of dye source used, dyeing methods, mordanting process, or the character of the substrate could be some of the reasons. Our results were in accordance with [4], as damage and exposure are not linearly related, and the curve slope for fading is steeper in the initial stage.

2- HPLC-DAD/HRMS analysis

A sample (0.01 g) of each was extracted with 3 mL solution according to the method explained in Chapter 3, section 3.5. Then, HPLC-DAD-MS was used to identify dyes on textiles and to detect their degradation products.

A previous study on the mordanted wool dyed with flavonoid dyestuffs aged by accelerated light showed detectable amounts of components added to the major components [5].

In the forthcoming study, the results of applying HPLC-DAD and UHPLC-HRMS/MS to identify the degradation products of artificially light-aged alum mordanted wool dyed will be presented.

By comparing a chromatogram of an extract of accelerated light-aged dyed wool samples with that of an unexposed reference and a mordanted wool blank (exposed for the same period), new compounds will be detected resulting from the photodegradation of yellow dye compounds.

148

The results of the degradation products identified under accelerated light aging conditions can be compared to analysis of historical textiles. Comparing the results with the historical textiles, not only can validate the accelerated aging experiment but also helps to identify the dye sources.

References

[1] Melo, M. J., & Claro, A. (2010). Bright light: microspectrofluorimetry for the characterization of lake pigments and dyes in works of art. *Accounts of Chemical Research*, 43(6), 857-866. Doi: 10.1021/ar9001894

[2] Feller, R. L. (1995). *Accelerated aging: photochemical and thermal aspects*. Getty Publications. ISBN 0892361255

[3] Sharif, S., Nabais, P., Melo, M.J., Pina, F. and Oliveira, M.C. (2021). Photoreactivity and stability of flavonoid yellows used in cultural heritage. *Dyes and Pigments*, 110051. Doi: 10.1016/j.dyepig.2021.110051

[4] Ferreira, E. S. B. (2001). *New approaches towards the identification of yellow dyes in ancient textiles* [Doctoral dissertation, University of Edinburgh]. University of Edinburgh Repository. http://hdl.handle.net/1842/12020

[5] Quye, A., Wouters, J., & Boon, J. J. (1996). A preliminary study of light-aging effects on the analysis of natural flavonoid-dyed wools by photodiode array HPLC and by direct temperature mass spectrometry. In *11th triennial ICOM committee for conservation conference* (pp. 704-713). James and James. ISBN 1873936508

General conclusion and future research

Discussion

Multi-analysis methods have been used more than ever in recent years to fully characterize dye sources of textiles. In this thesis, HPLC-DAD-MS, a highly selective and sensitive identification method, has been used in accordance with photochemical studies to confront the complicated task of identifying yellow dyes in historical textiles.

A survey about plant yellow dye sources in Iran has been provided in Chapter 2, and it has been followed with field research to select a list of plants currently used as dye sources in the center of Iran. It has also discussed the state-of-the-art studies that have identified yellow sources in Persian textiles.

In chapter 3, HPLC–DAD and UHPLC–HRMS/MS have been used to characterize the main yellow chromophores in the plants obtained from the workshops or collected from the central region of Iran, in addition to the wool samples dyed by those sources.

Chapter 4 has accurately quantified the photostability of the luteolin, quercetin, kaempferol, their glucosides, and eriodictyol. The results showed that the most stable yellows are luteolin-7-O-glucoside and all 3-O-glycosides of quercetin and kaempferol, (ϕ_R in order of 10^{-6} scale). The ϕ_R values of the more reactive yellows, quercetin, and kaempferol, were measured in the order of 10^{-5} scale. Characterization of the main degradation products by HPLC-DAD-MS and UHPLC-HRMS illustrates the occurrence of the solvent attack in position C2 or C3 for the studied flavonoids. By studying the solvent effects, an extreme loss of photostability in the proteinaceous media was revealed.

The knowledge gained from this Ph.D. project can bring a broad outlook in conservation science. The study of the degradation mechanism of natural yellow dye sources can gradually form a knowledge base for the identification of yellow or even orange and green dyes in historical textiles.

Natural dyeing technology and the specific regional plants all over the world can only be investigated by the combined efforts of botanists, chemists, and archeologists. Each dye source that goes through this methodology can eventually enrich the reference libraries and profoundly explore the museum textiles. Continuous development and expansion of these libraries can then help to classify and even identify unknown dye sources. In this way, our knowledge can be increased and applied to better understand

the vast dyeing world.

Future works

As a continuation of this work, the database of the reference yellow dye sources can be gradually completed. One can focus on other regions famous for their carpet-weaving and the local plants known as yellow dye sources in those areas. A complimentary helpful dataset would consider various harvesting times of the plants and different regions they have been obtained from, which might have an influence on the identification of dyes and quantification of the main chromophores. In this way, a seasonal and regional map of dye sources and the dyeing industry can be drawn over time.

Another significant step would be comparing the samples obtained from the historical museum textiles with the reference database of the dye compounds to identify the dye sources and the dyeing techniques.

Appendices

Appendix 1- General introduction

A1.1 Yellow dye sources in Iran from the literature point of view (this information is summarized from references [110–114] in Chapter 1).

Row	Botanical name	English name	Family	Colorant part	Mordant	Color on fiber
1	*Agrimonia eupatoria*	Agrimony	Rosaceae	Leaf, stem	Potash alum	Yellow
2	*Dahlia* spp.	Dahlia	Compositae	Flower	Potash alum	Yellow, orange
3	*Anthemis tinctoria*	Yellow chamomile	Compositae	Flower	Potash alum	Yellow
					Potassium di-chromate	Golden, orange
4	*Solidago* spp.	Goldenrod	Compositae	Flower, stem	Potash alum	Bright yellow, golden yellow
5	*Althaea officinalis*	Moorish mallow	Malvaceae	Flower	Potash alum	Yellow
6	*Galium verum*	Yellow bedstraw	Rubiaceae	Flower	Potash alum	Dull golden yel-low
7	*Tagetes* spp.	Marigold	Compositae	Flower	Potash alum,	Yellow
					Iron	Dark yellow, or-ange
8	*Calendula officinalis*	Calendula, marigold	Compositae	Flower	Alum	Orange yellow
					Iron	Deep yellow
9	*Crocus sativus*	Saffron	Iridaceae	Stigma	-	Yellow
10	*Cytisus palmensis*	Tagasate	Papilionaceae	Flower, green stem	Potash alum	Yellow
11	*Helianthus annus*	Sunflower	Compositae	Flower	Potash alum	Yellow
12	*Achillea millefollium*	Common yarrow	Compositae	Flower, stem	Potash alum	Yellow
13	*Zinnia elegans*	Common zinnia	Zingiberaceae	Flower	Potash alum, Chrome	Yellow
14	*Populous nigra* var *Italica*	Lombardy poplar	Salicaceae	Leaf, bark	Alum	Yellow

Row	Botanical name	English name	Family	Colorant part	Mordant	Color on fiber
15	*Ligustrum vulgare*	Privet	Oleaceae	Leaf	Alum	Lemon yellow
16	*Quercus* spp.	Oak	Fagaceae	Leaf	-	Orange, golden yellow
17	*Rumex obtusifolius*	Bitter dock	Polygonaceae	Branch, leaf, root	Alum	Gray yellow
18	*Genista tinctoria*	Common dyer's broom	Papilionaceae	Blossomed branch	Alum, chromium	Yellow
19	*Hypericum perforatum*	St. John's Wort	Hypericaceae	Blossomed shoot	Alum	Yellow
20	*Pteridium aquilinum*	Bracken	Hypolepidaceae	Stem	Potash alum	Golden yellow
21	*Delphinium semibarbatum*	Larkspur	Ranunculaceae	Stem, flower	Aluminum sulfate	Yellow
					Chrom potassium sulfate	Dull yellow
22	*Dorema aureum*	Dorema	Umbelliferae	Flower -All parts	Alum	Yellow
					Chromium	Bright yellow
					Iron	Deep yellow
23	*Curcuma longa*	Turmeric	Zingiberaceae	Root	Alum	Yellow
					Chromium	Bright Yellow
					Iron	Deep yellow
24	*Vitis vinifera*	Grape (vine)	Vitaceae	Leaf	Alum	Yellow
					Chromium	Orange
25	*Salix* spp.	Salix alba L.	Salicaceae	Leaf	Chromium	Dark lemon
					Alum	Canary yellow
26	*Thea sinensis*	Tea	Theeaceae	Leaf	Potash alum	Yellow
27	*Alnus* spp.	Alder	Betulaceae	Leaf, bark	-	Yellow

Row	Botanical name	English name	Family	Colorant part	Mordant	Color on fiber
28	*Betula* L.	Birch	Betulaceae	Leaf	Potash alum	Yellow
29	*Myrtus communis*	Myrtle	Myrtaceae		Alum	Yellow
					Chromium	Yellow mustard
30	*Sparterium* L.	Broom	Papilionaceae	Flower	Potash alum	Golden yellow
31	*Crataegus* L.	Hawthorn	Rosaceae	Fruit	Alum	Yellow
					Chromium	Deep yellow
					Iron	Dull yellow
32	*Castanea* Mill.	Chestnut	Fagaceae	Bark	Alum	Yellow
					Iron	Deep yellow
33	*Fumaria* L.	Fumitory	Fumariaceae	The whole plant	Alum	Bright yellow
34	*Platanus* L.	Plane	Platanaceae	Bark	Alum	Yellow, brown
				Leaf		Bright yellow
35	*Tamarix bachtiarica*	Tamarisk	Tamaricaceae	Flower	Chromium	Brown yellow
					Alum	Yellow
36	*Juglans regia*	Walnut	Juglandaceae	Leaf, fruit hull	Alum	Deep yellow
					Chromium	Brown yellow
37	*Viburnum lantana*	Wayfaring tree	Caprifoliaceae	All parts except the root	Alum	Lemon yellow
					Chromium	Bright yellow
					Iron	Dull yellow
38	*Humulus* L.	Hop	Cannabaceae	Leaf, flower	Alum, Chromium	Yellow
39	*Hedera* L.	Ivy	Araliaceae	seed	Alum	Yellow
40	*Allium porrum* L.	Leek	Liliaceae	Leaf	Alum	Dull yellow
41	*Primula macrocalyx*	Primrose	Primulaceae	Flower	Alum	Dull yellow

Row	Botanical name	English name	Family	Colorant part	Mordant	Color on fiber
42	*Chrysanthemum* L.	Chrysanthemum	Campositae	Leaf	Chromium	Yellow
43	*Trigonella* L.	Trigonella	Juncaginaceae	Seed	Alum, Chromium	Yellow
					Iron	Dark yellow
44	*Lauroceraus officinails*	Common laurel cherry	Rosaceae	Leaf	Alum, Chromium	Yellow
					Iron	Dark yellow
45	*Iris pseudoacorus*	Yellow flag iris	Iridaceae	Leaf	Alum	Yellow
46	*Pistacia vera*	Pistachio	Anacardiaceae	Fruit hull	Alum	Dull yellow
47	*Ziziphus* Mill.	Jujube	Rhamnaceae	Trunk	Alum	Yellow
					Iron	Dark yellow
48	*Terminalia* L.	Myrobalan	Combretaceae	Fruit	Alum	Yellow
					Iron	Deep yellow
49	*Prangos ferulacea*	Jashir (Persian name)	Umbelliferae	Leaf, stem	Alum	Bright canary yellow
					Chromium	Orange yellow
50	*Quercus persica*	Oak manna tree	Fagaceae	Parenchyma of the fruit	Chromium	Golden yellow
					Aluminum Sulfate	Light yellow
					Iron	Dark yellow
					Chromium and alum	Yellow
51	*Ficus carica*	Fig	Moraceae	Leaf	Aluminum Sulfate	Bright lemon
					Chromium potassium sulfate	Orange yellow

Row	Botanical name	English name	Family	Colorant part	Mordant	Color on fiber
52	*Punica granatum* L.	Pomegrante	Punicaceae	Fruit peel	Alum	Yellow
					Chromium	Deep yellow
53	*Allium cepa* L.	Onion	Liliaceae	Skin (yellow)	Alum	Orange
54	*Tanacetum* L.	Tancy	Campositae	Flower, stem	Potash alum	Yellow
55	*Coreopsis* L.	Tick-seed	Campositae	Flower, stem	Potash alum	Golden yellow
56	*Ulmus* L.	Elm	Ulmaceae	Leaf	Alum	Golden yellow
57	*Rubus persicus* Boiss.	Raspberry	Rosaceae	Leaf, Stem	Potassium di-chromate	Dark yellow
					Alum	Yellow
58	*Cosmos cav.*	Yellow cosmos	Compositae	Flower	Potash alum	Golden yellow
59	*Acacia farnesiana* L.	Sweet acacia	Mimosaceae	Leaf, stem	Potassium di-chromate	Yellow
					Alum	Yellow
60	*Amygdalus lycioides*	Almond	Rosaceae	Leaf, stem	Potassium di-chromate	Yellow
					Alum	Canary yellow
61	*Amygdalus eburnea*	Almond	Rosaceae	Leaf	Potassium di-chromate	Deep lemon yel-low
					Alum	Yellow
62	*Berberis integerrima Bunge*	Berberry	Berberidaceae	Leaf	Potassium di-chromate	Deep yellow
					Alum	Yellow
63	*Cachrys cheilanthifolia*	Prangos	Umbelliferae	Leaf	Potassium di-chromate	Yellow
					Alum	Lemon yellow

Row	Botanical name	English name	Family	Colorant part	Mordant	Color on fiber
64	*Capparis spinosa* L.	Caper	Capparidaceae	Leaf	Potassium di-chromate	Yellow
					Alum	Yellow
65	*Celtis caucarica* Willd.	Caucasian hackberry	Ulmaceae	Leaf, stem	Potassium di-chromate	Orange yellow
					Alum	Bright lemon yel-low
66	*Centaurea behen* L.	White behen	Campositae	Leaf	Potassium di-chromate	Lemon yellow
					Alum	Light lemon yel-low
67	*Centaurea virgata* Lam.	Centaurea	Campositae	Stem	Potassium di-chromate	Lemon yellow
					Alum	Bright lemon yel-low
68	*Cercis siliquastrum* L.	Judas tree	Caesalpinaceae	Leaf	Potassium di-chromate	Deep yellow
					Alum	Yellow
69	*Citrus bigaradia* L.	Sour orange	Rutaceae	Leaf	Potassium di-chromate	Light yellow
					Alum	Light lemon yel-low
70	*Colutea persica* Boiss.	Bladder senna	Papilioaceae	Leaf	Potassium di-chromate	Light yellow
					Alum	Bright lemon yel-low
71	*Convolvulus leio-calycinus*	Glorybind	Convolvulacoae	Leaf, stem, flower	Potassium di-chromate	Orange yellow

Row	Botanical name	English name	Family	Colorant part	Mordant	Color on fiber
72	*Delphinium oli-vieranum* DC.	Larkspur	Ranunculaceae	Stem, flower	Potassium di-chromate	Deep yellow
					Alum	Yellow
73	*Echinops ritrodes* Bunge.	Globe thistle	Compositae	Flower	Potassium di-chromate	Deep yellow
					Alum	Bright lemon yellow
74	*Eucalyptus camaldu-lensis* Dehnh.	Eucalyptus	Myrtaceae	Leaf	Potassium di-chromate	Yellow
					Alum	Light lemon yellow
75	*Euphorbia petiolata*	Eupatorium	Euphorbiaceae	Leaf, stem	Potassium di-chromate	Deep orange yellow
					Alum	Yellow
76	*Euphorbia macrostegia* Boiss.	Eupatorium	Euphorbiaceae	Leaf, stem, flower	Potassium di-chromate	Orange yellow
					Alum	Canary yellow
77	*Ferula assa- foetida* L.	Assafoetida	Umbelliferae	Leaf, stem	Potassium di-chromate	Yellow
					Alum	Bright lemon yellow
78	*Glycyrrhiza glabra* L.	Russian liquorice	Papilionaceae	Leaf	Potassium di-chromate	Deep lemon yellow
					Alum	Bright canary yellow
79	*Hesperis persica* Boiss.	Rocket	Cruciferae	Leaf	Potassium di-chromate	Light green yellow
					Alum	Light bright lemon yellow

162

Row	Botanical name	English name	Family	Colorant part	Mordant	Color on fiber
80	*Lactuca orientalis* Boiss.	Lettuce	Compositae	Stem, leaf	Potassium dichromate	Yellow
					Alum	Lemon yellow
81	*Lonicera caprifolium* L.	Sweet honeysuckle	Cprifoliaceae	Leaf	Potassium dichromate	Dark orange yellow
					Alum	Dull yellow
82	*Melia azedarach* L.	China berry	Meliaceae	Leaf	Potassium dichromate	Yellow
83	*Morus nigra* L.	Red mulberry	Moraceae	Leaf	Potassium dichromate	Orange yellow
					Alum	Bright canary yellow
84	*Morus alba* var. *pendula.*	Mulberry	Moraceae	Leaf, stem	Potassium dichromate	Yellow
					Alum	Lemon yellow
					Chromium	Dark lemon yellow
85	*Nerium oleander* L.	Common oleander	Apocyanaceae	Leaf, white flower	Potassium dichromate	Dark yellow
					Alum	Canary yellow
86	*Olea europaea* L.	Common olive	Oleaceae	Leaf	Potassium dichromate	Lemon yellow
					Alum	Yellow
87	*Platanus orientalis* L.	Oriental plane tree	Platanaceae	Leaf, stem	Potassium dichromate	Orange yellow
					Alum	Yellow
88	*Onosma syriacum*	Onosma	Boraginaceae	Flower	Potassium dichromate	Pale dull yellow

Row	Botanical name	English name	Family	Colorant part	Mordant	Color on fiber
					Alum	Light lemon yellow
89	*Phragmites australis* Cav.	Common reed	Gramineae	Leaf	Potassium di-chromate	Orange yellow
					Alum	Canary yellow
90	*Populus alba* L.	White poplar	Salicaceae	Leaf	Potassium di-chromate	Orange yellow
					Alum	Lemon yellow
91	*Pyrus syriaca* Boiss.	Pear	Rosaceae	Leaf	Potassium di-chromate	Deep yellow
					Alum	Bright lemon yellow
92	*Rosa canina* L.	Dog rose	Rosaceae	Leaf, flower	Potassium di-chromate	Brown yellow
					Alum	Yellow
93	*Salvia hydrangea* DC.	Sage	Labiatae	Leaf, flower	Potassium di-chromate	Lemon yellow
					Alum	Light lemon yellow
94	*Salvia palaestina* Benth.	Sage	Labiatae	Leaf, stem	Potassium di-chromate	Orange yellow
					Alum	Yellow
95	*Phlomis anisodonta* Boiss.	Jerusalem	Labiatae	Leaf	Potassium di-chromate	Yellow
					Alum	Light bright lemon yellow
96	*Thuja* sp. L.	Cypress	Cupressaceae	Leaf, stem	Potassium di-chromate	Orange yellow
					Alum	Yellow

Row	Botanical name	English name	Family	Colorant part	Mordant	Color on fiber
97	*Typha australis*	Cat's tail	Typhaceae	Leaf	Potassium di-chromate	Orange yellow
					Alum	Dark canary yel-low
98	*Verbascum spesiosum*	mullein	Scrophulariaceae	Leaf, flower	Potassium di-chromate	Dark lemon yel-low
					Alum	Dark lemon yel-low
99	*Verbascum sinuatum* L.	Mediterian mullein	Scrophulariaceae	Leaf	Potassium di-chromate	Dark lemon yel-low
					Alum	Plae lemon yel-low
100	*Amygdalus scoparia*	Almond	Rosaceae	Leaf, branch	Potassium di-chromate	Yellow
					Alum	Canary yellow
101	*Artemisia sieberi*	Sagebrush	Compositae	Leaf, stem	Potassium di-chromate	Orange yellow
					Alum	Yellow
102	*Ziziphus nummularia*	Camel thorn	Rhamnaceae	Leaf, stem	Potassium di-chromate	Yellow
					Alum	Lemon yellow
103	*Achillea micrantha* Willd.	Milfoil	Compositae	Leaf, stem, flower	Potassium di-chromate	Yellow
					Alum	
104	*Alcea aucheri* Boiss.	Alcea	Malvaceae	Leaf, stem	Potassium di-chromate	Canary Yellow
					Alum	Bright canary yellow

Row	Botanical name	English name	Family	Colorant part	Mordant	Color on fiber
105	*Astragalus* L.	Locoweed	Papilionaceae	Thin branch	Potassium di-chromate	Yellow
				Leaf, thin branch	Potassium di-chromate	Yellow
106	*Cardaria draba* L.	Cardaria	Cruciferae	Leaf, stem, root	Potassium di-chromate	Yellow
					Alum	Light lemon yellow
107	*Centaurea depressa* M.B.	Centaurea	Compositae	Leaf	Potassium di-chromate	Lemon yellow
					Alum	Bright lemon yellow
108	*Dianthus crinitus*	Pink	Cariophyllaceae	Leaf, stem	Potassium di-chromate	Yellow
					Alum	Lemon yellow
109	*Eryngium billadieri*	Eryngo	Umbelliferae	Stem, flower	Potassium di-chromate	Yellow
					Alum	Lemon yellow
110	*Eryngium bungei* Boiss.	Eryngo	Umbelliferae	Leaf	Potassium di-chromate	Yellow
					Alum	Lemon yellow
111	*Euphorbia heteradena*	Euphorbia	Euphorbiaceae	Leaf, stem, flower	Potassium di-chromate	Orange yellow
					Alum	Canary yellow
112	*Falcaria fabr.*	Falcaria	Umbelliferae	Leaf, stem, slower	Potassium di-chromate	Orange yellow
					Alum	Canary yellow
113	*Foeniculum vulgare*	Common fennel	Umbelliferae	Seed, leaf, stem	Potassium di-chromate	Orange yellow

Row	Botanical name	English name	Family	Colorant part	Mordant	Color on fiber
					Alum	Canary yellow
114	*Fraxinus rotundifolia*	Ash	Oleaceae	Leaf, branch	Potassium di-chromate	Yellow
					Alum	Lemon yellow
115	*Helicrysum leucoceph-alum* Boiss.	Everlasting flower	Asteraceae Compositaer	Leaf, stem	Potassium di-chromate	Orange yellow
					Alum	Canary yellow
116	*Hypericum helianthe-moides*	St. john's -Wort	Hypericacaea	Leaf, flower	Potassium di-chromate	Brown yellow
					Alum	Yellow
117	*Persica vulgaris* Mil-ler	Peach tree	Rosaceae	Leaf	Potassium di-chromate	Yellow
					Alum	Light yellow
118	*Phlomis elliptica* Benth.	Jerusalem sage	Labiatae	Leaf	Potassium di-chromate	Light yellow
119	*Phlomis olivieri* Benth.			Leaf, stem	Potassium di-chromate	Lemon yellow
120	*Lycopersicum esculen-tum* Mill.	Common tomato	Solanaceae	Bush	Potassium di-chromate	Orange yellow
					Alum	Lemon yellow
121	*Malva silvestris* L.	High mallow	Malvaceae	Leaf, stem	Potassium di-chromate	Lemon yellow
					Alum	Light yellow
122	*Pinus eldarica* Medw.	Pine	Pinaceae	Leaf, stem	Potassium di-chromate	Orange yellow
					Alum	Lemon yellow
		Pine	Pinaceae	Fruit	Potassium di-chromate	Yellow

Row	Botanical name	English name	Family	Colorant part	Mordant	Color on fiber
					Alum	Light lemon yellow
123	*Pyrus communis* L.	Common pear	Rosaceae	Leaf	Potassium di-chromate	Orange yellow
					Alum	Lemon yellow
124	*Reseda lutea* L.	Weld	Resedaceae	Stem, leaf	Potassium di-chromate	Dark yellow
					Alum	Light lemon yellow
125	*Salvia macrosiphon*	Sage	Labiatae	Leaf, stem	Potassium di-chromate	Orange yellow
					Alum	Yellow
126	*Salvia reuterana* Boiss.	Sage	Labiatae	Leaf, stem	Potassium di-chromate	Orange yellow
					Alum	Yellow
127	*Solanum melongena* L.	Garden eggplant	Solanaceae	Bush	Potassium di-chromate	Light yellow
					Alum	Light lemon yellow
128	*Tragopogon* L.	Salsify	Compositae	Stem, leaf, flower	Potassium di-chromate	Yellow
					Alum	Lemon yellow
129	*Zygophyllum euryp-terum*	Bean caper	Zygophyllaceae	Leaf, branch	Potassium di-chromate	Yellow
					Alum	Lemon yellow
130	*Datura stramonium* L.	Jimpson-weed datura	Solanaceae	Leaf	Alum	Canary yellow
131	*Cichorium hntybus* L.	Chicory	Asteraceae	Leaf	Alum	Yellow
132	*Elaeagnus angustifolia* L.	Russian olive	Elaeagnaceae	Leaf	Alum	light lemon color

Row	Botanical name	English name	Family	Colorant part	Mordant	Color on fiber
133	*Euphorbia cf. condy-locorpa.*	Euphorbia	Euphorbiaceae	Leaf	Alum	lemon color to Canary Yellow
134	*Euphorbia cf. osyridea.*	Euphorbia	Euphorbiaceae	Stem, flower	Alum	Yellow
135	*Evonymus japonica* L.f.	Evergreen evonymus	Celastraceae	Leaf, stem	Alum	Orangish yellow
136	*Medicago sativa* L.	Afaalfa	Papilionaceae	Leaf	Alum	Light bright lemon color
137	*Vicia villosa* Roth	Hairy vetch	Papilionaceae	Leaf	Alum	light lemon yellow
138	*Vitis sylvestris Gmelin*	Vine	Vitaceae	Leaf, stem	Alum	Yellow
139	*Ziziphus spina-Christi* L.	Christ's thorn	Rhamnaceae	Leaf, stem	Alum	Lemon yellow
140	*Acer monspessulanum* L.	Montpellier maple	Aceraceae	Leaf, stem	Alum	DarkcCanary Yellow
141	*Alcea aucheri* Boiss.	Alcea	Malvaceae	Leaf, stem	Alum	Bright canary yellow
142	*Alhagi camelorum* Fisch.	Camel's thorn	Papilionaceae	Leaf, branch, flower	Alum	light yellow
143	*Carthamus lanatus* L.	Wooly safflower	Compositae	Leaf, stem	Alum	Dark canary yellow
144	*Carthamus tinctorius* L.	Safflower	Compositae	Leaf, stem, flower	Alum	Canary yellow
145	*Cathalpa spesiosa* Worder.	Hardy cathapa	Bignoniaceae	Stem	Alum	Yellow
146	*Cedrus libani* Barrel.	Cedar of Lebanon	Pinaceae	Stem	Alum	Lemon yellow
147	*Cerasus microcarpa.*	Cherry	Rosaceae	Leaf, stem	Alum	Yellow
148	*Colchicum montanum* L.	Autumn crocus	Liliaceae	Leaf	Alum	Dark canary yellow
149	*Daphne mucronata*	Daphne	Thymelaceae	Leaf, stem, flower	Alum	Canary yellow

Row	Botanical name	English name	Family	Colorant part	Mordant	Color on fiber
	Royle					
150	*Daphne stapfii*	Daphne	Thymelaceae	Leaf, stem	Alum	Orange yellow
151	*Euphorbia helioscopia*	Sun euphorbia	Euphorbiaceae	Stem	Alum	Yellow
152	*Falcaria* Fabr.	Falcaria	Umbelliferae	Leaf, stem, flower	Alum	Yellow
153	*Juniperus exelsa* M.B.	Greek juniper	Cupressaceae	Leaf, branch	Alum	Canary yellow
154	*Poenix dactilifera* L.	Date	Palmaceae	Leaf	Alum	Light lemon color
155	*Pistacia mutica*	Turk terebinth pistache	Anacardiaceae	Leaf, branch	Alum	Bright canary yellow
156	*Pyrus glabra* Boiss.	Pear	Rosaceae	Leaf	Alum	Canary yellow
157	*Spartium junceum* L.	Weaver's-broom	Papilionaceae.	Leaf, flower	Alum	Canary yellow
158	*Tragopogon caricifolium.*	Salsifi	Compositae	Stem, leaf, flower	Alum	Lemon yellow
159	*Zataria multiflora* Boiss.	Thime	Labiatae	Stem, leaf	Alum	Lemon yellow

A1.2- Molecular mass and maximum absorbance of commonly seen flavonoid aglycones and glycosides structures

Flavonoid	Mass	λ_{max} (nm)
Apigenin	270	266-290sh-337
Luteolin	286	253- 267sh- 291sh- 350
Luteolin-7-*O*-glucoside	448	254-267sh-348
Kaempferol	286	248sh-266-295sh-318sh-366
Kaempferol-3-*O*-glucoside (Astragalin)	448	265-290sh-320sh-346
Quercetin	302	255-295sh-372
Morin	302	252-262sh-290sh-318sh-352
Quercetin-3-*O*-glucoside (Isoquercitin)	464	255-266sh-294sh-355
Quercetin-3-*O*-galactoside (Hyperoside)	464	255-266sh-294sh-355
Quercetin-3-*O*-rhamnoside (Quercitrin)	448	254-263sh-294sh-348
Isorhamnetin	316	255-266sh-306sh-326sh-372
Isorhamnetin-3-*O*-glucoside	478	255-266sh-294sh-355
Myricetin	318	252-263sh-298sh-371

A1.3- The methodology for interpretation of mass spectral data of flavonoid dye compounds[21]

1-Characterization of glycosylation type

MS/MS analysis in combination with CID allows the characterization of the carbohydrate and even the glycosylation position in several cases.

The most common carbohydrate in flavonoids is glucose, although other types like galactose, rhamnose, xylose, and arabinose are also encountered [59].

$^{k,l}X_i$, Y_i, and Z_i are the labels for the ions comprising the aglycone. The broken interglycosidic bonds are counted from the aglycone by i number, and the cleavages of carbohydrate rings are superscripted by k and l. The titles for the retained charges on the sugar residues are $^{k,l}A_i$, B_i, and C_i fragments representing hexoses, deoxyhesoses, and pentoses, respectively [70, 79] (Figure A1.3.1).
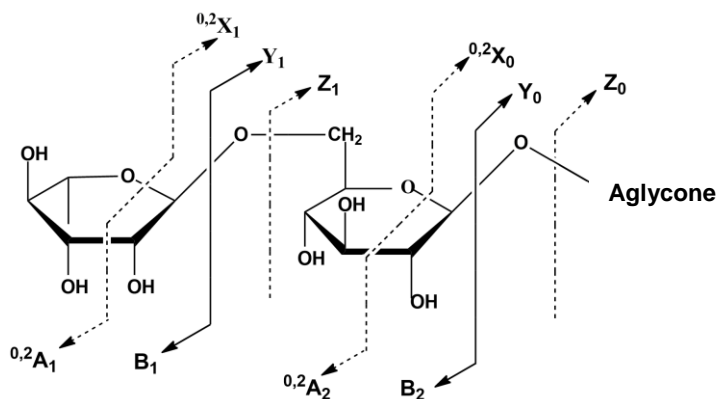
Figure A1.3.1- Nomenclature for labeling the *O*-glycoside fragmentation (reprinted from [65, 81])

The difference between the masses of the parent ions and the fragments of X_i, Y_i, and Z_i defines the type of sugar [70] (Figure A1.3.2 and Table A1.3.1). This value verifies the masses of the hexoses, deoxyhexoses, and pentoses with 162, 146, and 132 *Da*, respectively [65].

---

[21] The reported references are in accordance with the reference list of Chapter 1.
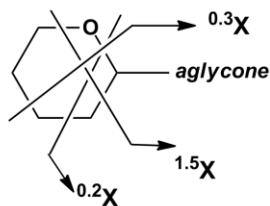
Figure A1.3.2- Cross-ring cleavages in hexoses and pentoses [59, 70]

Table A1.3.1- Characteristic loss of mass for *C*- and *O*- glycosides in case of hexoses deoxyhexoses and pentoses [59, 65]

Sugar types	$^{0,2}X$	$^{0,3}X$	$^{1,5}X$	Yi
Hexose	[M ± H – 120]	[M ± H – 90]	[M ± H – 134]	[M ± H – 162]
Deoxyhexose	[M ± H – 104]	[M ± H – 74]	[M ± H – 120]	[M ± H – 146]
Pentose	[M ± H – 90]	[M ± H – 60]	[M ± H – 104]	[M ± H – 132]

2- Position and number of glycosylation

The O or C atoms of the flavonoids usually attach to the glycoside residues; therefore, their glycosylation can be described in the forms of *O*-glycosides, *C*-glycosides, and *O,C*-glycosides [65].

O-glycosides can occur for flavonol glycosides and flavone glycosides, although *C*-glycosides or *O-C*-diglycoside can also occur in the case of flavone glycosides [82]. Low fragmentation energies provide distinct Y_i fragments for *O*-glycosides [70], while the use of higher levels of energy for fragmentation results in complex and ambiguous mass spectra [65]. For *C*-glycosides, at medium energy, $^{i,j}X$ and losses of water molecule are characteristic [70] (Figure A1.3.3).
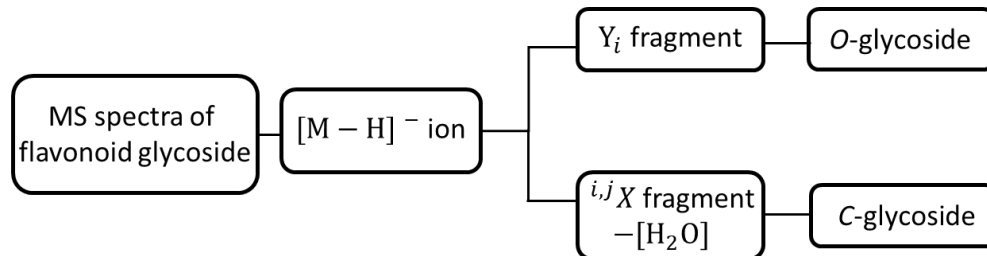
Figure A1.3.3- Decision tree supporting the proposed protocol for characterization of the position of flavonoids glycoside based on ion fragmentation of mass spectral data

The flavonoid glycoside isomers can be distinguished based on the position in which their sugar units are attached to the aglycones. Although, CID-MS–MS must be supported by the literature data [115].

In principle, *O*-glycosylation often attaches to the flavones at position 7, while the favored positions for the glycosylation of flavonols are 3 and 7 [59, 70]. On the other hand, *C*-glycosyl moiety has only been found attached to positions 6 or 8 of flavone (Figure A1.3.2; A1.3.5 and Table A1.3.2).
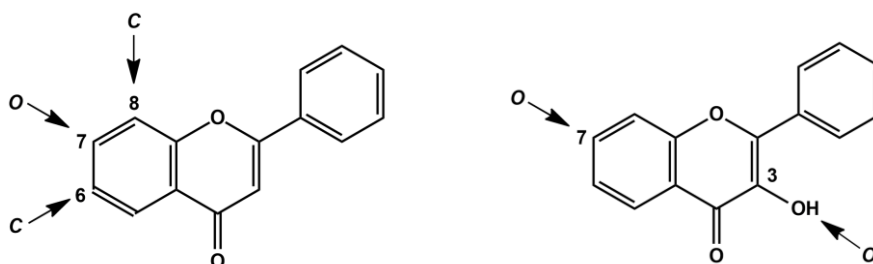
Figure A1.3.4- Flavone, flavonol with the indicated common O- and C-glycosylation positions

Table A1.3.2- Identical fragmentation for different positions of flavonoid *O*-glycoside [70]

Glycosylation		Fragment
7-*O*-monoglycosyl	$[Y_0 - CO]^-$	Loss of B-ring from aglycone and the $[M + Na]^+$
3-*O*-monoglycosyl	$[Y_0 - 2H - CO]^-$	Loss of the B-ring
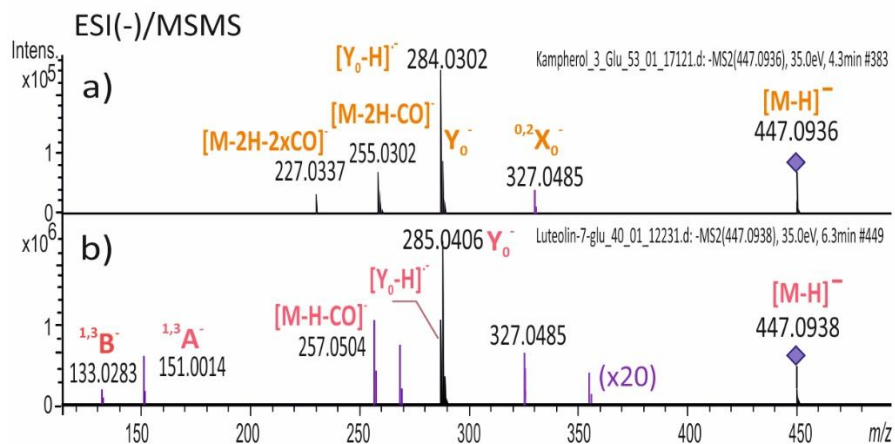
Figure A1.3.5- Differentiation of 3-*O*- and 7-*O*-glycosides. QTOF-MS/MS spectra of deprotonated (a) kaempferol-3-*O*-glucoside and (b) luteolin-7-*O*-glucoside, (formed under the same CID energy).

When two sugars are attached to the flavonoid aglycone, they can be at two different positions (monosaccharides) or at the same position (disaccharide). Z_i fragment, in the mass spectra, provides differentiating data to characterize these two types of sugars. Along with this data, the losses of Y_i fragments are other important decision parameters (Figure A1.3.6; A1.3.7).
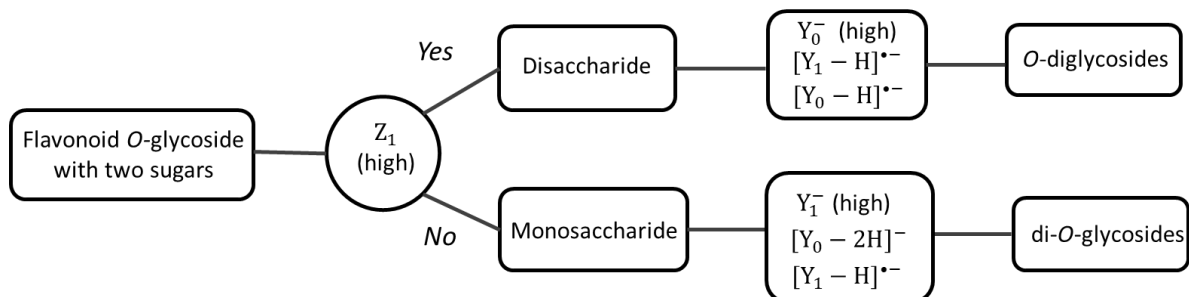
Figure A1.3.6- Decision tree supporting the proposed protocol for identification of monosaccharides and disaccharides based on the ion fragmentations mass spectral data [59, 65, 70]
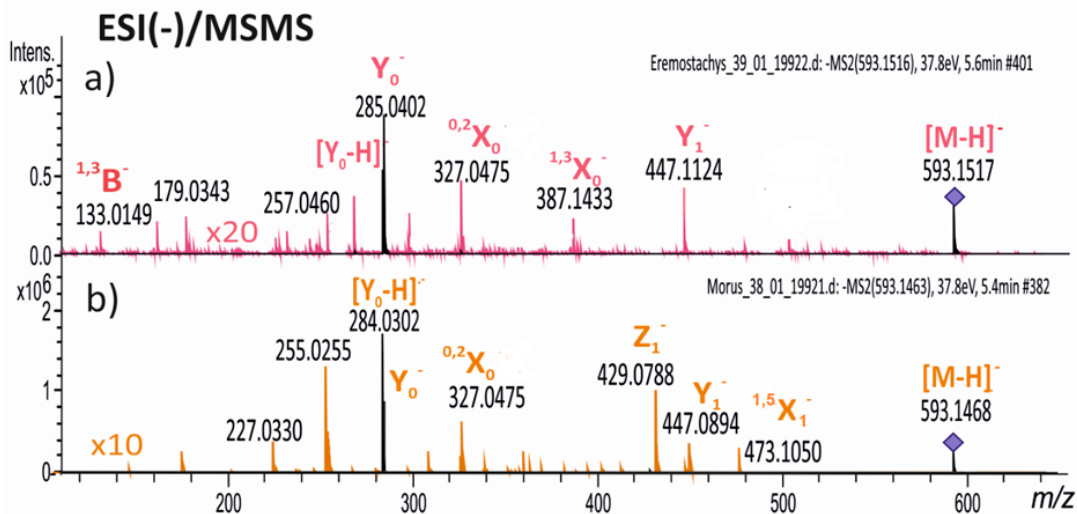
Figure A1.3.7- QTOF-MS/MS spectra of deprotonated a) luteolin-7-O-rutinoside with a 1→6 interglycosidic linkage; (b) kaempferol-3-O-rutinoside with a 1→2 interglycosidic linkage, (formed under 38 eV CID energy).

3- Characterization of aglycones

Analysis of the [M-H]$^-$ CID spectrum and selecting the Y_0 ion (Figure A1.3.1), characterizes unknown aglycones in flavonoids [59]. The identification of classes of the flavonoid aglycones is often achieved by the MS^2 spectra of compounds. In this regard, the retro Diels-Alder (RDA) fragmentation pathways and some small neutral losses appear to be characteristic.

3-1 RDA mechanism

The RDA mechanism is common for flavones, flavonol glycosides, and most flavonols [21]. The number and types of substituents in the A- and B- rings can be evaluated by the RDA mechanism. It also reveals the number of hydroxyl groups in the A ring of flavones and flavonols as structural information [21].

When identifying flavonoid aglycones, the most useful fragmentations occur in the cleavage of two C–C bonds of the C-ring at positions 1/3, 0/2, and 0/4, in positive ion electrospray and also 1/2 or 1/3 bonds in negative ion electrospray (Figure A1.3.8), providing structurally informative $^{i,j}A^{(+/-)}$ and $^{i,j}B^{(+/-)}$ ions, where superscripts i and j indicate the broken C-ring bond. This reveals the number and type of substituents in the A and B rings [35, 59, 65].
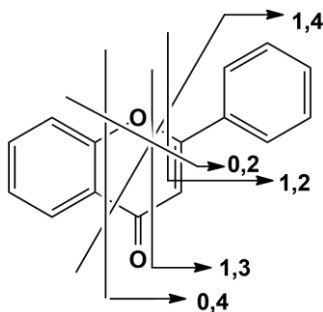
Figure A1.3.8- Nomenclature of different retrocyclization cleavages of C-ring of flavonoid structure (adapted from [20, 59, 65, 79])

The major fragment ion for all flavonoids in the negative and positive mode is often $^{1,3}A^-$. Direct cleavage of the bond between the B- and C-rings forms $[^{1,2}A^- - H]$ and $[^{1,2}B^- + H]$ ions providing information on the degree of hydroxylation on the B-ring for flavonols [20] (Table A1.3.3).

176

3-2 Loss of small molecules

Losses of CO (28 Da), CO_2 (44 Da), C_2H_2O (42 Da), H_2O (18 Da), and a combination of these neutral groups are commonly seen in MS^2 spectra of flavonoid analysis. This behavior provides some structural information during the fragmentation breakdown. For example, the loss of a $^\bullet CH_3$ radical (15 Da) is found to be characteristic of a flavonoid that contains phenolic methyl groups [20, 59] (Table A1.3.3 and Figure A1.3.9).

Table A1.3.3- MS (MS/MS) fragmentation ions of flavones and flavonols [20, 59, 70, 71, 79]

Flavones	0/2, 0/4, 1/3 RDA
	$^{1,3}A^+$, **$^{1,3}B^+$**, $^{0,2}B^+$, **$^{0,4}B^+$**, $[^{0,4}B^+ - H_2O]$
	losses of one and two C_2H_2O
	$^{1,3}A^-$, $^{1,3}A^- - CO_2$, **$^{1,3}B^-$**, $[^{1,4}B^- + 2H]$
Flavonols	0/2, 1/3 RDA
	$^{0,2}A^+$, $^{1,3}A^+$, $^{0,2}B^+$,
	losses of one and two C_2H_2O,
	$^{0,2}A^+ - CO$, $[^{1,4}A^+ + 2H]$, $[^{1,3}B^+ - 2H]$
	$^{1,2}A^-$, $^{1,2}A^- - CO$, $^{1,3}A^-$, **$^{1,2}B^-$**, $^{1,3}B^-$, $[^{1,2}A^- - CO - CO_2]$

177
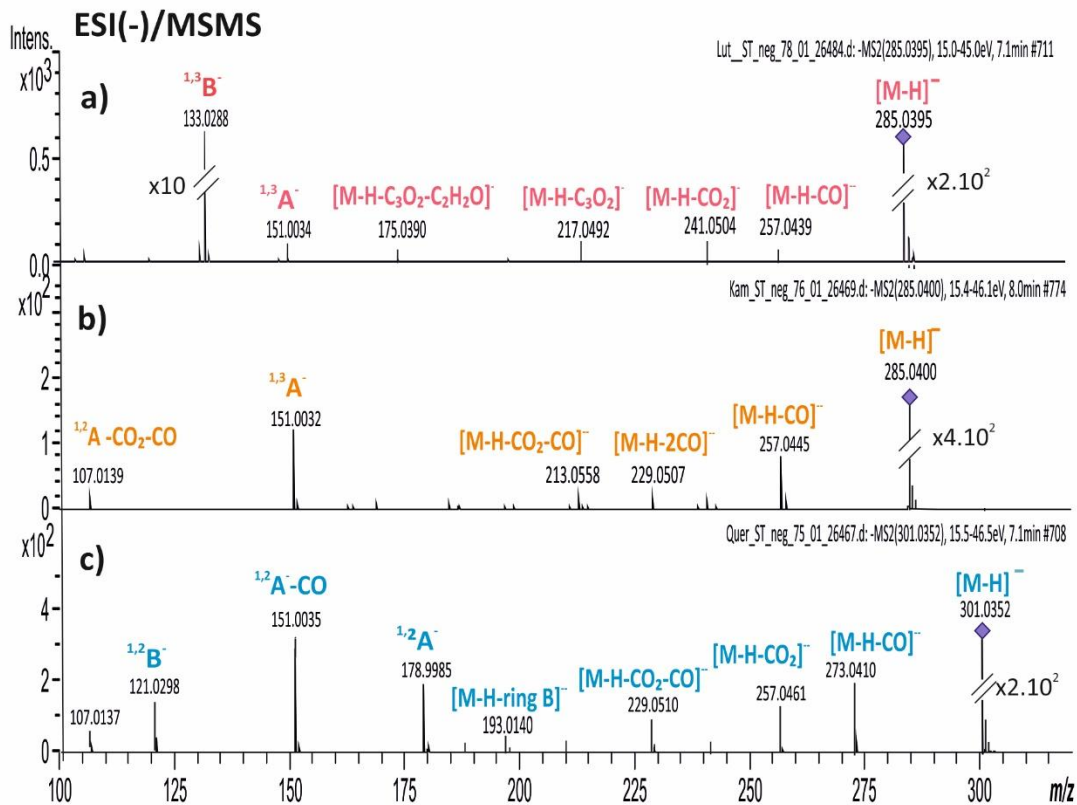
Figure A1.3.9- Differentiation of flavone and flavonol aglycones. QTOF-MS/MS spectra of deprotonated (a) luteolin, (b) kaempferol, and (c) quercetin (formed under the same CID energy).

Appendix 2- Natural yellow dye sources in Persian carpets: a review

Figure A2. 1-Morphology of *Pistacia vera*

Leaves
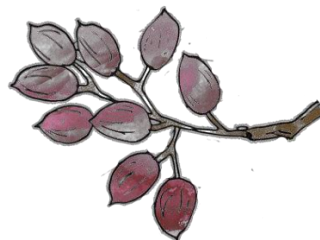
Cluster
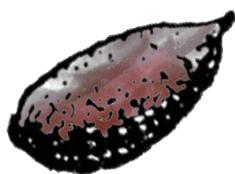
Fleshy hull (mesocarp)

Seed and shell (endocarp)

Appendix 3- Traditional yellow dyes used in the 21st century in central Iran

Table A3.1- HPLC-DAD and LC-ESI(-)-HRMS/MS characterization of the main yellow chromophores present in plant (Pl) and dyed wool (Tx) extracts.

	t_R (min)[1]		λ_{max} (nm)	Formula	[M-H]-		Δ ppm	MS/MS [m/z (Δppm) (attribution)]	Proposed compound	Pl	Tx
	HPLC	UHPLC			Obs. m/z	Calc. m/z					
Delphinium semibarbatum	17.55	5.85	256, 356	$C_{27}H_{30}O_{16}$	609.1467	609.1461	-1.0	300.0277 (-0.4) [Y0-H•]•- [$C_{15}H_8O_7$]•-	Que-3-O-deoxHex	1	1
	18.75	**6.42**	**255, 355**	**$C_{21}H_{20}O_{12}$**	**463.0876**	**463.0882**	**1.2**	**301.0347 (2.1) [Y0]- [$C_{15}H_9O_7$]-** **300.0277 (-0.4) [Y0-H•]•- [$C_{15}H_8O_7$]•-** **271.0250 (-0.7)[Y0-2H-CO]-[$C_{14}H_7O_5$]-**	**Que-3-O-Glc***	**2**	**2**
	19.55	6.79	264, 348	$C_{21}H_{20}O_{11}$	447.0929	447.0933	0.8	**284.0328 (-0.5) [Y0-H•]•- [$C_{15}H_8O_6$]•-** 255.0303 (-1.3)[Y0-2H-CO]- [$C_{14}H_7O_5$]-	Kae-Hex	3	3
	19.90	**7.04**	**264, 347**	**$C_{21}H_{20}O_{11}$**	**447.0931**	**447.0933**	**0.5**	**285.0402 (0.8) [Y0]- [$C_{15}H_9O_6$]-** **284.0328 (-0.5) [Y0-H•]•- [$C_{15}H_8O_6$]•-** **255.0291 (3.3) [Y0-2H-CO]- [$C_{14}H_7O_5$]-**	**Kae-3-O-Glc***	**4**	**4**
	20.19	**7.11**	**254, 354**	**$C_{22}H_{22}O_{12}$**	**477.1040**	**477.1038**	**-0.3**	**315.0505 (1.6) [Y0]- [$C_{16}H_{11}O_7$]-** **314.0433 (-0.2) [Y0-H•]•- [$C_{16}H_{10}O_7$]•-** **285.0409 (-1.6)[Y0-2H-CO]- [$C_{15}H_9O_6$]-**	**Irh-3-O-Glc**	**5**	**5**
	21.35	9.27	254, 371	$C_{15}H_{10}O_7$	301.0359	301.0354	-1.7	178.9980 (-0.4) [1,2A]- [$C_8H_3O_5$]- 151.0037 (-0.7) [1,2A-CO]- [$C_7H_3O_4$]- 121.0280 (10.0) [1,2B]- [$C_7H_5O_2$]-	Que*	n.a.	6
	22.87	10.63	264, 366	$C_{15}H_{10}O_6$	285.0413	285.0405	-2.9	151.0036 (0.7) [1,3A]- [$C_7H_3O_4$]-	Kae*	n.a.	7
	23.40	10.91	254, 370	$C_{16}H_{12}O_7$	315.0519	315.0510	-2.7	300.0282 (-2.0) [$C_{15}H_8O_7$]- 151.0037 (-0.7) [1,2A-CO]- [$C_7H_3O_4$]-	Irh*	n.a.	8
Eremostachys laev-igata	**18.37**	**6.18**	**254, 349**	**$C_{26}H_{28}O_{15}$**	**579.1362**	**579.1355**	**-0.7**	**447.0933 (-0.1) [Y1]- [$C_{21}H_{19}O_{11}$]-** **327.0512 (-0.6) [0,2X-] [$C_{17}H_{11}O_7$]-** **285.0404 (-0.2) [Y0]- [$C_{15}H_9O_6$]-**	**Lut-7-O-Hex-Pen**	**1**	**1**
	-	6.37	n.a.	$C_{27}H_{30}O_{15}$	593.1519	593.1512	-0.7	447.0936 (-0.3) [Y1]- [$C_{21}H_{19}O_{11}$]- 285.0404 (-1.3) [Y0]- [$C_{15}H_9O_6$]- 284.0328 (-0.5) [Y0-H•]•- [$C_{15}H_8O_6$]•-	Luteolin-7-O-Rut	n.a.	n.a.

| | t_R (min)[1] | | λ_{max} (nm) | Formula | [M-H]⁻ | | Δ ppm | MS/MS | Proposed compound | Pl | Tx |
	HPLC	UHPLC			Obs. m/z	Calc. m/z		[m/z (Δppm) (attribution)]			
	19.38	**6.49**	**256, 345**	$C_{21}H_{20}O_{11}$	**447.0938**	**447.0933**	**-0.5**	**327.0513 (-0.7) [^{0,2}X⁻] [$C_{17}H_{11}O_7$]⁻** **285.0406 (-0.3) [Y₀]⁻ [$C_{15}H_9O_6$]⁻** **284.0331 (-1.6) [Y₀-H•]•⁻ [$C_{15}H_8O_6$]•⁻**	**Lut-7-*O*-Glc***	**2**	**2**
	20.28	**7.18**	**254, 350**	$C_{23}H_{22}O_{12}$	**489.1040**	**489.1038**	**-0.1**	**327.0517 (-2.0) [^{0,2}X⁻] [$C_{17}H_{11}O_7$]⁻** **447.0932 (0.1) [$C_{21}H_{19}O_{11}$]⁻** **285.0407 (-0.8) [Y₀]⁻ [$C_{15}H_9O_6$]⁻** **284.0328 (-0.7) [Y₀-H•]•⁻ [$C_{15}H_8O_6$]•⁻**	**Lut-7-*O*-acetyl-Hex**	**3**	**3**
	21.55	8.08	254, 350	$C_{24}H_{22}O_{14}$	533.0939	533.0937	-0.3	489.10438 (0.1) [$C_{23}H_{22}O_{12}$]⁻ 285.0408 (-1.0) [Y₀]⁻ [$C_{15}H_9O_6$]⁻	Lut-malonyl-Hex	n.a.	4
	21.98	9.15	254, 350	$C_{15}H_{10}O_6$	285.0408	285.0405	-0.4	151.0034 (-0.7) [^{1,3}A]⁻ [$C_7H_3O_4$]⁻ 133.0283 (9.0) [^{1,3}B]⁻ [$C_8H_5O_2$]⁻	Lut*	n.a.	5
Morus Alba	**18.63**	**6.08**	**256, 356**	$C_{27}H_{30}O_{16}$	**609.14670**	**609.1461**	**-1.5**	**301.0346 (2.6) [Y₀]⁻ [$C_{15}H_9O_7$]⁻** **300.0278 (-0.4) [Y₀-H•]•⁻ [$C_{15}H_8O_7$]•⁻** **271.0250(-0.5) [Y₀-2H-CO]⁻[$C_{14}H_7O_6$]⁻**	**Que-3-*O*-Rut***	**1**	**1**
	19.03	**6.41**	**255, 355**	$C_{21}H_{20}O_{12}$	**463.0883**	**463.0882**	**-0.3**	**300.0276 (-0.1) [Y₀-H•]•⁻ [$C_{15}H_8O_7$]•⁻** **271.0250 (-1.9) [Y₀-2H-CO][$C_{14}H_7O_5$]⁻**	**Que-3-*O*-Glc***	**2**	**2**
	19.77	**6.66**	**264, 348**	$C_{27}H_{30}O_{15}$	**593.1513**	**593.1512**	**-0.2**	**447.0935 (-0.6) [$C_{21}H_{19}O_{11}$]⁻** **285.0403 (-0.5) [Y₀]⁻ [$C_{15}H_9O_6$]⁻** **284.0329(-0.8) [Y₀-H•]•⁻ [$C_{15}H_8O_6$]•⁻** **255.0302(-1.1) [Y₀-2H-CO]⁻[$C_{14}H_7O_5$]⁻**	Kae-3-*O*-Rut	3	3
	19.87	7.03	264, 347	$C_{21}H_{20}O_{11}$	447.0935	447.0933	-0.4	285.0397 (0.8) [Y₀]⁻ [$C_{15}H_9O_6$]⁻ 284.0331 (-1.6) [Y₀-H•]•⁻ [$C_{15}H_8O_6$]•⁻ 255.0303(-1.6) [Y₀-2H-CO]⁻ [$C_{14}H_7O_5$]⁻	Kae-3-*O*-Glc*	4	4
	20.33	7.49	264, 348	$C_{23}H_{22}O_{12}$	489.1044	489.1038	-1.1	285.0397 (2.7) [Y₀]⁻ [$C_{15}H_9O_6$]⁻ 284.0329 (-0.9) [Y₀-H•]•⁻ [$C_{15}H_8O_6$]•⁻ 255.0305(-2.6) [Y₀-2H-CO]⁻ [$C_{14}H_7O_5$]⁻	Kae-*O*-acetyl-Hex	5	5
Pistacia vera	**17.25**	**5.71**	**264, 358**	$C_{21}H_{18}O_{14}$	**493.0628**	**493.0624**	**-0.8**	**317.0307 (-1.3) [Y₀]⁻ [$C_{15}H_9O_8$]⁻** **299.0204 (-2.1) [$C_{15}H_7O_7$]⁻**	**Myr-3-*O*-Glr**	**1**	**1**
				$C_{21}H_{20}O_{13}$	**479.0834**	**479.0831**	**-0.6**	**316.0227(-0.6) [Y₀-H•]•⁻ [$C_{15}H_8O_8$]•⁻** **287.0206(-3.0) [Y₀-2H-CO]⁻ [$C_{14}H_7O_7$]⁻**	**Myr-3-*O*-Glc**		

t_R (min)[1]		λ_{max}	Formula	[M-H]⁻		Δ	MS/MS	Proposed	Pl	Tx
HPLC	UHPLC	(nm)		Obs. m/z	Calc. m/z	ppm	[m/z (Δppm) (attribution)]	compound		
17.88	5.91	278, 354	$C_{28}H_{24}O_{16}$	615.0992	615.0992	-0.1	463.0887 (-1.0) [Y₁]⁻ [C₂₁H₁₉O₁₂]⁻ 301.0349 (1.7) [Y₀]⁻ [C₁₅H₉O₇]⁻ 300.0281 (-1.7) [Y₀-H•]•⁻ [C₁₅H₈O₇]•⁻ 271.0260(-1.8) [Y₀-2H-CO]⁻[C₁₄H₇O₆]⁻	Que-3-galloyl-Glc	2	2
18.62	**6.45**	**258, 355**	**$C_{21}H_{18}O_{13}$**	**477.0675**	**477.0675**	**-0.1**	**301.0356 (-0.7) [Y₀]⁻ [C₁₅H₉O₇]⁻ 273. 0407 (-0.9))[Y₀-CO]⁻[C₁₄H₉O₆]⁻**	**Que-3-*O*-Glr**	**3**	**3**
			$C_{21}H_{20}O_{12}$	**463.0883**	**463.0882**	**-0.3**	**300.0220 (-4.8) [Y₀-H•]•⁻ [C₁₅H₈O₇]•⁻ 271.0251(-1.2) [Y₀-2H-CO]⁻[C₁₄H₇O₅]⁻**	**Que-3-*O*-Glc**		
19.10	6.82	265; 358	$C_{20}H_{18}O_{11}$	433.0777	433.0776	-0.2	300.0285 (-4.4) [Y₀-H•]•⁻ [C₁₅H₈O₇]•⁻ 271.0265(-4.8) [Y₀-2H-CO]⁻[C₁₄H₇O₆]⁻	Que-3-*O*-Pen	4	4
-	6.98	n.a.	$C_{21}H_{20}O_{11}$	447.0940	447.0933	-1.6	285.0406 (-0.3) [Y₀]⁻ [C₁₅H₉O₆]⁻ 284.0331 (-1.6) [Y₀-H•]•⁻ [C₁₅H₈O₆]•⁻	Lut-7-*O*-Glc*	n.a.	n.a.
19.82	7.69	266, 352	$C_{28}H_{22}O_{17}$	629.07837	629.0784	-0.4	477.0674 (0.1) [Y₁]⁻ [C₂₁H₁₇O₁₃]⁻ 301.0357 (-1.1) [Y₀]⁻ [C₁₅H₉O₇]⁻	Que-galloyl-Glr	5	5
22.00	**9.16**	**254, 350**	**$C_{15}H_{10}O_6$**	**285.0411**	**285.0405**	**-2.4**	**151.0035 (-1.0) [¹,³A]⁻ [C₇H₃O₄]⁻ 133.0284 (8.7) [¹,³B]⁻ [C₈H₅O₂]⁻**	**Lut***	**6**	**6**
18.60	**6.43**	**256, 354**	**$C_{21}H_{18}O_{13}$**	**477.0681**	**477.0675**	**-1.3**	**301.0358 (-1.8) [Y₀]⁻ [C₁₅H₉O₇]⁻**	**Que-3-*O*-Glr***	**1**	**1**
20.33	**7.24**	**254, 352**	**$C_{22}H_{20}O_{13}$**	**491.0832**	**491.0831**	**-0.1**	**315.0515 (-1.4) [Y₀]⁻ [C₁₆H₁₁O₇]⁻ 271.0252 (-1.4) [Y₀-2H-CO]⁻[C₁₄H₇O₆]⁻**	**Irh-3-*O*-Glr**	**2**	**2**
3.73	**2.24**	**257, 376**	**$C_{34}H_{22}O_{22}$**	**781.0521**	**781.0530**	**0.9**	**600.9899 (-0.5) [C₂₈H₇O₁₆]⁻ 300.9993 (-1.1) [Y₀]⁻ [C₁₄H₅O₈]⁻**	**Punicalin**	**1**	**1**
6.05	3.02	257, 377	$C_{48}H_{28}O_{30}$	541.0266#	541.0260	-0.6	[782.0564 (4.2) + 300.9995 (-1.6) [C₃₄H₂₂O₂₂]⁻ + [C₁₄H₅O₈]⁻	Punicalagin A	2	2
8.89	**3.69**	**257, 378**	**$C_{48}H_{28}O_{30}$**	**541.0268 #**	**541.0260**	**-0.7**	**[782.0564 (4.2) + 300.9995 (-1.6) [C₃₄H₂₂O₂₂]⁻ + [C₁₄H₅O₈]⁻**	**Punicalagin B**	**3**	**3**
15.51	5.46	256, 362	$C_{27}H_{22}O_{18}$	633.0629	633.0733	-0.8	463.0523 (-1.1) [C₂₀H₁₅O₁₃]⁻ 300.9989 (0.4) [Y₀]⁻ [C₁₄H₅O₈]⁻	Galloy-HHDP-Hex	4	4

P. ferulacea (rows with Que-3-*O*-Glr* and Irh-3-*O*-Glr)

Punica granatum (rows with Punicalin, Punicalagin A, Punicalagin B, Galloy-HHDP-Hex)

	t_R (min)[1]		λ_{max}	Formula	[M-H]⁻		Δ ppm	MS/MS	Proposed compound	Pl	Tx
	HPLC	UHPLC	(nm)		Obs. m/z	Calc. m/z		[m/z (Δppm) (attribution)]			
	16.45	5.70	254, 377	$C_{19}H_{14}O_{12}$	433.0403	433.0412	0.9	300.9987 (1.0) [Y_0]⁻ [$C_{14}H_5O_8$]⁻ 299.9911 (0.2) [Y_0-H•]•⁻ [$C_{14}H_4O_8$]•⁻	Ellagic acid-xylopyranoside	5	5
	17.01	5.88	252, 359	$C_{20}H_{16}O_{12}$	447.0565	447.0569	0.4	300.9978 (4.1) [Y_0]⁻ [$C_{14}H_5O_8$]⁻ 299.9913 (-0.4) [Y_0-H•]•⁻ [$C_{14}H_4O_8$]•⁻	Ellagic acid-Rha	6	6
	19.38	**6.24**	**250, 368**	**$C_{14}H_6O_8$**	**300.9996**	**300.9990**	**-0.6**	**273.0047 (-0.7) [$C_{13}H_5O_7$]- 257.0096 (-1.8) [$C_{13}H_5O_6$]- 229.0145 (-1.0) [$C_{12}H_5O_5$]-**	**Ellagic acid***	**7**	**7**
Vitis vinifera	**18.60**	**6.46**	**256, 354**	**$C_{21}H_{18}O_{13}$**	**477.0675**	**477.0675**	**-0.1**	**301.0356 (0.6) [Y_0]⁻ [$C_{15}H_9O_7$]⁻**	**Que-*O*-Glr***	**1**	**1**
	-	6.81	n.a.	$C_{21}H_{20}O_{11}$	447.0931	447.0933	0.3	284.0331 (-1.6) [Y_0-H•]•⁻ [$C_{15}H_8O_6$]•⁻ 255.0300(-0.2)[Y_0-2H-CO]⁻ [$C_{14}H_7O_5$]⁻	Kae-Glc isomer	n.a.	n.a.
	19.80	**7.02**	**264, 348**	**$C_{21}H_{20}O_{11}$**	**447.0933**	**447.0933**	**0.0**	**285.0404 (0.1) [Y_0]⁻ [$C_{15}H_9O_6$]⁻ 284.0331 (-1.6) [Y_0-H•]•⁻ [$C_{15}H_8O_6$]•⁻ 255.0306(-2.6) [Y_0-2H-CO]⁻ [$C_{14}H_7O_5$]⁻**	**Kae-3-*O*-Glc***	**2**	**2**
	21.23	**9.27**	**254, 370**	**$C_{15}H_{10}O_7$**	**301.0357**	**301.0354**	**-1.0**	**151.0030 (4.4) [$^{1,3}A$]⁻ [$C_7H_3O_4$]⁻ 121.0280 (10.0) [$^{1,2}B$]⁻ [$C_7H_5O_2$]⁻**	**Que***	**n.a.**	**3**
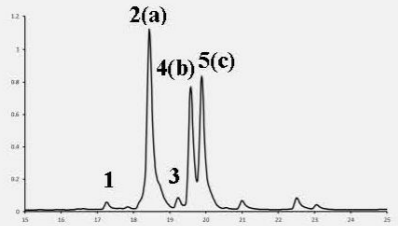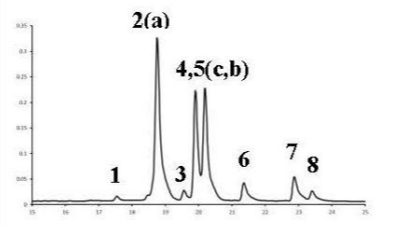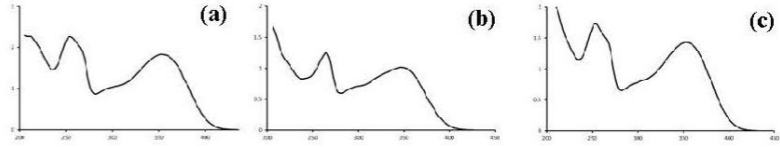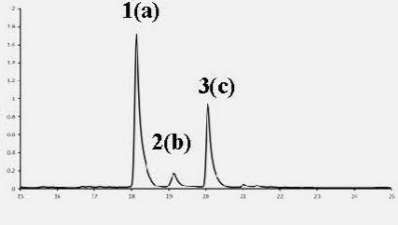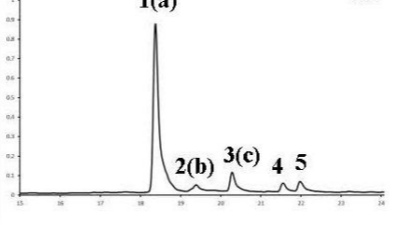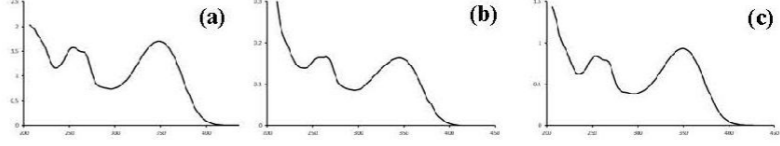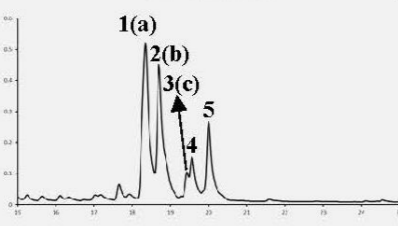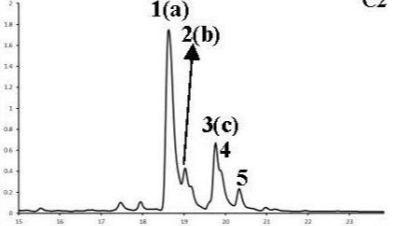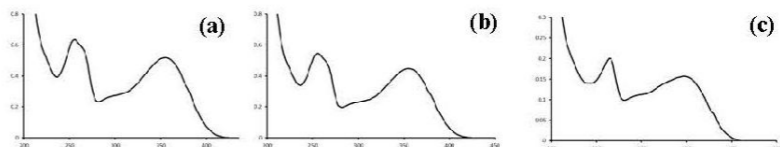
Abbreviations: Que, quercetin; Kae, kaempferol; Lut, luteolin; Irh, isorhamnetin; Rha, rhamnoside; Glc, glucoside; Glr, glucuronide; Gly, glycoside; DeoxHex, deoxyhexoside; Hex, hexoside, Pen, pentoside; Rut, rutinoside.

[1] The reported retention times are in accordance with the analysis of textile samples.

Double charged deprotonated molecules [M-2H]²⁻

* Identified with an analytical standard

Table A3.2- Chromatograms of both plant (left) and dyed wool extracts (right), retention times and correspondent absorbance maxima (λ_{max}) and mass, as well as UV-VIS spectra of the main peaks (A, B and C).

Chromatogram Plant	Peak	t_R (min)	λ_{max} (nm)	Chromatogram Textile	t_R (min)	λ_{max} (nm)	Mass (Da)	UV-Vis Spectra
Delphinium semibarbatum (A)	1	17.25	256, 355		17.55	256, 356	610	
	2	18.43	255, 355		18.75	255, 355	464	
	3	19.23	263, 347		19.55	264, 348	448	
	4	19.58	264, 347		19.90	264, 347	448	
	5	19.89	254, 354		20.19	254, 354	478	
	6	-	-		21.35	254, 371	302	
	7	-	-		22.87	264, 366	286	
	8	-	-		23.40	254, 370	316	
Eremostachys laevigata (B)	1	18.15	254, 348		18.37	254, 349	580	
	2	19.15	256, 345		19.38	256, 344	448	
	3	20.07	254, 350		20.28	254, 350	490	
	4	-	-		21.55	254 350	534	
	5	-	-		21.98	254,350	286	
Morus alba (C)	1	18.35	256, 356		18.63	256, 356	610	
	2	18.70	255, 355		19.03	255, 355	464	
	3	19.43	264, 348		19.77	264, 348	594	
	4	19.54	264, 347		19.87	264, 347	448	
	5	20.00	264, 348		20.33	264, 348	490	
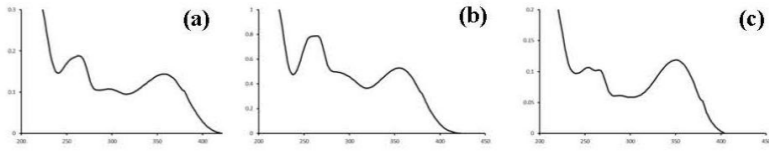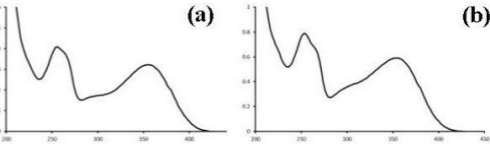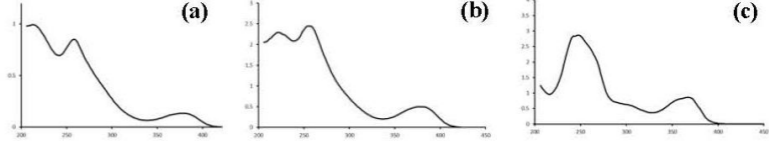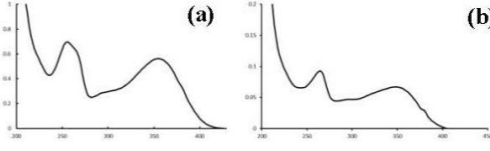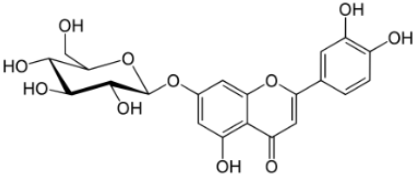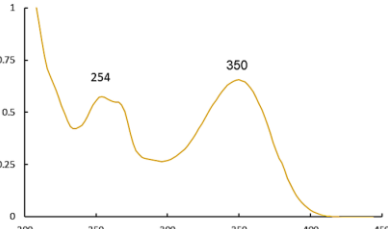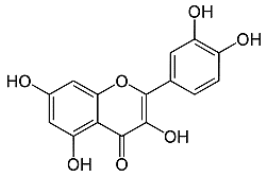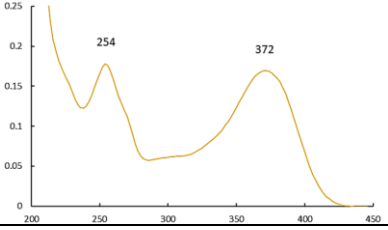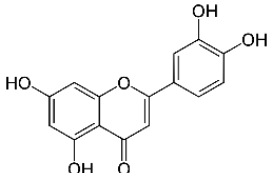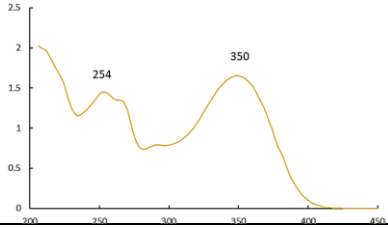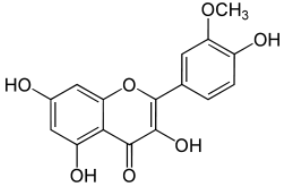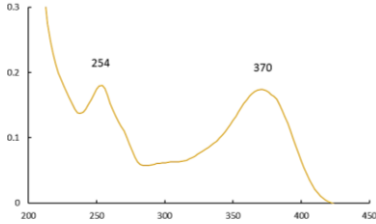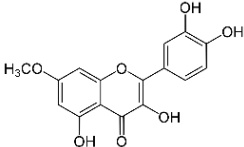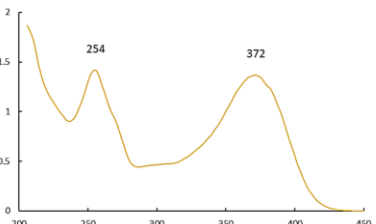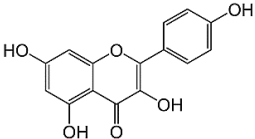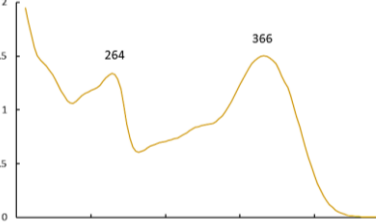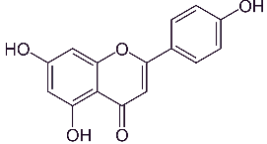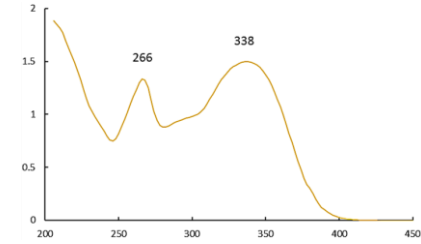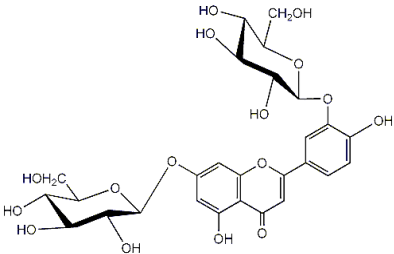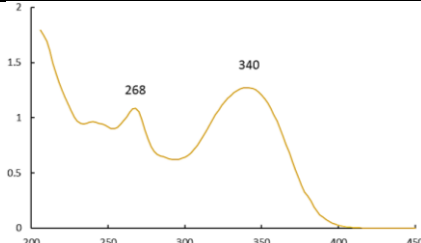
Chromatogram Plant	Peak	t_R (min)	λ_{max} (nm)	Chromatogram Textile	t_R (min)	λ_{max} (nm)	Mass (Da)	UV-Vis Spectra
Pistacia vera (D) D1	1	16.94	262, 357	D2	17.25	264, 358	480	(a) (b) (c)
	2	17.55	276, 353		17.88	278, 354	616	
	3	18.26	258, 355		18.62	258, 355	478	
	4	18.74	265, 358		19.10	265, 358	434	
	5	19.45	267, 350		19.82	266, 352	630	
	6	21.58	254, 350		22.00	254, 350	286	
Prangos ferulacea (E) E1	1	18.25	256, 354	E2	18.60	256, 354	478	(a) (b)
	2	20.02	254, 354		20.33	254, 352	492	
Punica granatum (F) F1	1	3.50	257, 378	F2	3.73	257, 376	782	(a) (b) (c)
	2	5.60	258, 378		6.05	257, 377	1084	
	3	8.43	256, 378		8.89	257, 378	1084	
	4	15.24	255, 363		15.51	256, 362	634	
	5	16.16	253, 378		16.45	254, 377	434	
	6	16.76	252, 359		17.01	252, 359	448	
	7	18.93	249, 368		19.38	250, 368	301	
Vitis vinifera (G) G1	1	18.25	256, 354	G2	18.60	256, 354	478	(a) (b)
	2	19.45	264, 348		19.80	264, 348	448	
	3	-	-		21.23	254, 370	302	

Table A3.3- Flavonoid references: common and scientific names, molecular structure, retention time, absorbance maxima and UV-VIS spectra as acquired by HPLC-DAD.

Name	Structure	t_R(min)	λ_{max} (nm)	Spectra UV-VIS
Luteolin-7-*O*-glucoside		18.40	254, 350	
Quercetin		20.90	254, 372	
Luteolin		21.76	254, 350	

Name	Structure	t_R(min)	λ_{max} (nm)	Spectra UV-VIS
Isorhamnetin		23.30	254, 370	
Rhamnetin		23.65	254, 372	
Kaempferol		22.39	264, 366	

Name	Structure	t_R (min)	λ_{max} (nm)	Spectra UV-VIS
Apigenin		22.80	266, 338	
Luteolin-3',7-di-*O*-gluco-side		17.3	268, 340	

Appendix 4- Photoreactivity and stability of flavonoid yellows used in cultural heritage
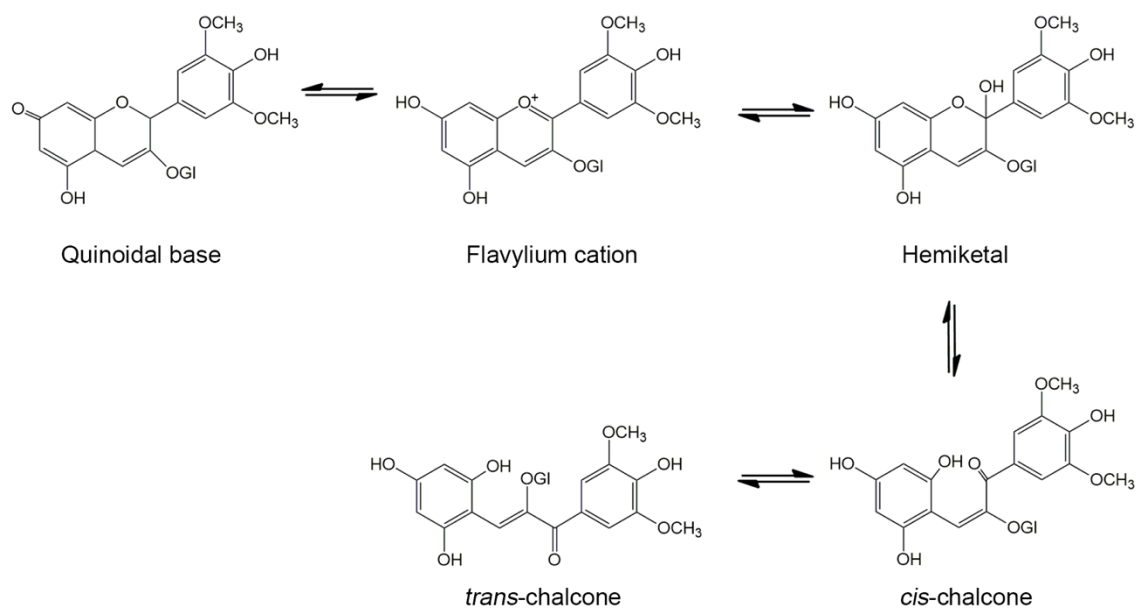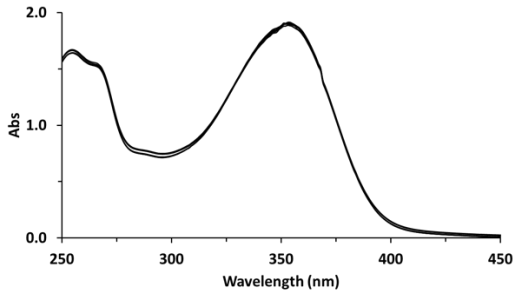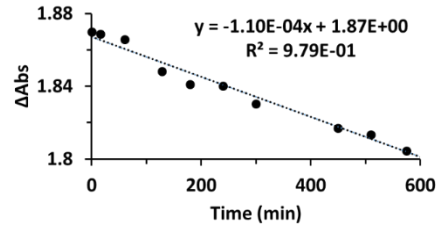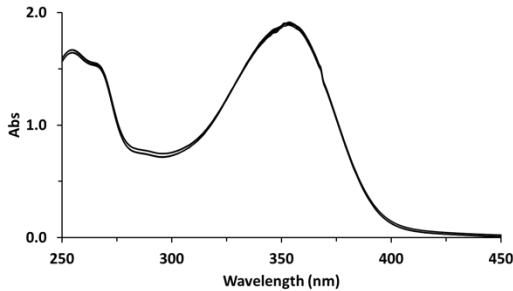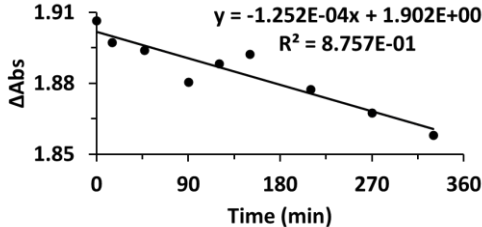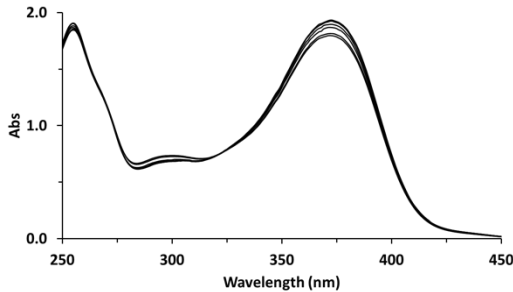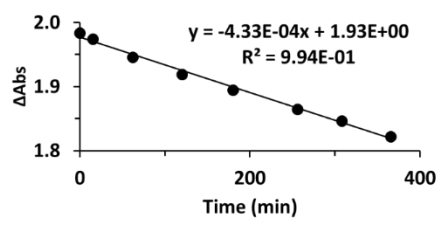
Scheme A4.1. Multi-equilibria, in water, for malvidin-3-*O*-glucoside (oenin) as an example for anthocyanins.
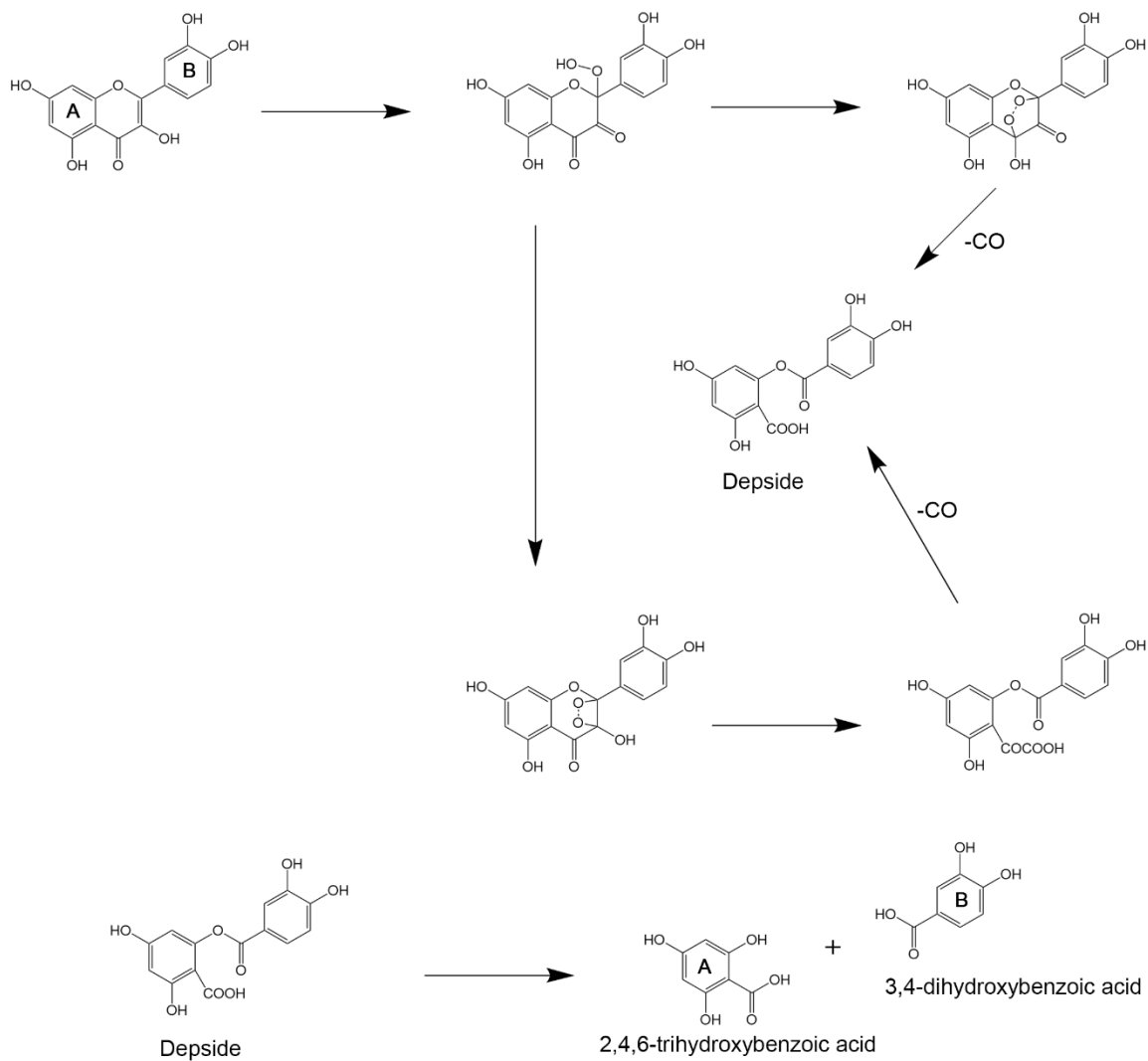
Scheme A4.2. Photooxidation of quercetin, adapted from Ferreira *et al.* [32][22].

---

[22] The reported references are in accordance with the reference list of Chapter 4.

193

Table A4.1. Experimental data used to calculate the quantum yields of reaction, Φ_R, at λ_{irr} = 313 nm and 293 K. Reference compounds were irradiated in homogeneous media, MeOH:H$_2$O (7:3).

Reference compound	UV-VIS spectra	Abs$_{max}$/ irradiation time
Luteolin 8.81 × 10^{-5} M Abs$_{max}$= 353 nm		 y = -1.10E-04x + 1.87E+00 R^2 = 9.79E-01
Luteolin-7OGlc 9.72 × 10^{-5} M Abs$_{max}$= 351 nm		 y = -1.252E-04x + 1.902E+00 R^2 = 8.757E-01
Quercetin 9.47 × 10^{-5} M Abs$_{max}$= 372 nm		 y = -4.33E-04x + 1.93E+00 R^2 = 9.94E-01

194

Reference compound	UV-VIS spectra	Abs$_{max}$/ irradiation time
Quercetin-3OGlr 9.99×10^{-5} M Abs$_{max}$= 360 nm		$y = -3.54\text{E-}04x + 1.97\text{E+}00$ $R^2 = 9.80\text{E-}01$
Kaempferol 7.70×10^{-5} M Abs$_{max}$= 368 nm		$y = -3.88\text{E-}04x + 1.97\text{E+}00$ $R^2 = 9.93\text{E-}01$
Kaempferol-3OGlc 1.12×10^{-4} M Abs$_{max}$= 353 nm		$y = -1.96\text{E-}04x + 1.86\text{E+}00$ $R^2 = 9.88\text{E-}01$
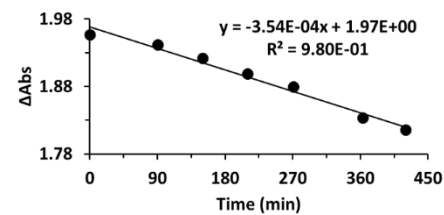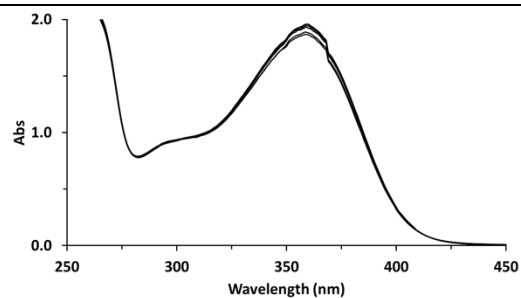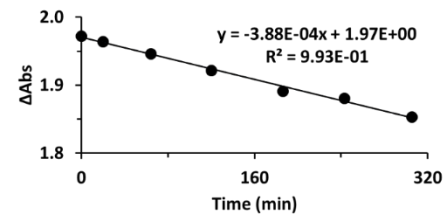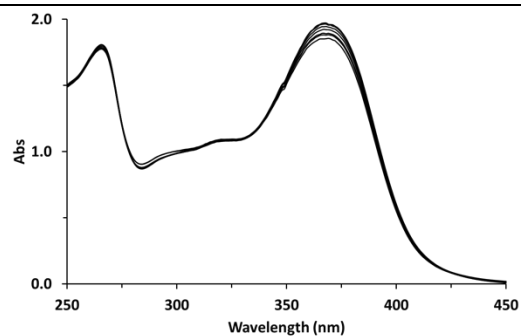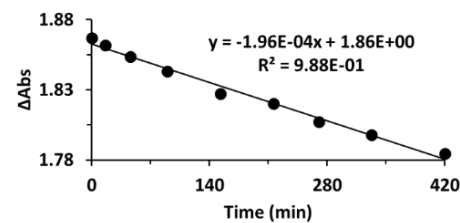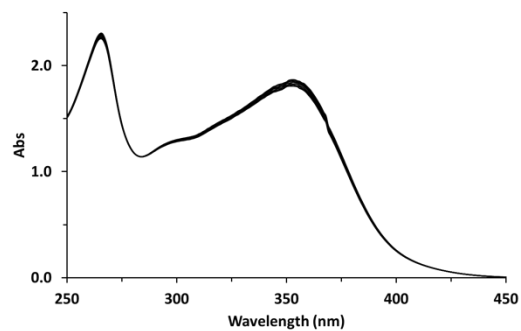
Reference compound	UV-VIS spectra	Abs_{max}/ irradiation time
Eriodictyol $1. \times 10^{-4}\,M$ $Abs_{max} = 290$ nm		
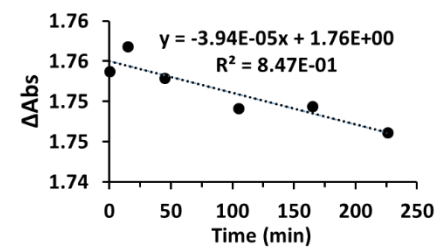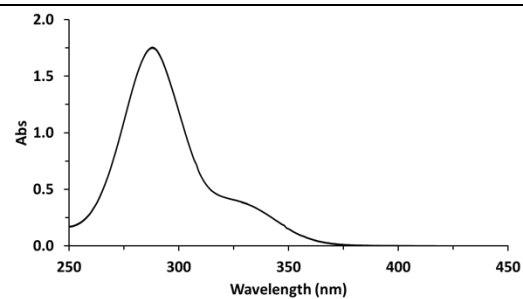
Table A4.2. Experimental data used to calculate the quantum yields of reaction, Φ_R, at λ_{irr} = 366 nm and 293 K. Reference compounds were irradiated in homogeneous media (HoM), MeOH:H$_2$O (7:3), and heterogeneous media (HeM), proteinaceous gel.

Reference compound	MeOH: H$_2$O	Proteinaceous gel
Luteolin HoM: 8.81 × 10^{-5} M HeM: 7.97 × 10^{-5} M Abs$_{max}$= 350 nm		
Luteolin-7OGlc HoM: 9.72 × 10^{-5} M HeM: 8.29 × 10^{-5} M Abs$_{max}$= 351 nm		
Quercetin HoM: 9.47 × 10^{-5} M HeM: 1.01 × 10^{-4} M Abs$_{max}$= 371 nm		

197

Reference compound	MeOH: H₂O	Proteinaceous gel
Quercetin-3OGlr HoM: 9.99×10^{-5} M HeM: 1.75×10^{-4} M Abs$_{max}$= 360 nm	 $y = -1.55\text{E-}04x + 1.77\text{E}+00$ $R^2 = 9.85\text{E-}01$	 $y = -3.30\text{E-}04x + 1.72\text{E}+00$ $R^2 = 8.96\text{E-}01$
Kaempferol HoM: 7.70×10^{-5} M HeM: 9.78×10^{-5} M Abs$_{max}$= 366 nm	 $y = -5.727\text{E-}04x + 1.852\text{E}+00$ $R^2 = 9.734\text{E-}01$	 $y = -2.32\text{E-}03x + 1.08\text{E}+00$ $R^2 = 9.18\text{E-}01$
Kaempferol-3OGlc HoM: 1.12×10^{-4} M HeM: 9.20×10^{-5} M Abs$_{max}$= 348 nm	 $y = -8.42\text{E-}05x + 1.92\text{E}+00$ $R^2 = 9.29\text{E-}01$	 $y = -3.93\text{E-}04x + 1.64\text{E}+00$ $R^2 = 8.17\text{E-}01$
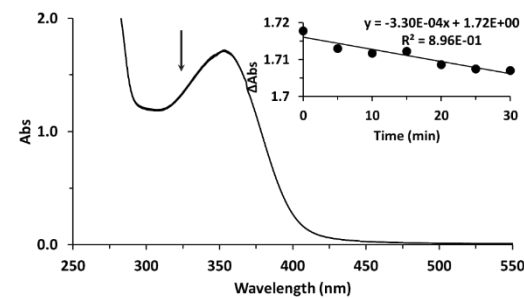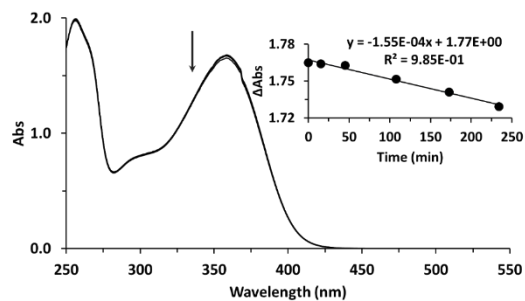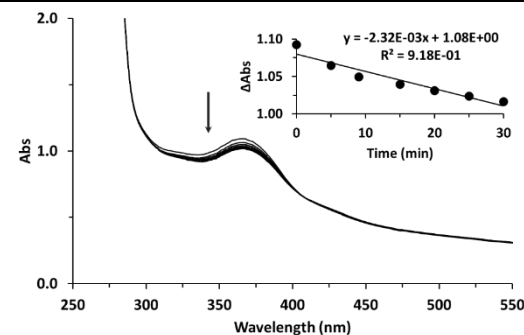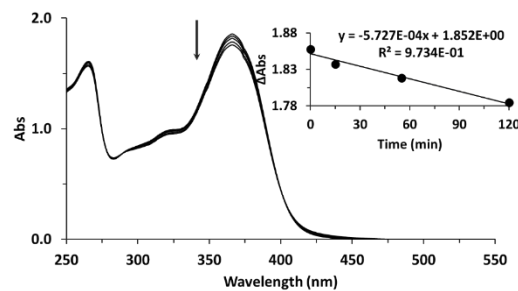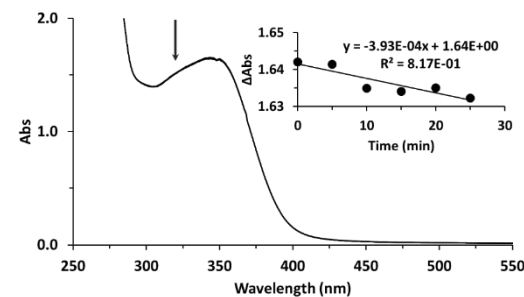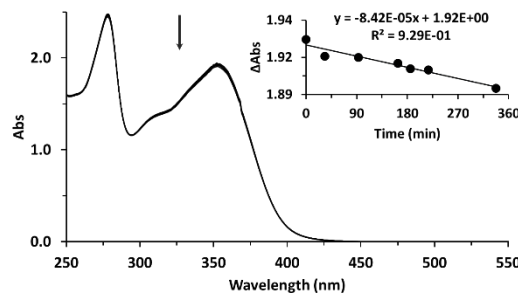
Table A4.3. Reference compounds (1x10^{-3}M), in MeOH irradiated with polychromatic Xenon-arc light source (λ_{irr}> 300 nm). Represented are the UV-VIS absorbance spectra and the decrease in absorbance for each compound throughout the irradiation times. For the scatter plot the maximum of absorbance of band I for each compound was considered.

Reference compound	UV-VIS spectra	Abs$_{max}$/ irradiation time
Luteolin		
Luteolin-7OGlc		
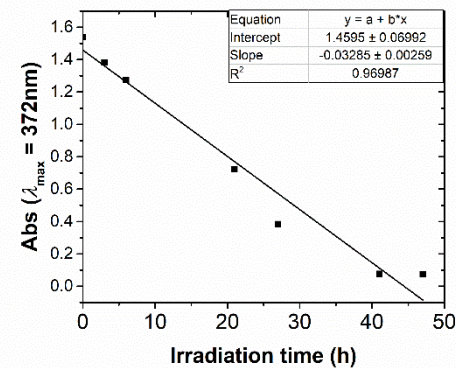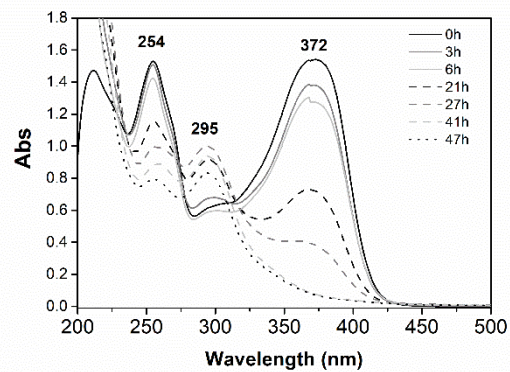
Reference compound	UV-VIS spectra	Abs$_{max}$/ irradiation time
Quercetin		
Quercetin-3OGlr		
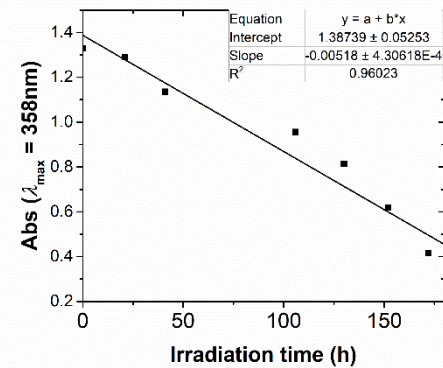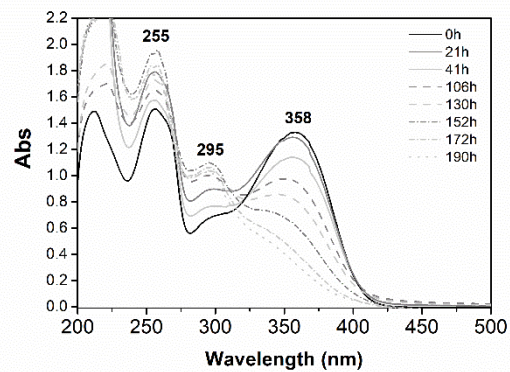
Reference compound	UV-VIS spectra	Abs$_{max}$/ irradiation time
Eriodictyol		
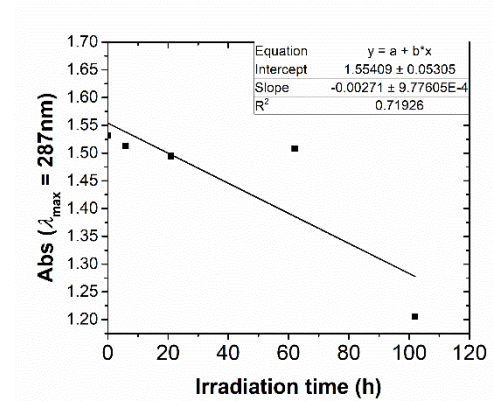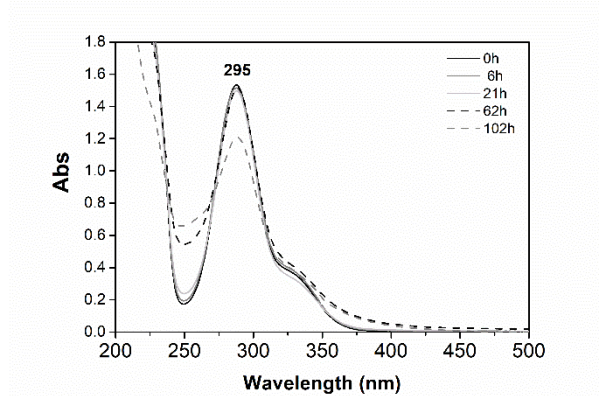
Table A.4.4- LC-DAD-MS data for flavonoid dyes and its irradiated solutions.

Compound	Irr time /h	t_R /min	λ_{max} /nm	[M-H]⁻	Code DP*
Quercetin	0h	11.51	254, 370	301	Que
		7.28	294	317	DP317
		8.43	292	331	DP331
				349	DP349
	3h	8.46	290	195	DP195
		9.14	260; 298	169	DP169
		10.21	296	363	DP363
		11.51	254; 370	301	Que
		6.66	274	179	DP179
		7.28	294	317	DP317
		8.43	290	331	DP331
				349	DP349
	6h	8.46	292	195	DP195
		9.14	260; 298	169	DP169
		10.21	274	333	DP333
			296	363	DP363
		11.51	254; 370	301	Que
		14.62	304; 362	601	DP601
		6.66	274	179	DP179
		9.14	260; 298	169	DP169
		9.64	266; 296	395	DP395
	41h	9.93	300	211	DP211
		10.11	292	395	DP395is
		12.02	298	347	DP347
		13.55	300	393	DP393
		9.64	266, 296	395	DP395
		9.93	300	211	DP211
	48h	10.11	292	395	DP395is
		12.02	298	347	DP347
		13.55	300	393	DP393
Que-3-*O*-Glr	0h	8.84	256; 354	477	Que-3OGlr
	21h	8.84	256, 354	477	Que-3OGlr
	41h	8.83	256; 354	477	Que-3OGlr
		7.27	260; 296	523	DP523
	106h	7.79	298; 296	587	DP587
		8.83	256; 354	477	Que-3OGlr
		9.64	262; 302	539	DP539
		7.27	260; 296	523	DP523
		7.79	260; 326	587	DP587
	130h	8.83	256; 354	477	Que-3OGlr
		9.64	262; 302	539	DP539
		9.94	300	539	DP539is
	190h	7.27	260; 296	587	DP587

Compound	Irr time /h	t_R /min	λ_{max} /nm	[M-H]⁻	Code DP*
		9.35	298	523	DP523is
		9.64	264; 302	539	DP539
		9.95	300	539	DP539is
Luteolin	0h	11.54	254; 348	285	Lut
	6h	11.54	254; 348	285	Lut
	21h	11.54	254; 348	285	Lut
	27h	11.54	254; 348	285	Lut
	41h	11.54	254; 348	285	Lut
	63h	11.54	254;348	285	Lut
	84h	7.87	304	347	PD347
		7.28	294	153	PD153
		8.67	302	317	PD317
		11.54	254; 348	285	Lut
	106h	6.74	294	177	PD177
		7.87	304	347	PD347
		7.28	294	153	PD153
		8.67	302	317	PD317
		10.22	304	393	PD393
		11.07	262; 304	333	PD333
		11.54	346	285	Lut
		12.43	318	331	PD331
		11.30	250; 320	333	PD333is
	147h	6.74	294	177	PD177
		7.87	258; 352	347	PD347
		7.27	294	153	PD153
		8.66	302	317	PD317
		10.22	302	393	PD393
		11.06	306	333	PD333
		11.48	330	331	PD331
		12.43	318	331	PD331is
		11.30	250; 320	333	PD333
Lut-7-O-Glc	0h	8.88	254; 342	447	Lut-7OGlc
	6 h	8.88	254, 342	447	Lut-7OGlc
	21h	8.88	254; 342	447	Lut-7OGlc
	27h	8.88	254 342	447	Lut-7OGlc
	41h	5.99	258; 290	509	DP509
		7.85	294	373	DP373
		8.88	254; 342	447	Lut-7OGlc
	63 h	5.99	258; 290	509	DP509
		6.42	258; 300	479	DP479
		7.85	294	373	DP373
		8.88	258; 348	447	Lut-7OGlc
		9.45	262; 328	493	DP493
		10.18	258; 320	511	DP511

Compound	Irr time /h	t_R /min	λ_{max} /nm	[M-H]⁻	Code DP*
Eriodictyol	0	11.2	288	287	ED
	6 h	11.2	288	287	ED
	21h	11.2	288	287	ED
		11.6	288	317	DP317
		13.3	288	349	DP349
	62h	8.8	288	275	DP275
		9.5	286	319	DP319
		11.2	288	287	ED
		11.4	288	333	DP333
		11.6	290	317	DP317
		12.6	282	333	DP333is
		13.3	288	349	DP349

* Identified degradation product
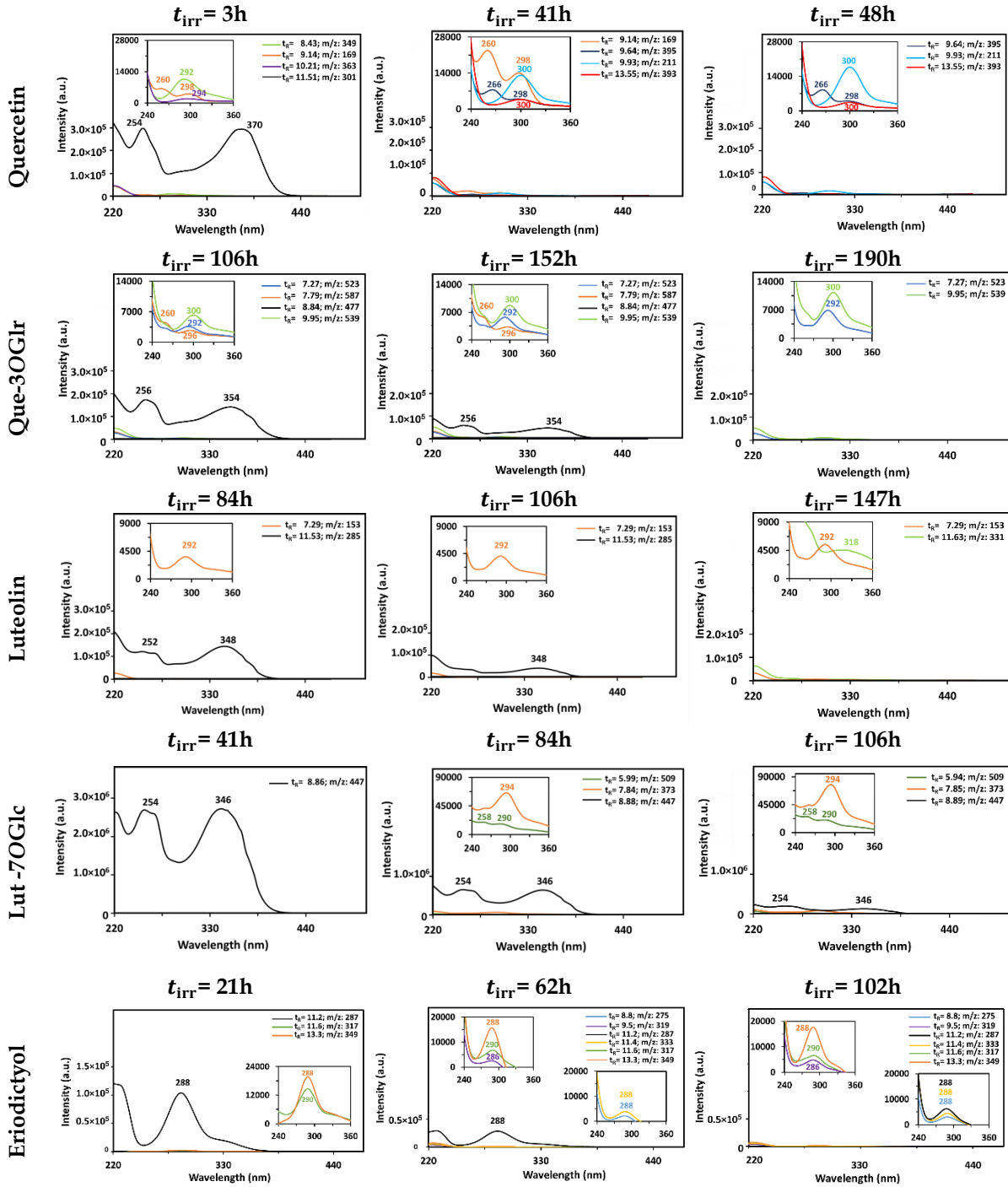
Figure A4.1- UV-VIS spectra of the main degradation compounds identified by HPLC-DAD-MS analysis
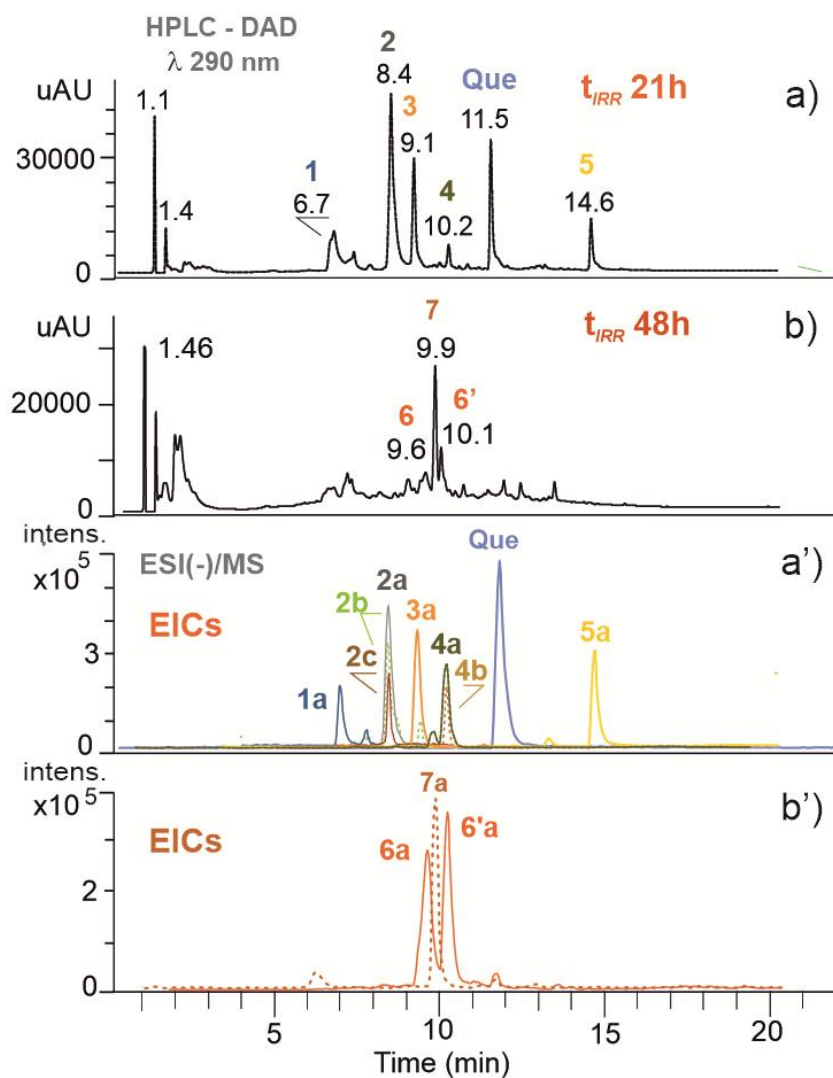
Figure A4.2. HPLC-DAD-MS analysis obtained in the ESI negative mode for two samples of Que in methanol, at 21h and 48h of irradiation: a) and b) DAD chromatograms obtained at 290 nm; a′) extracted ion chromatograms for the deprotonated molecules of: Que *m/z* 301; 1a *m/z* 179 DP179; 2a *m/z* 349 DP349; 2b *m/z* 331 DP331; 2c *m/z* 195 DP195; 3a *m/z* 169 DP169; 4a *m/z* 363 DP363; 4b *m/z* 333 DP333; 5a *m/z* 601 DP601; b′) extracted ion chromatograms for the deprotonated molecules of 6a and 6a′ *m/z* 395 isomers DP395; 7a *m/z* 211 DP211.
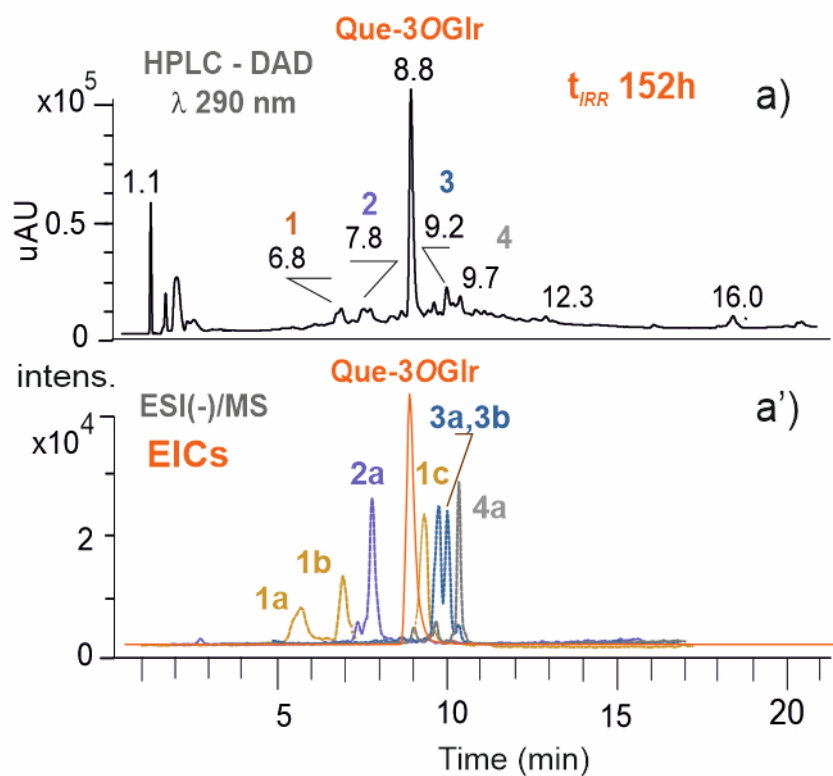
Figure A4.3. HPLC-DAD-MS analysis obtained in the ESI negative mode for a sample of Que-3OGlr in methanol, at 152h of irradiation: a) DAD chromatogram obtained at 290 nm; a') extracted ion chromatograms for the deprotonated molecules of: Que-3OGlr *m/z* 477; 1a,1b and 1c *m/z* 523 DP523 isomers; 2a *m/z* 587 DP587; 3a and 3b *m/z* 539 DP539 isomers, 4a *m/z* 537 DP 537.
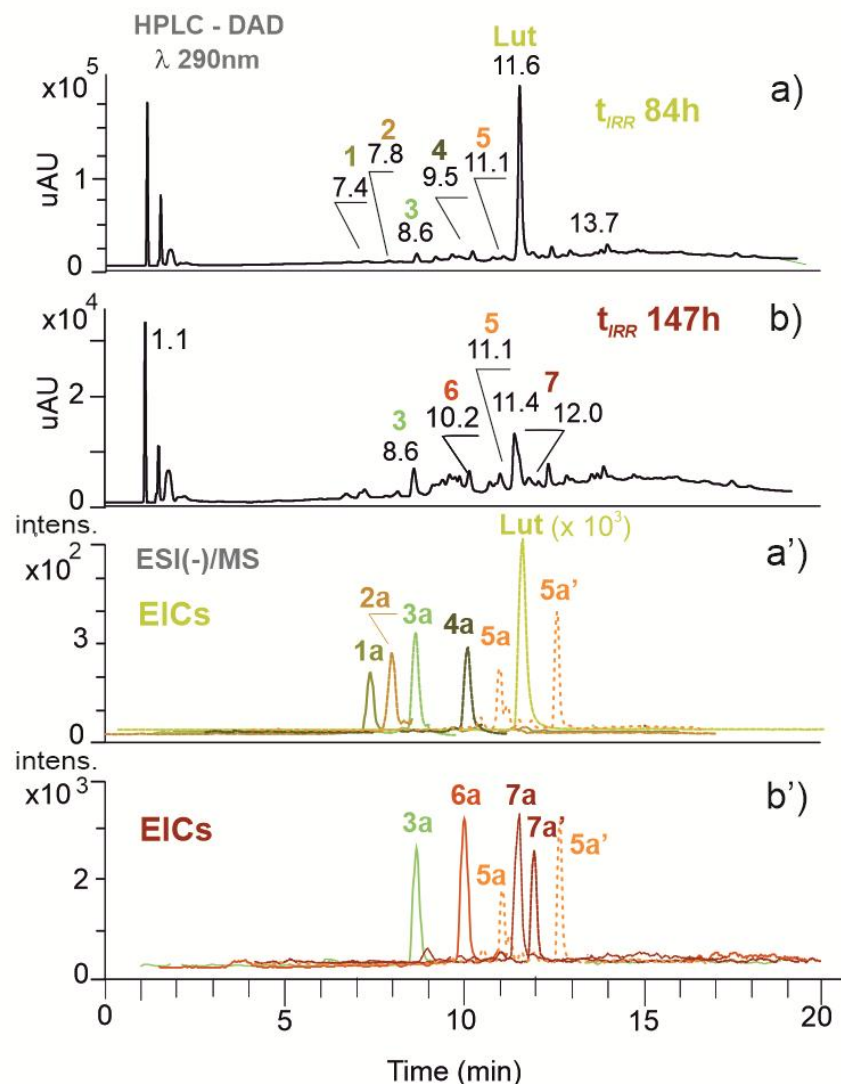
Figure A4.4. HPLC-DAD-MS analysis obtained in the ESI negative mode for two samples of Lut in methanol, at 84h and 147h of irradiation: a) and b) DAD chromatograms obtained at 290 nm; a') extracted ion chromatograms for the deprotonated molecules of: Lut *m/z* 285; 1a *m/z* 347 DP347; 2a *m/z* 153 DP153; 3a *m/z* 317 DP317; 4a *m/z* 393 DP393; 5a and 5a' *m/z* 333 DP333 isomers; b') extracted ion chromatograms for the deprotonated molecules of: Lut *m/z* 285; 3a *m/z* 153 DP153; 6a *m/z* 393 DP393; 5a e 5'a *m/z* 333 DP333 isomers; 7a and 7a' *m/z* 331 DP331 isomers.
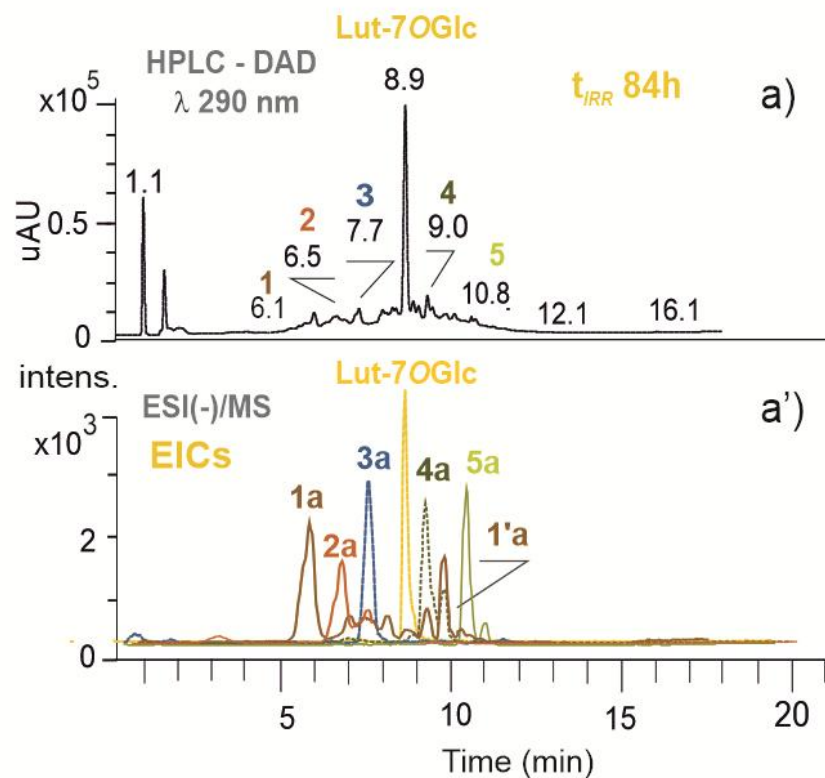
Figure A4.5. HPLC-DAD-MS analysis obtained in the ESI negative mode for two samples of Lut-7OGlc in methanol, at 84h of irradiation: a) DAD chromatograms obtained at 290 nm; a') extracted ion chromatograms for the deprotonated molecules of: Lut-7OGlc m/z 447; 1a and 1'a m/z 509 DP509 isomers; 2a m/z 479 DP479; 3a m/z 373 DP373; 4a m/z 493 DP493; 5a m/z 511 DP511.
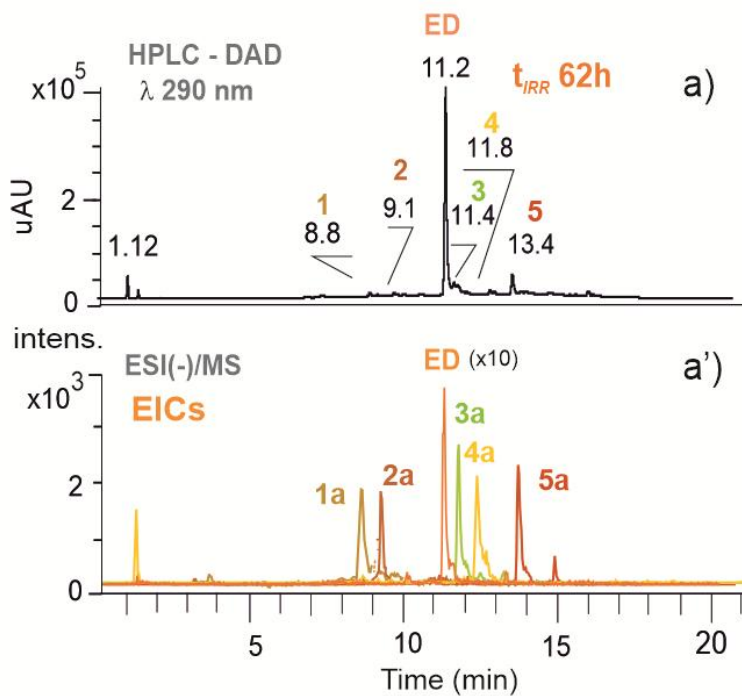
Figure A4.6. LC-DAD-MS analysis obtained in the ESI negative mode for one sample of eriodic-tyol in methanol, at 62h of irradiation: a) DAD chromatograms obtained at 290 nm; a') extracted ion chromatograms for the deprotonated molecules of: ED *m/z* **287; 1a** *m/z* **275 DP275; 2a** *m/z* **319 DP319; 3a** *m/z* **333 DP333; 4a** *m/z* **317 DP317; 5a** *m/z* **349 DP349.**
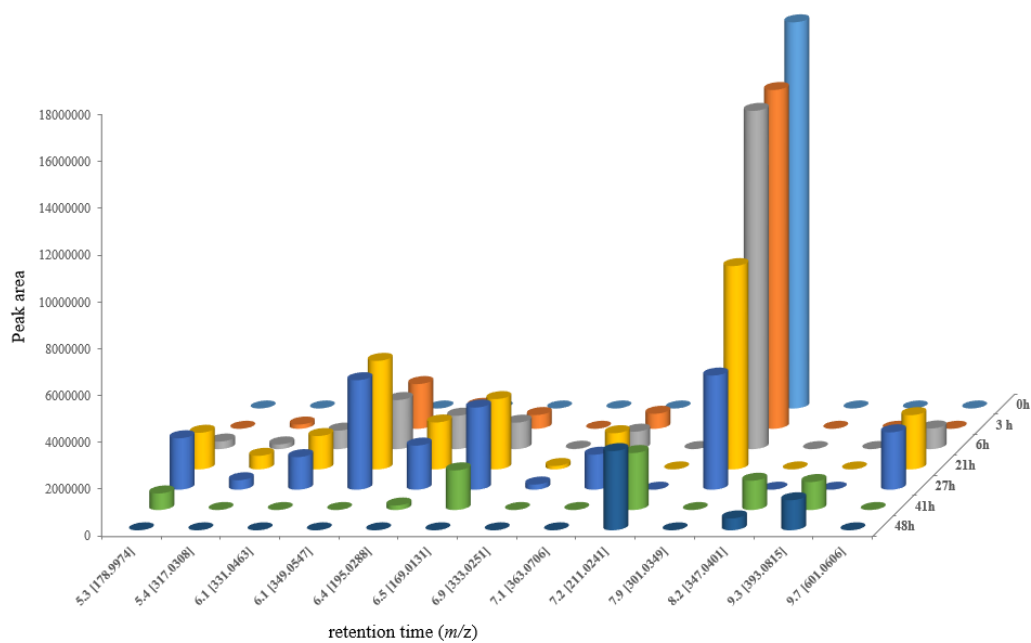
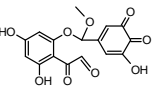**Figure A4.7. 3D-graph of the main photodegradation products of quercetin in methanol.**
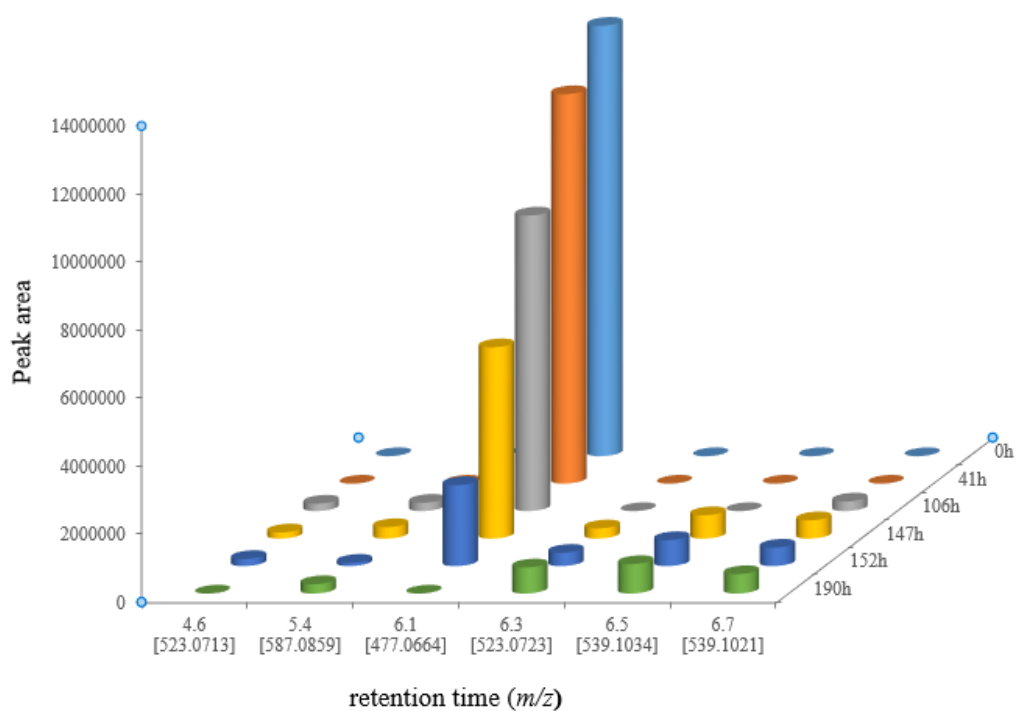
Figure A4.8. 3D-graph of the main photodegradation products of quercetin-3-*O*-glucuronide in methanol.
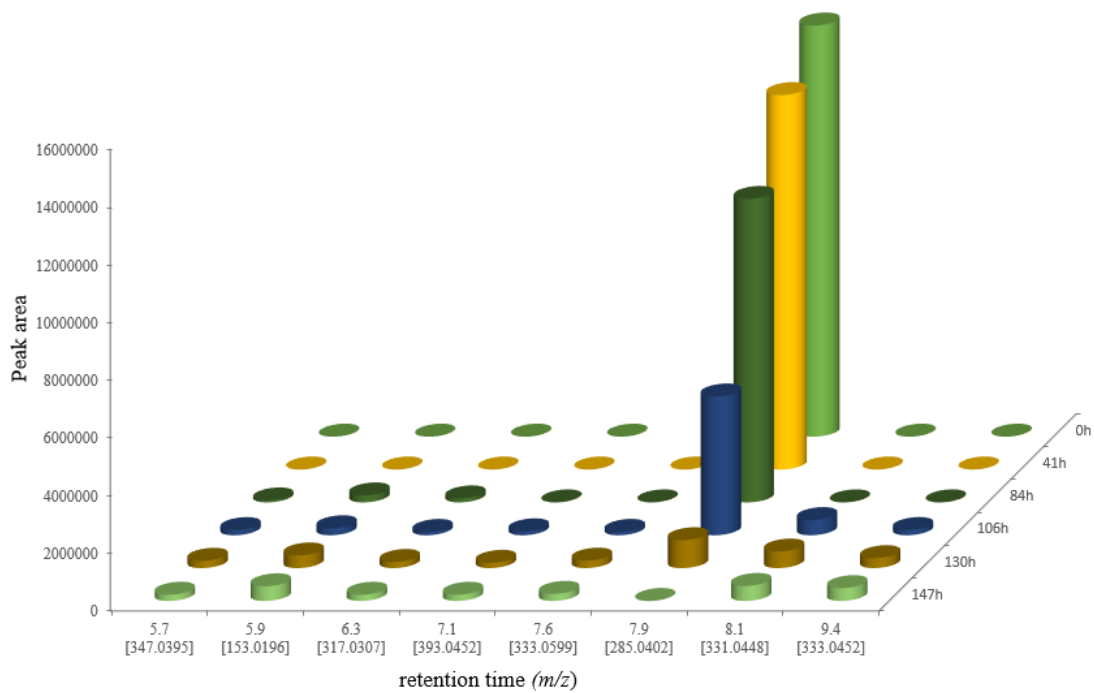
Figure A4.9. 3D-graph of the main photodegradation products of luteolin in methanol
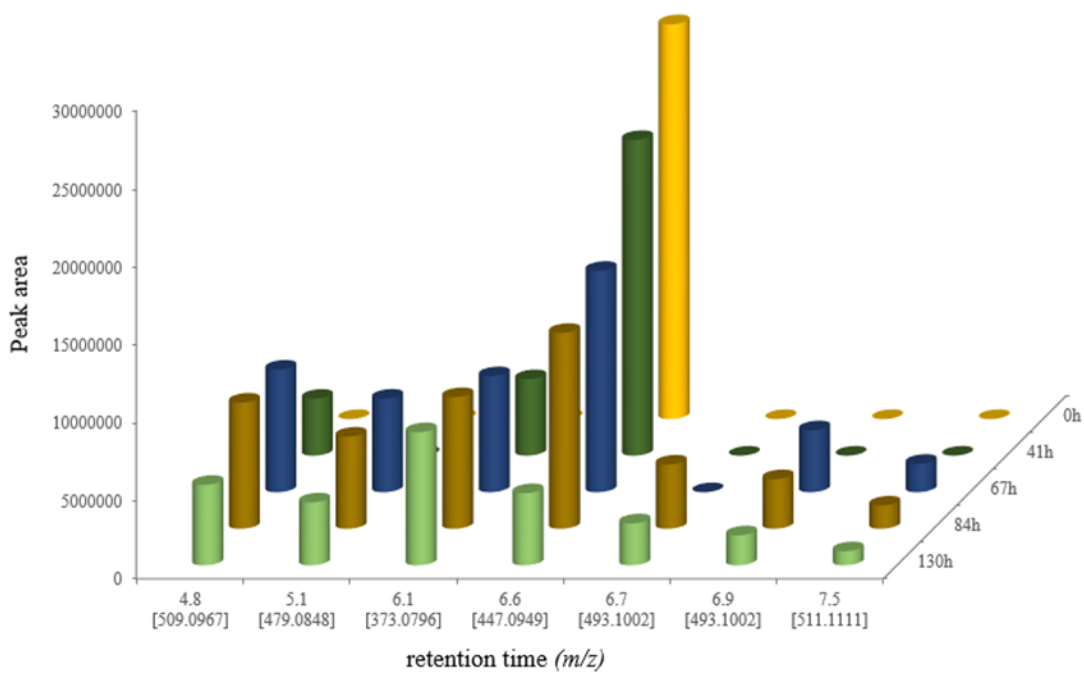
Figure A4.10. 3D-graph of the main photodegradation products of luteolin-7-*O*-glucoside in methanol
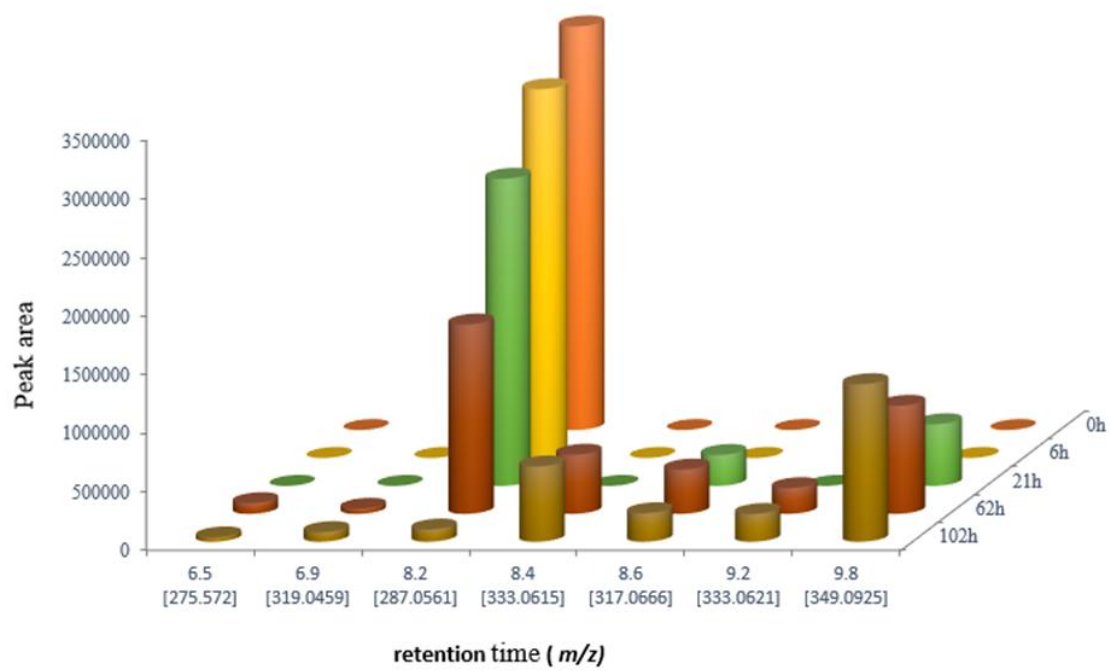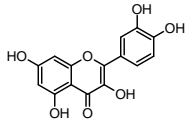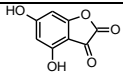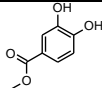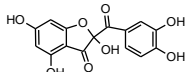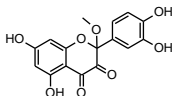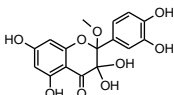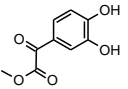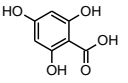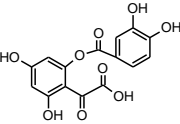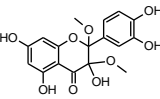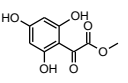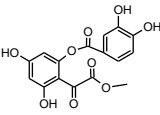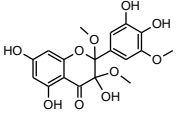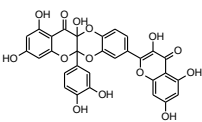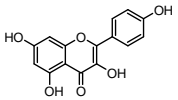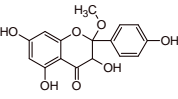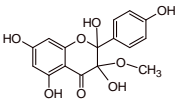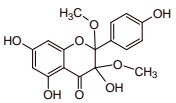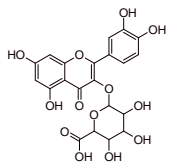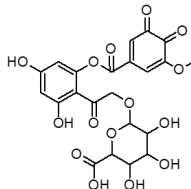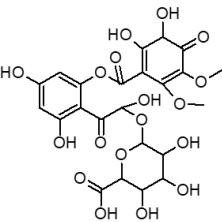
**Figure A4.11. 3D-graph of the main photodegradation products of eriodictyol in methanol**
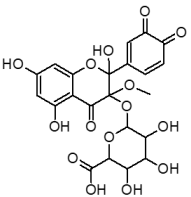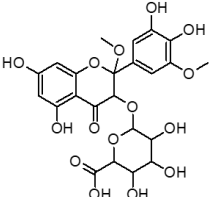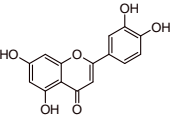
Table A4.5 – LC-ESI(-)-HRMS/MS identification of flavonoid dyes and their degradation products.
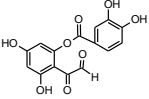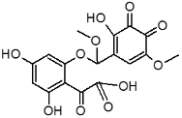
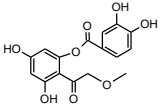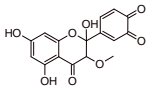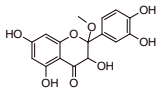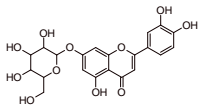| Compound/ proposed structure	t_R /min	Ion formula	[M-H]⁻ [m/z (Δ ppm); mSigma]	MS/MS [(m/z) (Δ ppm) (attribution)]	Code DP[1]
Quercetin					
	7.95	$C_{15}H_{10}O_7$	301.0355 (-0.5; 2.8)	273.0407 (-1.0) $[C_{14}H_9O_6]^-$ 257.0459 (-1.4) $[C_{14}H_9O_5]^-$ 229.0506 (-0.3) $[C_{13}H_9O_4]^-$ 193.0144 (-0.7) $[C_9H_5O_5]^-$ 178.9990 (-2.0) $[^{1,2}A^-]$ $[C_8H_3O_5]^-$ 151.0038 (-1.0) $[^{1,2}A^- - CO]$ $[C_7H_3O_4]^-$ 121.0296 (-0.6) $[^{1,2}B^-]$ $[C_7H_5O_2]^-$	Que*
	5.32	$C_8H_4O_5$	178.9989 (-1.9; 5.0)	151.0038 (-0.8) $[^{1,2}A^- - CO]$ $[C_7H_3O_4]^-$ 107.0139 (-0.3) $[^{1,2}A^- - CO-CO_2]$ $[C_6H_3O_2]^-$	DP179
	5.40	$C_8H_8O_4$	167.0322 (+4.8; 11.2)	152.0106 (+6.0) $[C_7H_4O_4]^{•-}$ 108.0209 (+8.2) $[C_6H_4O_2]^{•-}$	DP167
	5.45	$C_{15}H_{10}O_8$	317.0297 (0.2; 5.6)	299.0200 (-0.8) $[C_{15}H_7O_7]^-$ 273.0408 (-1.2) $[C_{14}H_9O_6]^-$ 255.0302 (-1.1) $[C_{14}H_7O_5]^-$ 206.9935 (-1.5) $[C_9H_2O_6]^-$ 178.9988 (-1.3) $[^{1,2}A^-]$ $[C_8H_3O_5]^-$ 151.0037 (-0.3) $[^{1,2}A^- - CO]$ $[C_7H_3O_4]^-$	DP317
	6.05	$C_{16}H_{12}O_8$	331.0463 (-1.2; 7.8)	301.0341 (-4.2) $[C_{15}H_9O_7]^-$ 300.0268 (-2.5) $[C_{15}H_8O_7]^{•-}$ 299.0191 (-2.1) $[C_{15}H_7O_7]^-$ 271.0244 (-1.5) $[C_{14}H_7O_6]^-$ 243.0293 (-2.6) $[C_{13}H_7O_5]^-$ 178.9984 (-1.0) $[^{1,2}A^-]$ $[C_8H_3O_5]^-$ 151.0032 (-3.2) $[^{1,2}A^- - CO]$ $[C_7H_3O_4]^-$ 107.0137 (-1.6) $[^{1,2}A^- - CO-CO_2]$ $[C_6H_3O_2]^-$	DP331
	6.05	$C_{16}H_{14}O_9$	349.0562 (+1.1; 4.3)	331.0463 (-1.2) $[C_{18}H_{11}O_8]^-$ 317.0302 (-0.4) $[C_{15}H_9O_8]^-$ 300.0268 (-2.6) $[C_{15}H_8O_7]^{•-}$	DP349
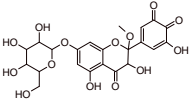
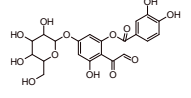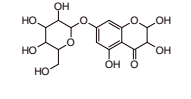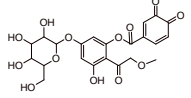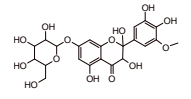| Compound/ proposed structure	t_R /min	Ion formula	[M-H]⁻ [m/z (Δ ppm); mSigma]	MS/MS [(m/z) (Δ ppm) (attribution)]	Code DP[1]
				299.0197 (+0.1) [$C_{15}H_7O_7$]⁻	
				243.0302 (-1.1) [$C_{13}H_7O_5$]⁻	
				178.9986 (-0.2) [$^{1,2}A^-$] [$C_8H_3O_5$]⁻	
				151.0039 (-1.2) [$^{1,2}A^-$ - CO] [$C_7H_3O_4$]⁻	
	6.37	$C_9H_8O_5$	195.0293 (-0.6; 3.2)	167.0345 (+0.5) [$C_8H_7O_4$]⁻	DP195
				136.0163 (-4.2) [$C_7H_3O_3$]⁻	
				108.0214 (-4.2) [$C_6H_3O_2$]⁻	
	6.54	$C_7H_6O_5$	169.0140 (+0.3; 1.6)	151.0034 (+2.1) [$C_7H_3O_4$]⁻	DP169
				125.0234 (+8.5) [$C_6H_5O_3$]⁻	
				107.0141 (-5.2) [$C_6H_3O_2$]⁻	
	6.97	$C_{15}H_{10}O_9$	333.0255 (-0.3; 4.7)	289.0356 (-0.2) [$C_{14}H_9O_7$]⁻	DP333
				245.0456 (-0.0) [$C_{13}H_9O_5$]⁻	
				217.0512 (-0.5) [$C_{12}H_9O_5$]⁻	
				178.9994 (-0.8) [$^{1,2}A^-$] [$C_8H_3O_5$]⁻	
				151.0037 (-0.0) [$^{1,2}A^-$ - CO] [$C_7H_3O_4$]⁻	
				107.0143 (-0.5) [$^{1,2}A^-$ - CO-CO$_2$] [$C_6H_3O_2$]⁻	
	7.13	$C_{17}H_{16}O_9$	363.0718 (-1.0; 4.4)	331.0457 (+0.8) [$C_{14}H_7O_6$]⁻	DP363
				300.0263 (+4.1) [$C_{15}H_8O_7$]•⁻	
				299.0197 (-0.1) [$C_{15}H_7O_7$]⁻	
				271.0248 (+5.4) [$C_{14}H_7O_6$]⁻	
				178.9981 (+2.8) [$^{1,2}A^-$] [$C_8H_3O_5$]⁻	
				151.0041 (-2.7) [$^{1,2}A^-$ - CO] [$C_7H_3O_4$]⁻	
	7.15	$C_9H_8O_6$	211.0248 (-3.8; 9.9)	178.9978 (+0.8) [$^{1,2}A^-$] [$C_8H_3O_5$]⁻	DP211
				151.0036 (+0.1) [$^{1,2}A^-$ - CO] [$C_7H_3O_4$]⁻	
				107.0143 (-0.5) [$^{1,2}A^-$ - CO-CO$_2$] [$C_6H_3O_2$]⁻	
	8.23	$C_{16}H_{12}O_9$	347.0422 (-3.9; 19.8)	303.0516 (-2.0) [$C_{15}H_{11}O_7$]⁻	DP347
				271.0252 (-1.6) [$C_{14}H_7O_6$]⁻	
				211.0254 (-2.4) [$C_9H_7O_5$]⁻	
				178.9991 (-2.6) [$^{1,2}A^-$] [$C_8H_3O_5$]⁻	
				151.0042 (-3.3) [$^{1,2}A^-$ - CO] [$C_7H_3O_4$]⁻	
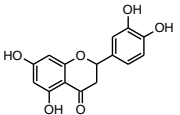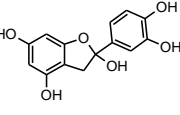
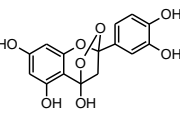| Compound/ proposed structure	t_R /min	Ion formula	[M-H]⁻ [m/z (Δ ppm); mSigma]	MS/MS [(m/z) (Δ ppm) (attribution)]	Code DP[1]
	9.29	$C_{18}H_{18}O_{10}$	393.0809 (+4.5)	303.0495 (+5.2) $[C_{15}H_{11}O_7]^-$ 289.0343 (+3.6) $[C_{14}H_9O_7]^-$ 206.9927 (+3.9) $[C_9H_3O_6]^-$ 151.0042 (-3.3) $[^{1,2}A^- - CO]$ $[C_7H_3O_4]^-$	DP393
	9.72	$C_{30}H_{18}O_{14}$	601.0628 (-0.7;10.7)	299.0191 (+0.6) $[C_{15}H_7O_7]^-$ 271.0246 (-0.2) $[C_{14}H_7O_6]^-$ 243.0299 (-0.0) $[C_{13}H_7O_5]^-$ 151.0042 (-3.3) $[^{1,2}A^- - CO]$ $[C_7H_3O_4]^-$	DP601
Kaempferol					
	8.04	$C_{15}H_{10}O_6$	285.0403 (+0.7; 10.6)	257.0455 (+0.3) $[C_{14}H_9O_5]^-$ 243.0306 (+2.9) $[C_{13}H_7O_5]^-$ 241.0500 (+2.4) $[C_{14}H_9O_4]^-$ 229.0507 (+0.4) $[C_{13}H_9O_4]^-$ 213.0558 (+0.5) $[C_{13}H_9O_3]^-$ 199.0404 (+0.3) $[C_{12}H_7O_3]^-$ 151.0032 (+3.0) $[^{1,2}A^- - CO]$ $[C_7H_3O_4]^-$	Kae*
	5.06	$C_{16}H_{14}O_7$	317.0654 (+4.9; 17.5)	299.0552 (+3.2) $[C_{16}H_{11}O_6]^-$ 285.0399 (+1.9) $[C_{15}H_9O_6]^-$ 267.0293 (+2.1) $[C_{15}H_7O_5]^-$ 257.0455 (+4.0) $[C_{14}H_9O_5]^-$ 239.0341 (+3.6) $[C_{14}H_7O_4]^-$ 221.0393(+5.6) $[C_{13}H_7O_3]^-$	DP317
	6.03	$C_{16}H_{14}O_8$	333.0604 (+3.6; 10.6)	315.0499 (+3.7) $[C_{16}H_{11}O_7]^-$ 284.0312 (+5.9) $[C_{15}H_8O_6]^{-•}$ 283.0239 (+3.0) $[C_{15}H_7O_6]^-$ 255.0289 (+4.9) $[C_{14}H_7O_5]^-$ 227.0339 (+4.0) $[C_{13}H_7O_4]^-$ 211.0394 (+3.3) $[C_{13}H_7O_3]^-$ 151.0032 (+3.0) $[^{1,2}A^- - CO]$ $[C_7H_3O_4]^-$	DP333

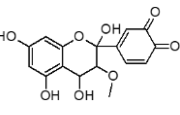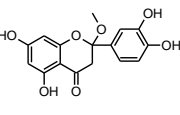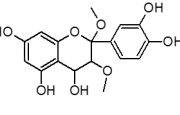| Compound/ proposed structure	t_R /min	Ion formula	[M-H]⁻ [m/z (Δ ppm); mSigma]	MS/MS [(m/z) (Δ ppm) (attribution)]	Code DP[1]
	7.26	$C_{17}H_{16}O_8$	347.0763 (+2.5; 15.6)	315.0378 (+3.1) $[C_{16}H_{11}O_7]^-$ 284.0317 (+3.2) $[C_{15}H_8O_6]^{-\bullet}$ 283.0242 (+2.2) $[C_{15}H_7O_6]^-$ 255.0292 (+2.7) $[C_{14}H_7O_5]^-$ 227.0340 (+4.5) $[C_{13}H_7O_4]^-$ 211.0402 (+0.8) $[C_{13}H_7O_3]^-$ 151.0032 (+3.0) $[^{1,2}A^- - CO] [C_7H_3O_4]^-$	DP347

Quercetin-3-O-glucuronide					
	6.10	$C_{21}H_{18}O_{13}$	477.0675 (+0.3;15.3)	301.0360 (-2.2) $[Y_0^-][C_{15}H_9O_7]^-$ 283.0257 (-3.0) $[C_{15}H_7O_6]^-$ 273.0411 (-2.2) $[C_{14}H_9O_6]^-$ 255.0308 (-3.6) $[C_{14}H_7O_5]^-$ 178.9990 (-2.2) $[^{1,2}A^-] [C_8H_3O_5]^-$ 151.0040 (-1.9) $[^{1,2}A^- - CO] [C_7H_3O_4]^-$	Que-3OGlr*
	4.63	$C_{22}H_{20}O_{15}$	523.0730 (-0.1; 23.1)	491.0473 (-1.1) $[C_{21}H_{15}O_{14}]^-$ 447.0547 (+4.9) $[C_{20}H_{15}O_{12}]^-$ 315.0139 (+2.5) $[C_{15}H_7O_8]^-$ 297.0046 (-1.9) $[C_{15}H_5O_7]^-$ 287.0221 (-8.3) $[C_{14}H_7O_7]^-$ 151.0040 (-2.2) $[^{1,2}A^- - CO] [C_7H_3O_4]^-$	DP523
	5.43	$C_{23}H_{24}O_{18}$	587.0859 (-2.3; 10.5)	569.0777 (+1.6) $[C_{23}H_{21}O_{17}]^-$ 525.0880 (+1.0) $[C_{22}H_{21}O_{15}]^-$ 349.0572 (-2.1) $[C_{16}H_{13}O_9]^-$ 317.0307 (-1.3) $[C_{15}H_9O_8]^-$ 289.0358 (-1.3) $[C_{14}H_9O_7]^-$ 231.0299 (+0.1) $[C_{12}H_7O_5]^-$ 193.0352 (+1.1) $[C_6H_9O_7]^-$	DP587

Compound/ proposed structure	t_R /min	Ion formula	[M-H]⁻ [m/z (Δ ppm); mSigma]	MS/MS [(m/z) (Δ ppm) (attribution)]	Code DP[1]
	6.30	$C_{22}H_{20}O_{15}$	523.0749 (-3.6;14.1)	479.0857 (-5.2) $[C_{21}H_{19}O_{13}]^-$ 347.0425 (-4.6) $[C_{16}H_{11}O_9]^-$ 303.0526 (-5.3) $[C_{15}H_{11}O_7]^-$ 271.0260 (-4.3) $[C_{14}H_7O_6]^-$ 243.0311 (-5.1) $[C_{13}H_7O_5]^-$ 151.0040 (-2.2) $[^{1,2}A^-$ - CO] $[C_7H_3O_4]^-$	DP523isom
	6.46	$C_{23}H_{24}O_{15}$	539.1054 (-2,1; 6.8)	507.0783 (-0.6) $[C_{22}H_{19}O_{14}]^-$ 475.0533 (-3.1) $[C_{21}H_{15}O_{13}]^-$ 363.0728 (-1.8) $[C_{17}H_{15}O_9]^-$ 331.0260 (-4.3) $[C_{16}H_{11}O_8]^-$ 299.0201 (-1.4) $[C_{15}H_7O_7]^-$ 233.0104 (-5.4) $[C_{11}H_5O_6]^-$ 178.9992 (-3.6) $[^{1,2}A^-]$ $[C_8H_3O_5]^-$ 151.0038 (-0.5) $[^{1,2}A^-$ - CO] $[C_7H_3O_4]^-$	DP539
Luteolin					
	7.96	$C_{15}H_{10}O_6$	285.0408 (-1.1; 13.9)	257.0448 (-3.4) $[C_{14}H_9O_5]^-$ 243.0289 (-1.2) $[C_{13}H_7O_5]^-$ 217.0499 (-2.9) $[C_{12}H_9O_4]^-$ 199.0393 (-2.3) $[C_{12}H_7O_3]^-$ 175.0395 (-2.3) $[C_{10}H_7O_3]^-$ 151.0035 (+1.5) $[^{1,3}A^-]$ $[C_7H_3O_4]^-$ 133.0293 (+1.8) $[^{1,3}B^-]$ $[C_8H_5O_2]^-$	Lut*
	5.66	$C_{16}H_{12}O_9$	347.0401 (+2.3; 10.1)	305.0298 (+1.6) $[C_{14}H_9O_8]^-$ 287.0221 (+0.1) $[C_{14}H_7O_7]^-$ 261.0410 (-1.9) $[C_{13}H_9O_6]^-$ 217.0148 (-2.7) $[C_{11}H_5O_5]^-$ 151.0035 (+1.5) $[^{1,3}A^-]$ $[C_7H_3O_4]^-$	DP347
	5.87	$C_7H_6O_4$	153.0192 (+0.6; 6.7)	125.0249 (-3.1) $[C_6H_5O_3]^-$ 107.0133 (+5.5) $[C_6H_3O_2]^-$	DP153

| Compound/ proposed structure	t_R /min	Ion formula	[M-H]⁻ [m/z (Δ ppm); mSigma]	MS/MS [(m/z) (Δ ppm) (attribution)]	Code DP[1]
	6.25	$C_{15}H_{10}O_8$	317.0295 (2.5; 1.3)	273.0405 (-1.3) $[C_{14}H_9O_6]^-$ 227.0341 (+3.7) $[C_{13}H_5O_4]^-$ 151.0036 (+0.6) $[^{1,3}A^-]$ $[C_7H_3O_4]^-$	DP317
	7.03	$C_{17}H_{14}O_{11}$	393.0468 (-1.1; 9.7)	375.0371 (-3.5) $[C_{17}H_{11}O_{10}]^-$ 333.0258 (-1.7) $[C_{15}H_9O_9]^-$ 273.0047 (-1.7) $[C_{13}H_5O_7]^-$ 245.0101 (-3.8) $[C_{12}H_5O_6]^-$ 201.0197 (-2.0) $[C_{11}H_5O_4]^-$ 151.0038 (-0.7) $[^{1,3}A^-]$ $[C_7H_3O_4]^-$	DP393
	7.60	$C_{16}H_{14}O_8$	333.0612 (+1.3; 12.2)	289.0718 (-1.4) $[C_{15}H_{13}O_6]^-$ 257.0456 (-0.4) $[C_{14}H_9O_5]^-$ 229.0498 (+3.6) $[C_{13}H_9O_4]^-$ 151.0038 (-0.7) $[^{1,3}A^-]$ $[C_7H_3O_4]^-$	DP333
	8.09	$C_{16}H_{12}O_8$	331.0448 (+3.2: 8.4)	287.0561 (+0.1) $[C_{15}H_{11}O_6]^-$ 272.0335 (-3.3) $[C_{14}H_8O_6]^{•-}$ 255.0287 (+4.6) $[C_{14}H_7O_5]^-$ 227.0355 (-2.4) $[C_{13}H_7O_4]^-$ 151.0046 (-5.6) $[^{1,3}A^-]$ $[C_7H_3O_4]^-$	DP331
	9.33	$C_{16}H_{14}O_8$	333.0616 (+0.1; 5,1)	301.0350 (+1.1) $[C_{15}H_9O_7]^-$ 259.0251 (-1.0) $[C_{13}H_7O_6]^-$ 214.0273 (-0.7) $[C_{12}H_6O_4]^{•-}$ 201.0195 (-0.9) $[C_{11}H_5O_4]^-$ 151.0038 (-0.7) $[^{1,3}A^-]$ $[C_7H_3O_4]^-$	DP333isom
Luteolin-7-O-glucoside					
	6.61	$C_{21}H_{20}O_{11}$	447.0933 (-0.0;4.5)	285.0398 (-2.6) $[Y_0^-][C_{15}H_9O_6]^-$ 284.0328 (-0.6) $[Y_0^- - H]^{•-}$ $[C_{15}H_9O_6]^{•-}$ 235,0249 (-0.3) $[C_{11}H_7O_6]^-$ 151.0039 (-1.1) $[^{1,3}A^-]$ $[C_7H_3O_4]^-$ 133.0294 (+1.0) $[^{1,3}B^-]$ $[C_8H_5O_2]^-$	Lut-7OGlc*

Compound/ proposed structure	t_R /min	Ion formula	[M-H]⁻ [m/z (Δ ppm); mSigma]	MS/MS [(m/z) (Δ ppm) (attribution)]	Code DP[1]
	4.79	$C_{22}H_{22}O_{14}$	509.0935 (-3.7; 6.4)	477.0677 (-0.6) $[C_{21}H_{17}O_{13}]^-$ 449.0718 (+1.6) $[C_{20}H_{17}O_{12}]^-$ 347.0404 (+1.3) $[C_{14}H_7O_7]^-$ 287.0183 (+1.6) $[C_{20}H_{17}O_{12}]^-$ 261.0397 (+3.0) $[C_{13}H_9O_6]^-$ 193.0142 (+0.4) $[C_9H_5O_5]^-$ 151.0030 (+4.4) $[^{1,3}A^-]$ $[C_7H_3O_4]^-$	DP509
	5.08	$C_{21}H_{20}O_{13}$	479.0848 (-3.6; 6.1)	435.0926 (+1.6) $[C_{20}H_{19}O_{11}]^-$ 317.0303 (+0.1) $[C_{15}H_9O_8]^-$ 273.0404 (+0.2) $[C_{14}H_9O_6]^-$ 229.0505 (+0.5) $[C_{13}H_9O_4]^-$ 151.0040 (-2.4) $[^{1,3}A^-]$ $[C_7H_3O_4]^-$	DP479
	6.18	$C_{15}H_{18}O_{11}$	373.0796 (-5.2; 10.1)	341.0526 (-2.3) $[C_{15}H_{17}O_{11}]^-$ 313.0573 (-1.7) $[C_{13}H_{13}O_9]^-$ 211.0252 (-2.0) $[C_9H_7O_6]^-$ 175.0040 (-1.9) $[C_9H_3O_4]^-$ 151.0039 (-1.4) $[^{1,3}A^-]$ $[C_7H_3O_4]^-$	DP373
	6.92	$C_{22}H_{22}O_{13}$	493.1000 (-2.6; 10.2)	447.0937 (-0.9) $[C_{21}H_{19}O_{11}]^-$ 331.0463 (-1.1) $[C_{16}H_{11}O_8]^-$~ 287.0565 (-1.4) $[C_{15}H_{11}O_6]^-$ 272.0328 (-0.6) $[C_{14}H_8O_6]^-$ 227.0351 (-0.7) $[C_{13}H_7O_4]^-$	DP493
	7.48	$C_{22}H_{24}O_{14}$	511.1110 (-3.3; 2.2)	479.0833 (-3.0) $[C_{21}H_{19}O_{13}]^-$ 465.0991 (+0.7) $[C_{21}H_{21}O_{12}]^-$ 379.0664 (+1.7) $[C_{17}H_{15}O_{10}]^-$ 349.0562 (+2.7) $[C_{18}H_{13}O_9]^-$ 287.0543 (+6.2) $[C_{15}H_{11}O_6]^-$	DP511
Eriodictyol					

| Compound/proposed structure	t_R /min	Ion formula	[M-H]⁻ [m/z (Δ ppm); mSigma]	MS/MS [(m/z) (Δ ppm) (attribution)]	Code DP[1]
	8.21	$C_{15}H_{12}O_6$	287.0564 (-1.1; 19.4)	151.0038 (-1.1) [1,3A⁻] [$C_7H_3O_4$]⁻ 135.0454 (-1.7) [1,3B⁻] [$C_8H_7O_2$]⁻ 125.0240 (+3.5) [1,4A⁻] [$C_6H_5O_3$]⁻ 107.0141(-2.2) [1,3A⁻-CO₂] [$C_6H_3O_2$]⁻	Eriodictyol*
	6.51	$C_{14}H_{12}O_6$	275.0563 (-0.8; 4.6)	257.0468 (-5.0) [$C_{14}H_9O_5$]⁻ 231.0678 (-6.8) [$C_{13}H_{11}O_4$]⁻ 149.0244 (-0.1) [$C_8H_5O_3$]⁻ 125.0247 (-2.5) [1,4A⁻] [$C_6H_5O_3$]⁻	DP275
	6.96	$C_{15}H_{12}O_8$	319.0459 (+0.3, 13.9)	301.0369 (-5.1) [$C_{15}H_9O_7$]⁻ 275.0541 (+2.3) [$C_{14}H_{11}O_6$]⁻ 257.0474 (+2.3) [$C_{14}H_9O_5$]⁻ 177.0187 (+3.3) [$C_9H_5O_4$]⁻ 125.0239 (+4.4) [1,4A⁻] [$C_6H_5O_3$]⁻	DP319
	8.45	$C_{16}H_{14}O_8$	333.0616 (-1.4; 7.5)	287.0563 (-0.7) [$C_{15}H_{11}O_6$]⁻ 257.0453 (+1.1) [$C_{14}H_9O_5$]⁻ 177.0191 (+1.0) [$C_9H_5O_4$]⁻ 151.0031 (+4.0) [1,3A⁻] [$C_7H_3O_4$]⁻ 125.0236 (+6.4) [1,4A⁻] [$C_6H_5O_3$]⁻ 107.0138 (+0.2) [1,3A⁻-CO₂] [$C_6H_3O_2$]⁻	DP333
	8.57	$C_{16}H_{14}O_7$	317.0669 (-0.6; 3.4)	285.0407 (-1.0) [$C_{15}H_9O_6$]⁻ 241.0510 (-1.7) [$C_{14}H_9O_4$]⁻ 165.0549 (+5.0) [$C_9H_9O_3$]⁻ 151.0030 (+4.5) [1,3A⁻] [$C_7H_3O_4$]⁻ 135.0450 (+0.7) [1,3B⁻] [$C_8H_7O_2$]⁻ 125.0235 (+7.5) [1,4A⁻] [$C_6H_5O_3$]⁻ 107.0140 (-1.5) [1,3A⁻-CO₂] [$C_6H_3O_2$]⁻	DP317
	9.83	$C_{17}H_{18}O_8$	349.0932 (-1.0; 5.9)	331.0683 (-3.4) [$C_{17}H_{15}O_7$]⁻ 317.0673 (-1.0) [$C_{16}H_{13}O_7$]⁻ 299.0570 (-2.9) [$C_{16}H_{11}O_6$]⁻ 207.0665 (-1.2) [$C_{11}H_{11}O_4$]⁻ 177.0198 (-2.5) [$C_9H_5O_4$]⁻	DP349

Compound/ proposed structure	t_R /min	Ion formula	[M-H]⁻ [m/z (Δ ppm); mSigma]	MS/MS [(m/z) (Δ ppm) (attribution)]	Code DP[1]
				165.0562 (-2.9) [C₉H₉O₃]⁻	
				151.0038 (-0.7) [¹,³A⁻] [C₇H₃O₄]⁻	
				135.058 (-3.4) [¹,³B⁻] [C₈H₇O₂]⁻	
				125.0246 (-1.5) [¹,⁴A⁻] [C₆H₅O₃]⁻	

[1] Identified degradation product

[*] Proposed fragmentation in according with Fabre, N. *et al.* (2001). Determination of flavone, flavonol, and fla-vanone aglycones by negative ion liquid chromatography electrospray ion trap mass spectrometry. *Journal of the American Society for Mass Spectrometry*, 12(6), 707-715.); as shown in Schemes A4.5-A4.10.
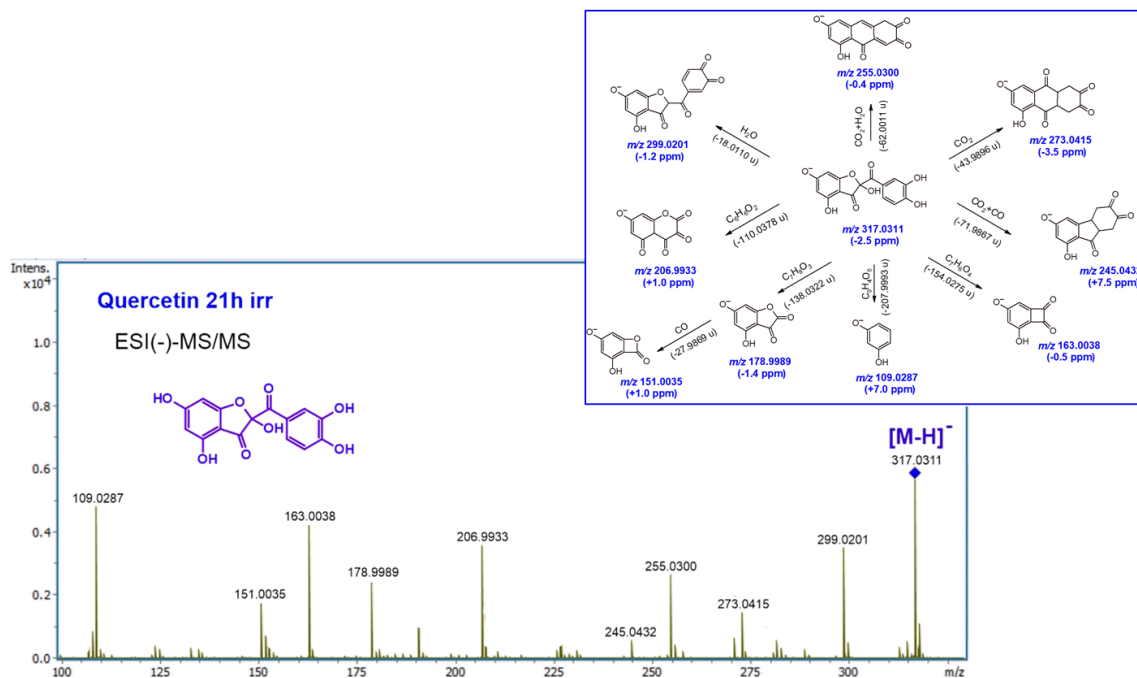
Scheme A4.3. Quercetin in methanol, tandem HR mass spectrum, and proposed fragmentation path for precursor ion of the degradation product *m/z* 317.0311 at *t*$_R$ 5.45 min, assigned to a benzo-furanona structure.
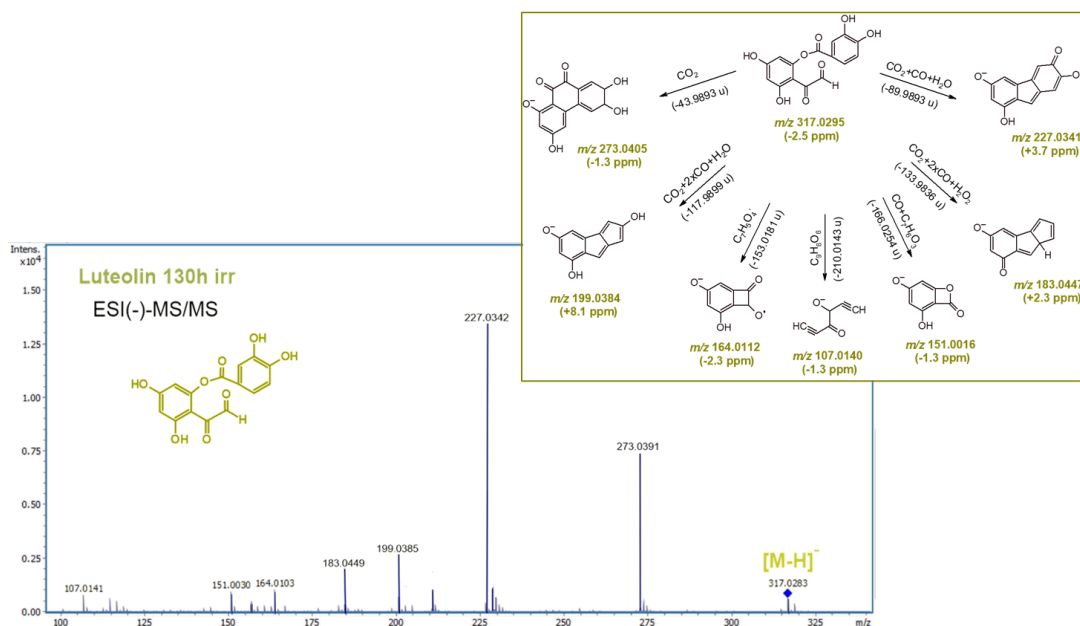

Scheme A4.4. Luteolin in methanol, tandem HR mass spectrum, and proposed fragmentation path for precursor ion of the degradation product *m/z* 317.0295 at *t*$_R$ 6.25 min, attributed to oxobenzal-dehyde depside form.
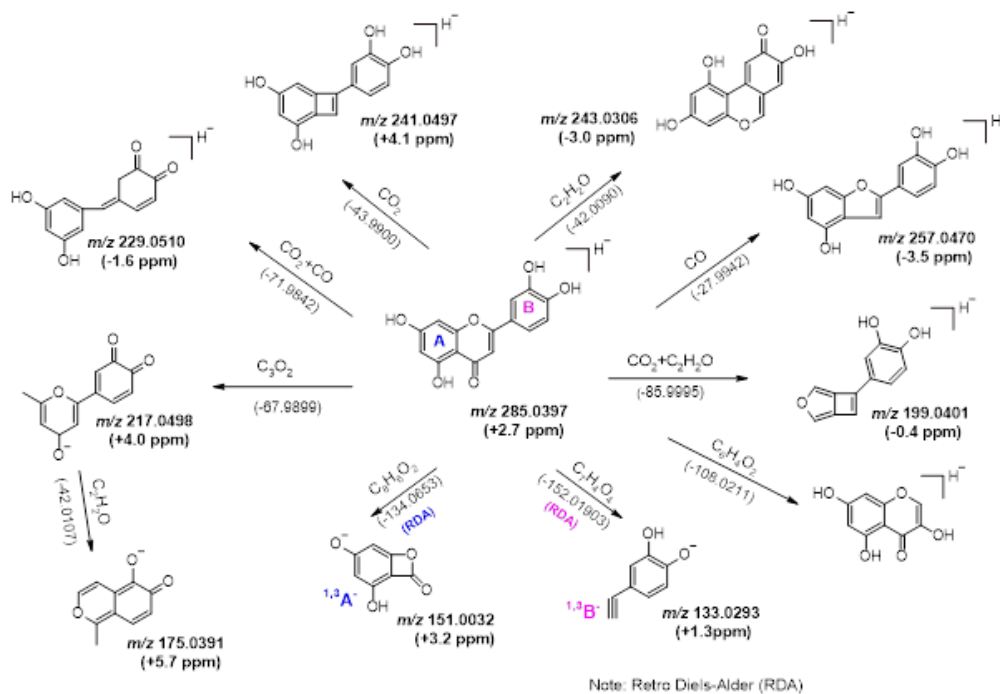
223
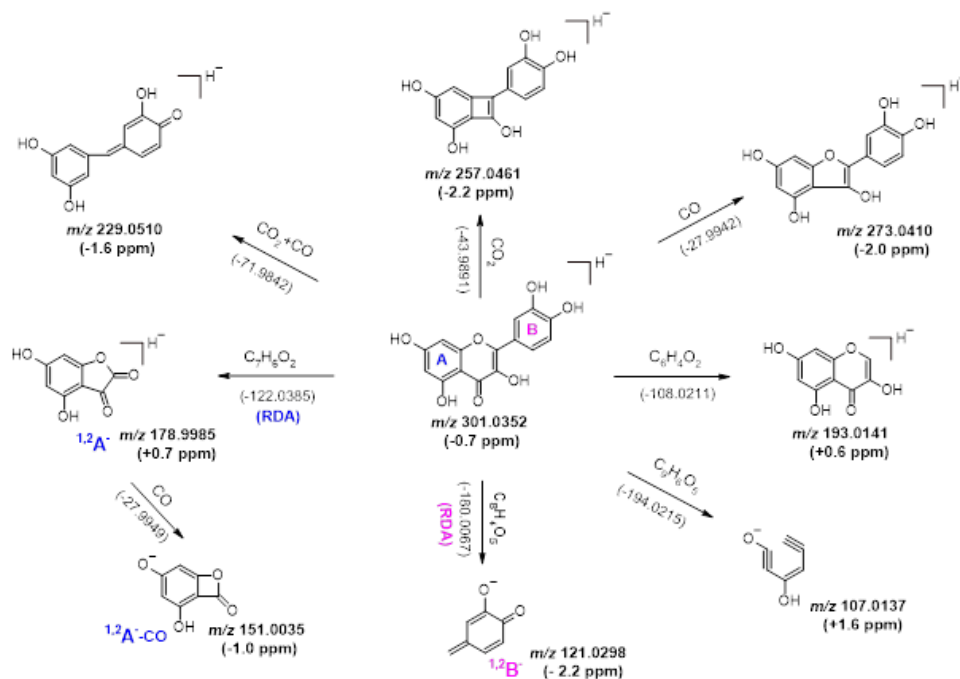
Scheme A4.5. Proposed fragmentation mechanism for precursor ion *m/z* 301.0352 assigned to the deprotonated molecule of quercetin.
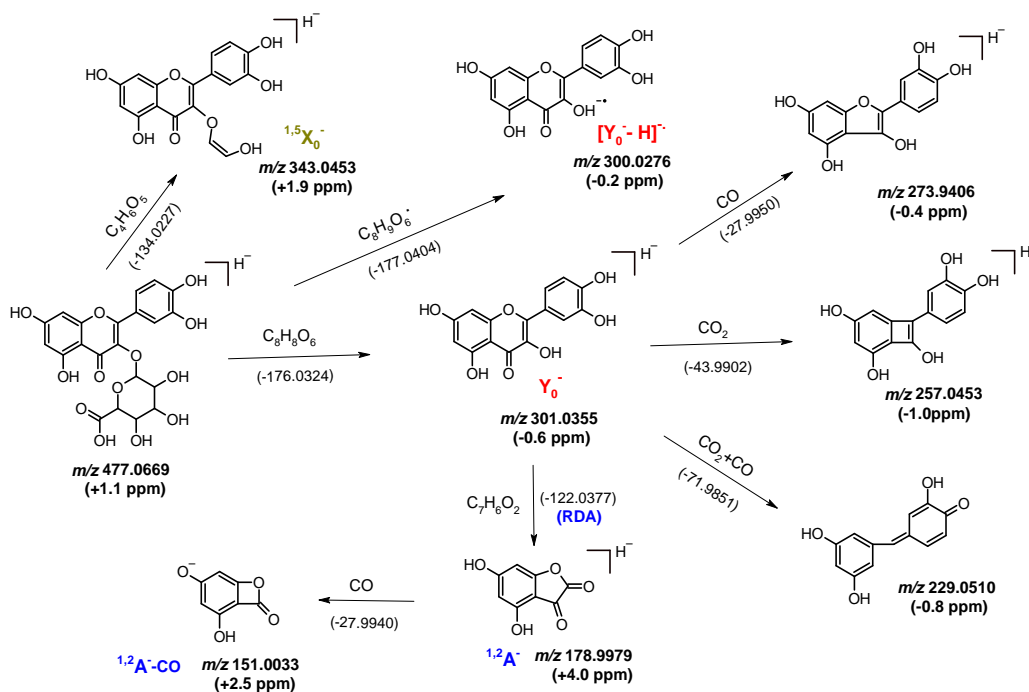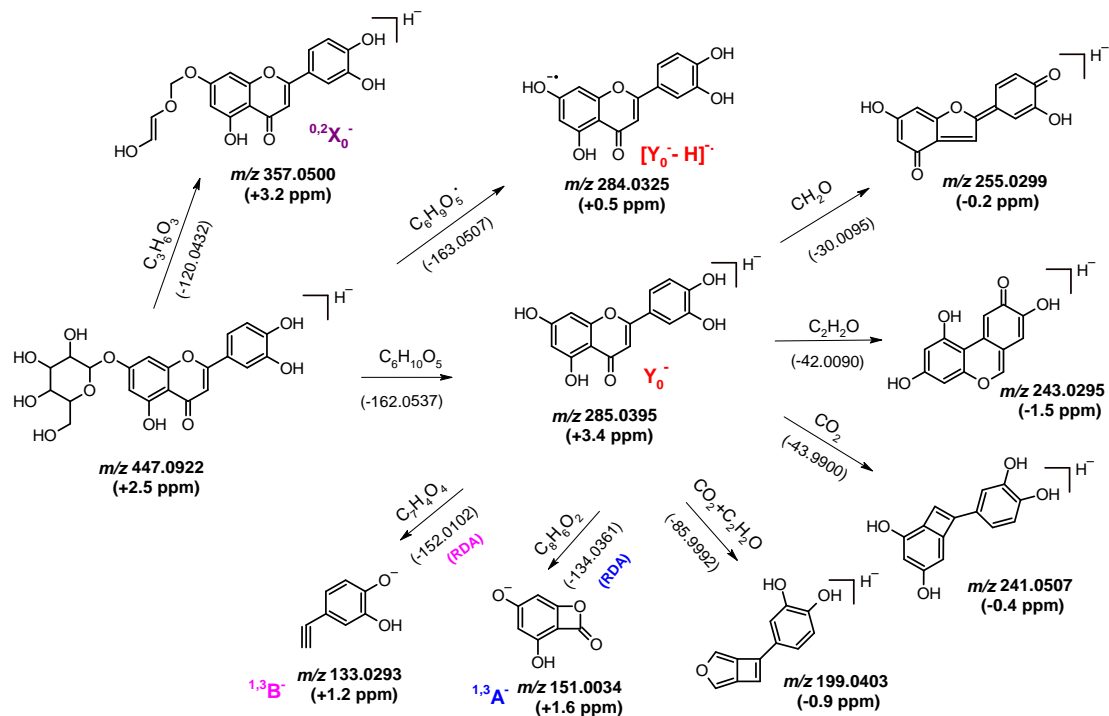

Scheme A4.6. Proposed fragmentation mechanism for precursor ion *m/z* 477.0669 assigned to the deprotonated molecule of quercetin-3-*O*-glucuronide.
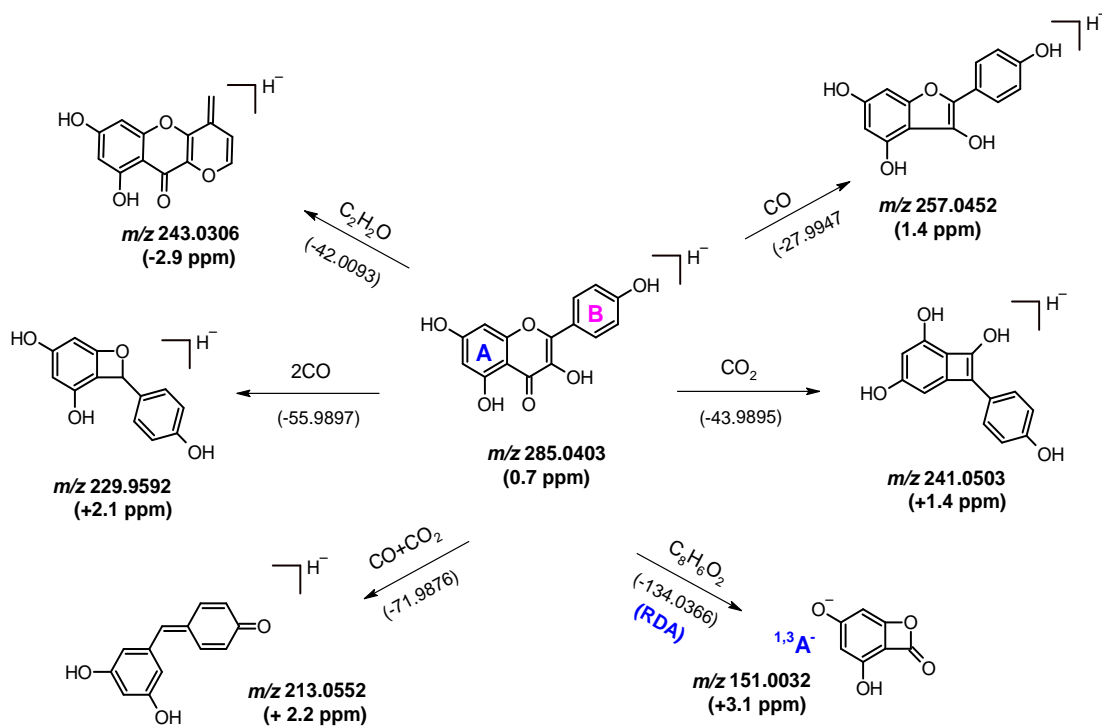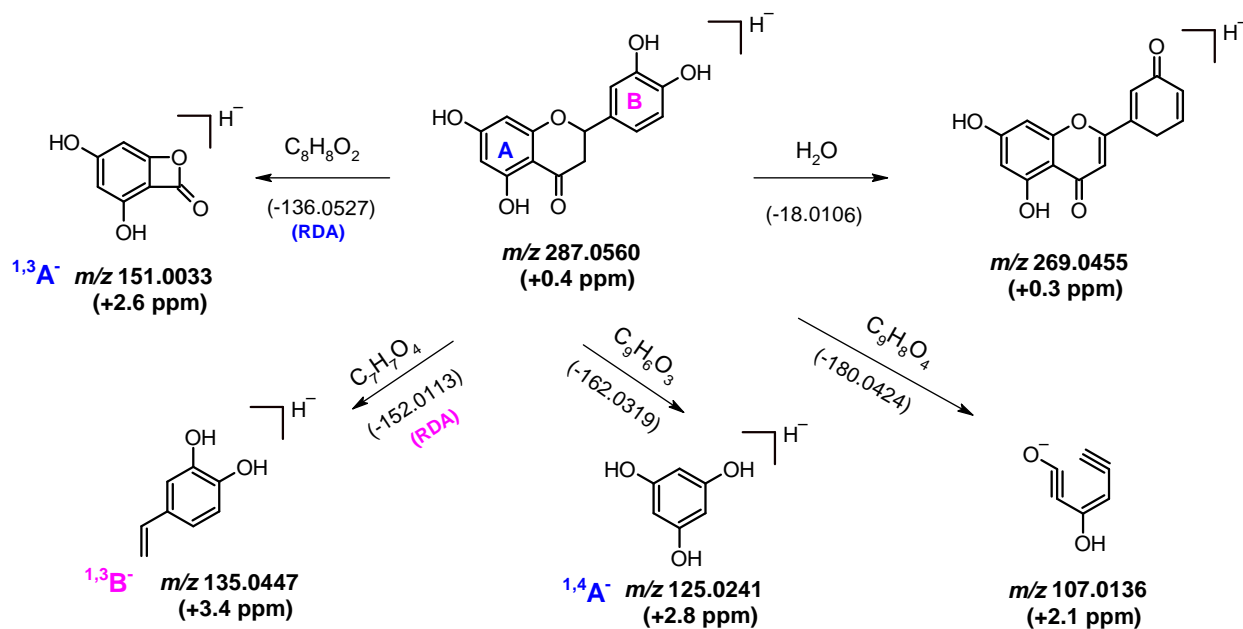
Scheme A4.7. Proposed fragmentation mechanism for precursor ion *m/z* 285.0403 assigned to the deprotonated molecule of kaempferol.

Scheme A4.8. Proposed fragmentation mechanism for precursor ion *m/z* 285.0397 attributed to the deprotonated molecule of luteolin.

Scheme A4.9. Proposed fragmentation mechanism for precursor ion *m/z* 447.0922 attributed to the deprotonated molecule of luteolin-7-*O*-glucoside.

Scheme A4.10. Proposed fragmentation mechanism for precursor ion *m/z* 287.0560 assigned to the deprotonated molecule of eriodictyol.

226